A Generalizable Mechanism of CD24 Signalling and Its Ability to Specifically Alter the Biogenesis of B Cell Extracellular Vesicles

By © D. Craig Ayre, B.Sc. (Hons.), B.Ed., M.Sc.

A Thesis Submitted to the School of Graduate Studies in Partial Fulfillment of the Requirements for the Degree of

Doctor of Philosophy

Faculty of Science, Department of Biochemistry

Memorial University of Newfoundland

August 2017

St. John's Newfoundland and Labrador

Abstract

CD24 is a variably glycosylated, glycophosphatidylinositol (GPI)-anchored cell surface protein. Its expression is dynamic during cellular differentiation and ligand interaction. While several decades of research have established that CD24 engages in many cell-type specific functions in many cases the ligands of CD24 are unknown, and researchers have relied on the use of antibodies to mimic ligand binding. Furthermore, as a GPI-anchored protein, CD24 must rely on *in cis* signalling partners, however little has been elucidated on the cell membrane-proximal signalling activities of CD24. Therefore, the work presented in this thesis presents a more comprehensive examination of CD24 expression, and function in multiple cell types, followed by an in-depth analysis in immature B lymphocytes. In B cells, CD24 is known to mediate the induction of apoptosis. To predict *in cis* and *in trans* partners of CD24, an analysis of CD24 mRNA expression, and its potential ligands was performed. In some tissues, such as B cells, an association was identified between CD24 and putative ligands, including Siglec-2. In other tissues, no significant associations were identified. Our previous investigation suggested that CD24 is involved in vesicle trafficking, Consistent with this, CD24 surface protein expression was shown to be dynamic within 1 h of Ab stimulation in WEHI-231 immature B cells and in *ex vivo* primary immature B cells. I found CD24 promotes the generation of plasma membrane-derived microvesicles (MVs). These MVs transported CD24 between cells. MVs also carried a variety of nucleic acid cargo, identified by RNA-Seq, and protein cargo as determined by mass spectrometry and flow cytometry. The incorporation of these cargos into MVs was variably influenced by CD24 stimulation. Overall, these

data suggest that MVs generated in response to CD24 play a role in regulating mitochondria, and immune cell activation. Finally, a unifying hypothesis on the function of CD24 is presented herein, proposing its role as a moderating rheostat of cellular signalling rather than a *de novo* signalling receptor. Together, this work has significantly advanced our understanding of CD24 in B cells, and may provide insight for studies in other cell types or in diseases such as leukemia.

Acknowledgements

Dedicating a thesis is a risky business. If you read a name written at the top, do you feel like they're more important than the dedications below? Have I created a ranked list of those who are important to me without realizing it? Humour is another tricky subject. This may be the only opportunity in your whole academic career to write an official, notarized joke. Some people crack under the pressure. Others reach for greatness only to be reminded years later that certain things just shouldn't be joked about. Like having a short supervisor, or the time you ground the objective lens of a microscope flat. Maybe it would be better to say nothing at all, and hope the people around you can intuit if they would have been thanked or mentioned. But then what if someone you *didn't* want to thank assumes they should be. Should have been a Vulcan. They don't worry about this kind of thing.

Anyway, I've used half my dedication space with no dedication. To those who helped craft this document, I believe they would call it in keeping with the trend of requiring half a page before they found a point.

I think that sums it up. Except for the actual dedicating.

To Sherri, Niki, Nicole, and Luke; There wouldn't be an awkward dedication without you. Remember always you helped create the life I get to enjoy now. I owe you a debt I can never repay. To Mom, Dad and Bryan; I owe you the past that got here and for the support to keep going. To Laura: You're the only reason any of it matters anyway.

Table of Contents

List of Tables

List of Figures

List of Abbreviations and Symbols

Ab	Antibody
Ag	Antigen
APC	Allophycocyanin
BCR	B cell receptor
CD	Cluster of Differentiation
CLP	Common Lymphoid Progenitor
CXCR	C-X-C Chemokine Receptor
Cy	Cyanine
DAMP	Danger Associated Molecular Pattern
DC	Dendritic Cell
DN	Double Negative
DP	Double Positive
EGFR	Epidermal Growth Factor Receptor
EV(s)	Extracellular Vesicle(s)
FACS	Fluorescent Activated Cell Sorting
FDR	False Discovery Rate
FITC	Fluorescein Isothiocyanate
FrA	Fraction A
FrB	Fraction B
FrC / FrC’	Fraction C / Fraction C’
FrD	Fraction D
FrE	Fraction E
FrF	Fraction F
GEF	Guanine Exchange Factor
FSC	Forward Scatter
GEO	Gene Expression Omnibus
GO	Gene Ontology
GPI	Glycophosphatidylinositol
GPT	Glutamic Pyruvate Transaminase
HMGB	High Mobility Group Box
HNK-1	Human Natural Killer-1
HSA	Heat Stable Antigen
HSC	Hematopoietic Stem Cell
Ig	Immunoglobulin
IgH	Immunoglobulin Heavy Chain
IgL	Immunoglobulin Light Chain

Il	Interleukin
INT	Intermediate
ITAM	Immunoreceptor Tyrosine-based Activation Motif
JNK	Jun Amino-Terminal Kinases
L1CAM	L1 Cell Adhesion Molecule
mAb	Monoclonal Antibody
MAPK	Mitogen Activated Protein Kinase
MHC	Major Histocompatibility Complex
MV(s)	Microvesicle(s)
NCAM	Neural Cell Adhesion Molecule
NCBI	National Center for Biotechnology
PBS	Phosphate Buffered Saline
PE	Phycoerythrin
PerCP	Peridinin chlorophyll
PI	Propidium Iodide
Pre	Precursor
Pro	Progenitor
PTK	Protein Tyrosine Kinase
QS	Quin Saline
SFK	Src Family Tyrosine Kinase
Siglec	Sialic Acid-Binding Immunoglobin-Type Lectins
SL	Surrogate Light Chain
SSC	Side Scatter
STAT	Signal Transducer and Activator of Transcription
TEM	Transmission Electron Microscope
TLR	Toll-Like Receptor
Tg	Transgenic
UTR	Untranslated Region
VCAM-1	Vascular Cell Adhesion Molecule-1
VLA-4	Very Late Antigen-4

List of Appendices and Supplemental Files

1. Appendix A: Copyright license agreements
2. Appendix B: R Scripts
3. Supplemental File 1 (Chapter 2): The mean and standard deviations from the microarray data analyzed, for all genes shown in Chapter 2
4. Supplemental File 2 (Chapter 4): Gene ontology enrichment analysis of the top 50 protein coding transcripts identified in EV from B cells released under isotype or anti-CD24 stimulation.
5. Supplemental File 3 (Chapter 4): Gene ontology, pathway, process and disease enrichments identified from the proteins enriched in EV released from B cells following anti-CD24 stimulation.

Chapter 1: Introduction

1.1 Identification of the CD24 cell surface receptor

The protein now termed CD24 was first identified in 1978 during a screen of mouse monoclonal antibodies (mAbs), for the identification of novel leukocyte antigens (1). During this screen, 5 cell lines produced mAbs (M1/75.21, M1/22.54, M1/89.1, M1/9.47 and M1/69.16) that recognized a common antigen, which was speculated to be carbohydrate-based due to its stability under high temperature.. Therefore, at the time, this antigen was termed the Heat Stable Antigen (HSA) and was found to be present on thymic-based leukocytes and red blood cells (RBCs). Of these mAbs, M1/69 was found to have the highest avidity for this newly identified antigen. Subsequently, other groups identified additional mAbs (J11d, B2A2) which bound to the same antigen (2). However, these groups disagreed as to the nature of the antigenic determinant. In parallel, studies in humans identified CD24 as a B lymphocyte (B cell) associated marker using the BA-1 mAb (3). Subsequently, it was found that the CD24 antigen was a glycoprotein, and differentially expressed during B cell development, with higher expression on developing versus. mature B cells (3, 4).

Concurrent studies began to examine the structural composition of the mature CD24 protein in greater detail (5-7). Cloning of mouse HSA/*CD24* identified the precursor peptide to be 76 amino acid residues in length (5). Furthermore, the initial 26 amino acids and the terminal 20 amino acids were predicted to be a cytoplasmic localization signal and a glycophosphatidylinositol (GPI)-anchor signal, respectively, and cleaved from the mature peptide (5). Ultimately, the mature peptide product was

predicted to be approximately 30 amino acids in length and have a size of approximately 3 kDa (6). Further refinement to the sequence analysis established the likely mature peptide to be 27 amino acids and approximately 2.7 kDa in size (7). In mouse, two other genomic sequences were identified with homology to *HSA/CD24*. The three sequences were denoted as HSA-A, HSA-B and HSA-C, where the B and C sequences were deemed to be intronless retroposons (7). A gene duplication event was thought to create HSA-C from –A, and HSA-B (containing a short poly-A tail) arose from a transcript originating from –C. While it has yet to be established if the –B or –C genes remain active, the –C transcript was functional in the evolutionary past.

Several studies confirmed that CD24 is anchored on the plasma membrane of multiple cell types via the GPI modification (2, 8). Cells treated with phospholipase C (PLC), which cleaves GPI anchor moieties from the plasma membrane, exhibit a profound reduction in CD24 protein levels. In multiple studies, however, this loss was not complete and a small amount of CD24 is retained by cells (2, 8). Due to this partial, but not complete loss, it was speculated that variants of CD24 may exist that are not GPI-anchored. However, another study found that patients with paroxysmal nocturnal hemoglobinuria do not express CD24 (8). This condition is caused by the inability to synthesize the GPI anchor structure, leading to a loss of all GPI-anchored proteins (9). The lack of CD24 expression in these patients therefore strongly argues against a secondary, non-GPI anchored isoform. Further, the retention of CD24 on cells following PLC treatment could be facilitated by *in cis* interactions with other proteins or structures on the plasma membrane (10) with the continued detection of CD24 following PLC treatment demonstrating that these *in cis* interactors cannot also be GPI anchored entities.

When the sequence of the human CD24 transcript was characterized, comparison of the sequencing information of CD24 and HSA established them to be homologous cell surface protein in human and mouse (5, 6). Similar to the mouse protein sequence, human CD24 was estimated to be 80 amino acids in length, with a 26-amino acid N-terminal signal domain and a 27 to 29 amino acid C-terminal GPI anchor sequence (6). Overall, this post-translational processing results in a mature peptide, then thought to be between 31 to 35 amino acids in length (6). While sequence homology was noted between the two species, it was determined that the most conserved regions were in the N- and C- terminal signal domains, and considerable variation existed in the mature protein core (6). As with the murine sequence, CD24 pseudogenes have also been identified in humans (11), with unknown expression or functional significance. Interestingly, transcript variants of mouse CD24, with unknown function, have been identified (12).

As sequencing data for more species has become available, CD24, and CD24-like sequences have been identified in numerous species (13). Overall, CD24 is evolutionarily at least 200 million years old and has been identified in reptiles, birds, and mammals (including aquatic species), however it has not been identified in marsupials or monotremes (13). The reason for its absence in these species is unknown. In each case, it was found that the evolution of the CD24 gene has more stringently conserved the N- and C- terminal processing sequences, while the core peptide has undergone considerable variation (13). Areas of higher conservation in the core mature peptide are primarily on amino acid residues capable of being glycosylated during post-translational modification. Furthermore, a conserved proline-rich domain has been identified in the C-terminal

region of the mature peptide. Overall, across evolutionary history, the CD24 gene encodes for a small protein that, following processing, is affixed to the outer leaflet of the plasma membrane via a GPI anchor (**Figure 1.1**).

1.2 CD24 is a heavily and variably glycosylated protein

Since its discovery, several groups have observed the CD24 protein does not have a well-defined mass, but instead ranges in size from approximately 20 to 70 kDa (2, 5, 14, 15). The discrepancy between predicted peptide size based on this sequence data and the measured sizes found in multiple studies was resolved by identifying CD24 as being post-translationally modified by extensive glycosylation. The glycosylation of the mature CD24 peptide had previously been established (2, 3), however the degree to which these glycosylations contributed to the mature protein size had not been appreciated. Glycosylation can occur on the nitrogen present in asparagine (Asn/N) residues, or on the oxygen present in serine (Ser/S) and threonine (Thr/T) residues, and is termed N-linked or O-linked, respectively. The first sequence analysis of murine CD24 showed there are four potential N-linked, and seven potential O-linked glycosylation sites (5).

Early studies on the structure of CD24 used tunicamycin to inhibit the N-linked glycosylation, which resulted in an approximately 20-kDa structure remaining. This was originally thought to be the core peptide, as it retained M1/69 binding (2). Later studies, removing N-linked glycosylations via endoglycosidases also produced a structure between 20 and 30 kDa in size, however with the combined sequence data, it was determined that O-linked glycosylation must contribute considerably to the remaining

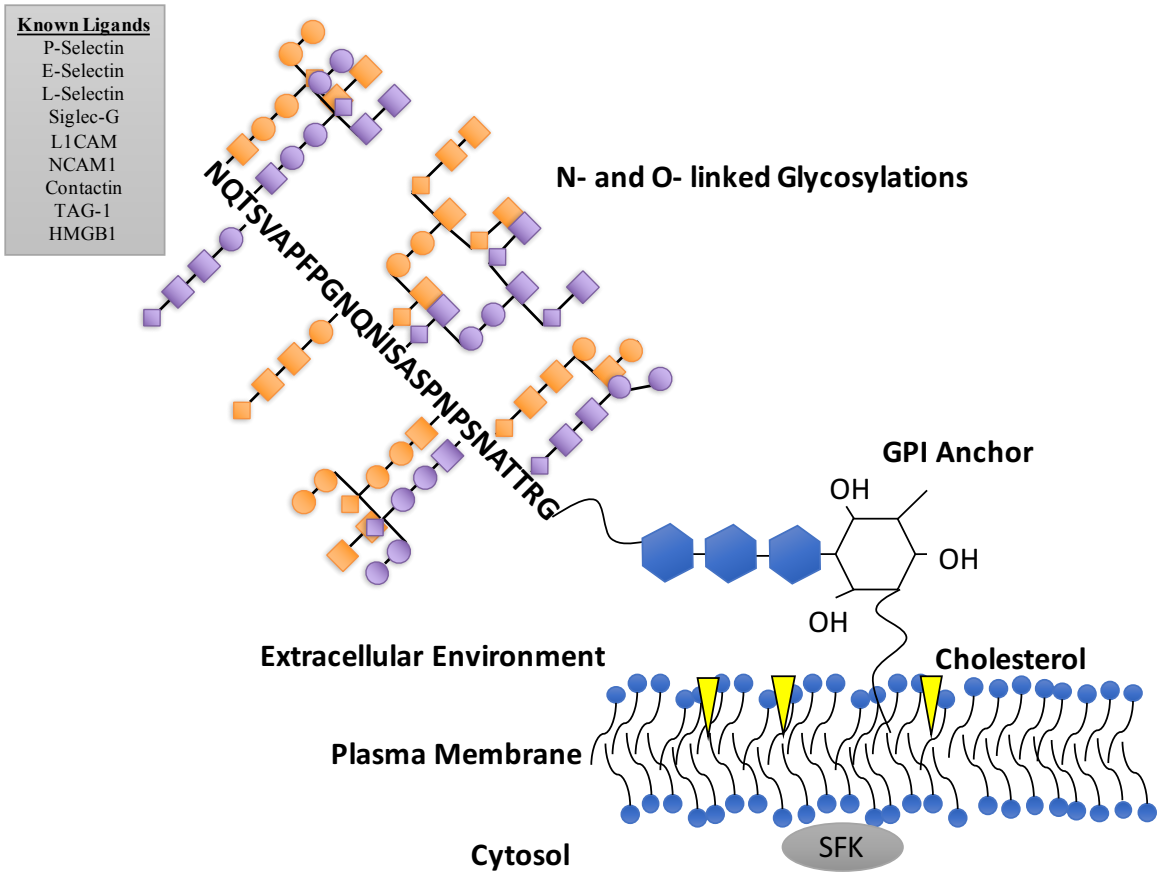

Figure 1.1: Schematic representation of the mature CD24 protein expressed on the cell surface. The consensus sequence of the mature CD24 core peptide across 56 species is shown in black. The conserved potential O- and N- linked glycosylation sites have representative glycosylations shown in purple and orange, respectively. Glycosylations are depicted as chains of carbohydrate monomers but do not represent a specific structure. The glycophosphatidylinositol anchor structure is represented by four hexose carbohydrate rings (blue circles) with a lipid tail inserted into the outer leaflet of the plasma membrane. Cholesterol esters, enriched in lipid raft microdomains are shown in yellow. Src family protein tyrosine kinases (SKFs) are a family of CD24-associated signalling proteins, and the multiple family members are represented by grey ovals. Known *in vivo* and *in vitro* CD24 ligands are indicated in the grey box

size of the peptide, since the peptide core is only 2.7 kDa in size (5). Treatment with sodium hydroxide to strip these O-glycans resulted in additional loss of size, confirming the presence of these O-linked glycans. Subsequently, it was determined that 4 of the 7 potential O-linked residues were glycosylated on erythrocyte-expressed CD24 (16). Stripping O-linked glycosylation also resulted in a loss of binding of the M1/69 mAb, clearly demonstrating that the M1/69 epitope is associated with one of these O-linked glycosylation sites (5). The overwhelming contribution of these glycosylations to the mature peptide size, as well as the strong conservation of the potential glycosylation amino acid residues in the mature peptide, argue that the underlying biological function(s) of CD24 are dependent on these moieties.

1.3 CD24 interacts with a wide variety of cell-specific ligands

One of the first identified roles for CD24 is its ability to modulate cell adhesion events. As previously stated, CD24 is expressed on B cells. Using mAbs, it was shown that blocking or sequestering CD24 restricts the ability of B cells to homoaggregate (17). Subsequently, it was shown that CD24 alters the ability of the integrin very late antigen (VLA-4) to bind to either vascular cell adhesion molecule-1 (VCAM-1) or fibronectin ligands (18). CD24 mediates adhesion in neuronal cells via *in cis* interactions with the L1 cell adhesion molecule (L1CAM), neural cell adhesion molecule (NCAM1) (19), and can also interact with contactin and TAG-1. Thus, CD24 can act as a cell adhesion molecule *de novo*, and can influence the behavior of other cell adhesion molecules.

Functionally, CD24 regulates neuronal outgrowth in a cell-type specific manner. The process of neurite outgrowth involves forming axonal connections between neurons, and is important for the developing nervous system and synaptic remodeling such as is required for learning and memory (20). CD24, via L1, restricts neurite outgrowth in dorsal root ganglia, but promotes outgrowth in cerebellar neurons (21). An overall functional significance of this CD24-mediated activity has not been elucidated, however these brain regions are responsible for processing sensory information, particularly pain (22) and motor activity (23).

CD24 has affinity for the selectin family of adhesion molecules. Leukocyte (L-), Platelet (P-) and Endothelial (E-) selectin have each been documented to bind to CD24 in various contexts (24-26). For example, CD24/P-Selectin binding mediates the binding of monocytes and neutrophils to endothelial cells (24), as well as cell rolling, a process involved in extravasation and metastasis, in the KS breast cancer cell line (27). In MCF-7 breast cancer cells, an *in vitro* assay of cell rolling showed this process is mediated through interaction between CD24 and E-selectin (26). Finally, though modest binding of CD24 to L-selectin is documented, no biological role has yet been identified (24). Based on these previous studies, however, it is reasonable to hypothesize that this interaction may be important for leukocyte cell adhesion, or potentially target cell recognition, or immune cell extravasation.

CD24 interacts *in cis* with a moderator of Toll-like receptor (TLR) signalling, Siglec-G, and *in trans* with the danger associated molecular pattern (DAMP) protein HMGB1 (28, 29). Cells release DAMPs while under physiological stress. These DAMPs promote immune responses to mitigate this stress, or in the event of unrecoverable cell

damage, to promote removal of the damaged cells (30). The DAMP HMGB1 can interact with TLRs on liver-derived DCs to promote inflammation (29, 31). Left unchecked, this leads to sepsis and death (29, 31). The role of Siglec-G is to restrict TLR signalling in response to these DAMPs, however Siglec-G cannot bind them *de novo*. In this case, CD24 acts as an adapter, binding both HMGB1 and Siglec-G, activating Siglec-G and ultimately inhibiting TLR-4 signalling (29). This mechanism of action represents a new paradigm of CD24-based ligand interaction. I have expanded on this idea into a general mechanism through which the cell-specific activity of CD24 may be explained (10). I propose that CD24 acts as a rheostat to properly attune other receptors to extracellular cues. It remains to be seen if this is a generalizable mechanism of CD24 activity, or a tissue-specific function, however I have also suggested a series of testable criteria through which this hypothesis may be evaluated, which is presented in Chapter 5 of this thesis.

A significant outstanding issue is that, in many cases, the tissue-specific ligands associated with CD24 activity have not been identified. For example, the ability of CD24 to regulate B cell survival has been known for nearly 30 years (32), however the endogenous ligand responsible for this activity has not been identified and thus CD24-mediated apoptosis has only been investigated using Ab-mediated stimulation (33). A second outstanding question with regard to CD24-ligand interaction is the tissue-specific nature of these associations. The evolutionary conservation of glycosylation sites in the mature CD24 sequence (13), as well as the substantial physical contribution of these modifications to the mature expressed protein suggests that CD24/environment interactions are mediated through glycans. Furthermore, CD24 is variably glycosylated,

even when isolated from a cell line or homogenous tissue. This variable mosaic of glycosylation may explain how CD24 interacts with different ligands in a cell type- and/or tissue-specific fashion (5, 10, 14, 15). The tissue-specific pattern of CD24 glycosylation points to a mechanism through which these interactions may be directed. By altering the nature and number of CD24 glycosylations, it may be possible for CD24 to selectively interact with ligands contextually. Thus, even though many cells express CD24, they do not necessarily possess equivalent ligand binding capacity and are limited in their ability to mediate specific interactions and events. As the cell-specific ligands of CD24 are largely unknown, even when the activity of CD24 itself has been well characterized, most studies rely on the use of mAbs to mimic CD24-ligand interactions. Considerable effort will therefore be required to identify the natural *in vivo* ligands of CD24 on a cell-by-cell basis.

1.4 CD24 expression and function in the immune system

1.4.1 Hematopoiesis and CD24 expression

All blood and immune cells arise from a common stem cell progenitor, the hematopoietic stem cell (HSC), in a process termed hematopoiesis (**Figure 1.2**). During this process, CD24 is known to be expressed on many of the immature, developing hematopoietic precursor cells, and is only retained once they reach maturity in some cases. This suggests that CD24 may regulate a common biological process or principle in HSC-lineage cells, and that elucidating the behaviour of CD24 in any of these cells may aid in furthering our understanding of its role in this group.

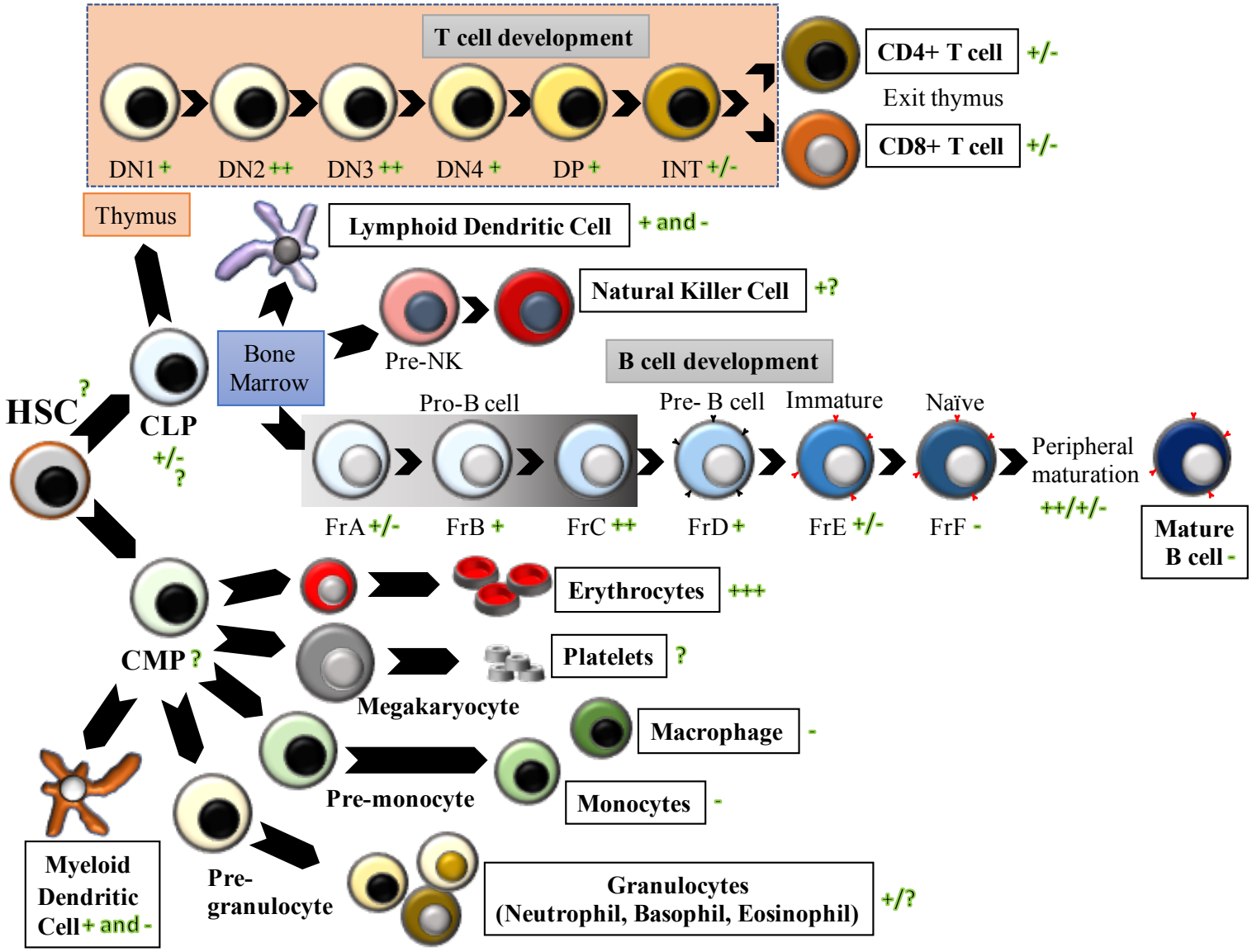
T cell development
DN1 +
DN2 ++
DN3 ++
DN4 +
DP +
INT +/-
CD4+ T cell +/-
Exit thymus
CD8+ T cell +/-
Thymus
Lymphoid Dendritic Cell + and -
Natural Killer Cell +?
Pre-NK
Bone Marrow
B cell development
HSC ?
CLP +/- ?
Pro-B cell
Pre- B cell
Immature
Naïve
Peripheral maturation ++/+/-
FrA +/-
FrB +
FrC ++
FrD +
FrE +/-
FrF -
Mature B cell -
Erythrocytes +++
CMP ?
Platelets ?
Megakaryocyte
Macrophage -
Pre-monocyte
Monocytes -
Myeloid Dendritic Cell + and -
Pre-granulocyte
Granulocytes (Neutrophil, Basophil, Eosinophil) +/?

Figure 1.2: Hematopoietic-lineage cells. Hematopoietic development begins in the bone marrow. HSC = Hematopoietic stem cell, CLP = Common lymphoid progenitor, CMP = Common myeloid progenitor. B cell development is divided into Hardy fractions (Fr) A to F. T cell precursors migrate to the thymus (orange) prior to the double negative (DN) 1 stage. T cell development progresses through DN stages before the double positive (DP) and intermediate single positive (Int) stages. Other developmental lineages of the CLP and CMP are shown in simplified progressions, indicating the first committed progenitor and mature cell form of each cell type. The relative expression of CD24 is indicated with a series of green +. Increasing numbers of + indicate higher levels of expression. A minimal, or relatively low level of expression is indicated by +/-. A question mark (?) indicates no data on expression of CD24 in a given cell type.

Hematopoiesis occurs through the differentiation of long-lived HSCs resident in highly specialized niches. The location of these niches changes throughout organismal development. In early embryogenesis in mammals, HSCs reside in the yolk sac (34). At this time, HSCs only give rise to selected cell types, dominated by the need for red blood cell (RBC) generation to support continuing embryonic development. This is referred to as primitive hematopoiesis. Later in embryogenesis, HSCs migrate into the developing aorta-gonad-mesonephros, seeding the developing aorta (34). In mid-gestation, they migrate further to the fetal liver (35). During this time, HSCs begin generating a wider range of effector lineages. This second wave of hematopoietic differentiation is referred to as definitive hematopoiesis, which may continue throughout an organism's life. Finally, near the end of gestation, HSCs migrate into the red bone marrow of the long bones such as the femur, among other bone marrow niches. By adulthood, hematopoiesis is restricted to a small number of bones such as the pelvis or sternum (36).

The HSC is a multipotent stem cell, capable of giving rise to many distinct effector lineages (37). It first differentiates into one of two oligopotent stem cells, which are restricted to a single effector sub-type. These restricted stem cells are called the common myeloid progenitor (CMP), and the common lymphoid progenitor (CLP) (38). The myeloid lineage ultimately gives rise to the effectors of the innate immune system, erythrocytes (red blood cells) and to megakaryocytes/platelets. The mature cells of the innate immune system are the granulocytes comprising basophils, neutrophils, eosinophils, as well as monocytes/macrophages, and mast cells. Each of these effector cells is generated through a further series of lineage-specific differentiation and

maturation stages from the common myeloid progenitor before the emergence of the mature cell from the bone marrow. In contrast, the lymphoid lineage cells comprise the adaptive immune system and include B, T and Natural killer (NK) cells. Both the myeloid and lymphoid cell lineages can give rise to a professional antigen presenting cell (APC) called a dendritic cell (DC).

1.4.2 CD24 function and expression in myeloid cells

Unlike lymphoid cells, comparatively less is known about the function of CD24 in myeloid cells. CD24 is expressed on neutrophil progenitors, and other granulocytes, but not in monocyte cells (39). Indeed, the use of CD24 expression was proposed as a potential discriminator of the pro-monocyte lineage, which were negative for CD24 expression (CD24-), from the granulocyte lineage. However, it has been found that CD24 appears to be a highly specific and sensitive marker for identifying acute myeloid leukemia, where cancerous, but not healthy, myeloid cells express CD24 (40). However, data from mice suggest that CD24 may in fact be expressed in at least some populations of monocytes, and that it is involved in their P-selectin-mediated adhesion (41). Further studies in granulocyte cells show that CD24 stimulation is capable of triggering caspase-mediated apoptosis in mature neutrophils in a manner consistent with that observed in B cells (42). Overall, there is a dearth of knowledge regarding the expression patterns and the functional consequences of CD24 in cells of myeloid origin.

1.4.3 CD24 expression in lymphoid cell development

The CLP gives rise to the effectors of the adaptive immune system, and CD24 has been most extensively studied during the differentiation, maturation and functioning of these effectors **(Figure 1.2**). Early in differentiation, the CLP first becomes lineage restricted into either immature DCs, progenitor (pro-) B cells or early double negative (DN) T cells. Comparatively little is known about the subsequent process of DC development, and upon maturity they are divided into at least two groups, by their expression of CD8, or lack thereof (43). It is known that these groups are not completely independent, and differentiation of CD8- to CD8+ DCs requires expression of CD24 (44), however its role is unknown. Other studies have demonstrated that CD24 is functionally important for mature DCs in directing immune responses, as will be described in section 1.4.4.

In contrast, B and T cell development has been exhaustively detailed, and more is known about roles for CD24 in these cells. B cells, like all cells of hematopoietic origin, are generated from HSC fate commitment through a highly coordinated, and well-defined differentiation process. This development occurs in the mammalian bone marrow during definitive hematopoiesis. Functionally, B cells are defined by their expression of the B cell receptor (BCR). Functionally, the BCR is activated via its ligation with soluble or particulate foreign material (usually protein), termed antigens (Ags). With co-stimulation via receptors such as CD40, this results in B cell activation and the production of antibodies (Abs) which bind and neutralize these Ags, and can recruit other immune effectors during immune challenge.

Unlike other proteins, there is not a single gene that encodes for the heavy and light chains of the BCR. Instead, gene segments comprising the immunoglobulin (Ig) gene loci are selectively rearranged together to form the final product (45). The mature receptor is a heterodimer composed of two identical heavy chains, generated from the heavy chain loci, termed IgH, each linked by disulfide bonds to two identical light chains called IgL, (**Figure 1.3**). Each heavy and light chain pair is anchored to the plasma membrane via a short transmembrane/intracellular domain. The BCR is partnered with a co-receptor heterodimer, CD79α and β (46). These co-receptors contain signaling domains called an immunoreceptor tyrosine-based activation motif (ITAM). This domain is responsible for initiating signal transduction from the BCR into the cytoplasm.

The earliest developing B cells are termed progenitor (pro-) B cells (**Figure 1.2**). At this stage of development, IgH rearrangement occurs. The IgH locus consists of 3 gene segments, termed Variable (V), Diversity (D), and Joining (J) responsible for the creation of the antigen binding domain, with a fourth region called the Constant (C) domain (47). Multiple alleles of each V, D and J segment exist to permit the generation of a diverse repertoire of BCRs in the B cell population. Rearrangement first occurs between the D and J segments, followed by the V segment. The VDJ chain is then linked to one of 5 C domains, termed Alpha (IgA), Gamma (IgG), Delta (IgD), Epsilon (IgE) or Mu (IgM) (47). Simultaneously, a surrogate light chain (SL) is also generated. At the end of pro-B cell development, the IgH and SL chains are linked via disulfide bonds in a manner like the association between IgH and IgL in the mature BCR. This IgH/SL complex is referred to as the pre-B cell receptor. (48). Expression of the pre-BCR on the plasma

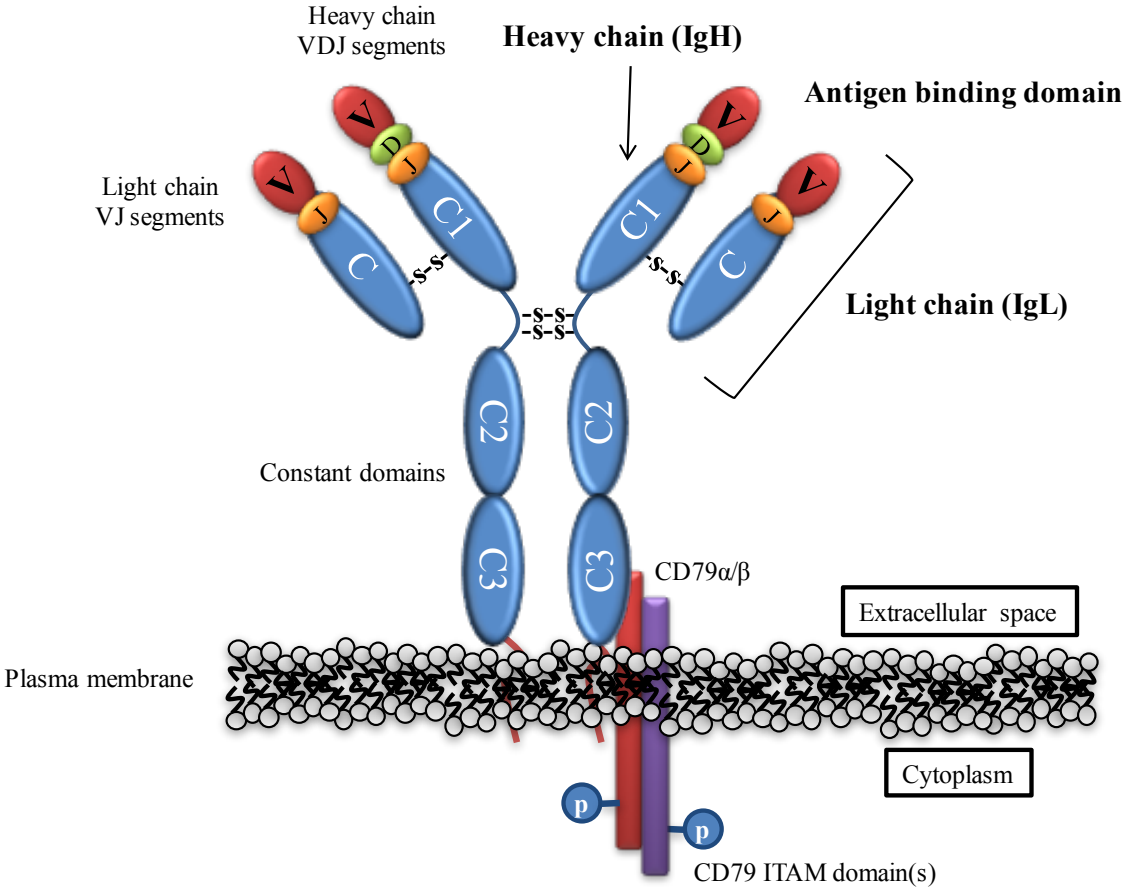

Figure 1.3 The B cell receptor. The mature B cell receptor (BCR) is comprised of a heterodimer of two heavy chains (IgH) and two light chains (IgL) with the associated CD79α/β heterodimer signalling partner. The IgH domains contain a small transmembrane domain. The V, D, and J segments of the antigen binding domains in the IgH and IgL chains are shown in red, green and orange, respectively. The constant domains (C) of IgH and IgL are shown in blue. The CD79α/β co-receptors, with associated ITAM domains are indicated.

membrane of the developing cell denotes the transition from the pro- to pre-B cell stage (**Figure 1.2**). Functionally, the pre-BCR is responsible for transducing pro-survival signals (49). However, this signalling occurs at a lower level than occurs following B cell activation via antigen binding. B cells undergo a developmental checkpoint at the pro- to pre-B cell transition whereby overactive pre-BCR signalling results in apoptosis, to prevent the generation of auto-reactive B cells (50).

During the pre-B cell development phase, rearrangement of the IgL gene segments occurs. Unlike IgH, the IgL antigen binding domain is composed of only the V and J gene segments, with their own antigen binding domain (47). Following successful rearrangement, the IgL and IgH chains are linked, and expressed on the cell surface. These cells are termed immature B cells (48, 51). After bone marrow development, naïve B cells leave the bone marrow for the periphery. These B cells simultaneously express IgM, and to a lesser degree IgD-class BCRs. Upon antigenic stimulation in the periphery, B cells become restricted to expressing a BCR of a single isotype. This process is termed class switch recombination (CSR). Due to the arrangement of the C domains, IgM and IgD may be expressed in a single cell via alternative RNA splicing. Switching to either IgG, IgE or IgA (in that order) requires the induction of DNA recombination via enzymes such as Activation Induced Cytidine Deaminase (AICDA) and the removal of upstream C domains from the genome, resulting in a permanent switch to a new BCR isotype (52). The generated Ab will also share this fate and B cells may switch to additional downstream C isotypes. B cells will thus express a BCR which may have any one of the 5 C domains, but each cell will generate a single BCR (46). Which of the C isotypes is expressed is dependent on the activity of cytokines including interleukin (Il)-4, Il-10 and

Il-6 (53). These activated B cells also produce soluble antibodies that are derived from the same rearranged IgH and IgL genes, but lack the transmembrane domain and are thus released into the extracellular environment.

The stages of B cell development were further refined using single-cell analysis via flow cytometry (54). The gain and loss of specific cell surface receptors and proteins, including CD24, during each developmental phase were used to classify cells into groups called Hardy fractions. Following commitment of HSCs to CLPs, the first three Hardy fractions represent the Pro-B cells (**Figure 1.2**). The earliest committed B cells acquire expression of the first pan-B cell marker, B220 and are termed Hardy fraction A. Hardy fraction B cells retain B220 and gain expression of CD24. Finally, Hardy fraction C cells increase their level of CD24 expression and acquire BP1/Ly56. Hardy fractions A, B and C all express CD43, which progressively declines as maturation continues. A sub-population of cells, termed Hardy fraction C', express the highest levels of CD24, and become bone marrow stroma-contact independent. When the pre-BCR is expressed, cells enter Hardy Fraction D as Pre-B cells. At this stage, CD24 expression declines, and continues to fall in subsequent Hardy fractions until it is expressed at low levels, if at all, by the end of bone marrow development. Immature, BCR expressing B cells are termed Hardy fraction E. Finally, freely circulating (naïve) B cells are termed Hardy fraction F.

CD24 is also expressed throughout T cell development (13). Unlike B cells, T cells mature primarily in the thymus. Analogous to B cells, T cells are defined by their expression of the T cell receptor (TCR), which is generated from rearrangement of the either the TCR-α and TCR-β gene segments, or in a minority of cells, the TCR-γ and

TCR-δ gene segments (55). Thymic T cell development is a process by which cells are educated to respond to foreign antigens without responding to endogenous proteins, only in the context of specific antigen presentation proteins called the Major Histocompatibility Complex (MHC) (55). Mature T cells are sub-divided based on expression of one of two mutually exclusive co-receptors, CD4 or CD8 (56). Acquisition of these co-receptors is used to differentiate T cell developmental stages. In the earliest four phases, double negative (DN1-4) cells do not express either CD4 or CD8, however CD24 is present on these cells. An intermediate, CD8 single positive phase is followed by the CD4/CD8 double positive (DP) stage (55). CD24 expression is mainly confined to these earlier developmental stages and is used as a marker for distinguishing the DN stages (57). At this point, T cells are selectively directed into either the CD4+ or CD8+ effector lineages and expression of the other receptor is lost. During this final commitment stage, CD24 expression declines and does not re-appear in T cells unless they are activated in an immune response.

1.4.4 CD24 is an important regulator of B cells

In addition to mediating B cell adhesion, CD24 is a potent negative regulator of pro-/pre-B cell survival and can alter the activation of mature B cells in the spleen. Ab-mediated engagement of CD24, using the M1/69 mAb, is capable of inducing apoptosis in isolated mouse bone marrow pro-B cells in a dose-dependent fashion (33). As Ab have two identical antigen binding domains, a single M1/69 Ab can interact with at most two CD24 molecules. However, the effect of Ab-mediated CD24 stimulation can be

potentiated by incubating the M1/69 Ab with a secondary Ab that enhances the ability to cross-link multiple CD24 molecules on the cell surface. The ability of Abs to induce apoptosis definitively requires engaging multiple CD24 molecules simultaneously, as treatment with a monovalent Ab fragment, containing only a single binding domain, had no effect on B cell apoptosis (33). Thus, the induction of CD24 apoptosis likely requires surpassing a signalling threshold involving the activation of multiple CD24 molecules on the surface. Mature B cells are insensitive to the apoptotic signal transduced by CD24, however they are rendered unable to respond to pro-proliferative stimulation (33).

The ability to induce cell death is also mediated by the anti-CD24 mAb 20C9. It is unknown if these Abs bind to unique, or overlapping epitopes. Therefore, identifying the various CD24 mAbs binding regions should be a future study to determine if CD24-mediated apoptosis is a universal response or is dependent on specific mAb/CD24 (and thus CD24/ligand) interactions.

The *in vivo* activity of CD24 to modulate B cell survival was examined through the creation of a whole body CD24 knockout (CD24 KO) mouse (58) and a lymphocyte-specific CD24 over-expressing transgenic (CD24 Tg) mouse (32). In CD24 KO mice, B cell development is disrupted at the pro- to pre-B cell transition stage (58). Compared to wild type (WT) mice, the absence of CD24 causes a loss of approximately 50% of the late pro-B cell (Hardy fraction C to D) population. Curiously, no losses were observed in either earlier or later B cell fractions, and the numbers of mature circulating B cells and plasma concentrations of Ab were not significantly different between CD24 WT or KO animals (58). This indicates that this developmental block is not absolute, or that the loss

of CD24 expression may be compensated for in B cells through other mechanisms such as increased proliferation at later stages of B cell development.

Unlike the CD24 KO mice, which have a total-body loss of CD24 expression, the CD24 over-expressing transgene is under the control of the TCR Vβ promoter, meaning it should only be active in thymocytes (T cells) and the hematopoietic T cell progenitors. However, this transgene is also active in B cells; potentially because B and T cells share a common hematopoietic lineage. The insertion of the CD24 transgene resulted in a 41% increase in CD24 expression in early (Hardy Fraction A) pro-B cells, a 23% increase in expression within late pro-B cells, and a 20% increase in pre-B cells but did not result in any increases in the immature B cell population. These CD24 Tg mice exhibited a loss of approximately 50% in the pro- and pre-B cell bone marrow fractions compared to WT controls. Unlike CD24 KO, however, immature, naïve populations of B cells were also reduced by approximately 25% in CD24 Tg mice (32) . Subsequently, this loss of B cells was shown to be the result of their increased apoptosis rather than a defect in hematopoiesis. Interestingly, CD24 Tg mice exhibit a loss of immature T cells at the CD4/CD8 double positive stage, but not in the earlier double negative phases (59). As previously discussed, CD24 expression can be highly dynamic. In combination with the data generated via CD24 KO and CD24 Tg mice, it is apparent that the function of CD24 is closely tied with the level and timing of its expression, and that an alteration of either of these parameters has a dramatic effect on its function in lymphocyte populations in general, and B cells, in specific.

Subsequent studies used human and mouse cell lines *in vitro* to determine mechanistic elements of CD24-mediated B cell apoptosis. Following on the work of

Chappel, *et al.* (1996), several studies have established a reproducible method for inducing apoptosis in multiple cell lines using primary anti-CD24 mAb pre-incubated with secondary Abs to form multimeric Ab complexes that enhance CD24 crosslinking and stimulation (33). Several primary anti-CD24 Abs have been used, including M1/69 and ALB-9 in mouse cell lines, or L30 in human cells (60-62). Multiple cell lines of different developmental stages have been examined, including: human Burkitt's lymphoma P32/SH and Namalwa cells (61); human Pro-B cell lines NALM-16, NALM-20, NALM-27, LC4-1 and KM-3; human Pre-B cells NALM-6, NALM-17 and P30/OHK (62); and mouse *ex vivo* primary B cells (33, 60). My own analysis, presented here in Chapter 3 demonstrates the WEHI-231 B cell lymphoma cell line to be sensitive to CD24-mediated apoptosis (60), further demonstrating that CD24-mediated apoptosis is not a result of a specific culture or experimental design, but is rather a global aspect of CD24 in B cell biology.

1.4.5 Functions of CD24 in T cells and DCs.

The ability of CD24 expressed on B cells to act as a co-stimulatory molecule for CD4+ T cells was among the first functions identified for CD24 in immune cells (63). In this case B cells acted as antigen presenting cells for CD4+ T cells. B cells presented antigens for TCR stimulation via MHC, and CD24 was responsible for providing a co-stimulatory signal. Blocking CD24 on B cells using the mAb 20C9 prevented this co-stimulation, indicating that CD24 interacted with an unknown partner on the T cell surface. Furthermore, while mature T cells generally lack CD24 expression, its

expression is transiently induced during CD4 and CD8 T cell activation. (64). When stimulated on these cells, it can also enhance proliferation in response to TCR and co-receptor stimulation. These data together showed that CD24 can act both *in cis* and *in trans* to promote T cell proliferation in response to activation.

Independent of their activation, T cells undergo a process called homeostatic proliferation required to maintain T cell numbers while at immunological rest (65). In addition to supporting T cell activation, CD24 is also known to regulate homeostatic proliferation of these cells (66, 67). Unlike in activated T cells, CD24 negatively regulates homeostatic proliferation signalling to restrict T cell growth. Without CD24, T cells rapidly proliferate *in vivo*, resulting in the death of their host mice (67). Interestingly, the ability for CD24 to restrict homeostatic proliferation was not dependent on being directly expressed on the T cells. Instead it could also operate *in trans* if expressed on DCs. This result strongly suggests that CD24 acts through an *in cis* partner on the T cell plasma membrane and can be acted upon *in cis* in CD24-expressing T cells, or *in trans* via DCs.

CD24 expressed on DCs is involved in regulating the induction of immune responses. As described in section 1.3, CD24 in partnership with Siglec-G is a negative regulator of DAMP-induced sepsis and is also a negative regulator of graft-versus-host (GVH) disease (68). When expressed on T cells, CD24 may be stimulated *in trans* via Siglec-G expressed on DCs. This interaction selectively inhibits T cell responses to the graft tissue. In the absence of Siglec-G on DCs, CD24-expressing T cells exhibit increased activation, leading to a shorter graft survival time (68). This response is contradictory with the pro-activation stimulatory effect CD24 during immune responses,

but may be explained by the potential for different *cis* interacting partners. CD24/Siglec-G signalling is consistently associated with the restriction of T cell activation; thus, it is possible that the pro-proliferative effect is mediated through a different partner.

Together, these data clearly show that CD24 is an important regulator of the immune system through selectively regulating T cell proliferation and activation, and altering DC-mediated immune activation.

1.5 Signalling in response to CD24 stimulation

Over a period of nearly 30 years, many studies, across diverse fields, have elucidated many aspects of CD24-mediated signalling, and its ability to affect cellular processes. Among the first evidence of CD24's signal transduction capability was demonstrated using human chronic lymphoblastic leukemia B cells. When stimulated using the mAb anti-CD24 VIBE3, no stimulation occurred, however enhancing CD24 crosslinking by treating cells with a goat-anti-mouse secondary Ab induced a modest increase in free intracellular calcium, as occurs during CD19 stimulation and B cell activation (8). Similarly, stimulation of CD24 on neutrophils via the same VIBE3 anti-CD24 primary and goat-anti-mouse secondary Ab also results in calcium flux (19) and can induce activation as indicated by a respiratory burst (8).

A series of studies elucidated several plasma membrane-proximal mediators of CD24 signaling. First, in the human small cell lung cancer cell lines SW2 and K562, CD24 was shown to be associated with the Src family tyrosine kinases (SFK) (69). The SFK proteins share a conserved SH2, SH3 and tyrosine kinase domains. The family

consists of 9 members; blk, fgr, fyn, hck, lck, lyn, src, yes, and yrk (70). Biologically, these proteins are involved in cytoplasmic signal transduction from associated transmembrane signalling receptors and mediate events such as cell adhesion, migration, and lymphocyte activation. Whereas their dysregulated activation is a mark of cellular transformation during cancer development (70). The association of CD24 with the SFK members appears to be cell specific, with SW2 showing an association with c-fgr, and lyn in K562 cells (69) while B cell lymphomas showed a signalling and physical association between CD24 and the SFKs lck, hck and lyn, but not fyn (71). An association between CD24 and lyn was shown in human Burkitt's lymphoma cells (61) whereas CD24 is associated with src in the MTLy breast cancer cell line (72). Collectively, these studies show that CD24 signals through multiple members of the Src family proteins.

Downstream from these proteins, CD24 is associated with a number of signalling intermediates that transduce multiple cellular outcomes. As a function of its induction of B cell apoptosis, CD24 induces a transient, but robust activation of the ERK1/2 mitogen activated protein kinase (MAPK), and a sustained activation of the p38 MAPK (62). The activation of p38 was necessary for the CD24-mediated progression of apoptosis, as inhibition of p38 via SC68376 abrogated its effect. The downstream cell death pathway was dependent on activation of multiple caspases, including Caspase 2, 3, 7 and 8 (62). Curiously, co-ligation of CD24 and the BCR did not promote B cell apoptosis at optimal concentrations for either antibody used independently, however sub-optimal antibody stimulation of both CD24 and the BCR simultaneously was capable of inducing B cell apoptosis. The nature of the association between CD24 and the BCR remains unknown.

Unlike the situation in B cells, CD24 signalling *promotes* colorectal cancer proliferation and survival through p38 signalling (73). Further clouding this issue, CD24 is capable of inducing apoptosis in DN and DP thymic T cells, however this process is caspase independent (74). The CD24 apoptosis pathway in these cells was independent of other death inducing receptors, such as Fas and tumor necrosis factor receptor (TNFR). Instead, this apoptotic program was mediated through the loss of the Bcl-2 pro-survival proteins in the mitochondria, a loss of mitochondrial membrane integrity and their release of pro-apoptotic components (74). Finally, in *ex vivo* human neutrophils, mAb stimulation of CD24 likewise induces apoptosis in a time-dependent fashion (42). In these cells, apoptosis occurs through mitochondrial membrane depolarization, as evidenced via fluorescent imaging, and requires the activation of caspases 3 and 9. It was also shown in these cells that CD24 expression was strongly influenced by stimulation with lipopolysaccharide (LPS), heat killed bacteria, or with the pro-inflammatory cytokines TNF-α, IFN-γ, or GM-CSF. By itself, IL-1β did not affect CD24 however in combination with sub-optimal TNF-α or IFN-γ, increases in CD24 expression were also observed. CD24 was down-regulated in neutrophils from sepsis patients, leading to a reduction in neutrophil apoptosis potentially indicating a role for CD24 in regulating the duration or intensity of the neutrophil response (42).

As CD24 is GPI-anchored, it does not possess transmembrane signalling potential, and must therefore operate through additional signalling intermediates on the plasma membrane. While there is ample evidence of the intracellular signalling intermediates influence by CD24, little is firmly established with regard to these

membrane-associated partners. The previously discussed associations between CD24 and L1, Siglec-G and integrins remain the only known membrane interactors. Thus, future studies will be required to better elucidate these partners. Furthermore, the ability for CD24 to interact with a variety of the SFKs means there are many potential combinations of cell-type specific CD24 signalling 'networks' which may be generated.

1.6 Extracellular vesicles (EV)

1.6.1 The identification, classification and biogenesis of EV subtypes

Extracellular vesicles (EVs) refer to the heterogeneous collection of membrane-enclosed structures that are released by cells. After their first identification in 1946, EVs were frequently discounted as cellular debris without a definitive biological function. Indeed, they were first named as 'platelet dust'. It was not until 1999 that researchers determined that this platelet dust was composed of several different vesicle subtypes, and that these structures mediated functions such as platelet aggregation and procoagulant activity. Subsequently, it was discovered that most, if not all, cells release EVs with varying compositions of proteins and nucleic acids and that they participate in numerous physiological processes. EVs are now broadly categorized, based on their size, morphology, mechanism of biogenesis, as well as their overall protein, lipid, and nucleic acid composition, into one of three major classifications: exosomes, microvesicles, or apoptotic bodies.

Exosomes are the smallest EV subtype, ranging in size from 30 to 100 nm. Unlike the other subtypes of EVs, exosomes are stored in the cytosol within structures called

multivesicular bodies (MVB) (75). The MVB is a cytosolic organelle that forms from invagination of the plasma membrane (PM) to form a vesicle called an endosome via endocytosis (76). During this invagination, proteins resident in the PM are internalized within the endosome. The resulting vesicle has an inverted topology from the original plasma membrane. Proteins internalized via endocytosis may be directed into multiple fates. Upon fission from the PM, endosomes are termed early endosomes. From here, they may be selected for recycling back to the PM (called a recycling endosome), exchange cargo with the trans-Golgi network (called a late endosome), or be selected for proteolytic degradation by fusion with a lysosome (77). In the early endosome, continued invagination results in the formation of smaller vesicles that remain inside the endosomal lumen. Additional small trans-golgi vesicles may also enter the endosome at this time. The accumulation of these smaller vesicles defines the formation of the MVB, with the interior vesicles referred to as exosomes. Release of exosomes from the MVB involves the early endosome re-fusing to the PM and discharging the exosomes into the extracellular space via exocytosis.

The selection of proteins for endocytic internalisation is incompletely understood, but thought to involve protein ubiquitination (76). Proteins appear to be selected for internalization via mono- or low-number ubiquitination, as opposed to polyubiquitination, which is associated with lysosomal degradation (76). However, there are also ubiquitin-independent selection mechanisms as well (78). Once ubiquitinated, these proteins are recognized by endosomal-sorting complex required for transport (ESCRT) proteins. Organization of the membrane components is thought to be mediated by tetraspannin proteins as well. These include CD63, CD9 and CD81, which have been

suggested as non-exclusive markers of exosomes (75, 79). During protein sorting to endosomes destined for MVB formation, PM-resident proteins are bound by ALIX and syntenin (80). These adapters redirect the ESCRT-mediated endosome formation from the lysosomal degradation pathway and towards MVB formation.

The direction of endosomes into their various fates is also regulated through the activity of Rab GTPases (81). The Rab family of proteins consists of over 60 members and it is thought that specific Rabs, or combination of Rabs, on the surface of vesicles is used as a protein sorting system within the cell (82). The Rab proteins act as adapter molecules to co-ordinate the activity of various cytoskeletal binding proteins, adapter proteins, and intracellular motors. GTP-bound Rab is recognized by Rab effector proteins, which serve as the linkers to the vesicle transport machinery (83). Inactivation of Rab by GTPase activity, either through auto-hydrolysis or via the action of Rab GTPase activating proteins (RabGAP) results in the loss of Rab-effector binding and serves as the "stop" signal during trafficking (81). Vesicle internalization is known to be regulated via Rab13, Rab21 and Rab5 (with potentially others). Direction of early endosomes into the late endosome occurs via Rab7, as does transition to the lysosome. Exocytosis, however is mediated through Rabs 14, 11, 25 and 27 (81-84).

Exosome production was first described during the process of reticulocyte maturation into mature RBCs. Here, cytosolic and membrane components, such as the transferrin receptor are packaged into exosomes within MVB for release as a means to removing components of the cell that are not necessary for RBC function (85). Ongoing research has since shown that exosomes are also involved in immune signal modulation,

antigen presentation, hemostasis and even act as transforming vectors during carcinogenesis (86, 87).

The next major category of EVs are microvesicles (MVs), which are distinguished from exosomes by their direct budding from the plasma membrane, with no cytosolic biogenesis or storage intermediates. On average, MVs tend to be larger, but more heterogeneous than exosomes, ranging from 100 to 1000 nm. The identification of MVs as a discrete EV population is relatively recent, with the recognition that platelets produce distinct EV populations which have distinct compositions: one from the surface and the other from the cytosol (88). Unlike exosomes, MV budding occurs via outward PM movement. MV biogenesis is thought to be associated with cholesterol-rich regions of the PM called lipid rafts (87, 89). MV are highly enriched in negatively-charged phospholipids, most notably phosphatidylserine (PS) (90). Whereas cells normally sequester PS to the inner leaflet of the PM, MVs are enriched for these lipids on their outer surface (75). This translocation has successfully been exploited as a potential biomarker of MVs through detection of PS with proteins like Annexin V or Lactadherin (88, 91).

The mechanism of formation is the major distinguishing feature between exosomes and MVs. Several studies have noted that cell surface receptor clustering, such as performed by the anti-CD24 antibody stimulation method described in this thesis, is frequently associated with MV formation (92). Canonically, MV biogenesis begins via calcium influx following receptor stimulation, to activate calpain (93). Calpain, does not act against a specific protein substrate but instead targets selected amino acid sequences present in any protein for cleavage. Among its targets are cytoskeletal and cell adhesion

proteins, including cadherins and actin organizational proteins (94). Thus, this calcium influx and calpain activation can render areas of the PM more fluid through the loss of these rigid structures. This process is not necessarily dependent on calcium/calpain as other proteins can selectively remodel the actin cytoskeleton such as the Arp2/3 complex and cofillin (95). Thus, it is likely that MV formation can also be induced through calcium-independent means.

During the process of membrane outward budding, the intrinsic organization of the PM is altered. PS is translocated from the inner to the outer leaflet of the PM under the guidance of the floppase enzyme (75, 90). The re-distribution of membrane charge and composition appears to be the driving force for outward membrane bending (90). Unlike exosomes, the organization of the membrane occurs, at least partially, independent of ESCRT activity (92). Following membrane budding, membrane scission occurs under the direction of small GTPases such as ARF6 (96). Related to the Rab proteins, ARF6 signalling recruits Erk to the PM, which subsequently recruits the molecular motor myosin light chain kinase (96). These, and likely other proteins that have yet to be identified, ultimately separate the MVs from the cell body.

The biogenesis of MVs has drawn parallels with viral shedding (97, 98), suggesting these processes may be evolutionarily related or that virus budding is a specialized form of MV release. Both viral and MV budding occur directly from the plasma membrane through disruption of the intrinsic membrane topology. Unlike MV budding, viral budding occurs under the direction of the Gag protein. In common, however, both MV and viral budding do not require the full ESCRT complex, but only recruit specific components (99). Functionally both MVs and viruses are capable of

transporting material that can induce cellular transformation in recipient cells, which is suggestive of a common biological functioning principle (98). Thus, it is possible that the process of MV biogenesis using intrinsic host proteins and DNA may have been co-opted evolutionarily by viruses. Future studies are required to further elucidate the functional and physical relationships between these processes.

Several studies and data presented in chapter 4 of this thesis also strongly point toward an active process driving cargo incorporation or exclusion in MV membranes rather than a random incorporation (100-103). MV composition is heterogeneous, and heavily dependent on the cell of origin (97, 104). The first evidence demonstrating selective compositional organization identified that the lipid composition of neutrophil EVs is enriched for cholesterol, diacylglycerol while maintaining consistent proportions of other phospholipids, relative to the cell PM (105).

The first MV protein sorting mechanism identified involves the selective inclusion of proteins with specific PM anchors, including myristoylation, phosphatidylinositol binding domains, prenylation and palmitoylation (100). These targeting specificities were identified by creating fusion proteins with C-terminal amino acid sequences to direct specific post-translational modification. The addition of unique post-translational modifications via these sequences to the C-terminal of proteins could selectively sort proteins to areas of MV generation on the PM. In contrast, specific site-directed mutagenesis to prevent this post-translational modification could abrogate the selection of proteins for MV incorporation. Interestingly, the inclusion of different post-translational modifications had different sorting efficiencies, ranging from 100% MV inclusion for myristoylated and palmitoylated proteins, to approximately 30% for

phosphatidylinositiol-binding domains, and 15% for prenylation (100). This strongly suggests that MV sorting is under the direction of multiple mechanisms, or that multiple domains within a protein may be required for efficient trafficking. The authors noted that the most efficient sorting tags were used by retrovirus budding and recognized the Gag protein, further suggesting a link between MV budding and virus release.

There is also evidence that extracellular post-translational modification is a determinant for EV-protein incorporation. In this case, proteins with modifications of N-linked glycans such as high mannose polyactosamine (Poly-LacNAc) and α2,6 sialic acids are preferentially incorporated into EVs (101). As with the previous example, manipulation of these glycosylations results in differential protein selection for EV release. The surface receptor EWI is intrinsically glycosylated with three N-linked chains, and present in EVs released from SK-Mel-5 human melanoma (101). When de-glycosylated on these N-linked residues using either glycosylation inhibiting enzymes, deglycosylases, or via mutation of the appropriate amino acids, incorporation of EWI into EVs was lost without loss of other EV-incorporated proteins (101).

Evidence for an mRNA sorting mechanism has also been identified. In this case, cells and EVs were shown to have differential inclusion of mRNA species (102). In the mouse liver cell line MLP29, mRNAs with a 12-nucleotide targeting sequence were selectively enriched in EVs when compared to the cell of origin. This sequence was enriched in the 3' UTR of nearly 40% of EV transcripts and forms a stem-loop structure (102). Incorporation of this sequence into other transcripts also induced their enrichment into EVs. Other studies have suggested a similar "mRNA zip code" of 25 nucleotides that

incorporate the miR-1289 binding site and are capable of promoting inclusion of transcripts into MVs (103). Taken together, these data strongly suggest that the packaging of EVs, and MVs in particular, is not a random process but a carefully regulated event, and further indicates that EVs are generated to mediate specific cell-specific processes.

The third type of EVs are apoptotic bodies. These EVs are distinct from exosomes and MVs in that they are not actively produced by viable cells, but are generated during apoptosis in a process called membrane blebbing. They are typically substantially larger than exosomes or MVs, and range in size from 1 to 5 μm (106). They may be formed via the breakup of the cell body in the execution phase of apoptosis (107), or through a recently-identified mechanism where cytoplasmic protrusions extend from the cell and bud off in a 'beads-on-a-string' formation (108). Apoptotic bodies tend to be short-lived *in vivo*, as they are rapidly removed by scavenging cells, such as macrophages (107). Functionally, these EVs are generated to prevent the release of harmful cytosolic contents into the extracellular environment during the cell death process, and potentially damaging neighboring cells (109). The larger size of apoptotic bodies allows them to incorporate cellular contents, such as nuclear material or organelles, which cannot be accommodated in smaller EVs. The initial stages of apoptotic body formation are similar to those of MVs in that the scramblase enzyme, functionally related to the flippase and floppase enzymes, induce PS redistribution to the outer leaflet of the PM (110). This membrane asymmetry is used by circulating immune cells to identify apoptotic cells and to initiate their clearance (111). While the precise recognition receptors for apoptotic cells and bodies by macrophages, and other cells, are completely characterized, evidence suggests that recognition involves recognition of N-glycosylated proteins on the apoptotic cell or body

and sialic-binding proteins, such as Siglec-1 (CD169) on immune cells (111, 112). As apoptotic bodies are generated during the execution-phase of regulated cell death, they are frequently termed cellular debris. As such, comparatively less has been established about their biological roles, or the physiological consequences of their interaction with other non-apoptotic cells.

1.6.2 EVs participate in numerous biological processes

1.6.2.1 EV functions in healthy cells

Ongoing research has identified EVs as important mediators of numerous processes in both healthy and diseased states, and has identified their potential utility as therapeutic tools. EV production may be ubiquitous as they have been identified as being generated from numerous cell types and isolated from virtually all body fluids (113). Thus, the use of EVs to influence their environment likely represents an intrinsic behaviour of cells. The manners by which EVs can affect recipient cells are not limited to a single mechanism, as delivery of cargo proteins, cell surface receptors, mRNA, miRNA and potentially other transcripts such as long non-coding RNA (lncRNA) have each been documented to influence recipient cells. Ultimately, the effect of EVs on cell behaviour appears to be highly dependent on their cell of origin.

Among the earliest studied functions for EVs are their role in modulating clotting responses to regulate coagulation and haemostasis. EVs released by platelets carry coagulation-modulating factors, including Tissue Factor (TF) and PS, which promote platelet aggregation (88, 113). These EVs may circulate freely through the blood, and

following a loss of haemostasis, be released by cells at wound sites to promote clot formation. However, these EVs can also restrict clotting through inactivation of clotting factors. For example, EVs can induce clotting factor V inactivation through active protein C or inhibition of Tissue Factor (114), possibly as a mechanism to prevent excess clot formation, which is of interest to research on obstructive arterial disease.

During immune challenge, EVs are known to act as regulators of antigen presentation, cellular activation and survival, or to induce immune tolerance to antigens. As early as 1996, it had been established that activated B cells release MHC-II bearing exosomes as a mechanism for antigen presentation and inducing immune responses (86). It is now understood that EVs can alter immune activation via APCs such as DCs and B cells through a variety of means. For example, cytomegalovirus infects endothelial cells, which in turn release EV-bearing viral antigens. These EVs can interact with MHC-bearing APCs *in vitro*, and allow for the activation of CD4+ T cells (115). Furthermore, it is possible for EVs to directly activate T cell responses. Here, APC-generated EVs selectively incorporate MHC-I-bound antigens, along with the ICAM cell adhesion molecule and the B7 T-cell costimulatory molecule. Binding of these APC-derived EVs can induce the activation of CD8+ cytotoxic T cells (116). The classical paradigm of immune activation requires the direct interaction of APCs with immune effectors in areas of high lymphocyte density, such as lymph nodes. These findings suggest it may be possible to elicit immune responses more systemically. These data may also be of interest in studies on immune function in areas of immune privilege, such as the brain, cornea or in tumours. EVs can cross physical barriers, like the blood brain barrier (117). Thus, in cases of traumatic injury or malignancy, EVs maybe capable of generating immune

responses that would otherwise not be possible due to the inability of immune effectors to directly interact with the tissue.

EVs do not necessarily transduce pro-activation signals in immune cells. As opposed to APC-derived EVs, those released directly by activated T cell effectors appear to be inhibitory, or even pro-apoptotic. For example, leukemic T and B cells may release the MICA/B, ULBP1 and ULBP2 ligands of the NKG2D receptor via exosomes (118). NKG2D is an activating receptor on NK cells, and promotes the recognition and destruction of malignant or infected cells (119). The secretion of NKG2D-ligand bearing exosomes by these cells acts via steric inhibition to prevent NKG2D-mediated NK cell activation by the leukemia cells, thus functioning as a decoy to prevent NK cells from destroying the tumour cells (118). T cells also release Apo2 and Fas-ligand via MVs to induce apoptosis in nearby T cells as a mechanism of immunomodulation (120). T cells may even be competitively inhibitory by altering the survival of APCs. Activated CD8+ T cells release exosomes bearing T cell receptors with their recognized antigen, and Fas-ligand. These exosomes can bind to antigen-bearing APCs via TCR-MHCI interactions, and induce apoptosis of the APCs via Fas-Fas ligand (121). Furthermore, the ligation of MHCI on the APC surface can induce its internalization, preventing antigen recognition by other T cells and thus inhibiting other CD8+ T cells (121). The purpose of these immunosuppressive EVs is to dampen and down-regulate already active immune responses rather than to initiate a response. In this regard, they may act as a counterbalance to prevent excessive response and destruction of healthy host cells. This is of interest in understanding the regulation of overactive immune responses, such as sepsis

or autoimmune diseases, but may also be relevant in non-pathological states like pregnancy.

EVs play critical roles in fertility and pregnancy. During spermatogenesis, EVs, called epididysomes, are released by epididymal cells as sperm transit along the reproductive tract. Epididysomes transfer a wide variety of cargo to sperm cells by fusing to the surface of the sperm (113). Among the most important in humans is the GPI-anchored P34H glycoprotein (122). Large quantities of P34H create a glyco-shell around the sperm head that permits binding to the zona pellucida of the oocyte and allows for fertilization. Without this epididysome-mediated transfer, oocyte penetration does not occur (123). Other cargo includes enzymes responsible for energy metabolism thought to enhance sperm motility (124). EVs from the prostate called prostasomes also carry key immune regulators to inhibit the destruction of sperm by the maternal immune system (113).

During pregnancy, syncytiotrophoblast cells release exosomes and other EVs called syncytial membrane-released microvesicles/microparticles (STBM) to regulate immune tolerance of the mother to the developing embryo (125, 126). A fetus represents a partially foreign entity to the maternal immune cells due to the contribution of paternally-derived cell surface receptors. Both exosomes and STMBs carry a variety of different immunomodulatory factors. These include Fas-ligand to induce apoptosis of immune cells (127) and NKG2D to inhibit NK cells in a manner analogous to that described with T cells (126). They also carry T cell inhibitory molecules PD-L1 which inhibit T cell activation through the PD-1 receptor (128). To permit engraftment and prevent rejection, the fetus secrets EVs into the amniotic fluid and at the maternal/fetal

interface to promote regulatory T cell development and inhibit effector T cell and other immune effector cells from responding to the fetus. These fetal-derived EVs were the first observed to carry CD24, and its association with EVs is a largely unexplored facet of CD24's biological functioning.

1.6.2.2 Cancer cells exploit EVs for multiple functions

The ability for EVs to alter cellular behaviour has been of significant interest in the study of cancer. The release of EVs from tumour cells was first documented in lymphocyte cell lines derived from a B cell Hodgkin's lymphoma patient (129). These EVs were reported to be 400 to 1200 angstroms in size (40 to 120 nm), which makes their identification as exosomes likely, despite the inability to classify them fully at the time.

As with their counterparts released from non-malignant cells, EVs from cancer cells carry a variety of protein and nucleic acid cargo that can influence recipient cells and aid tumour growth or metastasis. Furthermore, the production of EVs from cancer cells is correlated with their increased metastatic potential and invasiveness in patients (97).

Within two years of their identification from the Hodgkin's lymphoma patient-derived cell line, studies had demonstrated that EVs from malignant cells can act as transformation vectors, turning non-malignant, or low-grade malignant cells into more aggressive forms. EVs collected from the highly metastatic F10 sub-clone of the B16 mouse melanoma cell line transported material to the poorly metastatic F1 sub-clone (130). The transferred proteins were incorporated into the PM of the F1 sub-clone and

rendered the cells more aggressively metastatic in lung tissue. The PM-residency of the transferred components was demonstrated by showing CD8+ T cells reactive against F10 antigens could lyse F1 cells only following EV transfer, however, the determinants increasing the metastatic potential of the F1 cells were not identified.

Cancer cells can also secrete EVs to directly benefit the developing tumour and not simply to transform neighbouring cells. For example, hypoxia is a limiting factor of tumour growth and spreading. In response to hypoxic stress, A431 squamous cell carcinoma releases exosomes (and possibly other EVs) enriched with proteins involved in angiogenesis and extracellular matrix remodelling (131). These EVs can stimulate increased angiogenesis *in vivo.* Similarly, chronic lymphoblastic leukemic (CLL) B cells demonstrate an elevated release of EVs, which can incorporate into bone marrow stromal cells, in a time dependent fashion (132). Following incorporation, these stromal cells show increased activation of mTOR and AKT, leading to their production of vascular endothelial growth factor (VEGF) (132). Increased vascularization through the promotion of angiogenesis may represent a mechanism through which cancer cells can more easily spread during metastasis. EVs can also support tumour growth directly through the delivery of pro-survival, or pro-proliferative signalling receptors, such as a constitutively active variant of the epidermal growth factor receptor (EGFR) (133).

The ability for cancer-derived EVs to influence cells can be mediated through RNA transfer. Studies have shown that EVs package mRNA and miRNA transcripts that are biologically active in recipient cells. The human MDA-MB-231 breast cancer cell line is highly metastatic and produces exosome-sized EVs (134). When transfected with a Cre- recombinase reporter, these EVs incorporate the Cre mRNA (135). When

ultracentrifuge-isolated EVs carrying Cre were injected into mice carrying LoxP-transfected T47D breast cancer cells Cre was successfully integrated, translated, and became biologically active, demonstrating the ability for mRNA to generate functional products in recipient cells *in vivo* (135). The released MDA-MB-231 EVs were also enriched in mRNA that participates in cell migration and adhesion. Following incorporation of these EVs, T47D cells became more metastatic, with increased infiltration into surrounding tissues and distal sites (135) Similarly, miRNAs miR-105 and miR-181c transported by EVs have been shown to aid in metastasis through the blood brain barrier by disrupting tight junction proteins and actin localization, respectively, in endothelial cells (136, 137).

The most recent research has established that cells can release multiple types of EVs (such as exosomes and MVs) simultaneously (138). These EV sub-sets are compositionally distinct (138, 139). For example, MVs, but not exosomes, released from one prostate cancer cell line were heavily enriched in transcripts regulating prostate cancer, and more heavily for rRNA. Conversely, exosomes were more variable in the transcripts they carry (139). Therefore, future studies on the ability for EV to influence diseases, such as cancer, will be influenced heavily by the methodology used to isolate EV, and must account for the intrinsic intra-population heterogeneity of different EV sub-types.

1.6.2.3 The utility of EVs for diagnostics and therapeutics

Finally, a current trend in EV research is the investigation of their utility as diagnostic or therapeutic tools. Among the most simplistic but reliable diagnostic is the association between increased EV release in different biological or pathological conditions. This increase has been identified in the numbers of circulating EVs in plasma from melanoma, breast and esophageal squamous cell carcinoma cancer patients (140-142), in drug or alcohol-induced liver disease (143, 144), and in end-stage renal disease (145). Increased exosome production has been associated with advancing pregnancy, which has been suggested as a means for monitoring complications during gestation (146).

Beyond the simple monitoring of EV numbers, the composition of EVs has been examined for potential diagnostic utility. The ability for EVs to carry RNA, and their presence in, and ready isolation from, most biofluids have made them attractive targets for identifying signatures of disease. Ovarian cancer is frequently diagnosed at an advanced stage due to an absence of definitive symptoms, difficulties in early detection, and the lack of a non-invasive diagnostic which can be used for general population screening. In addition to increases in the numbers of circulating EVs, ovarian cancer EVs exhibit increases in miRNA previously established as biomarkers of the disease (147). The profile of miRNA isolated from these EVs was highly correlated with the originating tumour, and distinct from that of EVs isolated from healthy individuals. The ease of detection, as facilitated by routine blood collection makes this an attractive possibility for population screening.

Other tumours also shed EVs that have diagnostically relevant transcripts and proteins. These include glioblastoma, which frequently contain mRNA for the mutant EGFRvIII, which is absent in EVs from healthy tissue (148) Similarly, hepatocarcinoma cells release EVs enriched for the lncRNA ROR, a marker of Transforming Growth Factor β-induced treatment resistance (149). The resistance to treatment by the mAb Herceptin, an antagonist of Human Epidermal Growth Factor Receptor-2 (Her2), in human breast cancer can be mediated by exosomes. In this case, Her2 overexpressing tumours selectively release Her2+ exosomes to bind circulating Herceptin, allowing the tumour to escape the Herceptin-mediated inhibition (150). The monitoring of Her2+ EVs in patient plasma may therefore be useful in diagnosing treatment resistance and allow earlier therapeutic adjustment.

An early study on MV-mediated receptor transfer examined their role in mediating RBC survival. In paroxysmal nocturnal hemoglobinurina (PNH) patients, RBCs are deficient in the GPI-linked cell surface receptors CD55 and CD59. These receptors down-regulate complement-mediated cell lysis, and in their absence, cells are more susceptible to destruction via complement (9). CD55 and CD59 are present on MVs isolated from healthy donor RBCs. Transfer of these MVs, and their incorporated CD55 and CD59 *in vitro* protected RBCs isolated from PNH patients from complement-mediated lysis, however, this protection was lost when MVs were pre-treated with phospholipase C to cleave GPI-anchored proteins. (151). This study noted that long-term RBC storage increases RBC vesicle release, and it was hypothesized that blood stored for transfusion may be enriched for RBC MVs (152). Subsequently, it was demonstrated that

stored blood from healthy donors could be used to transfer CD55 and CD59 to PNH patients (152), however, remission of PNH was not evaluated in response to receptor transfer.

EVs have also been investigated for their potential to deliver small molecules or therapeutic agents to cells. In Parkinson's disease, neuron damage occurs through the generation of reactive oxygen species (ROS) (153). One possible therapeutic strategy being considered is the delivery of ROS scavengers, such as the catalase enzyme, to abrogate ROS-induced damage. *In vivo* studies in C57BL/6 mice showed EVs could be selectively loaded with active catalase, that these EVs could cross the blood brain barrier, and that the EVs could reduce brain inflammation (154).

EVs have been used to deliver apoptotic-inducing agents to cancer cells. Tumour Necrosis Factor-related Apoptosis Inducing Ligand (TRAIL) is a pro-apoptotic signalling receptor typically down-regulated in tumour cells (155). EVs have been used to deliver TRAIL to multiple cell lines *in vitro,* resulting in their apoptosis without affecting neighbouring healthy cells (156). Similarly, a caspase vector with a Schwann cell p0 promoter has been used to induce apoptosis in Schwann cell tumours in a mouse xenograft model (157). Interestingly, these cells also shed EVs (potentially as apoptotic bodies) containing the active vector, which destroyed neighbouring cells resulting in near complete tumour remission (157).

Recently, it has been shown that CD24 is released on EVs from both human and mouse cells *in vitro* and *in vivo.* CD24 was first identified on EVs derived from mouse and human urine and amniotic fluid (158). Interestingly, using CD24-knockout dams mated to CD24-positive males resulted in heterozygous pups. Vesicles isolated from the

amnion in CD24-knockout dams carried CD24, which demonstrates the vesicles isolated from amnion came from the developing fetus rather than being maternally derived. This study suggested that CD24 was not a driver of EV biogenesis, as comparable numbers of EVs were successfully isolated from WT and CD24 KO mice. Since that time, CD24 has been identified on EV freely circulating in blood plasma (159) and saliva (160), and it is incorporated in EV released from both healthy and cancerous tissues (159, 161). However, no functional role has been associated with CD24 on these EVs, and it remains unclear if it is simply incorporated or if CD24 may play some role in EV biogenesis.

Our lab first investigated the potential signalling mechanism of CD24 through a guilt-by-association bioinformatics analysis of publically available B cell transcriptomics data generated by the Immunological Genome Project (60). Our analysis showed that during B cell development, CD24 was co-expressed with 39 unique genes, suggesting a common regulatory scheme with potentially related, or complementary functions (60). Among these associations, there was an over-representation of genes associated with cytoskeletal organization and vesicle trafficking suggesting that CD24 may participate in these processes. I also identified that CD24 expression is highly dynamic following antibody-mediated stimulation of *ex vivo* isolated primary mouse B cells, with expression both decreasing and increasing. As other GPI-anchored proteins have been identified as signalling via endocytosis-based processes, I hypothesized that CD24 may signal through a balance of endocytosis and exocytosis-based events. However, the association between CD24 and EVs in other systems suggests that it may participate in signalling through these mediators as well. My research has thus focused on the investigation of these possibilities.

1.7 Research objectives

Given the current state of knowledge with respect to CD24-mediated cell signalling, my research focused on three major objectives:

1. Identify putative tissue-specific CD24 ligands to better elucidate potential interacting partners and their potential processes using publically available gene expression microarray data.

2. Examine the association between Ab-mediated stimulation changes in CD24 expression on the B cell surface with endocytosis, exocytosis, or EV release.

3. Characterize B cell EV released in response to Ab-mediated stimulation of CD24.

.

My work lead to the generation of a testable hypothesis on a generalizable mechanism of CD24 signalling based on its known *in cis* associations with transmembrane signalling co-receptors.

1.8 Publications arising from data presented in this thesis

The results presented in this thesis have all been published as follows:

1. **DC Ayre**, NK Pallegar, NA Fairbridge, M Canuti, AS Lang and SL Christian. (2016). Analysis of the structure, evolution, and expression of CD24, an important regulator of cell fate. *Gene* 590, 324-337 (13). This data is presented as chapter 2. The data presented in this chapter is used under copyright license from publisher Elsevier, with the copyright permission presented in appendix A.

   **This publication contains data generated from the co-first author that is not included within this thesis. Only data analysis performed by DCA is presented here.*

Author contributions: NKP performed the genomic structure analysis. DCA performed the transcriptomic expression and structural analysis. NKP, MC, and ASL performed the phylogenetic analysis. NAF, DCA, NKP, and SLC conceived the idea and participated in its design. All authors helped draft the manuscript and approved the final manuscript.

2. **DC Ayre**, M Elstner, NC Smith, ES Moores, AM Hogan and SL Christian. (2015). Dynamic regulation of CD24 expression and release of CD24-containing microvesicles in immature B cells in response to CD24 engagement. *Immunology* 146(2), 217-233 (60). This data is presented as chapter 3. The data presented in this chapter is used under copyright license from publisher John Wiley and Sons, with the copyright permission presented in appendix A.

**This publication contains data that was generated prior to the beginning of the PhD program. Only data collected during the PhD, and not contained in another thesis is presented here.*

Author contributions: DCA and SLC conceived the idea and designed the experiments. DCA performed FACS analysis on CD24 expression, as well as endocytosis and exocytosis inhibiting experiments. ME and DCA performed caspase analysis. Samples for TEM were stimulated by DCA and prepared with help from Kate Williams, Faculty of Medicine, Memorial University of Newfoundland. Flow cytometry of EVs was prepared and performed by DCA with assistance by Nicole Smith, CDRF, Memorial University of Newfoundland. ESM and AMH assisted with the preparation of samples for cell death assays. All authors approved the final manuscript.

3. **DC Ayre**, IC Chute, A Joy, D Barnett, AM Hogan, MP Grüell, L Peña-Castillo, AS Lang, SM Lewis and SL Christian (2017). CD24 induces compositional changes in B cell microvesicle RNA cargo, protein cargo and surface protein. *Scientific Reports* 7(1), 8642 (162). This data is presented as chapter 4. The data presented in this chapter are used under the Creative Commons Attribution 4.0 International License as stipulated by Scientific Reports. The full license is presented in appendix A.

Authors Contributions: DCA and AMH prepared samples for Western blot. DCA performed FACS and Western blot and gene/protein ontology analyses, and collected samples for mass spectrometry. DCA, MPG, ASL and LPC performed the RNA-sequencing and analysis. ICC, AJ, DAB and SML performed the mass spectrometry and

peptide annotation. ICC performed the nanosight tracking analysis, DCA performed the transmission electron microscopy sample preparation. DCA and SLC conceived and designed the experiments and prepared the final manuscript. All authors approved the final manuscript.

4. **DC Ayre** and SL Christian. (2016). CD24: A rheostat to modulate cell surface receptor signalling of diverse receptors. *Frontiers in Cell and Developmental Biology* 4:146 (10). This hypothesis is presented as a part of chapter 5. The data presented in this chapter are used under the Creative Commons Attribution 4.0 International License as stipulated by Frontiers in Cell and Developmental Biology. The full license is presented in appendix A.

Author Contributions: DCA and SLC conceived the hypothesis, prepared and edited the manuscript.

Chapter 2: Structure and Expression of CD24 and Potential Ligands

2.1 Introduction

As discussed in chapter 1 of this thesis, the CD24 protein is conserved in numerous mammalian, reptilian and avian species. In mice and humans, it is translated as a precursor protein of 80 or 76 amino acids, respectively, before the cleavage of N- and C-terminal sequences. These peptide sequences are responsible for directing the protein to the plasma membrane and for the attachment of the GPI anchor moiety, leaving a mature protein that is between 27 and 30 amino acids in length. This protein core is then heavily post-translationally modified with a variable mosaic of N- and O- linked glycosylations resulting in a final protein size which ranges between 20 and 80 kDa (14). This protein is then expressed in a wide variety of cells and tissues, and has demonstrated binding with numerous tissue-specific ligands. Furthermore, the relationship between CD24 and its ligands is highly complex. Multiple ligands have been identified for CD24 with many of these interactions known to be cell-type specific. No published research has attempted to predict which interactions may be present across different tissues based on the known expression of CD24 and its various potential ligands.

I performed an analysis of the consensus sequence of CD24 from 56 different species. I found within animal clades, there was a high degree of conservation, but between phyla this conservation was diminished (13). There was poor conservation of the mature CD24 protein across species. The most stringent conservation occurred in areas responsible for anchoring the glycosylation chains (13). However, the number of glycosylation sites, and whether these sites are conserved as N- or O-linked attachment

areas, varied between species. Therefore, I then examined the three-dimensional structure of CD24 to determine if there was a relationship between CD24 protein conservation, potential secondary or tertiary protein structures, and thus the ability for CD24 to interact with ligands. I examined the co-expression of CD24 with various known or potential ligands across multiple tissues. Overall, my analysis identified that the mature CD24 protein exists as an intrinsically disordered protein, with limited amino acid-directed structure. Furthermore, the expression of CD24 and its known ligands only occurs together in some tissues or cell types.

2.2 Materials and Methods

2.2.1 CD24 protein structure predictions.

The CD24 pro-peptide and mature peptide consensus sequences were generated using BioEdit from the unique amino acid sequences (Additional File 3) and visualized using WebLogo (163). These sequences were then analyzed by i-Tasser (164) and SPINE-D (165) for secondary structure predictions.

2.2.2 Gene expression analysis**.**

Microarray-based whole transcriptome data for the mouse tissues indicated were retrieved from the Gene Expression Omnibus (GEO) for the accession numbers listed in **Table 2.1**. Publication references for these data, where provided, are indicated. Robust Multi-Array Average (RMA) normalization of gene expression was performed in R 3.0.2 via R Studio 0.98.1091 using the Bioconductor, Biobase, and Oligo packages (166-169) and the pd.mogene.1.0.st.v1, pd.mouse430.2 and pd.moe430a annotation files. Using the online Affymetrix NetAffx tool, probe IDs for the selected genes of interest were identified for the three platforms. CD24, its known ligands, and closely related protein family members were included in each analysis, and appropriate lineage and non-lineage markers were included for each tissue (**Table 2.2**). RMA normalized data were then filtered using these probe IDs and gene expression data averaged between replicates. The Moe430a and Mouse430.2 arrays frequently contain multiple probe IDs for each gene. Therefore, each probe ID was examined individually and probes with values that did not represent known gene expression patterns or clear outliers were excluded from the analysis as indicated

Table 2.1 Mouse tissues used to determine expression profiles for CD24 and selected genes.

Cell / Tissue	GEO Accession Number and Reference	Platform
Bone marrow derived, developing B cells	GSE15907 (170)	GPL6246-Affymetrix Mouse Gene 1.0 ST Array
Developing T cell	GSE15907 (170)	GPL6246-Affymetrix Mouse Gene 1.0 ST Array
Dendritic cells	GSE15907 (170)	GPL6246-Affymetrix Mouse Gene 1.0 ST Array
Embryonic liver	GSE13149 (171)	GPL1261-Affymetrix Mouse Genome 430 2.0 Array
Mature, adult liver post-hepatectomy	GSE4528 (No associated publication)	GPL339-Affymetrix Mouse Expression 430A Array
Prenatal whole brain	GSE8091 (172)	GPL1261-Affymetrix Mouse Genome 430 2.0 Array
Post-natal and adult whole brain	GSE11528 (173)	GPL6886 - Mouse Genome 430 2.0 Array[a]
Foetal placenta	GSE11220 (174)	GPL1261-Affymetrix Mouse Genome 430 2.0 Array
Maternal decidua	GSE11220 (174)	GPL1261-Affymetrix Mouse Genome 430 2.0 Array
Embryonic whole testis	GSE6881 (175)	GPL1261-Affymetrix Mouse Genome 430 2.0 Array
Embryonic whole ovary	GSE6882 (175)	GPL1261-Affymetrix Mouse Genome 430 2.0 Array
Embryonic and mature cornea	GSE43155 (176)	GPL6246-Affymetrix Mouse Gene 1.0 ST Array

[a] Platform GPL6886 - Mouse Genome 430 2.0 Array is identical to the GPL1261-Affymetrix Mouse Genome 430 2.0 Array. The authors used custom annotation files in analysis, which were not required for this analysis.

Table 2.2 Gene symbols, names and Probe IDs for all genes used in expression analysis.

MGI Gene Symbol	Gene Name	Alternative Name	MoGene 1.0 Probe ID	affy_moe430a Probe ID(s)[a]	affy_mouse430_2 Probe ID(s)[a]
CD24A	n/a	CD24, Heat Stable Antigen (HAS) / Nectadrin, Ly-52	10362896	1416034_at, 1437502_x_at, 1448182_a_at	1416034_at, 1437502_x_at, 1448182_a_at
SELL	L-Selectin	SEL-L[b], CD62L, LECAM-1, Lnhr, Ly-22, Lyam-1, Ly-m22	10351197	1419480_at, 1419481_at	1419480_at, 1419481_at
SELP	P-Selectin	SEL-P [b], CD62P, Grmp	10351206	1420558_at, 1449906_at	1420558_at, 1440173_x_at, 1449906_at
SELE	E-Selectin	SEL-E [b], CD62E, Elam	10351182	1421712_at	1421712_at
L1CAM	L1 Cell Adhesion Molecule	CD171, L1, L1-NCAM, NCAM-L1	10605113	1421958_at, 1450435_at	1421958_at, 1450435_at
CD22	Siglec-2 (Human)	Lyb8, Lyb-8	10562132	1419768_at, 1419769_at	1419768_at, 1419769_at
Siglece	Sialic Acid Binding Ig-like Lectin E	Siglec-5 (Human), mSiglec-E, SiglecL1	10552369	1424975_at	1424975_at
Siglecg	Sialic Acid Binding Ig-like Lectin G	mSiglec-G, Siglec-10 (Human)	10552380	N/A	1435955_at
CD80	n/a	B7-1, B7.1, CD28l, Ly-53, Ly53	10435704	1427717_at, 1451950_a_at	1427717_at, 1451950_a_at
CD86	n/a	B70, B7-2, B7.2, CD28l2, Ly58, Ly-58, MB7-2	10439312	1420404_at, 1449858_at	1420404_at, 1449858_at
Itgam	n/a	CD11b, CD11b/CD18, CD11B(p170), Complement component receptor 3 alpha, complement receptor type 3, Cr3, Ly-40, Mac-1, Mac-1a, Mac-1 alpha	10557862	1422046_at	1422046_at
Il3ra	Interleukin 3 receptor, Alpha Chain	CD123, IL-3 receptor alpha chain, SUT-1	10412760	1419712_at	1419712_at

Gapdh	Glyceraldehyde-3-phosphate dehydrogenase	Gapd, G3PD	10545765	1418625_s_at, AFFX-GapdhMur/M32599_3_at, AFFX-GapdhMur/M32599_5_at, AFFX-GapdhMur/M32599_M_at	1418625_s_at, AFFX-GapdhMur/M32599_3_at, AFFX-GapdhMur/M32599_5_at, AFFX-GapdhMur/M32599_M_at
Rplp0	ribosomal protein, large, P0	36B4, Arbp, L10E, LP0	10524718	1419441_at	1419441_at
Actb	Actin, Beta	Actx, A-X actin-like protein, beta-actin	10535381	1419734_at, 1436722_a_at, AFFX-b-ActinMur/M12481_3_at, AFFX-b-ActinMur/M12481_5_at, AFFX-b-ActinMur/M12481_M_at	1419734_at, 1436722_a_at, AFFX-b-ActinMur/M12481_3_at, AFFX-b-ActinMur/M12481_5_at, AFFX-b-ActinMur/M12481_M_at
CD19	n/a	B4, CVID3	10567863	1450570_a_at	1450570_a_at
CD4	n/a	L3T4, Ly-4	10547894	1419696_at, 1427779_a_at	1419696_at, 1427779_a_at
CD8b1	n/a	Ly-3, Ly-C, Lyt-3, Leu2, P37	10538979	1426170_a_at	1426170_a_at
CD8a	n/a	Ly-2, Ly-35, Ly-B, Lyk-2, Leu2, p32	10538993	1425335_at, 1451673_at	1425335_at, 1444078_at, 1451673_at
Gpt	Glutamic pyruvic transaminase, soluble	AAT1, ALT1, GPT1	10424979	1426502_s_at	1426502_s_at
NCAM1	Neural cell adhesion molecule 1	CD56, E-NCAM, NCAM, NCAM-1, NCAM-120, NCAM-140, NCAM-180, MSK39	10593293	1426865_a_at, 1450437_a_at	1426865_a_at, 1450437_a_at

[a]Probe IDs in red were removed from analysis as the gene expression values obtained were inconsistent with other Probe IDs or with known expression.

[b]Selectin genes were labelled as either Sele-L, Sele-P, Sele-E in expression profile figures for ease of identification.

(**Table 2.2**). When a single gene was represented multiple times within an array, gene expression values for all probe IDs representing a single gene were averaged (see **Supplemental File 1** for means and standard deviations for each gene).

2.2.3 Statistical analysis

High and low gene expression was defined as values within 25% of the maximum and the minimum gene expression within each panel, and shown as green and pink bars, respectively. Statistically significant changes to CD24 gene expression were determined by 1-way ANOVA followed by Tukey post-hoc test, if significant. Positive correlation between the expression of CD24 and all other genes was determined using a one-tailed Spearman's rank correlation analysis at a p-value of 0.05. All statistics were done in R (167).

2.3 Results

2.3.1 The Structure of CD24

I used the consensus sequence of CD24 derived from the alignment of the previously analyzed species to predict secondary structure and organization at the protein level. The consensus sequence was longer than the sequence for any individual species as it includes rare and unique amino acid insertions from each species added into the single sequence. Secondary structure prediction of the precursor CD24 protein using i-Tasser suggested that there are two alpha-helical regions (**Figure 2.1A**). One is in the N-terminal region, from residues 3 to 29, which corresponds to the signal sequence. The second is in the C-terminal domain, from residues 86 to 96, which corresponds to a portion of the GPI-anchor signal sequence. No secondary structure could be predicted for the region of the precursor protein that corresponds to the mature peptide between residues 42 to 77. As the N- and C-terminal regions are cleaved from the mature peptide during post-translational processing (14), I also analyzed the mature core peptide in isolation (**Figure 2.1B**). Similarly, no discrete secondary structure was predicted for the mature peptide in isolation. As expected from the secondary structure prediction results, no tertiary structure was confidently predicted for either the precursor or the mature peptide.

In agreement with the secondary structure prediction, analysis of the intrinsic disorder of the CD24 precursor protein via SPINE-D revealed that this protein is likely to be highly intrinsically disordered, with an average probability score of 0.62 (**Figure 2.1A**). In the N-terminal region of the precursor protein, the region from residues 24 to 37 has a probability of disorder of 0.32, indicating it is likely an ordered region. This area

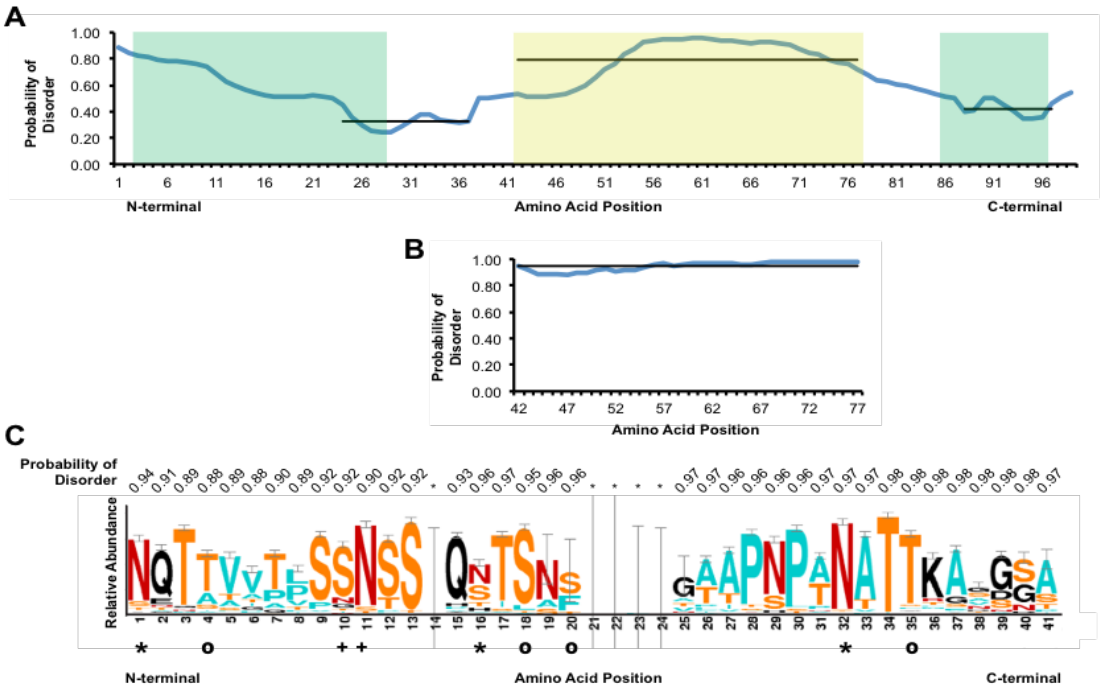

Figure 2.1: Visualization of CD24 secondary structure motifs and sequence alignment. The predicted secondary structures of the CD24 (**A**) pro-peptide and (**B**) mature peptide were assessed using i-Tasser and SPINE-D. The predicted disorders of the pro- and mature peptide are represented with a blue line. Areas predicted by i-Tasser to contain alpha-helical domains are shown in green. Black bars represent the average probability of disorder predicted by SPINE-D for two ordered domains in the N- and C-terminal regions and the mature peptide. (**C**) A graphical representation of the mature CD24 peptide alignment is shown. Letter height indicates relative abundance of a given amino acid in each position. Error bars show a Bayesian 95% confidence interval. Asn and Arg residues are shown are red, while Ser and Thr residues are shown in orange. Hydrophobic amino acids are in blue and all other amino acids are in black. Known *Mus musculus* N-glycosylated residues are indicated with * and known O-linked glycoslyations are indicated with °. Potential N-linked glycosylation sites are shown with $^{+}$, based on the Asn x(Ser/Thr) glycosylation motif. Amino acid positions 14 and 21-24 are shown as gaps as they do not align or are not present in most sequences analyzed (Additional File 3). The likelihood of a given residue existing in a disordered state was predicted using SPINE-D and the probability of disorder is shown above the sequence.

partially overlaps with the alpha-helical domain predicted by i-Tasser (**Figure 2.1A**). In the C-terminal region, there is another ordered region from residues 88 to 97, with a probability of disorder of 0.42, overlapping with the predicted alpha-helical region of the GPI-anchor signal sequence. The central domain of the precursor protein containing the mature core peptide from positions 42 to 77 had a high average probability of disorder value of 0.80. Furthermore, when analyzed in isolation, I found that the intrinsic disorder of the mature peptide increased to an average of 0.94, primarily due to a loss of order at the N-terminus (**Figure 2.1B**). Therefore, post-translational processing of the CD24 protein causes reduced order in the peptide core, however, it is not precisely known how the addition of glycosylations and/or the GPI-anchor influence the structure or disorder of the surface protein.

Visualization of the alignment of the mature core peptide clearly reveals that several of the known O-glycosylation sites as well as known and predicted N-glycosylation sites (177) are highly conserved (**Figure 2.1C**). Specifically, there were 12 highly conserved Ser or Thr residues that could be modified by O-linked glycosylation, and five highly conserved Asn residues that can be N-glycosylated, based on the consensus sequence of Asn-X-(Thr/Ser) where X can be any amino acid except proline (178). Of the potentially glycosylated residues, there are three highly conserved residues that are known to be N-linked, and four highly conserved residues that are likely to be O-linked, at least in the case of erythrocyte-derived mouse CD24 (16).

In addition to the glycosylation sites, there are two clearly identifiable regions with highly conserved sequences, from positions 9 to 19 and 28 to 35 of the mature protein. The second, a proline-rich region, partially overlaps with the CD24 domain as

annotated by the Pfam database (PF14984) (179), which begins at position 26 and ends within the GPI-anchor signal peptide at position 75. However, as the Pfam domain PF14894 includes the GPI-anchor peptide it does not accurately represent the mature core peptide. Nevertheless, the high conservation of key glycosylation residues supports previous work showing that glycosylation of CD24 dictates ligand specificity and therefore function of CD24 (6, 31, 180).

2.3.2 Dynamic regulation of CD24 gene expression and its putative ligands during cellular development

CD24 is dynamically regulated throughout development at the mRNA and protein levels in multiple cell types (14, 15, 181, 182), and is highly expressed in the developing embryo (183). Multiple ligands for CD24 have been identified, which interact with CD24 either *in cis* or *in trans*. Putative *in cis* interactions can be predicted using global transcriptomic analysis of purified populations of cells at different stages of development while putative *in trans* interactions can be predicted using global transcriptomic analysis of whole tissues. Thus, I performed analyses on the expression levels of *CD24* and previously identified ligands and closely related family members in developing cells of the immune system, in immune privileged sites, in developing and regenerating liver cells, and in the whole embryonic and adult brain. For each cell type, I also analyzed the expression of key lineage markers and genes known to have high or low expression to confirm that the transcript data of interest accurately represented the cell type and stage at the transcript level. I analyzed the correlation between the expression of *CD24* and the

genes of interest as well as establishing boundaries for low/no, moderate, and high expression, as described in section 2.2.3. The GEO accession numbers and appropriate publication references are provided in table 2.1, as previously indicated.

2.3.2.1 Immune cells

I analyzed the expression of *CD24* and genes encoding putative ligands in B cells (**Figure 2.2A**), T cells (**Figure 2.2B**), and DCs (**Figure 2.2C**), in which CD24 is known to positively regulate apoptosis, homeostatic proliferation, and repression of activation, respectively (15).

B cells develop in the bone marrow occurs through discrete stages from multi-lymphoid progenitor (MLP) to the common lymphoid progenitor (CLP) and then to committed B cell stages (Hardy fractions A through F). I used *CD19* expression to confirm lineage specificity (48) and found that, as expected, *CD19* expression increases at the Fraction B stage, where irreversible B cell commitment occurs, until the Fraction E (immature) phase whereupon expression plateaus (**Figure 2.2A**). In agreement with the original studies (54), I found that while *CD24* expression is generally moderate during B cell development, its expression increases from moderate to high at the committed B cell stage, Fraction B, followed by a decline when cells reach maturity and then remains moderate with a slight decline in plasma cells (**Figure 2.2A**).

I found that the expression patterns of *Siglec-2*, *Siglec-G* and *CD19* significantly correlated with *CD24* expression (**Figure 2.2A**). *Siglec-2* and *-G* are expressed at a low level at the onset of B cell development, and their expression increases

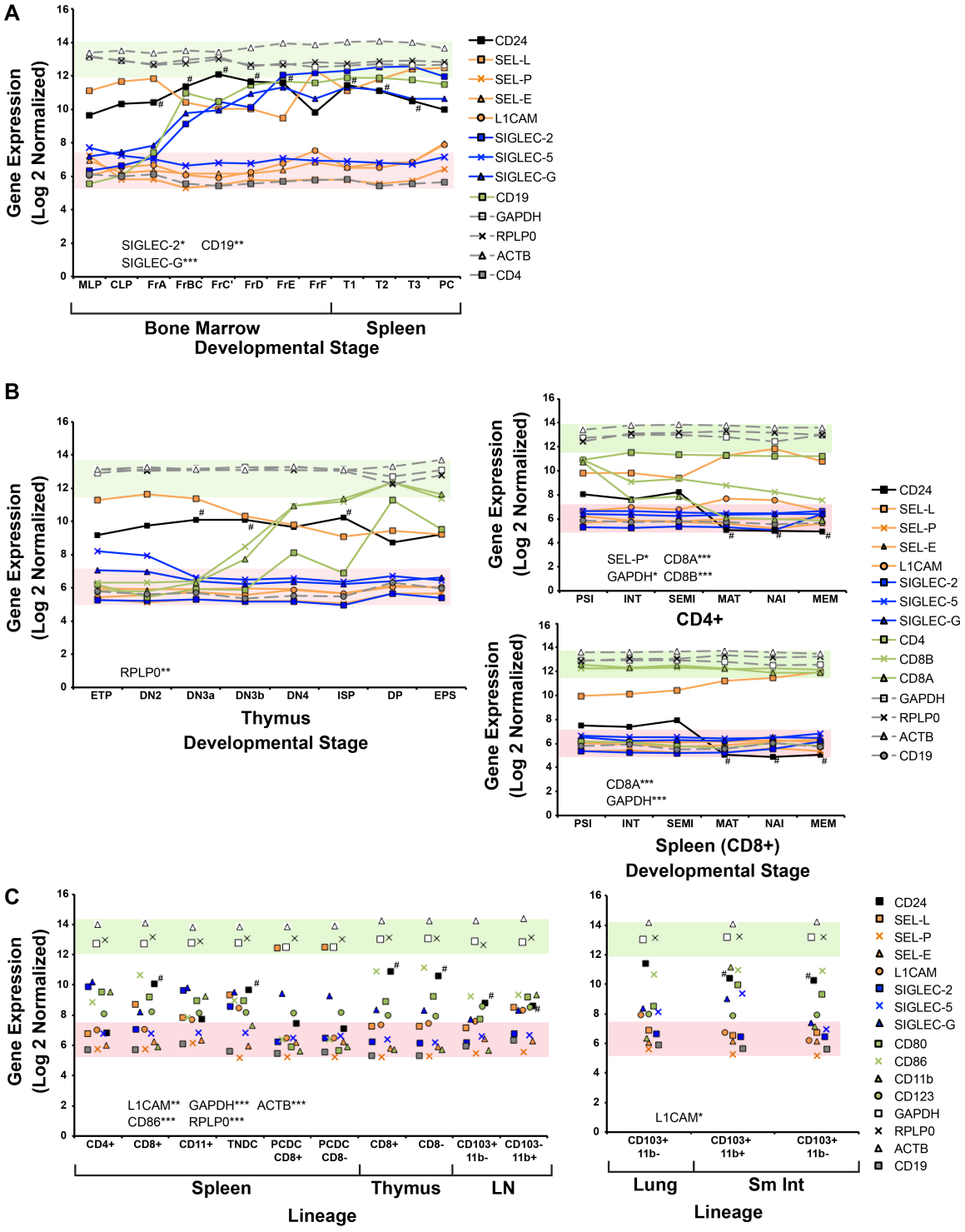
A
Gene Expression (Log 2 Normalized)
SIGLEC-2* CD19**
SIGLEC-G***
MLP CLP FrA FrBC FrC' FrD FrE FrF T1 T2 T3 PC
Bone Marrow
Spleen
Developmental Stage
CD24
SEL-L
SEL-P
SEL-E
L1CAM
SIGLEC-2
SIGLEC-5
SIGLEC-G
CD19
GAPDH
RPLP0
ACTB
CD4
B
Gene Expression (Log 2 Normalized)
RPLP0**
ETP DN2 DN3a DN3b DN4 ISP DP EPS
Thymus
Developmental Stage
SEL-P* CD8A***
GAPDH* CD8B***
PSI INT SEMI MAT NAI MEM
CD4+
CD8A***
GAPDH***
Spleen (CD8+)
Developmental Stage
CD8B
CD8A
C
L1CAM** GAPDH*** ACTB***
CD86*** RPLP0***
CD4+ CD8+ CD11+ TNDC PCDC CD8+ PCDC CD8- CD8+ CD8- CD103+ 11b- CD103- 11b+
Spleen
Thymus
LN
Lineage
L1CAM*
CD103+ 11b- CD103+ 11b+ CD103+ 11b-
Lung
Sm Int
Lineage
CD80
CD86
CD11b
CD123

Figure 2.2: *CD24*, CD24 ligand, and lineage marker expression during immune cell development. Data show expression of *CD24* (black), known CD24 ligands (orange), Siglecs (blue), lineage markers (green), and normalizer genes and non-lineage markers (grey), n=3-4. (**A**) B cell development is divided into bone marrow and splenic stages. MLP, multilineage progenitor stem cells; CLP, common lymphoid progenitor cells; FrA through FrF, Hardy Fractions A, B/C, C', D, E and F; T1-T3, splenic transitional B cells, stages 1 through 3; and PC, terminally differentiated plasma cells. (**B**) T cell development is divided into Progenitor T cells (left panel) and Splenic $CD4^+$ and $CD8^+$ T cells (right panel). ETP, early T progenitor; DN2, double negative 2; DN3a, double negative 3a; DN3b, double negative 3b; DN4, double negative 4; ISP, immature single positive; DP, double positive; EPS, early positive selection; CD4-PSI, $CD4^+$ positive selection intermediate; CD4-INT, $CD4^+$ intermediate; CD4-SEMI, $CD4^+$-semi-mature; CD4-MAT, $CD4^+$-mature; CD4-NAI, naïve $CD4^+$; CD4-MEM, $CD4^+$-memory; CD8-PSI, $CD8^+$ positive selection intermediate; CD8-INT, $CD8^+$ intermediate; CD8-SEMI, $CD8^+$-semi-mature; CD8-MAT, $CD8^+$-mature; CD8-NAI, naïve $CD8^+$; and CD8-MEM, $CD8^+$-memory. (**C**) DCs are divided into immune organ-derived (left panel; spleen and thymus) and non-immune organ-derived (right panel; lung, lung lymph node and small intestine). DC lineages are classified by expression of CD4, CD8, CD11b and CD103. TNDC, triple negative DC; PCDC-$CD8^+$, CD8+ plasmacytoid DC; and PCDC-$CD8^-$, $CD8^-$ plasmacytoid DC. Significant changes in CD24 expression compared to the leftmost stage shown per panel by 1-way ANOVA and Tukey post-hoc analysis $^{\#}P<0.05$. Genes with significant positive correlation to CD24 indicated within graph * $P<0.05$, ** $P<0.01$, *** $P<0.005$.

rapidly and peaks in Fraction E cells. While *Siglec-G* showed a moderate decline in expression in splenic cells, *Siglec-2* expression was maintained at higher levels throughout B cell development and activation. Although L-selectin was highly expressed at the same stages as *CD24*, its expression pattern did not correlate significantly with *CD24*. Neither *P-* nor *E-selectin* was expressed to a significant level at any of the stages. As epithelial cells were not present in this purified population, identification of *trans* ligands between different cell types was not possible. High expression of *L-selectin* suggests that interactions between B cells could be mediated by L-selectin and CD24, however, there are no published reports on such an interaction. While Siglec-2 has not previously been demonstrated to be a CD24 ligand, it can bind the α2, 6-linked sialic acids that are present on CD24 suggesting that Siglec-2 could be a potential ligand for developing B cells (68, 184).

T cells develop from CLP cells that migrate from the bone marrow to the thymus where they further develop through the double negative (DN) stages, through the double positive (DP) stage and then to the early positive selection stage. As expected, *CD4* and *CD8* mRNA expression were both high by the DP stage and remained high in CD4-positive or CD8-postive T cells, respectively (**Figure 2.2B**). In comparison to B cells, *CD24* is more equally expressed through T cell development (**Figure 2.2B**). Both CD4- and CD8-positive T cell populations maintain *CD24* expression until they reach maturity whereupon it declines dramatically and remains low. Mature, naïve and memory T cells are equally capable of re-entering the cell cycle given the correct activation signals but are considered effector cell types, like antibody-producing plasma cells.

Moderate expression of *Siglec-5* and *Siglec-G* is detectable in the Early T Progenitor phase (ETP) followed by loss of expression in every other phase of T cell development. Unlike the expression patterns in B cell development, none of the Siglec genes would be viewed as strong candidates for ligands of CD24 to mediate homotypic interactions. This is consistent with the role that CD24 expression plays in co-stimulation of T cells (63). I found a significant correlation between *CD24* and *P-selectin* expression patterns, however, since *P-selectin* is expressed at very low levels, this correlation likely does not have biological meaning.

DCs can be found in lymphoid organs, such as the spleen, thymus, and lymph nodes, as well as in non-lymphoid tissue, where they act as the sentinels of the immune system and present antigen to T cells (185). I found that *CD24* expression was highly variable among DC subsets (**Figure 2.2C**). In general, *CD24* expression was moderate to high in all the DC subsets except in CD4+ splenic DC and plasmacytoid DC where CD24 expression was low.

Expression of genes encoding putative and known CD24 ligands was also highly variable (**Figure 2.2C**). Overall, *Siglec-G* was moderately expressed in most DC subsets consistent with the known *cis* inhibition of Siglec-G by CD24 in bone marrow-derived DCs (29). Even though bone marrow-derived DCs are not represented in this expression dataset, I would predict that the Siglec-G - CD24 interaction may also be an important interaction in many other DC subsets, particularly in non-lymphoid organs but less likely in lymph node DCs or $CD8^{+}(CD4^{-}CD11^{-})$ splenic DCs. Plasmacytoid DCs (PCDCs) arise from CLPs whereas other DC subsets originate from the myeloid lineage (185). Interestingly, *L-selectin* is highly expressed in both subsets of PCDCs but not in any

other DC subset. I found there was no strong correlation between *CD24* levels and any ligand except for *L1CAM*, however this correlation may not be biologically meaningful as the expression of *L1CAM* is low in nearly all of the DC subsets analyzed.

Overall, these data support a putative role for Siglec-2 and Siglec-G acting as *cis* ligands in B cell development, but do not support a role for these ligands in developing T cells. Analysis of individual DC subsets at the biological level will be necessary to identify ligands due to the large variability of CD24 and ligand expression in the different subsets.

2.3.2.2 Immune-privileged sites

Sites of immune privilege are maintained to prevent the immune system from recognizing and responding to endogenous antigens by inhibiting classical immune responses in these areas. Sites of immune privilege include the maternal/fetal interface, the gonads and the cornea (186). As CD24 is best characterized as an immunoregulatory protein, it may also have a role in mediating responses at immune-privileged sites.

During pregnancy, the maternal decidual tissue and the fetal placenta maintain the maternal/fetal interface and establish immune privilege (187). This must be maintained through the pregnancy as its loss can lead to rejection of the fetus (188). Transcriptomic analysis clearly shows that *CD24* is expressed in both the placenta and the decidua at moderate levels during all stages of murine gestation (**Figure 2.3A-B**). Of the known CD24 ligands, I identified that only *L1CAM* has elevated expression in these tissues. In the mouse placenta *L1CAM* expression is constant throughout pregnancy (**Figure 2.3A**)

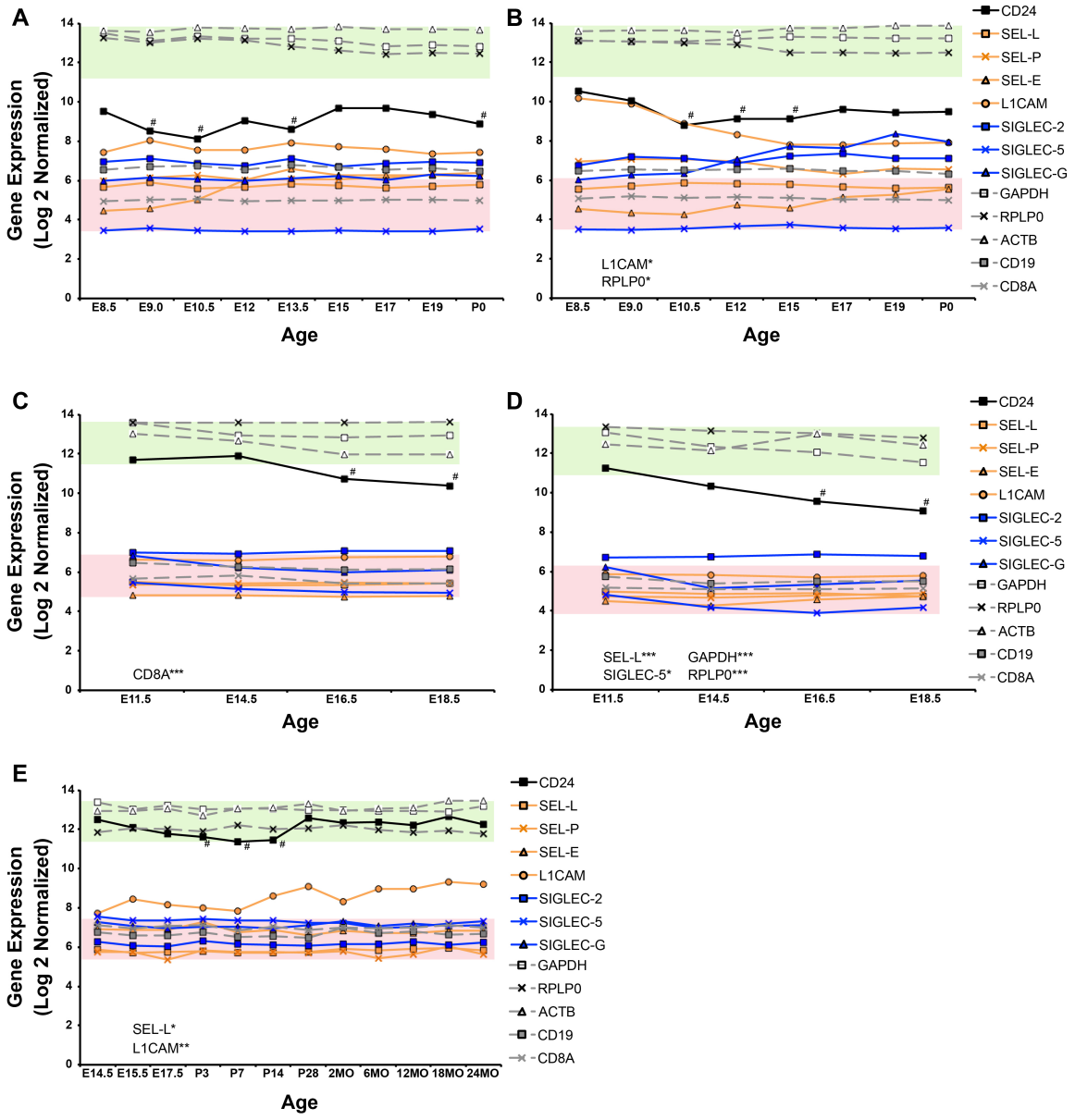

Figure 2.3. *CD24*, CD24 ligand and lineage marker expression in immune-privileged sites. Data show expression of *CD24* (black), known CD24 ligands (orange), Siglecs (blue), lineage markers (green), and normalizer genes and non-lineage markers (grey); n=3-4. Development is divided into embryonic (E) and postnatal (P) days in (**A**) Placenta, (**B**) Decidua, (**C**) Testis, (**D**) Ovary and (**E**) Cornea. Significant changes in CD24 expression compared to the earliest stage shown per panel by 1-way ANOVA and Tukey post-hoc analysis $^{\#}P<0.05$. Genes with significant positive correlation to CD24 indicated within graph * P<0.05, ** P<0.01, ***P<0.005.

while in the decidual tissue *L1CAM* expression is initially comparable to that of *CD24* but steadily declines through pregnancy until birth (**Figure 2.3B**). Accordingly, I found a significant correlation of *CD24* expression with *L1CAM* in decidual, but not placental tissue. Also, in the decidua, but not the placenta, there is an increasing trend of *Siglec-2* and *Siglec-G* expression during pregnancy reaching moderate levels at birth (**Figure 2.3B**). While no known function for CD24 has been shown in these tissues, CD24-bearing exosomes, originating from the fetus, have been found to accumulate in amniotic fluid (158).

I also found that *CD24* is expressed at high levels in both the embryonic testes and ovaries (**Figure 2.3C-D**). In both cases, expression of *CD24* is elevated in the earlier stages of fetal development and declines to a moderate level closer to birth. Even though changes in *CD24* expression showed significant correlation to *Siglec-G* in testes, and *L-selectin* and *Siglec-5* in ovary, expression of the selectins, siglecs and *L1CAM* is low throughout testicular or ovarian development.

Immune privilege is also maintained in the eye (186) where CD24 has been shown to be involved in wound healing and where *CD24* promoter hypomethylation and resultant overexpression is associated with the tissue overgrowth induced by corneal damage in humans (189). I found that *CD24* is highly expressed in corneal tissue through embryonic development and into post-natal life (**Figure 2.3E**). With respect to putative CD24 ligands, *L1CAM* is also expressed in the cornea, appearing at moderate levels 2-3 weeks after birth and maintained at a relatively constant level (**Figure 2.3E**). This trend in expression correlated significantly with CD24 expression. There is no appreciable expression of any of the other putative CD24 ligands or family members in the cornea.

Combined, these data clearly show that *CD24* is generally highly expressed in areas of immune privilege, with little dynamic regulation of expression in contrast to what is seen in immune effector cells. The maintenance of *CD24* expression suggests that CD24 likely serves a specific function in these tissues that has not yet been described. Surprisingly, its expression was not well correlated with any known CD24 ligands in any of these tissues. Since these expression studies were performed in whole tissue, identification of both *cis* and *trans* ligands is possible. Therefore, in these tissues it is possible that CD24 may act as its own ligand, or that an as-yet unknown ligand remains to be identified.

2.3.2.3 Brain and Liver

CD24 is also a biomarker for stem cells or progenitor cells, capable of differentiation and proliferation, in the brain (190), liver (191), small intestine (192), and mouse mammary tissue (193).

Brain tissue undergoes rapid development and proliferation during fetal maturation before entering a more quiescent state upon maturity. The fetal liver is responsible for hematopoietic cell development while the adult liver has critical roles in digestion and detoxification, and is capable of full regeneration of function following injury. Using these tissues as examples of rapid embryonic growth followed by a shift in function and/or growth, I examined the expression of *CD24* and genes encoding its putative ligands.

In whole brain, *CD24* is highly expressed throughout all the fetal time points examined (**Figure 2.4A**). *CD24* expression remains elevated at birth followed by a decline by 14 days of age, with a further reduction by 56 days of age (**Figure 2.4B**). *NCAM1*, chosen as a lineage marker since its expression was best described in brain, showed increasing expression during fetal development, which remained high in the adult. The *CD24* expression pattern correlated significantly with both *L1CAM* and *NCAM1* expression in developing and mature brain tissue. CD24, NCAM1, and L1CAM have been shown to be functionally related in neuronal signalling (19). In these studies, it was shown that CD24, L1CAM and NCAM1 co-migrate on the cell surface suggesting they may form cooperative signalling complexes. However, the comparatively low expression of *CD24* with respect to *L1CAM* or *NCAM1* in mature brain tissue suggests that L1CAM and NCAM1 participate in other biological roles distinct from their role with CD24.

In the fetal liver, I found that *CD24* expression is high throughout all stages of embryonic development whereupon it drops to low levels between 3 and 21 days after birth (**Figure 2.5A**). During the time frame when *CD24* expression is high, I observed very low transcript expression of known CD24 ligands. *CD24* expression correlated with *L-selectin* expression, however due to the very low level of *L-selectin* expression, this correlation not likely biologically relevant. I observed the gain of glutamic pyruvate transaminase (*GPT*) expression, a gene expressed by liver hepatocytes (194), that occurred at the same times as the drop in *CD24* expression.

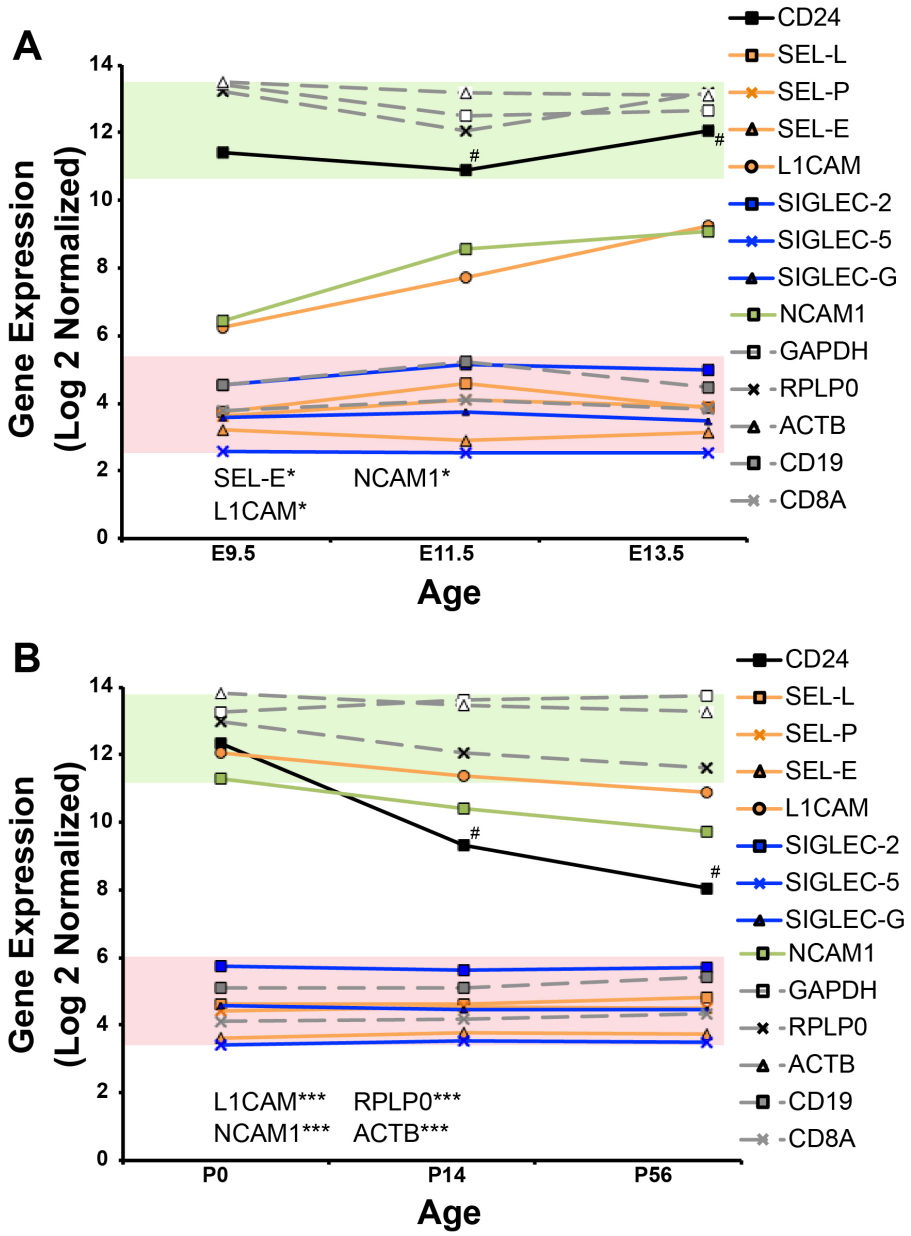

Figure 2.4. *CD24*, CD24 ligand and lineage marker expression during embryonic and postnatal brain development. Data show expression of *CD24* (black), known CD24 ligands (orange), Siglecs (blue), lineage markers (green), and normalizer genes and non-lineage markers (grey); n=3-6. (**A**) Embryonic brain development is divided by embryonic (E) day. (**B**) Postnatal brain development is divided by postnatal (P) days where P0 is day of birth. Significant changes in CD24 expression compared to the earliest stage shown per panel by 1-way ANOVA and Tukey post-hoc analysis $^{\#}P<0.05$. Genes with significant positive correlation to CD24 indicated within graph * $P<0.05$, ***$P<0.005$.

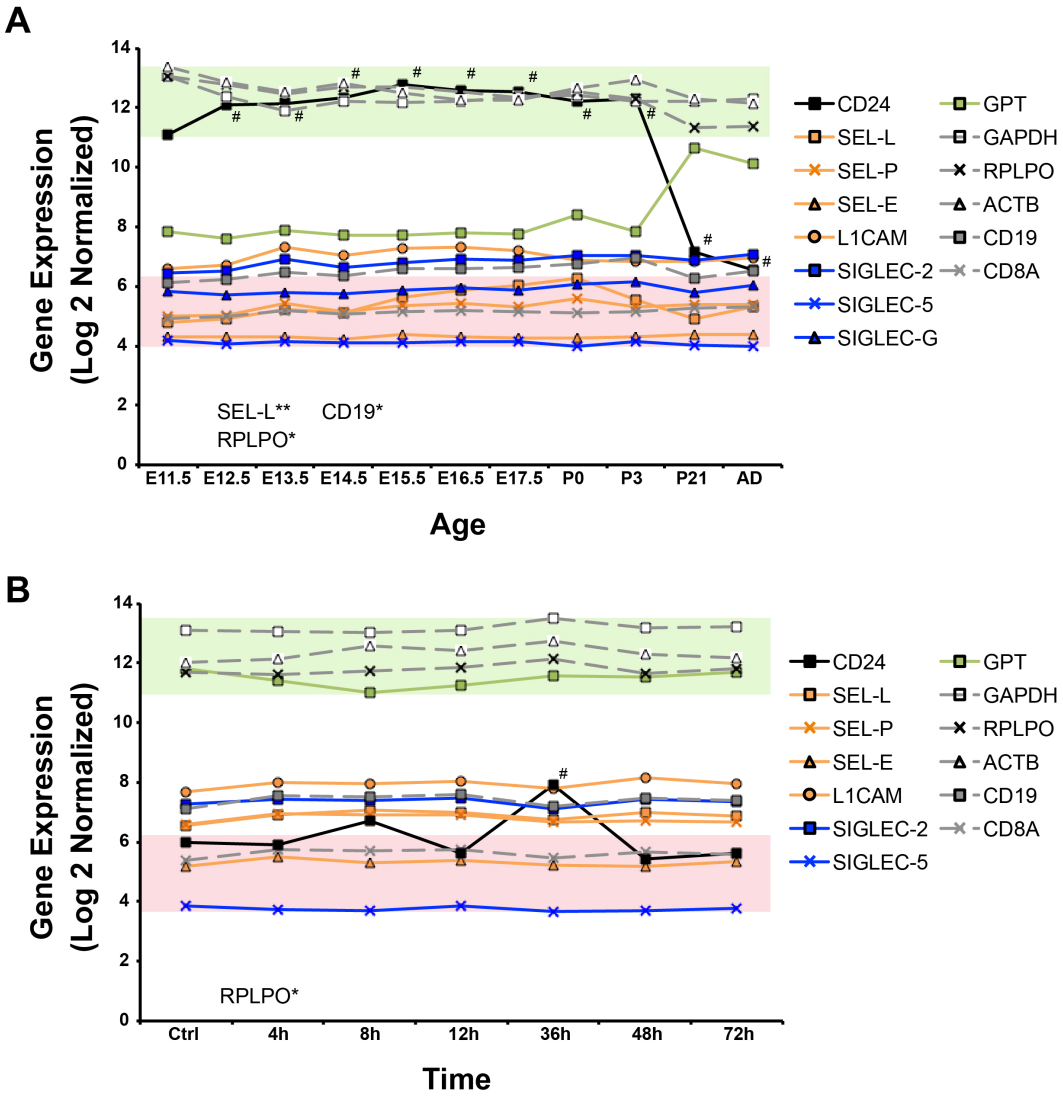

Figure 2.5. *CD24*, CD24 ligand and lineage marker expression during liver development and post-partial hepatectomy. Data show expression of *CD24* (black), known CD24 ligands (orange), Siglecs (blue), lineage markers (green), and normalizer genes and non-lineage markers (grey); n=2. (**A**) Liver development is divided into Embryonic (E) and Post-natal (P) periods with numbers indicating days where P0 is day of birth and AD is adulthood. (**B**) Samples from liver are divided into pre-operative (Ctrl) and post-operative samples denoted by hours post-hepatectomy. Significant changes in CD24 expression compared to the earliest stage shown per panel by 1-way ANOVA and Tukey post-hoc analysis $^{\#}P<0.05$. Genes with significant positive correlation to CD24 indicated within graph * $P<0.05$, ** $P<0.01$.

Gain in *GPT* expression is consistent with the shift in liver function from hematopoietic cell development in the fetal liver (35) to metabolic regulation in the post-fetal liver (195) providing an overall indicator of the progression of liver maturation.

As CD24 expression is frequently associated with highly proliferative cells, or as a marker of cells that are more stem-cell like, I analyzed the expression of *CD24* in liver responding to partial hepatectomy.

I found that after partial hepatectomy *CD24* expression remains low, comparable to that of normal adult liver, except for a brief increase at 36h (**Figure 2.5B**). The expression levels of CD24-associated ligands are likewise unaffected by surgical resection of the liver and remained low or absent. *CD24* expression did not correlate with any known ligands.

2.4 Chapter 2 Discussion

This is the first comprehensive analysis of CD24 regarding its sequence homology across species, and expression in multiple tissues and developmental states. Although the mature CD24 peptide is only between 26 and 41 residues, depending on the species from which it is isolated, I was able to generate a consensus sequence among 56 disparate species which highlights the constraints on CD24 sequence diversity among species Moreover, using transcriptomic data covering the development of multiple cell types I was able to link the dynamic regulation of *CD24* expression in the murine model with putative ligands or, in some cases, suggest that novel ligands may exist in tissues that do not express any of the known ligands.

Analysis of the predicted structure of the consensus mature peptide sequence did not reveal any secondary structure for CD24. As such, CD24 may be considered an intrinsically disordered protein. Intrinsically disordered proteins represent a comparatively new paradigm in understanding protein structure and the suggestion is that many proteins exist without a defined secondary or tertiary structure as a basis of their molecular function (196). Protein functions thought to depend on intrinsic disorder include flexible linker domains and phosphorylation sites (196, 197). Given that CD24 is heavily glycosylated in its mature form, it is also plausible that this disorder gives the mature protein additional flexibility to maximize its glycosylation potential through minimizing steric interactions. The glycosylations may impose order on the structure, thereby making structure prediction from the amino acid sequence alone not possible.

As mentioned, the amino acid sequence of CD24 possesses conserved glycosylation sites, as well as a proline-rich domain near the C-terminal region of the

mature peptide. The conservation of glycosylation sites strongly suggests that they are critical regions that define the biological activity of CD24, including the localization of CD24 to the extracellular surface of the plasma membrane. Interestingly, the sites and degree of glycosylation can also vary within and between species. For example, the comparison of CD24 between humans and mouse reveals human CD24 is enriched in Ser and Thr, and missing two Asn residues, compared to mouse (6). This may result in greater O-linked and fewer N-linked glycosylations. The mature core protein only contributes approximately 3.5 kDa with the remaining and variable mass of CD24 is made up by differing glycosylations (6, 14). Thus, while the presence of multiple potential glycosylation sites is maintained, the number and type varies in a cell- and species-dependent manner.

Physically, the gain or loss of these glycosylation sites may have a significant impact on the size or shape of the mature CD24 peptide. O-linked glycans may contribute up to 2.5Å to total protein length (198). Thus, mouse CD24 would be predicted to extend at least 10Å beyond the plasma membrane. The presence of significantly more O-linked glycosylation sites in the human sequence suggests that it may be held in a more rigid conformation and extend even further from the cell surface. The evolution of the conserved glycosylation sites in CD24 suggests that the function of the protein is critically dependent on its status as a glycophosphoprotein, with additional flexibility depending on the nature of the individual glycosylations.

Functionally, CD24 has been associated with a wide range of biological processes. Gene ontology annotation by NCBI has associated mouse CD24 with 59 processes, including apoptotic signalling, cell migration, adhesion, lipid homeostasis, cell

proliferation and neuronal development. To analyze the expression of CD24 over the course of cellular development, I chose to examine published expression data from specific cell types and whole tissues, where roles for CD24 have been identified or could be predicted based on the function of the tissue. In addition, I selected transcriptomic datasets with well-defined cellular stages isolated by fluorescence-activated cell sorting (FACS) or whole tissues isolated at multiple times over the course of development.

As expected, I observed a dynamic regulation of *CD24* expression during B cell development, and I have clearly found that there is dynamic expression in T cell development. In both B and T cells, *CD24* expression is high in immature populations and declines or is absent in mature cells. My data also support previous observations that DCs demonstrate lineage-dependent expression of *CD24* where it functions as a co-stimulator molecule for the specific activation of both $CD4^+$ and $CD8^+$ T cells (199).

In my analysis of whole tissues, I found that *CD24* was not regulated as dynamically as compared to isolated cells, which likely reflects the presence of multiple types of cells at multiple stages of development, each contributing to the total observed expression level. I observed high levels of *CD24* expression in the major immunologically privileged sites including the testes, ovaries and cornea, which did not change substantially over the course of development. These results suggest that CD24 is actively maintained through development into maturity. In contrast, I found that in brain and liver tissue, *CD24* is highly expressed during fetal development, but drops rapidly after birth and is either lost, or maintained at substantially diminished levels after maturity. Interestingly, in liver, *CD24* expression remains suppressed even following surgical resection during which time liver cells rapidly proliferate to reconstitute organ

volume. The regrowth of liver, however, involves mature hepatocytes rather than relying on the proliferation and differentiation of naïve or stem cell populations (195). As such, it may be that CD24 is not involved in regulating proliferation *per se*, but is involved in organizing or moderating the growth and development of undifferentiated or stem-cell like populations into mature tissue. This hypothesis is consistent with recent data showing that CD24 expression levels mark reprogramming-responsive cells during pluripotent stem cell development (200).

CD24 is also associated with regulating homeostatic proliferation and fate determination (14, 15). The role of CD24 in regulating matrix remodelling and stromal proliferation in corneal tissue (189) and in regulating similar processes in adult brain and epithelial tissues (201) suggests that CD24 may be a more generalized regulator of cell fate, by controlling the number and rate of cells that are allowed to proliferate and differentiate into mature tissues, and thus its expression is maintained in tissues where this capacity is maintained. In contrast, CD24 expression is not maintained in other self-renewal processes, such as in liver regeneration that is dependent on the division of mature cells.

The association of CD24 with its known ligands is similarly complex to its known cell-type specific roles, with many different tissue-specific interactions. My analysis suggests that there may be novel associations between known ligands, or that novel ligands exist in some tissues. For example, there is a correlation between *CD24* expression and *Siglec-G* and *Siglec-2* (*CD22*) in B cells. At present, the ligand for CD24 in B cells is unknown but given the known association between CD24 and Siglec-G in DCs, it is a likely candidate in B cells. Furthermore, interaction of CD24 with Siglec-2,

another member of the Siglec family, warrants additional investigation. In decidual tissue, *L1CAM* expression is more closely related to *CD24* expression than other potential ligands. The interaction between L1CAM and CD24 has only been shown in neurons, but their co-expression in these tissues suggests it is possible this interaction may occur in the decidua during gestation.

As CD24 is GPI-linked and cannot intrinsically signal through the plasma membrane, it must be associated with *cis*-acting elements to propagate signals into the cell on which it is expressed. However, CD24 can engage in *trans* and *cis* interactions simultaneously. For example, the *cis* interaction of CD24 with Siglec-G (human Siglec-10) along with the *trans* interaction with HMGB1 can down-regulate the damage-induced immune response (29). Future discovery of CD24 ligands must include an analysis of both *cis* and *trans* ligands.

Overall, I have also shown that the CD24 protein exists in an intrinsically disordered state and that the most evolutionarily constrained regions are related to sites of N- and O-linked glycosylation, which mediate CD24-ligand interactions and possibly affect the protein structure. Moreover, *CD24* is dynamically expressed in multiple tissues throughout cellular development in the mouse model. The regulation of CD24 expression is not necessarily related to cell proliferation, but is more likely associated with developmental maturity. Furthermore, *CD24* expression across tissues and cell types is not well correlated with any given known CD24 ligand, indicating roles for numerous ligands in mediating the biological activity of CD24. Overall, the data presented here are a valuable resource for further elucidation of CD24-mediated biology, including ligand discovery.

Chapter 3: CD24 stimulation is associated with the formation of plasma membrane-derived microvesicles

3.1 Section introduction

The CD24 cell surface receptor lacks an intracellular signalling domain. Despite this, it has been shown conclusively antibody-mediated engagement of CD24 can induce the activation of the Src-family tyrosine kinases (SFKs) (61, 62), calcium influx (8), and leads to activation of multiple mitogen activated protein kinase (MAPK) signalling intermediates with a variety of downstream consequences. In human and mouse B cells, CD24 signalling results in the activation of the MAPK Jnk, and initiates the caspase cascade resulting in cell death (61, 62).

The dynamic nature of the rise and fall of CD24 expression in B cell maturation defines a signature I used to identify 39 co-expressed genes (60). Among these genes, I found significant associations with cytoskeletal organization and vesicle trafficking processes, suggesting that CD24 may be associated with these events. Other GPI-anchored receptors are known to initiate signalling events via their endocytosis, such as with CD48 (202), and CD55 (203). Thus, here I have examined the possibility that CD24 operates through endocytosis and/or exocytosis processes.

I first validated the use of the mouse WEHI-231 B cell lymphoma cell line as a model for CD24-mediated apoptosis in B cells. I found that that CD24 expression is highly dynamic following Ab-mediated stimulation within 1 hour, however the inhibition of endocytosis and exocytosis did not influence the expression dynamics of CD24. Instead, CD24 activation was associated with the formation of plasma membrane-derived

EVs, with characteristics consistent with classifying them as MVs. Furthermore, I found that these MVs are predominantly CD24-positive. Once stimulated, populations of B cells were capable of exchanging CD24 between stimulated cells. As the GPI-anchor is intrinsic to the plasma membrane, and required for CD24 retention this process is likely mediated through the membrane incorporation of CD24-bearing MVs exchanged by these cells. While these findings do not identify a cell-intrinsic signalling mechanism, or an *in cis* signalling partner, they do identify a novel mechanism through which CD24 signalling may be capable of affecting cell behaviour in an endocrine or paracrine-similar fashion.

3.2 Materials and Methods

3.2.1 Cell Culture

All materials for cell culture were obtained from Life Technologies (Carlsbad, CA) unless otherwise indicated. Isolated bone-marrow derived immature B cells and the BALB/c x NZB mouse WEHI-231 pre-B cell lymphoma cell line (ATCC, Manassas, VA) were maintained in RPMI 1640 media supplemented with 10% heat-inactivated fetal bovine serum (FBS), 1% antibiotic/antimycotic (100 units of Penicillin, 100 units of streptomycin and 0.25 μg/mL amphotericin B) 1 % sodium pyruvate and 0.1% β-mercaptoethanol (complete media) at 37°C and 5% CO_2.

3.2.2 Primary Bone Marrow B Cell Isolation

Male C57BL/6 mice (3 to 6 weeks of age) were sedated using isoflurane and euthanized via cervical dislocation following Memorial University of Newfoundland animal care, and CCAC guidelines. Femurs were removed and bone marrow was flushed out with Quin saline (QS; 25 mM NaHEPES, 125 mM NaCl, 5 mM KCl, 1 mM $CaCl_2$, 1 mM Na_2HPO_4, 0.5 mM $MgSO_4$, 1 g/L glucose, 2mM Glutamine, 1 mM Sodium pyruvate, 50 μM 2-Mercaptoethanol, pH 7.2), using a 21-gauge needle. Single-cell suspensions were produced using a 100 μm nylon mesh. The EasySep Mouse B Cell Isolation Kit (cat no. 19854, StemCell Technologies, Vancouver, BC, Canada) was used to enrich bone marrow isolates following the manufacturer's protocol. Fc-receptors were blocked on the B cells in this isolation using anti-mouse CD16/CD32 (Fc γ III/II receptor) Abs. All experiments and analyses were performed on total isolated bone marrow-derived B cells.

3.2.3 Flow Cytometry

Cells were resuspended in 0.2 µm-filtered Phosphate Buffered Saline (PBS; 18.6 mM $NaH_2PO_4•H_2O$, 84.1 mM Na_2HPO_4, 1.5 M NaCl) containing 1% heat-inactivated fetal bovine serum (Thermo Fisher) (refered to as FACS buffer) unless stated otherwise. Flow cytometry data were collected on a FACSCalibur flow cytometer using CellQuest Pro v4.0.2 software (BD Biosciences, San Jose, CA) or a FACSAria II cell sorter using FACSDiva v8.0 software (BD Biosciences), at the Medical Education and Laboratory Support Services or the Cold-Ocean Deep-Sea Research Facility of Memorial University, respectively. Analysis was performed using FlowJo v10.0.5 (Tree Star, Ashland, OR.). Cell death experiments using Annexin V and Propidium iodide (PI) were analyzed ungated while CD24 expression was analyzed after gating on the live cell population based on FSC/SSC.

3.2.4 Apoptosis Assay

3.2.4.1 Annexin V / PI staining:

WEHI-231 cells ($5x10^5$ cells/mL) in complete media were treated for up to 24 h with either functional grade 10 µg/ml primary mAb M1/69 rat anti-mouse CD24 (cat no. 16-0242-85) or 10 µg/mL matching primary isotype Ab (cat no. 16-4031-85) both from eBioscience (San Diego, CA), or with primary Abs that had been pre-incubated with 5 µg/ml goat anti-rat secondary Ab (secondary; cat no. 112-005-003, Jackson ImmunoResearch, West Grove, PA). Primary and secondary antibodies were always pre-incubated prior to addition to cells at a 2:1 ratio to ensure efficient cross-linking of

primary Ab and to ensure no excess secondary Ab was present. Furthermore, I have confirmed that isotype pre-incubated with secondary Ab did not bind to either WEHI-231 or primary B cells. Cells with treatment times less than 24 h were centrifuged to remove Ab-treated media and then resuspended in complete media and incubated at 37˚C for a total of 24 h and then analyzed for cell death. For staining, cells were resuspended in Annexin V binding buffer (10 mM HEPES buffer, 70 mM NaCl, 2.5 mM $CaCl_2$) at pH 7.4. Apoptosis was measured using AnnexinV-Alexa488 and PI using the Dead Cell Apoptosis kit (Life Technologies) following the manufacturer's instructions. Cells were analyzed by flow cytometry on a FACSCalibur flow cytometer using CellQuest Pro v4.0.2.

3.2.4.2 Caspase activation:

Cells were treated for up to 3 h as described above. Thirty minutes prior to the indicated time, cells were incubated with 5 μM CellEvent^{Tm} Caspase-3/7 Green Detection Reagent (Life Technologies) following the manufacturer's protocol, and then analyzed by flow cytometry on a FACSCalibur flow cytometer using CellQuest Pro v4.0.2..

3.2.5 CD24 surface expression

WEHI-231 cells ($5x10^5$ cells/ml in QS) were rested at 37°C for 15 min. Cells were then incubated with 10 μg/ml of M1/69 anti-mouse CD24 Ab that had been pre-incubated with 5 μg/ml of biotinylated goat-anti-rat secondary Ab for 1, 5, 15, 40 or 60 min, or left untreated. Cells were arrested in 3 mL of ice-cold FACS buffer and then washed with

FACS buffer followed by staining with 0.25 µg streptavidin-linked FITC (cat no. 11-4317-87, eBioscience) for 30 min in FACS buffer at 4°C. Cells were washed 3 times with FACS buffer and then analyzed by flow cytometry. To determine if CD24 epitopes were saturated by the addition of the pre-incubated primary and secondary Ab, cells were stimulated as above, or left untreated, followed by fixation with 4% paraformaldehyde for 20 min at room temperature, followed by 3 washes with FACS buffer. Fixed, untreated cells (control) were incubated with 10 µg/ml of M1/69 anti-mouse CD24 Ab that had been pre-incubated with 5 µg/ml of biotinylated goat-anti-rat secondary Ab for 30 min at 4°C. All cells were then stained with 0.25 µg streptavidin-linked FITC and with 0.06 µg M1/69-APC (cat. no. 17-0242-80, eBioscience) for 30 min at 4°C. Cells were then washed with FACS buffer and analyzed by flow cytometry on a FACSCalibur flow cytometer using CellQuest Pro v4.0.2.

3.2.6 Inhibition of Endocytosis and Exocytosis

WEHI-231 cells, resuspended at $5.0x10^5$ cells/mL in QS, were pre-incubated in 200 µM Pitstop 2 (Abcam, Cambridge, UK), 50 µM Dynasore (Abcam), 40 µM Exo1 (Abcam), 10 µM Brefreldin A (Life Technologies) or vehicle control (DMSO) at 37˚C for 30 min and then treated with primary and secondary Ab, as above, with inhibitor concentrations maintained at half the original concentration, for up to 1 h.

3.2.7 CD24 exchange

Isolated bone marrow B cells or WEHI-231 cells ($5x10^5$ cells/ml in QS) were resuspended as above and were rested at 37°C for 15 min. Cells were then incubated for

15 min at 37˚C with 10 µg/mL M1/69 anti-CD24 Ab that had been pre-incubated with 5 µg/mL biotinylated secondary Ab and either Streptavidin-FITC (0.25 µg) or Streptavidin-eFluor660 (0.125 µg, cat no. 50-4317-80, eBioscience). Cells were centrifuged at 500 x g for 5 min to remove unbound Ab and then resuspended in QS. Equal amounts of FITC-labelled and eFluor660-labelled cells were mixed at either on ice (control) or at 37˚C for the indicated times. Cells were washed with FACS buffer and then analyzed by flow cytometry on a FACSCalibur flow cytometer using CellQuest Pro v4.0.2.

3.2.8 Transmission electron microscopy

WEHI-231 cells were stimulated as described above and then centrifuged and resuspended in Karnovsky fixative for 24 h. TEM was performed by the Medical Education and Laboratory Support Services facility of Memorial University according to standard protocols. Briefly, 85 nm resin-embedded sections were mounted on 300 mesh copper grids, and then stained with 3% Uranyl acetate in a 30% ethanol. Grids were examined using a JEOL 1200 EX electron microscope (JEOL, Peabody, MA) and images captured using a SIA-L3C digital camera (SIA, Duluth, GA).

3.2.9 Isolation of EV

WEHI-231 cells in QS were left untreated, or stimulated as described above for 15 min or 60 min at 37°C with either 10 µg/ml of M1/69 anti-mouse CD24 Ab that had been pre-incubated with 5 µg/ml of biotinylated goat-anti-rat secondary Ab. Enrichment of EV was performed similarly to previously published studies (132, 204). All steps were

performed at 4˚C. Briefly, cells were centrifuged for 5 min at 400 x g to pellet cells then the supernatant was centrifuged for 5 min at 2000 x g to pellet cell debris. M1/69 anti-mouse CD24 Ab (10 µg/ml) pre-incubated with 5 µg/ml of biotinylated goat-anti-rat secondary Ab was added to the supernatant from untreated cells, when indicated. The supernatant was centrifuged for 1 h at 16,800 x g to pellet EV. The pelleted EV were resuspended in a residual volume of 25 µl QS, and 25 µL of 2x Annexin V binding buffer was added. EV were stained with 5 µl of Annexin-V Alexa 488 and 0.06 µg streptavidin-APC (eBioscience). EVs were analyzed on the FACSAria II with 0.2 µm and 0.4 µm beads (Bangs Laboratories, Inc., Fishers, IN) used to establish a sizing gate for EV using SSC following established protocols (205, 206).

3.2.10 Statistical Analysis.

Statistical analyses were performed in R v3.0.2 (167). Student's t-test was used to determine differences between 2 groups. ANOVA was used to determine differences between more than 2 groups followed by either *a priori* analysis using a generalized linear model (207) for more than two groups or Student's t-test for two groups with significance given in each figure. Tukey HSD was used for *a posteriori* analysis of all pairwise comparisons if the ANOVA was found to be significant.

3.3 Results

3.3.1 Antibody-mediated engagement of CD24 causes apoptotic cell death in the WEHI-231 B cell line.

In order to test the hypothesis that engagement of CD24 may regulate vesicle-mediated transport or associated processes, I first validated that engagement of CD24 would induce apoptosis, a well-established function of CD24, in the WEHI-231 B cell lymphoma cell line, which expresses high level of CD24. To mimic ligand engagement, the cells were treated for 24 h with primary rat anti-mouse CD24 Ab or isotype antibody either with or without additional cross-linking induced by pre-incubating the primary Ab with a secondary anti-rat IgG Ab. The secondary Ab was added to increase the cross-linking of CD24 as well as to increase the avidity of anti-CD24 Ab binding.

I found that WEHI-231 cells did not undergo apoptosis in response to the isotype alone or with secondary Ab, or anti-CD24 primary Ab engagement alone but did undergo significant induction of apoptosis when stimulated with both primary and secondary Ab (**Figure 3.1A-B**). In addition, enhanced clustering with primary and secondary Ab, but not with primary Ab alone, significantly increased very late apoptotic or necrotic cell death.

CD24 crosslinking has been shown to activate multiple caspases, including Caspases-2, -3, -7 and -8. Similar to previous reports (62), I found that there was significantly upregulated caspase-3/7 activity in WEHI-231 cells after 3 hours of Ab stimulation (**Figure 3.2A**). Similarly, caspase-3/7 activity was significantly upregulated

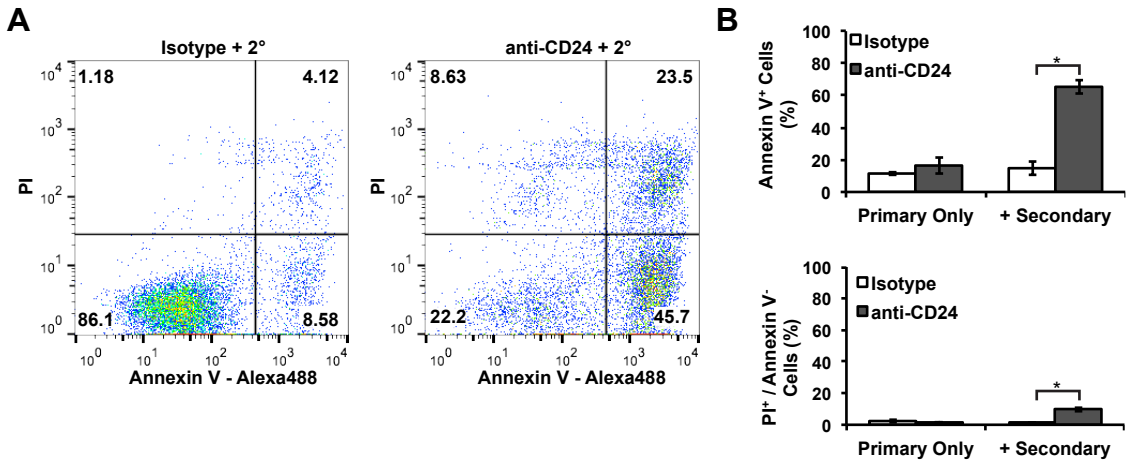

Figure 3.1. Enhanced crosslinking of CD24 induces cell death in the WEHI-231 B cell line. Cells were treated with isotype control or anti-CD24 primary Ab, with or without secondary for 24 h. Cell death was assessed after 24 h of antibody stimulation using Annexin V-Alexa488 and Propidium iodide staining. (A) Shown are representative dot plots, and (B) mean ± SEM of percent Annexin V-positive apoptotic cells or necrotic Annexin V-negative, PI-positive cells, n=3, Student's paired t-test, * $P< 0.05$, ** $P<0.01$

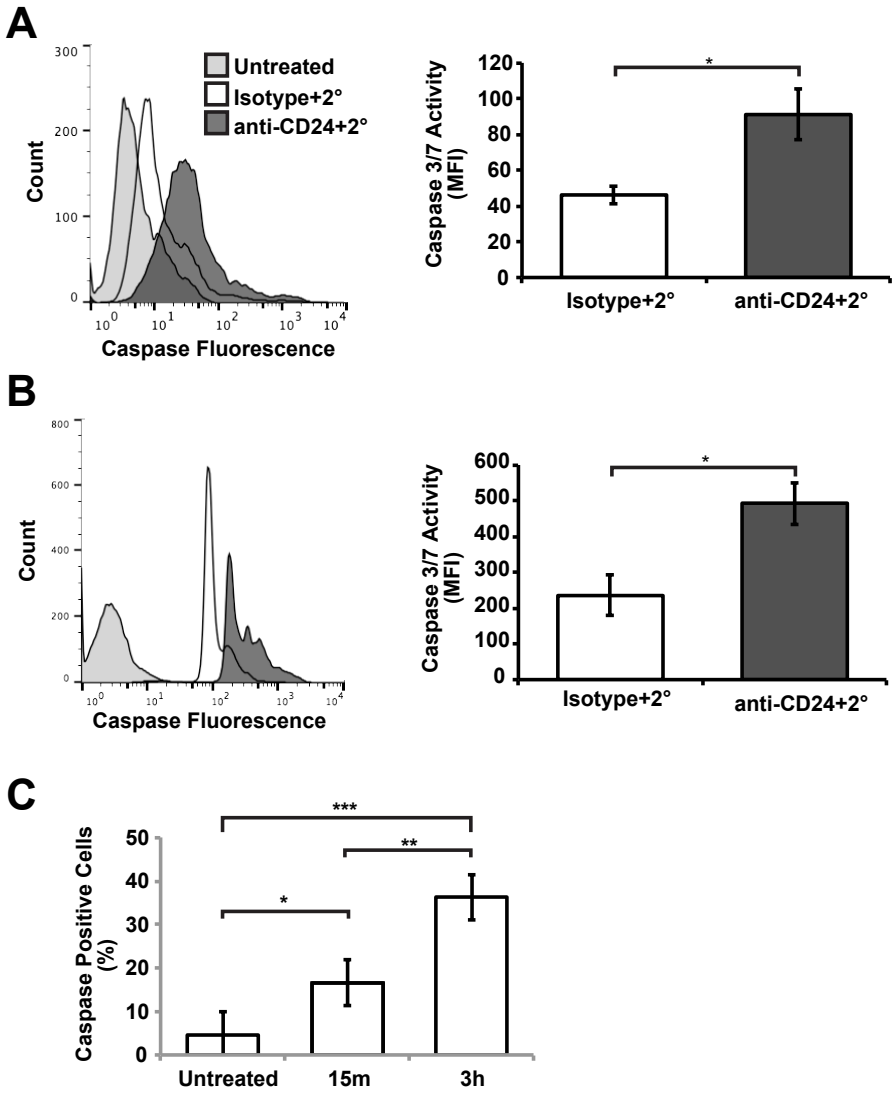

Figure 3.2. CD24 engagement activates caspase-3/7 in WEHI-231 and primary B cells. (A) WEHI-231 cells or (B) Primary cells were treated as for Figure 3.1. Shown are representative histograms of caspase-3/7 activation (left panel) and the mean ± SEM of the mean fluorescent intensity (right panel), n=3, Statistical significance was assessed using Students' paired t-test * $P<0.05$, ** $P\leq0.01$. (C) WEHI-231 cells were removed from the Ab-treated media after 15 min of stimulation and replaced with untreated media for 2 h 45 min, or left with Ab for 3 h. Shown is the mean ± SEM of the mean fluorescent intensity, n=3, statistical significance was assessed using a 1-way ANOVA followed by *a posteriori* analysis by Tukey post-hoc, * $P<0.05$, ** $P<0.01$, *** $P<0.001$.

in primary cells at the same time point (**Figure 3.2B**) demonstrating that CD24 mediated cell death operates in an analogous fashion in WEHI-231 cells to that of primary cells.

I next investigated whether prolonged engagement with anti-CD24 Ab stimulation was required to induce caspase-3/7 activation, by removing unbound Ab from WEHI-231 cells after 15 min of stimulation. I found with only 15 min of Ab exposure, there was significantly less caspase activity after 3 h, compared to cells exposed continuously to Ab (**Figure 3.2C**). These data demonstrate that effect CD24-mediated apoptosis induction requires prolonged, engagement in conditioned media, rather than a transient engagement, to induce the maximum amount of caspase 3/7 activation.

Together, these data demonstrate that CD24-induced cell death occurs in a comparable fashion between WEHI-231 cells and primary *ex vivo* bone marrow cells (33, 61) and that WEHI-231 can serve as a model for elucidating the function of CD24 in B cells.

3.3.2 Ab-mediated engagement of CD24 dynamically regulates CD24 surface expression

Engagement of receptors by their ligand can cause changes to their own surface expression, which may be mediated by vesicle formation and/or membrane re-organization, as exemplified by the BCR (208, 209). Therefore, I next examined if expression of CD24 surface protein was altered following Ab-mediated engagement.

I found that WEHI-231 cells responded with a time-dependent, dynamic change in CD24 surface expression. I have previously shown that primary cells increase their expression of CD24 over the course of 1 h, following antibody-mediated CD24

stimulation (60). In comparison, WEHI-231 cells showed an immediate loss of CD24 expression by 1 min before recovering baseline CD24 surface expression by 15 min and then further increasing the amount of cell surface protein over the course of 60 min (**Figure 3.3 A-B**).

I confirmed that the changes to CD24 surface expression was not an artefact of the short incubation times by determining if there were any epitopes available for binding of anti-CD24 Ab after stimulation. To do this, cells were fixed after treatment and then incubated with an APC-conjugated anti-CD24 antibody, which will label any unbound epitopes (**Figure 3.3C**). CD24 on untreated cells was readily detected by the anti-CD24-APC (**Figure 3.3D**, APC only). However, this binding was significantly diminished in cells that had previously been treated with anti-CD24 primary plus secondary Ab (**Figure 3.3D**). Furthermore, the degree of binding of the anti-CD24-APC Ab did not vary with the different incubation times with stimulating Ab indicating that the surface CD24 had been saturated by the stimulating Ab at all times examined.

3.3.1 The dynamic regulation of CD24 protein expression does not depend on classical endocytosis or exocytosis processes.

To test the hypothesis that CD24 is associated with endocytosis and/or exocytosis, I disrupted these processes in WEHI-231 cells through chemical inhibition. Primary cells were not able to withstand treatment with the chemical inhibitors without undergoing cell death so these cells were not analyzed further. Endocytosis was disrupted

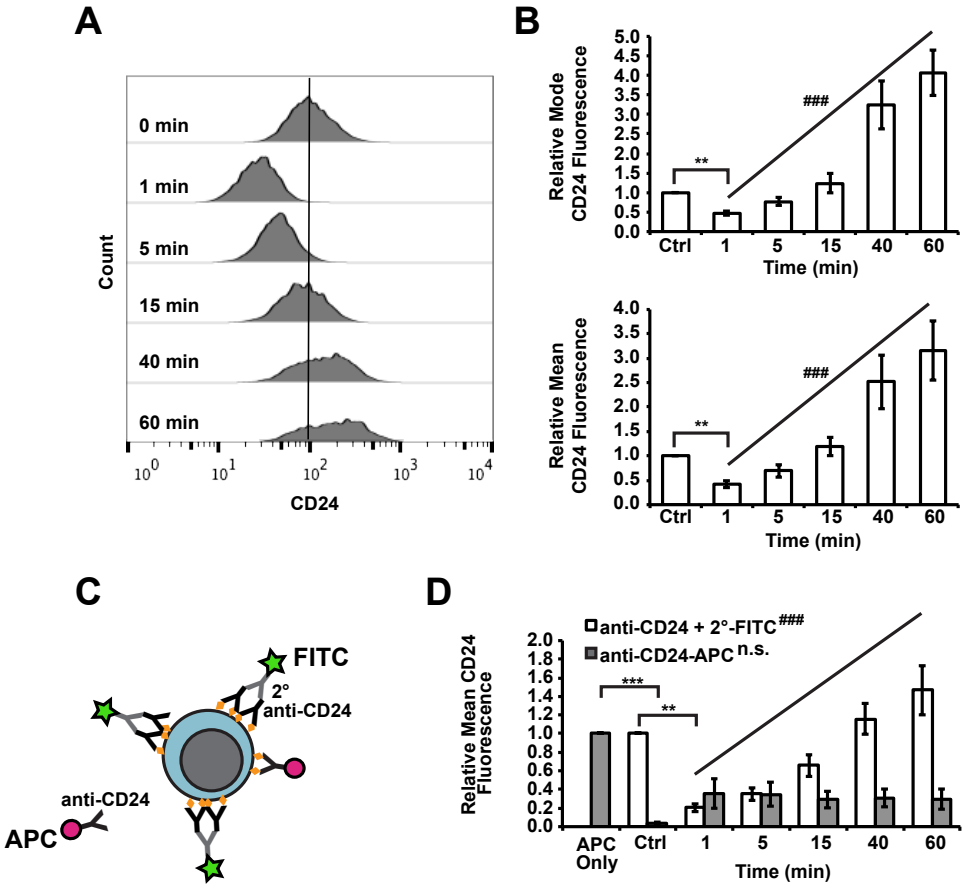

Figure 3.3. CD24 protein expression is dynamically regulated after CD24 engagement in WEHI-231 cells. (A) WEHI-231 cells were stimulated for the indicated times with anti-CD24 primary Ab and biotinylated secondary Ab. Surface CD24 expression was assessed using streptavidin-FITC. Shown are representative histograms. (B) Mean ± SEM of the relative mean or the modal fluorescence intensity, n=3, statistical significance was assessed using a 1-way ANOVA followed by *a priori* analysis of 0 min to 1 min via Student's one-tailed, uneven variance t-test * $P<0.05$, and from 1 min to 60 min via generalized linear model regression analysis. ### $P<0.001$. (C) Schematic of CD24 epitope availability assessment. Cells were stimulated for 1 min to 60 min with anti-CD24 primary Ab and biotinylated secondary Ab, followed by detection with streptavidin-FITC (green star) as in A and B. Cells were then fixed and available CD24 epitopes (orange diamond) detected by addition of anti-CD24 Ab directly conjugated to APC (red circle). (D) WEHI-231 were stimulated for the indicated times as above and relative surface CD24 expression (white) and free epitopes (grey) detected. The mean ± SEM of the relative mean fluorescence intensity, n=3, statistical significance was assessed using a 1-way ANOVA followed by *a priori* analysis of 0 min to 1 min via Student's one-tailed, uneven variance t-test ** $P<0.01$, *** $P<0.005$, and from 1 min to 60 minvia generalized linear model regression analysis. n.s. not significant, ### $P<0.001$.

by pre-incubation with Pitstop2, which disrupts both clathrin and non-clathrin mediated endocytosis, or Dynasore, which prevents dynamin-mediated internalization. Analysis of surface expression showed that Pitstop 2 pre-treatment alone significantly increased CD24 protein expression on the cell surface (**Figure 3.4A**). However, Pitstop2 pre-treatment did not prevent the loss or subsequent increase in CD24 surface expression. Treatment with Dynasore had no effect on either the decrease or increase in CD24 surface expression in response to Ab-mediated cross-linking (**Figure 3.4A**).

To determine if the dynamic changes in CD24 surface expression depend on exocytosis, a process that regulates the formation of exosomes (210) and synaptic vesicle release (211), cells were pre-treated with the ER to Golgi transport inhibitors Exo1 or Brefeldin A. I found that treatment with either of these inhibitors did not alter CD24 dynamics at any time point examined, indicating that CD24 surface protein levels are not regulated via classical exocytosis of newly packaged vesicles (**Figure 3.4B**).

3.3.2 CD24 expression is not a function of endocytosis or exocytosis

Since neither endocytosis nor exocytosis were involved in regulating the levels of CD24 surface expression, I next analyzed if CD24 could be lost from the cell surface by the generation of plasma-membrane derived EV released into the extracellular environment. I first analyzed changes in size and surface complexity of B cells using flow cytometry following Ab-mediated crosslinking. Both WEHI-231 cells and primary cells showed a large increase in subcellular-sized objects within 15 min of CD24 engagement (**Figure 3.5A**), a time-point that is generally considered too early to be

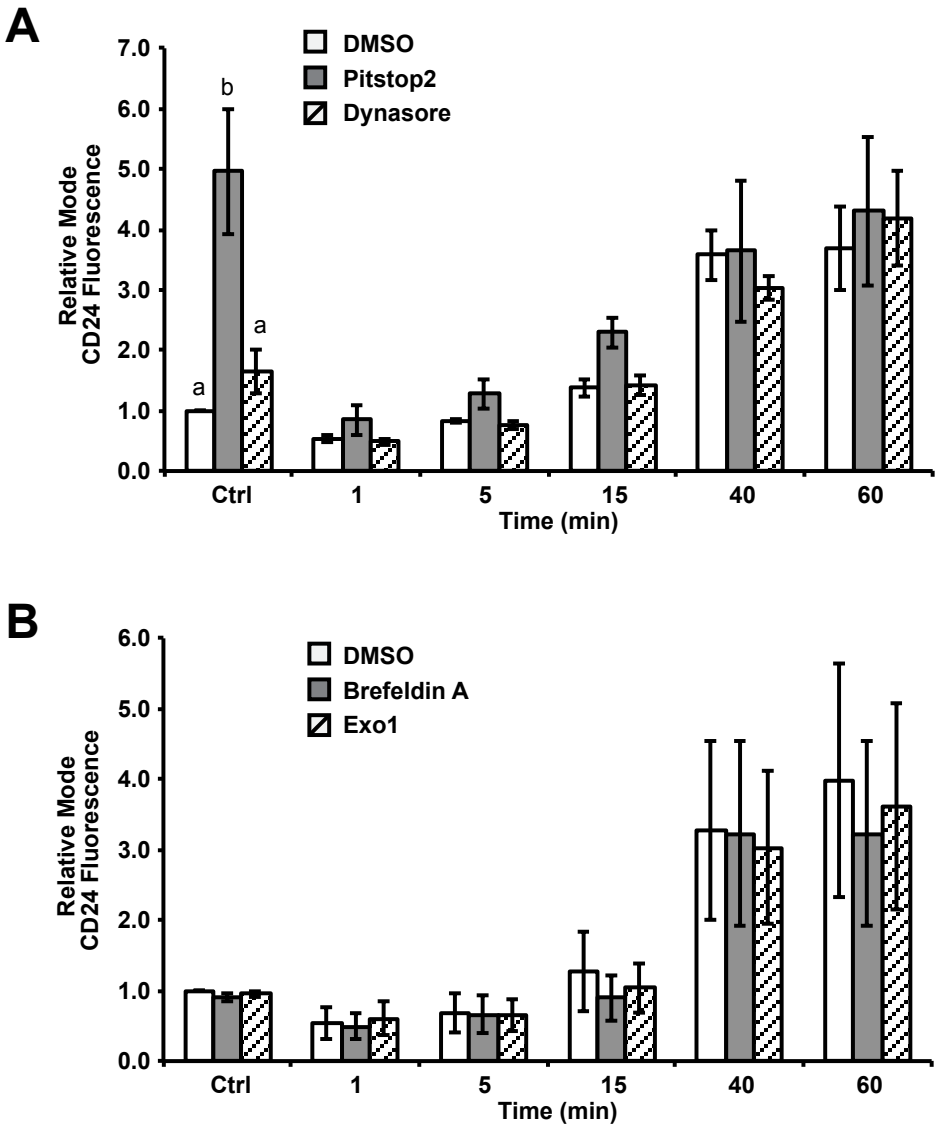

Figure 3.4. **Changes to CD24 cell surface expression are not dependent on classical endocytosis or exocytosis.** WEHI-231 cells were pre-treated with (A) Dynasore, or Pitstop2, and (B) Brefeldin A, or Exo1. DMSO was used as a vehicle control in all cases. Cells were treated as described for Figure 3.3 and CD24 detected using streptavidin-FITC. Mean ± SEM of the relative modal fluorescence intensity relative to DMSO control treated (Ctrl) is shown, n=3, statistical significance was determined by *a priori* analysis of each time point using 1-way ANOVA, different letters represent different groups at $P<0.05$.

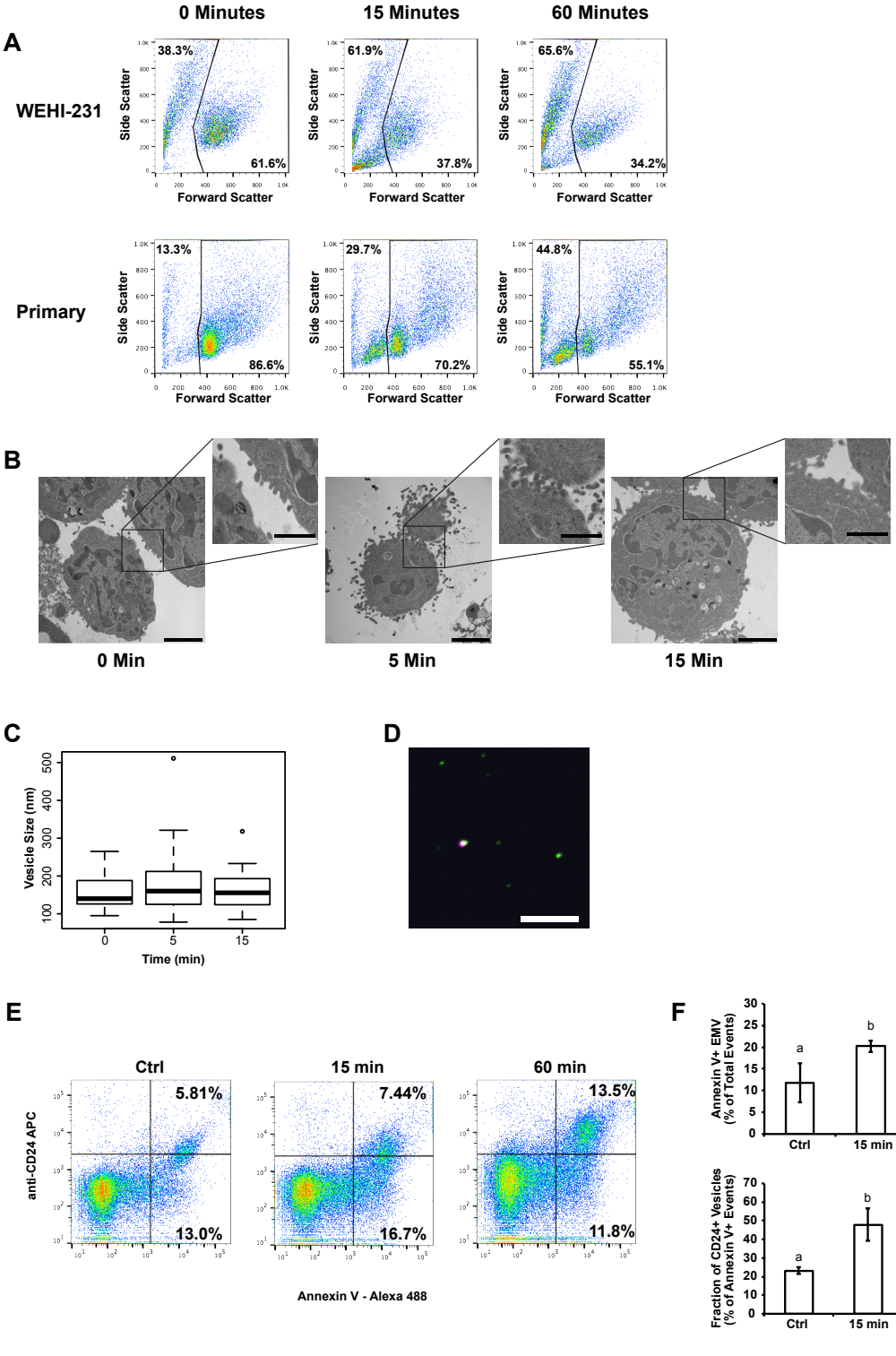
A
0 Minutes
15 Minutes
60 Minutes
WEHI-231
Primary
Side Scatter
Forward Scatter
38.3%
61.6%
61.9%
37.8%
65.6%
34.2%
13.3%
86.6%
29.7%
70.2%
44.8%
55.1%
B
0 Min
5 Min
15 Min
C
Vesicle Size (nm)
Time (min)
D
E
Ctrl
15 min
60 min
anti-CD24 APC
Annexin V - Alexa 488
5.81%
13.0%
7.44%
16.7%
13.5%
11.8%
F
Annexin V+ EMV (% of Total Events)
Fraction of CD24+ Vesicles (% of Annexin V+ Events)
Ctrl
15 min
60 min

Figure 3.5. **CD24 antibody-mediated cross-linking induces release of extracellular microvesicles.** (A) WEHI-231 and Primary B cells stimulated with primary and secondary Abs as described for Figure 3.1, for the indicated times. Shown are representative dot plots with the percentage of sub-cellular sized objects in the upper left corner, n=7-8 for primary cells, n=3 for WEHI-231. (B) Transmission electron micrographs of WEHI-231 treated with anti-CD24 primary and secondary Ab for the indicated times. Scale bar=2 μm for the main image and 1 μm for the inset. (C) Box-and-whisker plot of vesicle sizes observed from the TEM. A minimum of 3 images were analyzed with 17, 58 and 46 EV analyzed at 0, 5, and 15 min, respectively. No significant differences in EV size were found by 1-way ANOVA. (D) Microvesicles isolated from WEHI-231 cells after 15 min of treatment with anti-CD24 primary and eFluor660-labeled secondary Ab analyzed by confocal microscopy. CD24 (purple), Annexin V-Alexa488 (green), and DAPI (blue) were detected by confocal microscopy. Note: no DAPI-positive particles were observed. Scale bar= 10 μm. (E) Analysis of isolated microvesicles from WEHI-231 cells. Cells were left unstimulated for 60 min (ctrl) or stimulated with anti-CD24 primary and biotinylated secondary anti-rat Ab for 15 or 60 min. Representative dot plots of isolated vesicles were detected using AnnexinV-Alexa488 and streptavidin-APC, after gating on the EV-sized population, n=4. (F) Mean ± SEM of the total percentage of AnnexinV+ EV (upper panel) and the percentage of AnnexinV+ EV that are CD24+ (lower panel). n=4, significance was assessed via 1-way ANOVA followed by Tukey post-hoc test. Different letters represent significantly different groups at $P<0.05$.

associated with the generation of apoptotic bodies and would be prior to significant induction of caspase based on my data. In addition, the appearance of this sub-cellular fraction was coincident with the time frame showing dynamic changes in CD24 surface expression.

3.3.3 CD24 is associated with extracellular microvesicle formation.

To determine if WEHI-231 cells could produce EV in response to CD24 engagement, I used transmission electron microscopy (TEM) to image WEHI-231 cells after treatment with anti-CD24 primary and secondary Abs (**Figure 3.5B**). These images show that engagement of CD24 causes the generation of large numbers of small, plasma membrane-derived EV within 5 min. By 15 min (a time-point that is coincident with the appearance of large numbers of subcellular sized particles in the bulk population), the number of EVs closely associated with the cell was reduced.

As described in chapter 1, EVs are heterogeneous in both composition and size, ranging from 50 nm to above 1000 nm in diameter (212, 213). The EVs imaged by TEM ranged in size between 78 nm and 511 nm, with no significant change in size in response to CD24 engagement (**Figure 3.5C**). The morphology of these vesicles by TEM indicates that they are formed and released directly by budding from the PM, a defining characteristic of MVs (214). While a definitive surface marker for EV has not yet been identified they are unlike exosomes in that they are enriched in surface phosphatidylserine (75, 215), which can be detected by Annexin V binding. Thus, to further characterize the plasma-membrane derived vesicles, I viewed EV that has been

isolated from WEHI-231 cells after 15 min of CD24 engagement under confocal microscopy (**Figure 3.5D**). The isolated EV are sub-cellular sized and do not contain DNA as evidenced by their DAPI-negative character. Moreover, CD24 co-localized with Annexin V in a portion of these EV, demonstrating that the EV maintained the same orientation of surface proteins as the plasma membrane. When treated with Triton X-100, a non-ionic detergent that disrupts the plasma membrane, I observed an essentially complete loss of Annexin-V positive particles (data not shown), further demonstrating that these are membrane bound particles.

To quantify the number of EV that contain CD24, I analyzed isolated EV released after treatment of WEHI-231 cells using the FACSAria II, which can identify particles less than 1 μm in diameter. Using established strategies, I gated on particles in the size range of 0.2 to 0.4 μm and quantified the number of AnnexinV-positive and CD24-positive EV released after 15 or 60 min of treatment (**Figure 3.5E-F**). Overall, I found that supernatant from unstimulated cells contained an average of $6.9x10^5 \pm 3.1x10^5$ EV-sized particle after 60 min at 37°C (Figure 7E). After 15 or 60 minutes of Ab stimulation, an average of $5.1x10^5 \pm 4x10^4$ to $5.6x10^5 \pm 1.7x10^4$ EV-sized particles were detected, respectively (Figure 7E), however this was not significantly different from control cells when analyzed by one-way ANOVA ($P>0.05$). The technical limitations of the FACSAria II instrument limit EV detection to particles greater than 200-300 nm in diameter, thus EV counts from both conditions may be under-represented.

In contrast, Annexin V-positive particles, which are generated from and retain the orientation of the plasma membrane, increased significantly following 15 min and 60 min

of CD24 stimulation (**Figure 3.5F**). Moreover, the percentage of Annexin V-positive EV that carried CD24 increased significantly from 23.1 ± 1.9% in control cells to 47.8 ± 8.8% and 61.8 ± 3.5% after 15 min and 60 min, respectively **Figure 3.5F**). These findings show that engagement of CD24 promotes the formation of CD24-bearing EVs, in addition to altering the composition of EVs released by B cells.

3.3.4 CD24-bearing EV can transport CD24 between cells

EV can be taken up by other cells via multiple mechanisms to deliver both their intracellular and membrane bound cargo (104, 214). Therefore, I next investigated if the CD24-bearing EV generated in response to CD24 engagement can be taken up by neighbouring cells and thus potentially participate in cell-cell communication. I independently stimulated two different populations of WEHI-231 cells for 15 min with primary and secondary Ab and labelled each with either streptavidin-conjugated FITC or eFluor660. After removal of excess Ab, the differentially labelled cells were mixed together for up to 60 min at 37˚C. I found that upon mixing, there was a time- and temperature-dependent exchange of CD24 between both WEHI-231 cells and primary cells (**Figure 3.6A-B**). When WEHI-231 cells were mixed on ice (i.e. Ctrl), fewer than 5% were double-labelled. There was a statistically significant time-dependent increase in the number of cells containing both labels over 60 min of co-incubation (**Figure 3.6A**, right panel). In contrast, if the cells were paraformaldehyde-fixed prior to mixing, the exchange of CD24 between WEHI-231 cells was essentially abolished and did not vary with time (**Figure 3.6A**). Thus, the exchange of CD24 was dependent on active cellular

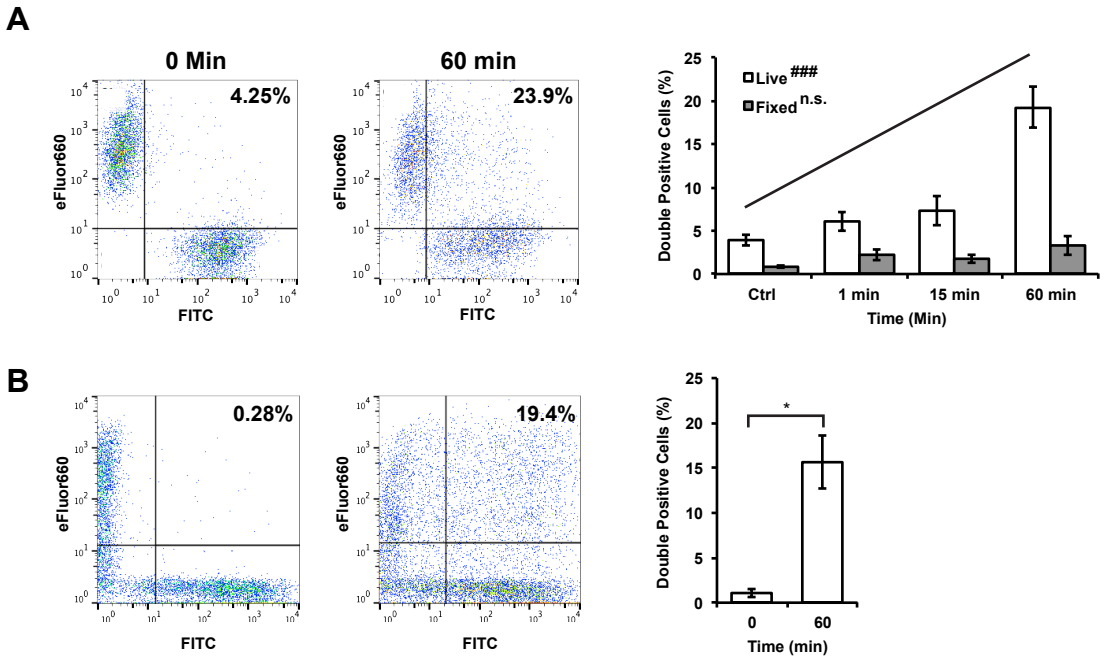

Figure 3.6. **CD24 protein is re-distributed within the B cell population in response to engagement of CD24.** (A) WEHI-231 cells were treated with anti-CD24 primary and secondary anti-rat Ab conjugated to either eFluor660 or FITC. The two populations of cells (live or fixed) were then mixed and left on ice or incubated at 37˚C for up to 60 min. Shown are representative dot plots (left panel) and mean ± SEM of the percent of double-positive cells (right panel), n=3, statistical significance was determined by 1-way ANOVA followed by generalized linear model regression analysis. $^{n.s}$ not significant, $^{###}$ P<0.001. (B) Primary B cells were treated with anti-CD24 primary and secondary anti-rat Ab. The two populations were mixed immediately before analysis, or were mixed for 60 min at 37˚C. Shown are representative dot plots (left panel) and the mean ± SEM of the percent double-positive cells (right panel), n=3, statistical significance was determined by Students' T-test, * P<0.05.

processes and not due to movement of the anti-CD24 primary Ab, secondary Ab, or streptavidin-conjugated fluorophore from one cell population to the other. I found that primary cells also exchanged CD24 when differentially labelled populations were mixed in a similar manner to WEHI-231 cells (**Figure 3.6B**). Thus, engagement of CD24 causes a clear exchange of CD24 protein within a homogenous population of cells in the case of WEHI-231, or a more heterogeneous population of bone-marrow derived B cells at various stages of development.

3.4 Chapter 3 Discussion

CD24-mediated cell death has been observed in several mouse and human cell lines, as well as in longer-term, *in vitro* cultures of murine bone marrow extracts co-cultured with bone marrow stromal cells (33, 61, 62). This study is the first to establish that the WEHI-231 cell line may serve as a model system for investigating CD24-mediated apoptosis. Unlike previous reports, in which engagement of CD24 by primary Ab alone was sufficient to induce apoptosis (33), I found that these cells require more extensive crosslinking of CD24 via primary and secondary Abs to initiate a substantial increase in apoptosis. Therefore, my findings, in agreement with the previously published reports (33) suggest that CD24 signalling requires a minimum threshold of stimulation that is surpassed upon the additional clustering of CD24 or increased avidity of Ab binding.

During my validation of WEHI-231 cells as appropriate models for understanding CD24-mediated signalling, I refined the timeline of events related to CD24 signalling with respect to the induction of apoptosis. I found that upon engagement of CD24 caspase-3 / -7 activity is substantially and significantly upregulated within 3 hr in both primary cells and WEHI-231 cells. The caspase family is divided into initiator caspases, such as caspase-8 and executioner caspases, such as caspase-3 and -7 (216). Caspases-3 and 8 activation, as detected by western blot, occurs within 24 h of anti-CD24 Ab stimulation in Pre-B HPB-Null cells (62). My data clearly demonstrates that CD24 signalling engages apoptotic machinery in primary B cells and WEHI-213 cells by 3 h. Furthermore, my results show that removing unbound Ab after a 15 min incubation, which is prior to reaching the highest levels of CD24 expression in the timeframe

examined, reduced the degree of apoptosis within the population. This suggests that the presence of the higher levels of surface CD24 may be necessary to promote maximal apoptosis following CD24 engagement.

In support of my hypothesis that CD24 is associated with cellular organization, I found that CD24 surface protein expression is complex and dynamic in response to Ab-mediated engagement. WEHI-231 cells show an initial decline, followed by a sustained increase in CD24 surface expression. These data demonstrate that in addition to its regulation during B cell development, engagement of CD24 can rapidly alter its own expression at the single cell level. Thus, these data demonstrate that there is a positive feedback loop that increases CD24 surface expression in response to its own engagement.

I have also established that the loss of CD24 surface expression that occurs within 1 min in WEHI-231 cells is not due to classical exocytosis or endocytosis but via loss of CD24 protein on EV. Through both TEM and flow cytometry, I have established that EV appear within 15 min of Ab stimulation and continue to accumulate in the extracellular space through 60 min of stimulation. In addition, I observed an increase in both the total percentage of Annexin V-positive EV and the percentage of CD24-bearing EV following CD24 stimulation. There is not a significant increase in the percentage of CD24+ EV at 60 min compared to 15 min after CD24 engagement. This likely reflects the steady-state equilibrium of EV where EV are continually being released and taken up by the cells.

The gain of CD24 surface expression that occurs over the course of 60 min in WEHI-231 cells is not mediated via classical exocytosis pathways, which transport protein from the ER via the Golgi to the cell surface. My data clearly show that isolated EV can mediate the exchange of CD24 between Ab stimulated cells. There is a broader

distribution of CD24 surface expression at later time points suggesting that some cells acquire more CD24 than other cells. Therefore, at least some of the increase in CD24 surface protein may be due to the uptake of CD24-bearing EV. However, as both the mean and mode of CD24 expression increase at the single cell level, there must be additional mechanisms that increase CD24 expression, which are independent of ER to Golgi trafficking. For example, it is possible that the increase in CD24 surface expression is due to alterations in epitope availability due to conformational changes in response to CD24 engagement or due to fusion of pre-formed vesicles proximal to the plasma membrane.

The loss of CD24 due to release of CD24-bearing EV is consistent with the lack of effect of both endocytosis and exocytosis inhibitors on CD24 surface expression. Previously, CD24 has been associated with exosomes found in urine and amniotic fluid that were secreted by maternal and fetal kidney cells (158). However, as these CD24-bearing vesicles express phosphatidylserine, are not associated with the appearance of secretory vesicles, and have an average size of 165±5 nm, these EV cannot be classified as exosomes (217). The appearance of CD24 on plasma membrane derived EV is consistent with a general role for CD24 on membrane-bound structures released from cells.

Previous studies on EV have shown they can participate in a wide range of cell processes including the regulation of lymphocyte activation, cellular proliferation, the transfer of signalling molecules, the epigenetic modification of cells and the delivery of active second messengers or microRNAs into cells (104, 212-215, 218, 219). The transfer of EV in blood transfusions can deliver CD55 and CD59, inhibitors of complement-

mediated lysis, to host RBCs, preventing their complement-mediated destruction (151, 152). While defining the precise function of CD24-bearing EV in B cell development requires further investigation, given their broad range of functions and their ubiquitous nature, the production of these CD24-bearing microvesicles from immature B cells may have the potential to affect differentiating B cells as well as the supporting stromal cell environment.

Chapter 4: The Composition of CD24-Associated EV

4.1 Introduction

EV production likely represents an innate, basal cellular process to serve as a cell to cell communication vehicle to influence local, or potentially even distant, recipients. Therefore, examining EV cargo is critical to understanding how EVs affect the cellular microenvironment.

To better understand the role of EVs induced by CD24 stimulation, I have performed a systematic examination of the EVs released by the mouse WEHI-231 B cell line following stimulation of CD24. Using a combination of morphology, RNA-Seq, proteomics, and flow cytometry I have firmly established that CD24 stimulation promotes MV and not exosome release. I found that the RNA cargo and the MV proteome are relatively stable in response to stimulation, but MV receptor composition is distinct from that of the cell surface. Overall, these data show that B cells constitutively release MVs, but that CD24 signalling affects the surface composition in a manner that does not reflect their cellular origin, suggesting a regulated system for packaging surface proteins in these MV.

4.2 Materials and Methods

4.2.1 Cell Culture

Cell culture materials were obtained from Thermo Fisher Scientific (San Jose, CA) unless otherwise indicated. The WEHI-231 pre-B cell lymphoma cell line (ATCC; Manassas, VA) was maintained in RPMI 1640 media supplemented with 10% heat-inactivated fetal bovine serum (FBS), 1% penicillin and streptomycin, 1% sodium pyruvate and 0.1% β-mercaptoethanol (RPMI complete) at 37°C and 5% CO_2.

4.2.2 EV Production

4.2.2.1 Vesicle-free media

Two aliquots of RPMI complete media were prepared as described (220), with the following changes: 20% heat-inactivated FBS (RPMI-20%) was centrifuged at 100,000x g for 18 h at 4°C in an SW-28 rotor (Beckman Coulter, Brea, CA) to deplete endogenous vesicles from the FBS, and filtered through a 0.22 μm filter and stored at 4°C. Vesicle-free RPMI for culturing was prepared by mixing equal volumes of vesicle-free RPMI-20% and FBS-free RPMI-complete media.

4.2.2.2 Stimulation of EV production

For stimulation and vesicle collection, 5.0 x10^5 WEHI-231 cells were removed from RPMI-complete, washed 1X in vesicle-free RPMI, re-plated in 1 mL vesicle-free media and allowed to rest for 5 min at 37˚C. Cells were then stimulated at 37˚C with either 10 μg/mL functional grade primary (1°) isotype control Ab (cat no. 16-4031-85) or

M1/69 rat anti-mouse CD24 Ab (cat no. 16-0242-85) from eBioscience (San Diego, CA), which had been pre-incubated with 5 μg/ml goat anti-rat secondary (2°) Ab (Jackson ImmunoResearch; West Grove, PA) for 10 min at room temperature. Either unconjugated (cat no. 112-005-003) or biotinylated (112-065-003) 2° Ab was used depending on the subsequent analysis. These stimulations are referred to as isotype and anti-CD24, respectively. Isotype antibody has previously been demonstrated to not bind to WEHI-231 cells (60) and is used in place of an unstimulated control.

4.2.3 Nanoparticle Tracking Analysis

WEHI-231 cells were stimulated as described using biotinylated 2° Ab to remain consistent with previous Ab stimulations. Following stimulation, the cells were centrifuged at 500 x g for 5 min at 4°C to pellet cells and then centrifuged at 2000 x g for 5 min at 4°C to pellet cell debris and larger vesicles. Conditioned media from isotype-treated or anti-CD24-treated WEHI-231 cells were diluted 1:25 in 0.1-μm-filtered PBS and immediately analyzed on an LM10 Nanosight system with software version 3.2 (Malvern; UK). Five videos of 30 sec each were acquired using camera level 15 for all samples as well as a background media control. The quintuplicate videos for each sample were batch analyzed using a detection threshold of 10. Mean number of particles/ml for each batch was used to estimate the original concentration.

4.2.4 Isolation of extracellular vesicles (EVs)

4.2.4.1 Immunoaffinity isolation

WEHI-231 cells were stimulated as described using biotinylated 2° Ab. Following stimulation, the cells were centrifuged at 500 x g for 5 min at 4°C to pellet cells. Cells were stained for FACS as described below as needed. Supernatant containing vesicles was then centrifuged at 2000 x g for 5 min at 4°C to pellet cell debris and larger vesicles. Protease and phosphatase inhibitors (1 mM phenylmethylsulfonyl fluoride (PMSF; Sigma-Aldrich, St. Louis MO), 1 mM sodium orthovanadate (Sigma-Aldrich) and 1 μM aprotinin (Sigma-Aldrich)) were added to the supernatant. Anti-CD24 M1/69 (10 μg/mL) and biotinylated 2° Ab (5 μg/mL) were added to supernatant from isotype-treated cells. Supernatant (1 ml) was then incubated with $2.2x10^6$ streptavidin-coated magnetic beads (average diameter 4.0 μm; Spherotech; Chicago IL) pre-blocked in 5% bovine serum albumin (BSA) in phosphate-buffered saline (PBS) with rotation, overnight at 4°C. Beads and the bound EVs were then isolated using an EasySep magnetic separation system (StemCell; Vancouver, Canada) followed by FACS analysis (see below).

4.2.4.2 Vn96 peptide

WEHI-231 cells were stimulated as described using unconjugated 2° Ab. Supernatant (1 ml) and cells were collected, centrifuged and treated with protease inhibitors as above. Vn96 peptide (22.5 μg) was suspended in 9 μL ME-buffer (New England Peptide; Gardner MA) and added to approximately 750 μL of cleared supernatant. Vn96 was incubated with supernatant with rotation, overnight at room

temperature. Vn96 with bound EV was pelleted by centrifugation at 17,000 x g for 15 min at room temperature, producing a translucent pellet, following the manufacturer's instructions. No pellet was produced from the supernatant in the absence of Vn96. The pellet was further enriched for EV by adding a second aliquot (750 µL) of vesicle-containing RPMI-media, followed by disrupting the pellet using a 1000-µL pipette and incubating with rotation for 1 h at room temperature. Vn96-EV were isolated again by centrifugation at 17,000 x g for 15 min at room temperature. Pellets were washed once in 0.1 µm-filtered PBS and centrifuged at 16,000 x g for 10 min at room temperature. Vn96-EV pellets were resuspended in buffers appropriate for the subsequent analysis as described below.

4.2.5 Transmission electron microscopy

EV were isolated using Vn96 from supernatant from isotype and anti-CD24 treated cells as described above. Two 750-µL aliquots of vesicle-containing media were pooled for each Vn96 pull-down. Pellets were resuspended in 20 µL of PBS and MV were dispersed by digestion overnight with 25 µg proteinase K enzyme (221) at 37°C. The digested samples were centrifuged at 17,000 x g for 15 min at room temperature to remove undigested Vn96-EV material. All subsequent steps were performed at room temperature. Dispersed EV (10 µl) were placed on formvar-carbon electron microscope grids (Canemco; Montreal, Canada) and allowed to dry for 30 min. Grids were floated sample-side down pyrogen-free water. Grids were then fixed with 3.7% paraformaldehyde for 15 min, followed by two washes with 0.1 µm-filtered water by

flotation. Grids were contrasted with 2% uranyl acetate (w/v), followed by one additional water wash. All solutions were filtered using 0.1-μm syringe filters (4611; Pall Corp; Port Washington, NY). Dried grids were then viewed using a Tecnai Biotwin Transmission Electron Microscope (TEM) (FEI; Hillsboro OR). Images were captured using an XR-41 camera with an AMT capture engine V602 (Advanced Microscopy Techniques; Woburn, MA).

4.2.6 Transcriptome analysis

4.2.6.1 RNA sequencing

All sequencing materials and equipment are from Thermo Fisher Scientific unless otherwise noted. 3 biological replicates of EVs from 2 mL each of isotype, or anti-CD24 treated cells were isolated by Vn96. Vn96-EV pellets were resuspended in 1 mL of TRIzol reagent. Following RNA extraction following the manufacturers protocol, RNA quantity was measured by Nanodrop spectrophotometer (Thermo Fisher Scientific). RNA samples were then assessed for size and integrity using the Agilent Bioanalyzer with the RNA 6000 Pico kit (Agilent; Santa Clara CA). Using RNA concentration values from the Bioanalyzer, samples were prepared for sequencing on the IonTorrent PGM per the manufacturer's protocol. In brief, all recovered MV RNA was concentrated to 3 μL by vacuum centrifugation. Library preparation (without RNA fragmentation) followed the guidelines for the IonTotal RNA-Seq Kit v2. Barcode adapters were used in the cDNA amplification process to differentiate isotype (barcode 1) from anti-CD24 (barcode 2) stimulated cells. Amplified cDNA was enriched using the Ion PGM Template OT2 200

Kit and the Ion OneTouch 2 System. Library density on the IonSphere particles was assessed via Qubit (Thermo Fisher Scientific) fluorometric quantitation. Libraries were then loaded onto an IonTorrent 316 v2 Chip and sequenced for 550 cycles. All RNA-Seq gene expression data have been deposited in the Gene Expression Omnibus (GEO) repository under accession number GSE94778.

4.2.6.2 Bioinformatics analysis

IonTorrent transcript read counts were pre-processed as per Anders et al. (2013). For quality control checks, I used the FastQC software (http://www.bioinformatics.babraham.ac.uk/projects/fastqc/). Read trimming was performed with the FastQ quality trimmer as part of the FASTX toolkit (http://hannonlab.cshl.edu/fastx_toolkit/) using the parameters –Q 33, -t 22, -I 28. Read mapping was performed by tmap with parameters –B 18, -a 2, -v stage 1, map1, map2, map3. For feature counting, I used the HTSeq framework (222). Analysis of sequencing data was performed using R 3.3.1 (167) accessed by RStudio 0.99.902 (166). RNA annotation was performed using BioMart (223). Differential gene expression analysis was performed using edgeR (224) with Counts Per Million filters of 1.0 and 0.1.

4.2.7 Proteomics

Stimulation of EV release, in response to either isotype or anit-CD24 Ab-mediated stimulation was performed at Memorial University of Newfoundland. EV were isolated using Vn96 and provided to the Atlantic Cancer Research Institute (ACRI;

Moncton, Canada) for proteomics processing. Sections 4.2.7.1 through 4.2.7.3 were performed by staff at ACRI. Mass spectrometry assays were designed to capture qualitative data on protein inclusion into EVs and were not optimized for the generation of quantitative data on protein abundance between samples. Data analysis (4.2.7.4) was performed at Memorial University of Newfoundland.

4.2.7.1 In-Gel Tryptic Digest

The EV-Vn96 complexes (pellets) were re-suspended in 25 µL of PBS followed by addition of 2X Laemmli buffer containing ß-mercaptoethanol (BioRad; Hercules CA), heated for 5 min at 95°C and then stored at -20°C. Protein mixtures (45 µL) were separated on a 10% SDS-PAGE gel and visualized with Coomassie EZBlue stain (Sigma-Aldrich). Each gel lane was excised into 12 bands that were distributed into individual micro-centrifuge tubes for tryptic digestion. Each of the bands was sequentially treated with 10 mM dithiothreitol (Sigma-Aldrich) and 25 mM iodoacetic acid (Sigma-Aldrich) to reduce internal disulfide bonds and alkylate free cysteine residues, respectively. Fifty µL of a 10 ng/µL solution of modified trypsin (Promega; Madison, WI) in 100 mM ammonium bicarbonate (Sigma-Aldrich) were added to each tube for overnight enzymatic digestion. The extraction of peptides was achieved using 50% acetonitrile (VWR; Mississauga, ON) containing 5% acetic acid (Sigma-Aldrich,). The total volume of each sample was reduced by vacuum centrifugation to approximately 45 µL, adjusted to 1% acetic acid and stored at -80°C.

4.2.7.2 Offline C-18 Solid-Phase Extraction

Peptide extracts were prepared for offline C-18 clean-up by adding 2% formic acid (Sigma-Aldrich)/20% ACN to each sample at a ratio of 1:3. C-18 mini spin-filter cartridges (Canadian Life Science; Peterborough, ON) were initially activated with 50% ACN and then equilibrated with a 0.5% formic acid/5% ACN solution. Extracted protein digests were bound to the C-18 resin, washed with 0.5% formic acid/5% ACN, and eluted from each filter with a 70% ACN solution. Sample volumes were then reduced by vacuum centrifugation to 45 µL and adjusted to 0.1% aqueous formic acid.

4.2.7.3 Mass Spectrometry Analysis

Protein tryptic digests were analyzed by gradient nanoLC-MS/MS using a hybrid Quadrupole Orbitrap (Q-Exactive, Thermo-Fisher Scientific, San Jose, CA) mass spectrometer interfaced to a Proxeon Easy Nano-LC II (Thermo-Fisher Scientific). Samples were injected (2 µL) onto a narrow bore (20 mm long x 100 µm inner diameter; i.d.) C-18 pre-column packed with 5 µm ReproSil-Pur resin (Thermo-Fisher Scientific). High resolution chromatographic separation was then achieved on a Thermo-Scientific Easy C-18 analytical column with dimensions of 100 mm by 75 µm i.d. with 3 µm diameter ReproSil-Pur particles. Peptide elution was achieved using an acetonitrile/water gradient system, with LC-MS grade solvents (VWR, Mississauga, ON). Solvent A consisted of 0.1% formic acid in water and solvent B was made up of 90/9.9/0.1 acetonitrile/water/formic acid. A linear acetonitrile gradient was applied to the C-18 column from 5-45% solvent B in 60 min followed by 100% B for 10 min at a flow rate of

300 nL/min. The outlet diameter of the nano-flow emitter on the Q-Exactive (15 μm) was biased to +1.9 kV and positioned approximately 2 mm from the heated (250°C) transfer capillary. The S-lens of the mass spectrometer was maintained at 100 V. The Q Exactive mass spectrometer was calibrated in positive ion mode with a commercial standard solution containing caffeine, MRFA peptide and Ultramark polymer. Mass spectrometric data were acquired in data dependent acquisition (DDA) mode, whereby a full mass scan from 350 to 1500 This was followed by the acquisition of fragmentation spectra for the ten most abundant precursor ion intensities above a threshold of 20,000 intensity units. Precursor ion spectra were collected at a resolution setting of 70,000 and an AGC (automatic gain control) value of $1x10^6$. Peptide fragmentation was performed using high energy collision induced dissociation in the HCD cell and MS/MS spectra were collected in the Orbitrap at a resolution of 17,500 and an AGC setting of $1x10^5$. Peptide precursors were selected using a repeat count of 2 and a dynamic exclusion period of 20 s. Mass spectrometric protein identification data were analyzed using Proteome Discoverer version 1.4 (Thermo-Fisher Scientific) employing the SEQUEST scoring algorithm (225). FASTA databases were obtained from Uniprot (226) for *Mus musculus* (44,435 kb) and from the Global Proteome Machine (227) for contaminants using the contaminant repository for affinity purification (cRAP) entries (41 kb).

Searches were performed with the following settings: (a) enzyme specificity of trypsin with 2 allowed missed cleavages, (b) precursor and fragment mass accuracy tolerances were 10 ppm and 0.8 Da, respectively, (c) variable modifications of methionine oxidation (+ 15.994 Da), and lysine acetylation (+42.011 Da) and ,(d) a fixed modification of cysteine carboxymethylation (+58.005 Da). Proteome Discoverer 1.4

calculated a strict false discovery rate (FDR) of 0.1% based on the results of a decoy (reverse) database search. Peptides were scored with Sequest using minimal Xcorr values of 1.62 for +2 ions and 1.79 for +3 ions. Scaffold (Scaffold 4.3.4, Proteome Software Inc., Portland, OR) was then used to validate MS/MS based peptide and protein identifications. Peptide identifications were accepted if they could be established at greater than 95.0% probability by the Scaffold Local FDR algorithm. Protein identifications were accepted if they could be established at greater than 99.0% probability and contained at least 2 unique identified peptides. Protein probabilities were assigned by the Protein Prophet algorithm (228). Proteins that contained identical peptides were grouped to satisfy the principles of parsimony. The mass spectrometry proteomics data have been deposited to the ProteomeXchange Consortium via the PRIDE partner repository with the dataset identifier PXD005919.

4.2.8 Ontology Enrichment Analysis

Transcriptomics and proteomics data were assessed to identify gene ontologies (GO) from EVs using the ToppFun program in the ToppGene suit (229) using official gene symbols. P-values were obtained using the probability density function. Other associations, including human disease, drug and published proteomics analyses were also captured via ToppGene. Bonferroni multiple testing correction (q-value) was performed and results were reported with $q<0.05$. The proteomics GO terms for common and CD24-enriched MV proteins were compared using the Venn diagram tool from the Bioinformatics Institute Ghent (http://bioinformatics.psb.ugent.be/webtools/Venn/). GO

terms were grouped into common categories using the online REVIGO tool (230) using the associated Bonferroni FDR values from Toppfun and the default REVIGO settings. Box sizes for REVIGO plots are reflective of GO enrichment P-values.

4.2.9 Western Blot

4.2.9.1 Cells

Cells were stimulated with either isotype or anti-CD24 Ab for 1 h. Cells were pelleted and resuspended in 100 μL of Tris-based RIPA lysis buffer (50 mM Tris-HCl; pH 7.6, 0.02% sodium azide, 0.5% sodium deoxycholate, 0.1% SDS, 150 mM NaCl) supplemented with 1 mM PMSF (Sigma-Aldrich), 1X HALT protease inhibitor cocktail (Thermo Fisher Scientific) and 1 μM aprotinin (Sigma-Aldrich). Cells were lysed for 10 min on ice, then centrifuged at 17,000 x g for 10 min at 4°C to pellet cell debris. Protein was quantified with the Bicinchoninic Acid Protein Assay (Thermo Fisher Scientific) per the manufacturer's protocol. Cell lysates were then prepared in SDS sample buffer (62.5 mM Tris base, 2% glycerol, 2.3% SDS, 100 mM dithiothreitol, 0.02% bromophenol blue, pH 6.8) and boiled for 5 min. Protein (5 μg) was loaded onto a 12% SDS-PAGE gel followed by transfer to nitrocellulose membrane. Blocking was performed using 5% (w/v) skim milk in TBST. Anti-mouse Ab were diluted in tris-buffered saline with 0.05% Tween-20 (TBST) + 5% BSA as follows: 1:1000 HSP90α/β (SC-13119; Santa Cruz; Santa Cruz CA), 1:750 SHMT2 (12762S; Cell Signaling Technology; Danvers, MA), 1:1500 EEF1G (ab72368; Abcam; San Francisco CA), 1:1000 GRB2 (3972S; Cell Signaling Technology) and 1:1500 HMGB2 (14163S; Cell Signaling Technology). HSP90 was detected using goat-anti-mouse IgG (SC-2005; Santa Cruz) and all others

were detected using goat-anti-rabbit IgG (SC-2004; Santa Cruz). Secondary antibodies were diluted 1:2000 in TBST + 5% BSA. Immobilon Western chemiluminescent horse radish peroxidase substrate (Millipore; Billerica MA) was used for detection. Images were acquired using the AlphaImager gel documentation system with FluorChem HD2, v3.4.0 (Protein Simple; San Jose CA). Image manipulation was limited to adjusting brightness and contrast to the entire image using Adobe Photoshop CS6 .

4.2.9.2 Extracellular vesicles

EV were isolated using Vn96 from isotype and anti-CD24 Ab treated cells as described above. Two 1-mL aliquots of vesicle-containing media were pooled for each Vn96 pull-down representing the total 1 h vesicle production from $1.0x10^6$ cells. Vn96-EV pellets were dissolved in SDS loading buffer and boiled for 5 min. Half of each Vn96-EV sample was loaded onto each 12% SDS-PAGE gel. Proteins were transferred, probed and detected as described for cells.

4.2.10 Flow Cytometry

A FACSAria II SORP cell sorter was used to collect flow cytometry (FACS) data using FACSDiva v8.0 software (BD Biosciences; San Jose CA), at the Cold-Ocean Deep-Sea Research Facility (Memorial University of Newfoundland). Data analysis was performed using FlowJo v10.0.5 (Tree Star; Ashland, OR). All reagents were from eBioscience (San Diego, CA) and are rat anti-mouse antibodies, unless otherwise stated. Colour compensation was performed using single-stained OneComp beads (catalogue

number 01-1111) with all fluorophores. Cells were stimulated to produce EV as described above using 1° Ab pre-incubated with biotinylated 2° Ab. Isotype or anti-CD24-treated cells were stained with 0.5 µg M1/69 CD24-FITC (11-0242) or Streptavidin-FITC (11-4317), respectively. All cells were stained with 1.25 µg Siglec-2-PE (126111; Biolegend; San Diego, CA), 0.625 µg CD63 PerCP-eFluor710 (46-0631), 1.25 µg IgM PE-Cy7 (25-5790), 0.625 µg Siglec-G APC (17-5833), MHC-II (I-A/I-E) Alexa Fluor 700 (56-5321), and 0.625 µg Ter119 APC-eFluor780 (47-5921). Matching isotype Ab controls were used to confirm the absence of non-specific Ab binding and to set thresholds. Captured MV were stained with the same fluorophores except with 5 µL Annexin V Alexa488 (Thermo Fisher Scientific) instead of anti-CD24-FITC or Streptavidin-FITC.

4.2.10.1 Cells

Cells were suspended in phosphate buffered saline (PBS; 18.6 mM $NaH_2PO_4•H_2O$, 84.1 mM Na_2HPO_4, 1.5 M NaCl) that contained 1% heat-inactivated fetal bovine serum (FACS buffer) unless stated otherwise. Pelleted cells were washed at 4°C in 500 µL FACS buffer and resuspended in 100 µL of FACS buffer containing FITC-conjugated streptavidin, and the directly conjugated Siglec-2 (CD22), CD63, IgM, Siglec-G, MHC-II and Ter119 Ab diluted as above. Cells were stained for 30 min at 4°C, followed by the addition of 500 µL of FACS buffer. Cells were again washed in 500 µL FACS buffer prior to fixation in 100 µL of 4% paraformaldehyde for 20 min at room temperature in the dark. FACS buffer (400 µl) was added to cells, which were then

assessed on the FACSAria II. For analysis, single cells were gated using the FSC/SSC parameters.

4.2.10.2 Extracellular vesicles

EV were isolated by immunoaffinity isolation. Following magnetic isolation, bead-bound MV were washed in 1X Annexin V binding buffer (5 mM HEPES buffer, 140 mM NaCl, 2.5 mM $CaCl_2$; pH 7.4). Bead-MV complexes were resuspended in 100 µL of Annexin V binding buffer containing the directly conjugated Siglec-2, CD63, IgM, Siglec-G, MHC-II and Ter119 Ab diluted as above and incubated for 20 min at room temperature. Samples were diluted with 400 µL of 1X Annexin V binding buffer and placed at 4°C until analyzed the same day on the FACSAria II. Analysis was performed on singlet beads, gated using FSC/SSC parameters. Non-specific antibody binding to beads was established with pre-blocked beads, which were used to set the negative fluorescence threshold for all MV fluorescence parameters.

4.3 Results

4.3.1 EV released from isotype and anti-CD24 stimulated WEHI-231 cells are morphologically similar.

As discussed in chapter 3, I found that Ab-mediated stimulation of CD24 induced the formation of CD24-bearing EVs from B cells, that I concluded were plasma-membrane derived MVs (60). Here I further characterized the size, shape and quantity of the EVs released by WEHI-231 cells after anti-CD24 stimulation compared to isotype control treatment **(Figure 4.1**).

Particles of MV size were detected using nanoparticle tracking analysis (NTA) following 1 h stimulation in both conditions (**Figure 4.1A**). The mean size from isotype-treated samples was 122 +/- 54 nm, and from anti-CD24 treated samples was 122 +/- 56 nm (**Figure 4.1B** left), consistent with the upper range of exosomes and the lower range of MVs (75). Isotype-treated cell supernatant contained an average of $114.7x10^8$ particles/mL, whereas anti-CD24 stimulated cell supernatant contained an average of $141.3x10^8$ particles (**Figure 4.1B**, right). While not reaching statistical significance, each supernatant from CD24 treated cells trended towards more particles than the matching isotype supernatant, and there was an overall trend towards increased particle numbers following CD24 stimulation ($p=0.07$).

I next quantified the population of CD24-bearing EVs that express phosphatidylserine by flow cytometric-detection of Annexin V on CD24+ EVs captured on streptavidin-coated magnetic beads. While individual EVs cannot be analyzed using this approach, I found a statistically significant increase in the number of Annexin V+

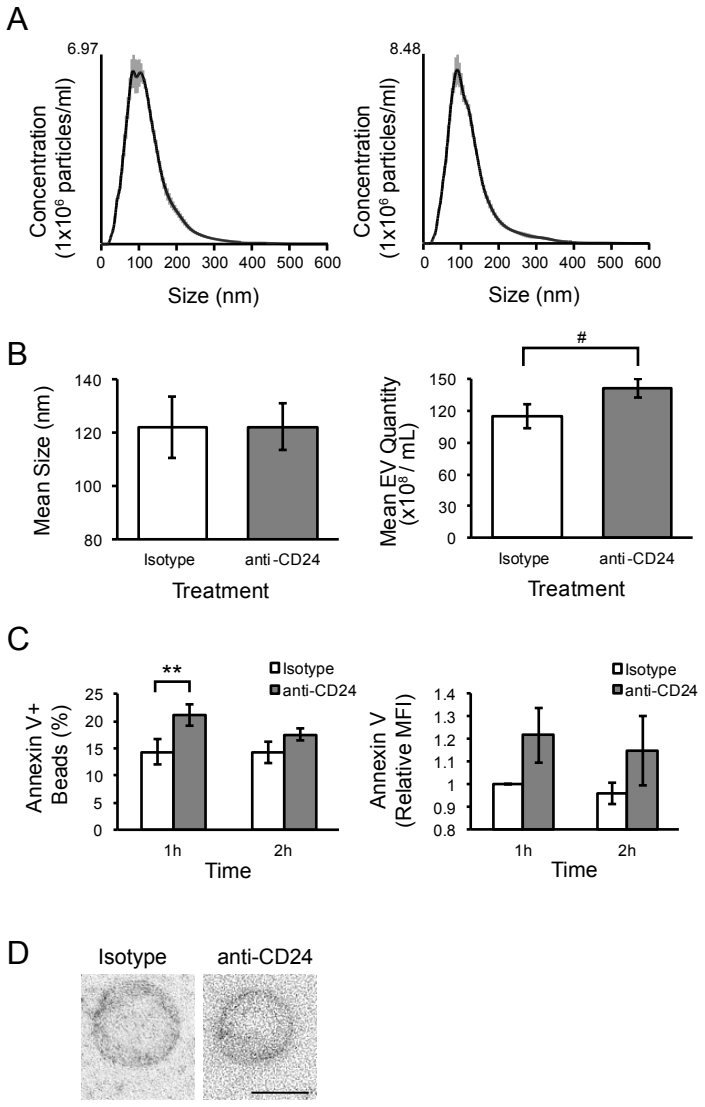

Figure 4.1: The quantification and morphology of MVs released from B cells with and without CD24 stimulation. (A) Representative nanoparticle tracking (NPT) plots of particle sizes and concentrations in supernatants from cells stimulated with either isotype (right) or anti-CD24 (left) Ab after 1 h. Grey lines show ± 1 standard deviation of the mean in measurements. n=3 biological replicates with 5 technical replicates each. (B) The mean size (left) and concentration (right) ± SEM of particles from supernatants analyzed by NPT, n=3. Statistical significance was assessed using Students' paired t-test, # p=0.08. (C) Mean % positive (left) and relative mean fluorescent intensity (MFI; right) of Annexin V-FITC beads used to capture CD24-bearing MVs released from isotype or anti-CD24 stimulated cells for the indicated times, n=3. Statistics assessed by a two-tailed Student's paired t-test. **p<0.01. (D) Representative transmission electron microscopy (TEM) images of Vn96-isolated EVs from cells stimulated with either isotype or anti-CD24 for 1 h. Scale bar =100 nm.

beads in response to 1 h anti-CD24 stimulation (**Figure 4.1C** left) with 14.3 ± 2.3% of beads from isotype-treated samples, and 21.2 ± 2.0% of beads from anti-CD24 treated samples being Annexin V+ ($p=0.009$). After 2 h of anti-CD24 stimulation, the number of Annexin V+, bead-captured EV was comparable to that of isotype treatment indicating that the promotion of Annexin V+ EV formation by CD24 was transitory.

I isolated EVs from both isotype and anti-CD24 stimulated cells for transmission electron microscopy (TEM) analysis using the Vn96 peptide-based capture, as previously validated (221). I isolated round structures consistent with the size estimates from the NTA, and my previous results using FACS-based bead sizing that showed that CD24 was associated with EVs smaller than 200 nm in diameter (**Figure 4.1D**) (60). There was no difference in morphology between EVs isolated from isotype or anti-CD24 stimulated cells.

Together these results indicate that B cells constitutively release EVs that are approximately 120 nm in diameter and these vesicles do not vary in their size or morphology following CD24 stimulation; however, there is a statistically significant increase in the number of phosphatidylserine-positive EVs, indicative of MVs, following 1 h of anti-CD24 stimulation that does not persist over time.

4.3.2 Individual transcripts are not preferentially packaged but overall protein coding transcripts are reduced in EV in response to CD24 stimulation.

I next used RNA-seq to characterize the RNA carried by EVs released by WEHI-231 cells. I found that both isotype and anti-CD24 stimulated cells produce EVs that

carry RNA of approximately 200 bp, consistent with other reports of RNA isolated from MVs (**Figure 4.2A**; (204)). As there was no evidence of 18S or 28S RNA by Bioanalyzer analysis in the EV population, I sequenced all EV RNA without rRNA depletion.

I did not identify any individual transcripts that were differentially incorporated between EVs from 3 biological replicates of isotype or anti-CD24 stimulated cells. Surprisingly, I found that 89.5% of the transcripts in all 6 EV samples were annotated as either rRNA or ribozyme by BioMART (223). The majority (95.2%) of these transcripts were annotated as 5.8S (72.7%) and 5S (22.5%) rRNA, (**Figure 4.2B**). Indeed, most annotated reads from all 6 samples mapped to a single 5.8S rRNA transcript: n-R5-8s1. The RNA carried by EVs is strongly influenced by their sub-type and cell of origin; however, the lack of 18S and 28S, but presence of 5/5.8S rRNA, is consistent with other reports on MV RNA (204, 231). Of the remaining transcripts, approximately 29.1 ± 2.9 % (3.1% of the total RNA) were mitochondrial non-coding mt-rRNA and mt-tRNA (**Figure 4.2C**).

Interestingly, I found a statistically significant decrease in the total number of protein-coding transcripts in EVs from CD24-stimulated cells ($p=0.002$). Of the top 50 protein coding transcripts, 14 were mitochondrial genes. There was also a trend towards increased abundance of miRNA transcripts in the EVs ($p=0.08$) (**Figure 4.2**C). Even though my analysis did not identify any individual statistically significant differentially expressed transcripts, these data show there are changes in the overall distribution of RNA incorporated into these EVs.

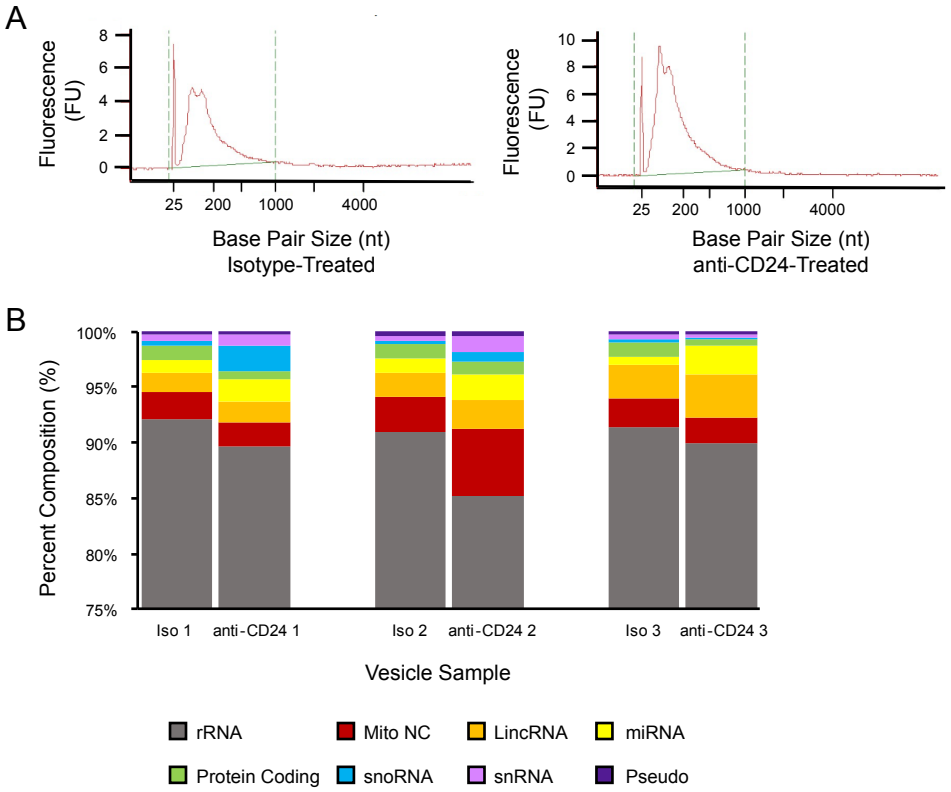
A
Fluorescence (FU)
8
6
4
2
0
25
200
1000
4000
Base Pair Size (nt)
Isotype-Treated
Fluorescence (FU)
10
8
6
4
2
0
25
200
1000
4000
Base Pair Size (nt)
anti-CD24-Treated
B
Percent Composition (%)
100%
95%
90%
85%
80%
75%
Iso 1
anti-CD24 1
Iso 2
anti-CD24 2
Iso 3
anti-CD24 3
Vesicle Sample
rRNA
Mito NC
LincRNA
miRNA
Protein Coding
snoRNA
snRNA
Pseudo
C
Percent Composition Without rRNA (%)
40%
30%
20%
10%
0%
Isotype
anti-CD24
*
#
Mito NC
LincRNA
Protein Coding
miRNA
snRNA
snoRNA
Processed Tr.
Pseudo

Figure 4.2: CD24 stimulation alters the abundance of protein coding transcripts loaded into B cell MVs. (A) Representative RNA size distributions of MVs collected from cells stimulated with either isotype (right) or anti-CD24 (left) Ab after 1 h. (B) The RNA incorporated into MVs from cells after 1 h of either isotype or anti-CD24 Ab stimulations categorized into one of 8 sub-categories containing >0.2% of the total RNA, n=3 biological replicates. (C) The mean ± SEM percentage of the 8 major non-rRNA transcripts with greater than 2% of RNA abundance from MVs isolated from either isotype (white bars) or anti-CD24 (grey bars) stimulated cells. n=3, statistics were assessed using a two-tailed Student's t-test, $^{\#}p=0.07$; $*p<0.05$.

I next performed gene ontology (GO) enrichment analysis on the 50 most abundant protein coding transcripts using ToppFun (**Table 4.1**). These were enriched for 16 Biological Process (BP) terms, 13 Molecular Function (MF) terms and 9 Cellular Component (CC) terms, at a Bonferroni-corrected P-value (q-value) of q=0.05 (**Supplemental File 2**). Using REVIGO, I visualized the associations between GO terms based on their associations to one another (**Figure 4.3**). The BP terms belonged to one of two major groups: Electron transport chain and the Generation of precursor metabolites and energy. Similarly, four of the five MF groups belonged to mitochondrial-associated functions: NADH dehydrogenase activity, Hydrogen ion transmembrane transporter activity, Oxidoreductase activity, and Electron carrier activity. Finally, the CC terms were primarily associated as Mitochondrial inner membrane, and Respiratory chain. Overall, these data demonstrate that protein-coding transcripts in EVs released by these B cells are associated with mitochondrial functions, regardless of CD24 stimulation.

Finally, across the six samples, I found there were on average 22 distinct miRNA transcripts, of which 12 were common to all EVs. Only two, mir6236 and mir5099, were annotated and there was a trend towards increased incorporation in these transcripts in EVs from anti-CD24 stimulated cells (p=0.09 for both). As the remainder of the common transcripts were unannotated or predicted, no functional enrichment analysis could be performed.

.

Table 4.1 The top 50 most abundant protein coding transcripts from B cell MV.

Ensmbl	Gene Name	Gene Description	Isotype		Anti-CD24	
			Average CPM	SD	Average CPM	SD
ENSMUSG00000035202	Lars2	Leucyl-trna synthetase, mitochondrial	537.00	467.43	889.67	249.85
ENSMUSG00000064351	mt-Co1	Mitochondrially encoded cytochrome c oxidase I	174.67	77.39	505.00	284.69
ENSMUSG00000064356	mt-Atp8	Mitochondrially encoded ATP synthase 8	231.00	51.96	386.33	276.41
ENSMUSG00000064354	mt-Co2	Mitochondrially encoded cytochrome c oxidase II	89.33	28.29	270.67	176.02
ENSMUSG00000064345	mt-Nd2	Mitochondrially encoded NADH dehydrogenase 2	59.00	13.00	205.67	139.41
ENSMUSG00000064341	mt-Nd1	Mitochondrially encoded NADH dehydrogenase 1	36.33	1.53	175.33	130.13
ENSMUSG00000064370	mt-Cytb	Mitochondrially encoded cytochrome b	51.00	16.09	169.00	116.01
ENSMUSG00000064357	mt-Atp6	Mitochondrially encoded ATP synthase 6	47.00	4.36	186.67	118.33
ENSMUSG00000064367	mt-Nd5	Mitochondrially encoded NADH dehydrogenase 5	61.33	8.74	175.00	86.13
ENSMUSG00000064363	mt-Nd4	Mitochondrially encoded NADH dehydrogenase 4	27.00	3.46	118.33	74.41
ENSMUSG00000064358	mt-Co3	Mitochondrially encoded cytochrome c oxidase III	45.00	19.16	134.00	80.17
ENSMUSG00000065947	mt-Nd4l	Mitochondrially encoded NADH dehydrogenase 4L	49.67	18.01	85.00	42.67
ENSMUSG00000019428	Fkbp8	FK506 binding protein 8	11.00	15.72	24.67	40.13

ENSMUSG00000051627	Hist1h1e	Histone cluster 1, h1e	10.33	11.02	29.67	5.77
ENSMUSG00000022957	Itsn1	Intersectin 1 (SH3 domain protein 1A)	8.00	2.00	34.00	4.36
ENSMUSG00000064368	mt-Nd6	Mitochondrially encoded NADH dehydrogenase 6	5.00	1.73	24.67	11.93
ENSMUSG00000037375	Hhat	Hedgehog acyltransferase	4.33	7.51	5.00	8.66
ENSMUSG00000064360	mt-Nd3	Mitochondrially encoded NADH dehydrogenase 3	2.00	1.73	8.00	5.57
ENSMUSG00000032850	Rnft2	Ring finger protein, transmembrane 2	9.67	13.32	9.33	4.04
ENSMUSG00000030560	Ctsc	Cathepsin C	0.00	0.00	3.00	4.36
ENSMUSG00000060275	Nrg2	Neuregulin 2	0.00	0.00	2.67	4.62
ENSMUSG00000005442	Cic	Capicua homolog	0.67	1.15	3.33	3.51
ENSMUSG00000031779	Ccl22	Chemokine (C-C motif) ligand 22	2.67	2.89	5.33	2.08
ENSMUSG00000066026	Dhrs3	Dehydrogenase/ reductase (SDR family) member 3	6.00	3.00	3.00	3.61
ENSMUSG00000025092	Hspa12a	Heat shock protein 12A	6.00	5.29	4.00	2.00
ENSMUSG00000000184	Ccnd2	Cyclin D2	0.00	0.00	3.33	2.52
ENSMUSG00000063550	Nup98	Nucleoporin 98	0.33	0.58	2.33	3.21
ENSMUSG00000003970	Rpl8	Ribosomal protein L8	6.33	6.66	6.00	2.65
ENSMUSG00000031502	Col4a1	Collagen, type IV, alpha 1	1.33	2.31	3.00	2.65
ENSMUSG00000037754	Ppp1r16b	Protein phosphatase 1, regulatory (inhibitor) subunit 16B	3.33	4.93	3.67	1.53
ENSMUSG00000031659	Adcy7	Adenylate cyclase 7	1.67	2.89	2.33	2.52
ENSMUSG00000035828	Pim3	Proviral integration site 3	1.00	1.73	2.67	2.08

ENSMUSG00000037896	Rcor1	REST corepressor 1	0.00	0.00	2.00	2.65
ENSMUSG00000020431	Adcy1	Adenylate cyclase 1	0.33	0.58	1.67	2.89
ENSMUSG00000030830	Itgal	Integrin alpha L	0.67	0.58	2.67	2.52
ENSMUSG00000036499	Eea1	Early endosome antigen 1	0.33	0.58	1.67	2.89
ENSMUSG00000041417	Pik3r1	Phosphatidylinositol 3-kinase, regulatory subunit, polypeptide 1	0.33	0.58	1.67	2.89
ENSMUSG00000045318	Adra2c	Adrenergic receptor, alpha 2c	3.33	3.51	1.67	2.89
ENSMUSG00000059436	Max	Max protein	0.00	0.00	1.67	2.89
ENSMUSG00000034994	Eef2	Eukaryotic translation elongation factor 2	20.67	19.40	11.33	7.02
ENSMUSG00000039477	Tnrc18	Trinucleotide repeat containing 18	6.00	6.24	4.67	5.03
ENSMUSG00000049517	Rps23	Ribosomal protein S23	0.33	0.58	3.00	1.73
ENSMUSG00000063457	Rps15	Ribosomal protein S15	5.00	7.00	4.67	2.08
ENSMUSG00000039844	Rapgef1	Rap guanine nucleotide exchange factor (GEF) 1	0.67	1.15	2.33	1.53
ENSMUSG00000075014	*Gm10800*	*Predicted gene*	81.33	106.46	47.33	34.24
ENSMUSG00000095280	*Gm21738*	*Predicted gene*	14.33	16.65	9.33	2.52
ENSMUSG00000095891	*Gm10717*	*Predicted gene*	36.33	39.88	15.00	11.36
ENSMUSG00000095547	*Gm10719*	*Predicted gene*	27.33	32.75	13.33	8.08
ENSMUSG00000091028	*Gm10722*	*Predicted gene*	23.67	29.70	13.67	9.02
ENSMUSG00000096385	*Gm11168*	*Predicted gene*	32.33	43.50	11.00	6.24

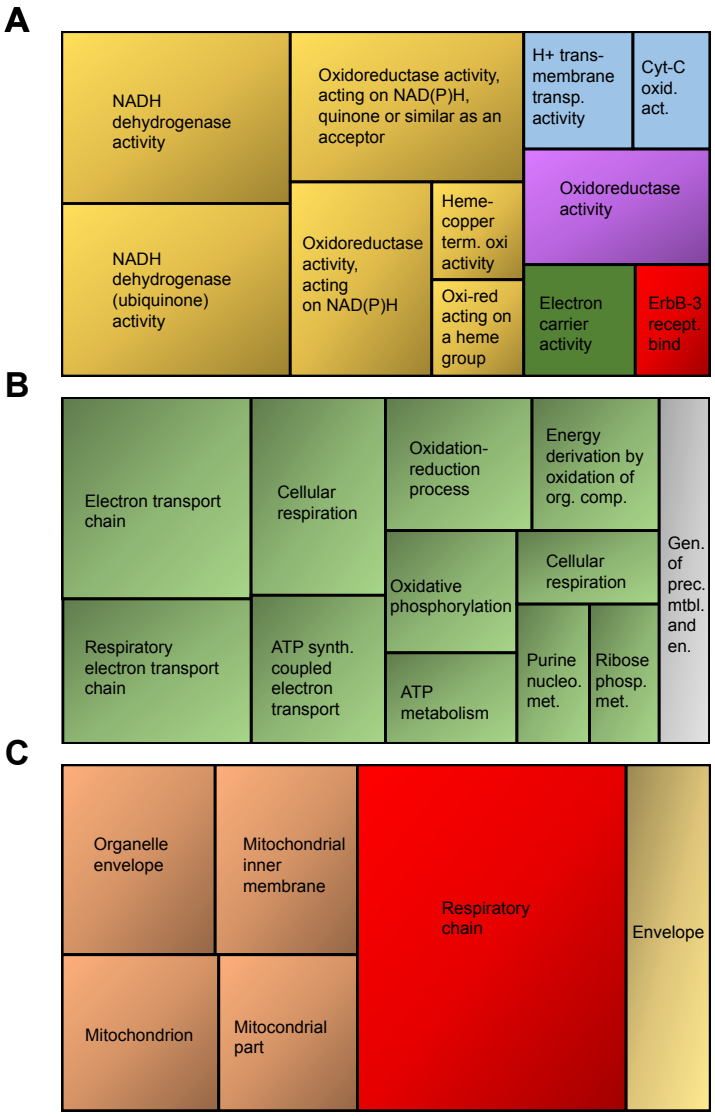

Figure 4.3 REVIGO analysis of Gene Ontologies of RNA Cargo. The 50 most abundant protein coding RNA transcripts from isotype or anti-CD24 Ab stimulated cells are predominantly associated with mitochondrial function GO terms. No differentially expressed transcripts were identified in response to the different Ab treatments. (A) Biological processes (BP): NADH dehydrogenase (ubiquinone) activity (yellow), hydrogen ion transmembrane transporter activity (blue). (B) Molecular functions (MF): Electron transport chain (green). (C) Cellular components: Mitochondrial inner membrane (pink). Act. = activity, comp. = compounds, Cyt-c = cytochrome C, gen. = generation, en. = energy, mtbl. = metabolites, nucelo. = nucleotide, org. = organic, oxi = oxidase, oxi-red = oxidoreductase, phosp. = phosphate, prec. = precursor, recept. = receptor, Transp. = transport, term. = terminal

4.3.3 CD24 stimulation may enrich specific proteins in the EV cargo of WEHI-231 cells

I next used mass spectrometry (MS; specifically, nanoLC-MS/MS) to analyze the protein cargo in Vn96-isolated EVs from both isotype and anti-CD24 stimulated cells. The total EV secretome of cells were assessed in a qualitative way, as equal amounts of EV protein could not be compared between samples. I found that the EVs carried a total of 460 unique proteins, detected at the 2-peptide cut-off level (**Supplemental file 3**). Fifty-eight proteins (mapping to 41 annotated genes) were common to all EVs (**Table 4.2**). There was considerable heterogeneity among EV samples, as no peptides uniquely distinguished EVs released by isotype-treated cells from anti-CD24 treated cells. However, 79 proteins (mapping to 77 annotated genes) were found in two or more of the anti-CD24 stimulated EVs, but present in only a single EV sample from isotype-treated cells (**Table 4.3**), suggesting these proteins may be preferentially enriched into EVs by CD24. I did not observe the reciprocal effect of peptides preferentially enriched into EVs from isotype-treated cells. Finally, 153 peptides were detected in only one of the replicates, suggesting they are incorporated at low abundance, or randomly.

I used Toppfun to identify the biological functions of proteins enriched in EVs from CD24-stimulated cells, by identifying their unique GO terms for the 41 common EV proteins. I found that proteins enriched in EVs from CD24-stimulated cells were associated with 41 BP (**Figure 4.4**A), 12 MF (**Figure 4.4**B) and 13 CC terms (**Figure 4.4**C). I identified five major GO associations within the 41 BP, with most terms categorized as Cellular amide metabolism, Macromolecular complex assembly, or Protein localization to nuclear body (**Figure 4.4**A). Similarly, I found three major associations in MF ontologies, with the largest two being Damaged DNA binding and Transferase

Table 4.2 41 peptide sequences common to MV isolated from cells stimulated for 1 h with either isotype or anti-CD24.

Peptide Identifier	MGI Symbol	Gene / Protein Name
AK1A1_MOUSE	Akr1a1	Aldo-keto reductase family 1, member A1 (aldehyde reductase)
A6ZI44_MOUSE	Aldoa	Aldolase A, fructose-bisphosphate
ANXA2_MOUSE	Anxa2	Annexin A2
CALR_MOUSE	Calr	Calreticulin
EF1A1_MOUSE	Eef1a1	Eukaryotic translation elongation factor 1 alpha 1
ENOA_MOUSE	Eno1	Enolase 1, alpha non-neuron
H4_MOUSE	Hist1h4a	Histone cluster 1, h4a
HS90A_MOUSE	Hsp90aa1	Heat shock protein 90, alpha (cytosolic), class A member 1
HS90B_MOUSE	Hsp90ab1	Heat shock protein 90 alpha (cytosolic), class B member 1
ENPL_MOUSE	Hsp90b1	Heat shock protein 90, beta (Grp94), member 1
Q3U2G2_MOUSE	Hspa4	Heat shock protein 4
GRP78_MOUSE	Hspa5	Heat shock protein 5
HSP7C_MOUSE	Hspa8	Heat shock protein 8
GRP75_MOUSE	Hspa9	Heat shock protein 9
Q58E56_MOUSE	Igh	Immunoglobulin heavy chain complex
PLSL_MOUSE	Lcp1	Lymphocyte cytosolic protein 1
G5E8N5_MOUSE	Ldha	Lactate dehydrogenase A
LDHB_MOUSE	Ldhb	Lactate dehydrogenase B
MDHC_MOUSE	Mdh1	Malate dehydrogenase 1, NAD (soluble)
Q8CD23_MOUSE	Ncl	Nucleolin
PDIA3_MOUSE	Pdia3	Protein disulfide isomerase associated 3
PGAM1_MOUSE	Pgam1	Phosphoglycerate mutase 1
6PGL_MOUSE	Pgls	6-phosphogluconolactonase
Q3ULZ3_MOUSE	Psat1	Phosphoserine aminotransferase 1
PSA1_MOUSE	Psma1	Proteasome (prosome, macropain) subunit, alpha type 1
PSA3_MOUSE	Psma3	Proteasome (prosome, macropain) subunit, alpha type 3
PSA4_MOUSE	Psma4	Proteasome (prosome, macropain) subunit, alpha type 4
PSA6_MOUSE	Psma6	Proteasome (prosome, macropain) subunit, alpha type 6
PSA7_MOUSE	Psma7	Proteasome (prosome, macropain) subunit, alpha type 7
G3X9V0_MOUSE	Psme2	Proteasome (prosome, macropain) activator subunit 2 (PA28 β)
B2CY77_MOUSE	Rpsa	Ribosomal protein SA
A2BE93_MOUSE	Set	SET nuclear oncogene
TALDO_MOUSE	Taldo1	Transaldolase 1
TKT_MOUSE	Tkt	Transketolase
TPIS_MOUSE	Tpi1	Triosephosphate isomerase 1
sp|P21107-2|TPM3_MOUSE	Tpm3	Tropomyosin 3, gamma
TERA_MOUSE	Vcp	Valosin containing protein
1433E_MOUSE	Ywhae	Tyrosine 3-monooxygenase/tryptophan 5-monooxygenase activation protein, epsilon polypeptide
1433G_MOUSE	Ywhag	Tyrosine 3-monooxygenase/tryptophan 5-monooxygenase activation protein, gamma polypeptide
1433F_MOUSE	Ywhah	Tyrosine 3-monooxygenase/tryptophan 5-monooxygenase activation protein, eta polypeptide
1433Z_MOUSE	Ywhaz	Tyrosine 3-monooxygenase/tryptophan 5-monooxygenase activation protein, zeta polypeptide

Table 4.3 77 peptide sequences enriched in MV from CD24 stimulated cells.

Peptide Identifier	MGI Symbol	Description
ACON_MOUSE	Aco2	Aconitase 2, mitochondrial
ACTN4_MOUSE	Actn4	Actinin alpha 4
ARP3_MOUSE	Actr3	ARP3 actin-related protein 3
Q3U4D1_MOUSE	Ahcy	S-adenosylhomocysteine hydrolase
Q3UJW1_MOUSE	Aldh2	Aldehyde dehydrogenase 2, mitochondrial
APEX1_MOUSE	Apex1	Apurinic/apyrimidinic endonuclease 1
ARC1B_MOUSE	Arpc1b	Actin related protein 2/3 complex, subunit 1B
sp|P18572|BASI_MOUSE	Bsg	Basigin
CAZA1_MOUSE	Capza1	Capping protein (actin filament) muscle Z-line, alpha 1
A2AMW0_MOUSE	Capzb	Capping protein (actin filament) muscle Z-line, beta
TCPB_MOUSE	Cct2	Chaperonin containing Tcp1, subunit 2 (beta)
TCPG_MOUSE	Cct3	Chaperonin containing Tcp1, subunit 3 (gamma)
G5E839_MOUSE	Cct4	Chaperonin containing Tcp1, subunit 4 (delta)
Q3UDB1_MOUSE	Cct7	Chaperonin containing Tcp1, subunit 7 (eta)
CLIC1_MOUSE	Clic1	Chloride intracellular channel 1
KCY_MOUSE	Cmpk1	Cytidine monophosphate (UMP-CMP) kinase 1
DDB1_MOUSE	Ddb1	Damage specific DNA binding protein 1
DLDH_MOUSE	Dld	Dihydrolipoamide dehydrogenase
A0A087WS46_MOUSE	Eef1b2	Eukaryotic translation elongation factor 1 beta 2
EF1G_MOUSE	Eef1g	Eukaryotic translation elongation factor 1 gamma
IF2A_MOUSE	Eif2s1	Eukaryotic translation initiation factor 2, subunit 1 alpha
EIF3F_MOUSE	Eif3f	Eukaryotic translation initiation factor 3, subunit F
EIF3I_MOUSE	Eif3i	Eukaryotic translation initiation factor 3, subunit I
IF4A1_MOUSE	Eif4a1	Eukaryotic translation initiation factor 4A1
FA49B_MOUSE	Fam49b	Family with sequence similarity 49, member B
sp|P97807-2|FUMH_MOUSE	Fh1	Fumarate hydratase 1
FLNB_MOUSE	Flnb	Filamin, beta
Q3UC72_MOUSE	Gdi2	Guanosine diphosphate (GDP) dissociation inhibitor 2
sp|Q9CPV4|GLOD4_MOUSE	Glod4	Glyoxalase domain containing 4
E9Q070_MOUSE	Gm8730	Ribosomal protein, large, P0 pseudogene
B1AT92_MOUSE	Grb2	Growth factor receptor bound protein 2
GSTO1_MOUSE	Gsto1	Glutathione S-transferase omega 1
HMGB2_MOUSE	Hmgb2	High mobility group box 2
sp|O88569|ROA2_MOUSE	Hnrnpa2b1	Heterogeneous nuclear ribonucleoprotein A2/B1
IMPA1_MOUSE	Impa1	Inositol (myo)-1(or 4)-monophosphatase 1
INO1_MOUSE	Isyna1	Myo-inositol 1-phosphate synthase A1
KCD12_MOUSE	Kctd12	Potassium channel tetramerisation domain containing 12
FUBP2_MOUSE	Khsrp	KH-type splicing regulatory protein
IMB1_MOUSE	Kpnb1	Karyopherin (importin) beta 1
MDHM_MOUSE	Mdh2	Malate dehydrogenase 2, NAD (mitochondrial)
NACAM_MOUSE	Naca	Nascent polypeptide-associated complex alpha polypeptide

NUDT5_MOUSE	Nudt5	Nudix (nucleoside diphosphate linked moiety X)-type motif 5
Q05BN2_MOUSE	Pa2g4	Proliferation-associated 2G4
PABP1_MOUSE	Pabpc1	Poly(A) binding protein, cytoplasmic 1
PCBP1_MOUSE	Pcbp1	Poly(rc) binding protein 1
Q3TJL8_MOUSE	Pdia6	Protein disulfide isomerase associated 6
PUR4_MOUSE	Pfas	Phosphoribosylformylglycinamidine synthase (FGAR amidotransferase)
6PGD_MOUSE	Pgd	Phosphogluconate dehydrogenase
PGK1_MOUSE	Pgk1	Phosphoglycerate kinase 1
PHB_MOUSE	Phb	Prohibitin
PHB2_MOUSE	Phb2	Prohibitin 2
SERA_MOUSE	Phgdh	3-phosphoglycerate dehydrogenase
IPYR_MOUSE	Ppa1	Pyrophosphatase (inorganic) 1
B1AXW5_MOUSE	Prdx1	Peroxiredoxin 1
PSA2_MOUSE	Psma2	Proteasome (prosome, macropain) subunit, alpha type 2
G3UXZ5_MOUSE	Psme1	Proteasome (prosome, macropain) activator subunit 1 (PA28 alpha)
Q3TE70_MOUSE	Ptpn6	Protein tyrosine phosphatase, non-receptor type 6
Q3TJ52_MOUSE	Rad23b	RAD23 homolog B, nucleotide excision repair protein
RANG_MOUSE	Ranbp1	RAN binding protein
A2AFJ1_MOUSE	Rbbp7	Retinoblastoma binding protein 7
RCC2_MOUSE	Rcc2	Regulator of chromosome condensation 2
Q3UK56_MOUSE	Rps3	Ribosomal protein S3
Q3V1Z5_MOUSE	Rps4l	Ribosomal protein S4-like
Q3UXP2_MOUSE	Ruvbl2	Ruvb-like protein 2
G3UZ26_MOUSE	Shmt1	Serine hydroxymethyltransferase 1 (soluble)
Q3TFD0_MOUSE	Shmt2	Serine hydroxymethyltransferase 2 (mitochondrial)
SPSY_MOUSE	Sms	Spermine synthase
Q3UJL7_MOUSE	Srm	Spermidine synthase
F10A1_MOUSE	St13	Suppression of tumorigenicity 13
Q3THQ5_MOUSE	Stip1	Stress-induced phosphoprotein 1
TBB5_MOUSE	Tubb5	Tubulin, beta 5 class I
Q91Y95_MOUSE	Txnrd1	Thioredoxin reductase 1
UCHL3_MOUSE	Uchl3	Ubiquitin carboxyl-terminal esterase L3 (ubiquitin thiolesterase)
Q3THL7_MOUSE	Vdac1	Voltage-dependent anion channel 1
VDAC2_MOUSE	Vdac2	Voltage-dependent anion channel 2
Q60950_MOUSE	Ybx1	Y box protein 1
sp|Q9CQV8-2|1433B_MOUSE	Ywhab	Tyrosine 3-monooxygenase/tryptophan 5-monooxygenase activation protein, beta polypeptide

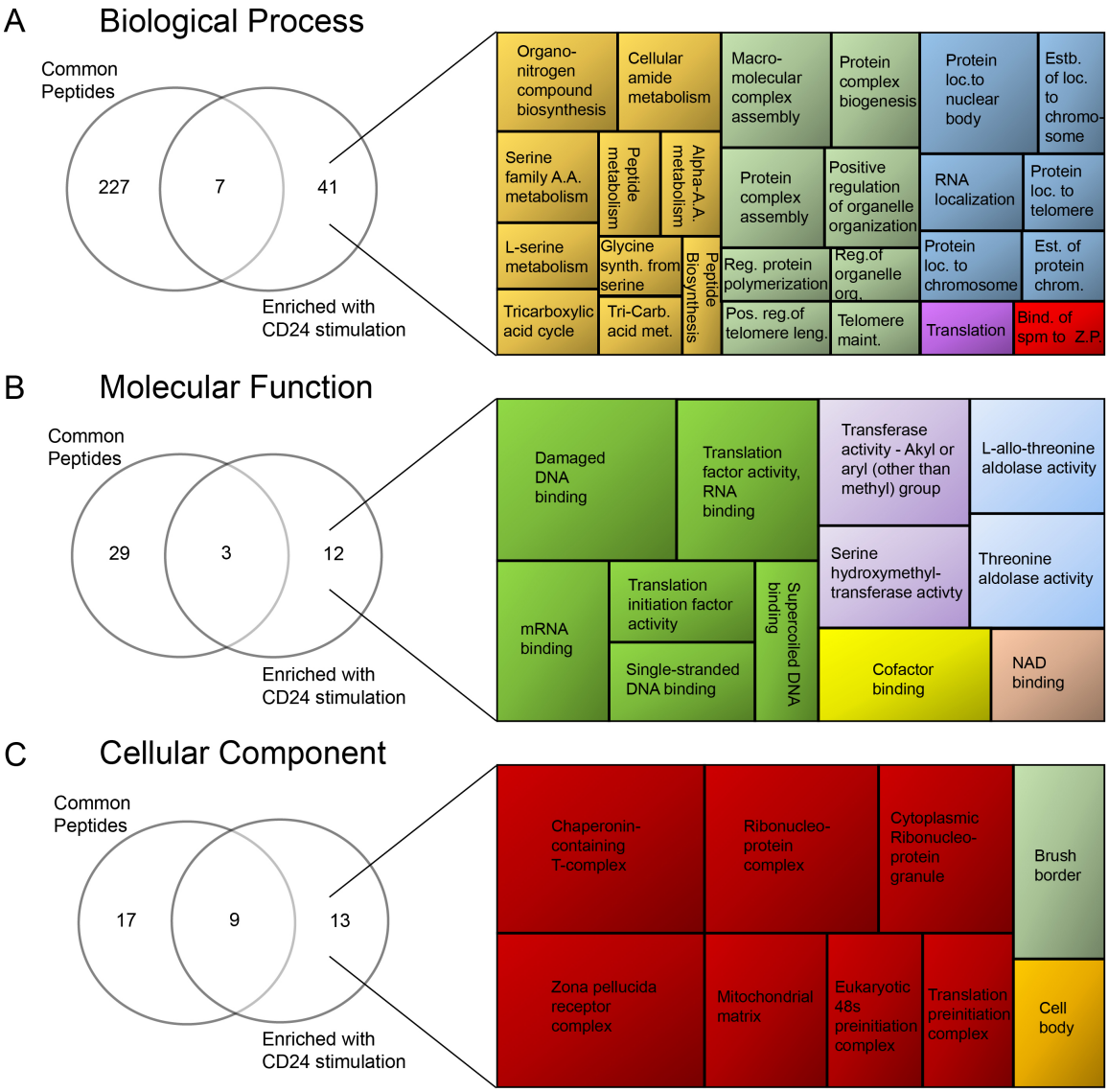
A
Biological Process
Common Peptides
227
7
41
Enriched with CD24 stimulation
Organo-nitrogen compound biosynthesis
Cellular amide metabolism
Macro-molecular complex assembly
Protein complex biogenesis
Protein loc.to nuclear body
Estb. of loc. to chromo-some
Serine family A.A. metabolism
Peptide metabolism
Alpha-A.A. metabolism
Protein complex assembly
Positive regulation of organelle organization
RNA localization
Protein loc. to telomere
L-serine metabolism
Glycine synth. from serine
Peptide Biosynthesis
Reg. protein polymerization
Reg.of organelle org.
Protein loc. to chromosome
Est. of protein chrom.
Tricarboxylic acid cycle
Tri-Carb. acid met.
Pos. reg.of telomere leng.
Telomere maint.
Translation
Bind. of spm to Z.P.
B
Molecular Function
Common Peptides
29
3
12
Enriched with CD24 stimulation
Damaged DNA binding
Translation factor activity, RNA binding
Transferase activity - Akyl or aryl (other than methyl) group
L-allo-threonine aldolase activity
Serine hydroxymethyl-transferase activty
Threonine aldolase activity
mRNA binding
Translation initiation factor activity
Supercoiled DNA binding
Single-stranded DNA binding
Cofactor binding
NAD binding
C
Cellular Component
Common Peptides
17
9
13
Enriched with CD24 stimulation
Chaperonin-containing T-complex
Ribonucleo-protein complex
Cytoplasmic Ribonucleo-protein granule
Brush border
Zona pellucida receptor complex
Mitochondrial matrix
Eukaryotic 48s preinitiation complex
Translation preinitiation complex
Cell body

Figure 4.4: Proteomics analysis suggests that CD24 stimulation causes enrichment of proteins from specific functional categories into MVs. Gene Ontology (GO) enrichment analysis was performed on proteins common to MVs from all 6 isotype and anti-CD24 samples in comparison to the proteins enriched in MVs after 1 h anti-CD24 stimulation (**Tables 4.2 and 4.3**). Venn diagrams (left panels) show GO terms associated with all MVs or those associated with the proteins enriched in MVs after anti-CD24 stimulation. The numbers indicate the number of unique GO terms associated with the respective protein lists. Enriched GO terms were visualized by REVIGO (230) (right panels). (A) CD24-enriched biological process (BP): Cellular amide metabolism (yellow), macromolecular complex assembly (green) and protein localization to nuclear body (blue). (B) CD24-enriched molecular functions (MF): Damaged DNA binding (green), transferase activity (purple) and threonine aldolase activity (blue). (C) CD24-enriched cellular component annotations were primarily grouped as chaperonin-containing T-complex (red). A.A. = amino acid, Synth = synthesis, Carb = carboxylic, Reg = regulation, Pos. = positive, Leng. = length, org = organization, Maint = maintenance, Loc = localization, Est = Establishment, Spm = sperm, Z.P = zona pellucida.

activity related to one carbon metabolism (**Figure 4.4**B). Finally, the CC terms were primarily categorized as Chaperonin-containing T complex, or other protein-binding complexes (**Figure 4.4**C), which function to regulate protein-protein interactions (232) and protein folding. Interestingly, both BP and CC ontologies identified an association of binding to the zona pellucida. This glycoprotein structure is composed of proteins and glycoproteins on the oocyte surface and is important for spermatozoa binding (233). It is well-known that CD24 is a heavily glycosylated protein (101), and this suggests potential biological similarity in MV proteins enriched by CD24 and those facilitating sperm:egg recognition.

Overall, as with the transcript analysis, there was a strong association between EV protein cargo, and mitochondrial or metabolic functions; however, I found other associations that suggest the regulation of protein localization or protein complexes.

The ToppFun analysis identified associations between the list of CD24-enriched EV proteins to multiple published proteomics studies, disease associations and Reactome pathways (**Supplemental File 3**). There were significant correlations with four different publications that examine exosome-associated protein cargo from B cells, podocytes, prostrate secretions and urine (234-237). B cell CD24-EVenriched proteins were also associated with one disease, squamous cell carcinoma of the esophagus ($q= 6.54x10^{-6}$). The most significant pathway associations were metabolism-related, such as carbon metabolism ($q = 4.95x10^{-6}$), serine/glycine biosynthesis ($q= 3.9x10^{-4}$), TCA cycle ($q= 3.9x10^{-4}$) and conversion of glucose to acetyl CoA ($q= 3.9x10^{-4}$), supporting the identified associations with mitochondrial-related functions.

To validate the proteomics data, I selected five proteins for Western blot analysis. Owing to the heterogeneity in the MS data, I again selected proteins found in two or more anti-CD24 stimulated EV samples, but present in no more than one sample from isotype-treated cells, with each protein having different biological associations (**Table 4.4**). I examined the expression of these proteins in both isotype or anti-CD24 stimulated cell lysates, and their respective Vn96-isolated EVs. Heat Shock Protein (HSP) 90 was used as a loading control (using an Ab that detects both HSP90 alpha and beta), as it is ubiquitously expressed in cells and was present in all six EV samples analysed by MS. By Western blot, HSP90 was found to be readily detectable and comparably expressed in all cell lysate and EV samples, and did not vary in response to anti-CD24 stimulation (**Figure 4.5**). SHMT2, EEF1G, HMGB2 and GRB2 were also easily detected in all cell lysates; however, GRB2 was detectable only at low level. The expression of these proteins in cell lysates was not affected by stimulation (**Figure 4.5**). In contrast with my MS analysis, I observed SHMT2 and EEF1G in EVs from both isotype and anti-CD24 stimulated cells, with no difference in abundance in response to anti-CD24 stimulation. GRB2 was not detected in any EV sample, potentially due to its overall low abundance. Finally, there was considerable heterogeneity in HMGB2 in EVs, with two apparent phenotypes observed. In two replicates, HMGB2 was present in EVs from the anti-CD24 stimulated cells, but absent or minimally present in EVs from isotype stimulated cells, as predicted by MS. However, in three other replicates, HMGB2 was not detected.

Table 4.4 Selected proteins from mass spectrometry data for validation by Western blot

Protein Name	Symbol	Rationale
Heat shock protein 90	HSP90α/β	Ubiquitously expressed in cells, and present in all EV. Used as Western blot loading control (221).
Serine hydroxymethyltransferase 2 (mitochondrial)	SHMT2	Enrichment of mitochondrial functions seen in transcriptome and proteomics data (238)
Eukaryotic translation elongation factor 1 gamma	EEF1G	Enrichment of gene transcription / translational processes, and ribosomal elements (239, 240).
High mobility group box 2	HMGB2	Stress inducible protein and highly orthologous to known CD24-interacting protein HMGB1 (241-243).
Growth factor receptor bound protein 2	GRB2	Important downstream effector of B cell signalling (244).

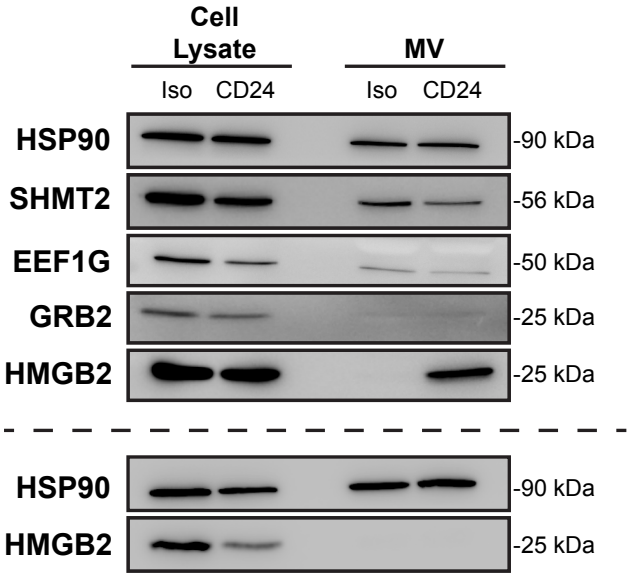

Figure 4.5: Proteins identified by proteomics analysis of B cell MVs are detectable in both cell lysates and MVs of isotype and anti-CD24 stimulated B cells by Western blot analysis. Cell lysates (5 µg; equivalent to approximately $2.3x10^5$ cells) and the corresponding protein from MVs (from $1.0x10^6$ cells) were analyzed for expression of SHMT2, EEF1G, GRB2 and HMGB2. HSP90 was used as a loading control after stimulation with isotype (Iso) or anti-CD24 (CD24). n=5. Two different outcomes were observed for HMGB2, with MVs from CD24 stimulated cells containing high HMGB2 (Upper panels, n=2) or HMGB2 being low/absent in all vesicles (lower panels n=3).

Overall, my proteomics analysis suggests that CD24 stimulation may enrich EVs with proteins involved with mitochondrial or metabolic functions. While MS analysis suggests specific protein enrichments following anti-CD24 stimulation, I was unable to confirm these enrichments via Western blot, likely due to differences in the sensitivity between the techniques, and intrinsic heterogeneity between EV samples.

4.3.4 CD24 stimulation produces EVs with a distinct surface composition

I next examined surface protein expression on cells and EVs by FACS in response CD24 stimulation. Two receptors, Siglec-2 (CD22) and Siglec-G were selected based on their potential in acting as CD24 signalling partners (13, 31, 245). CD63 was selected as a marker of EVs (87). The B cell receptor (BCR), detected as IgM, is known to share downstream signalling pathways and synergize with CD24 (61). MHC-II was selected as a marker of B cell activation and previous associations with activated B cell exosomes (235). Finally, Ter119 was selected as a putative negative control as its expression has been shown to be limited to erythroid-lineage cells (246).

CD24 stimulation causes a statistically significant decrease in the number of CD24+ cells compared to isotype-treated cells after 1 h (**Figure 4.6A**). No effect of stimulation time (1 h vs 2 h) was observed. The number of cells that expressed IgM, MHC-II, Siglec-2 and Siglec-G did not change in response to either Ab stimulation or time (**Figure 4.6**A), while the number of cells expressing CD63 increased significantly in

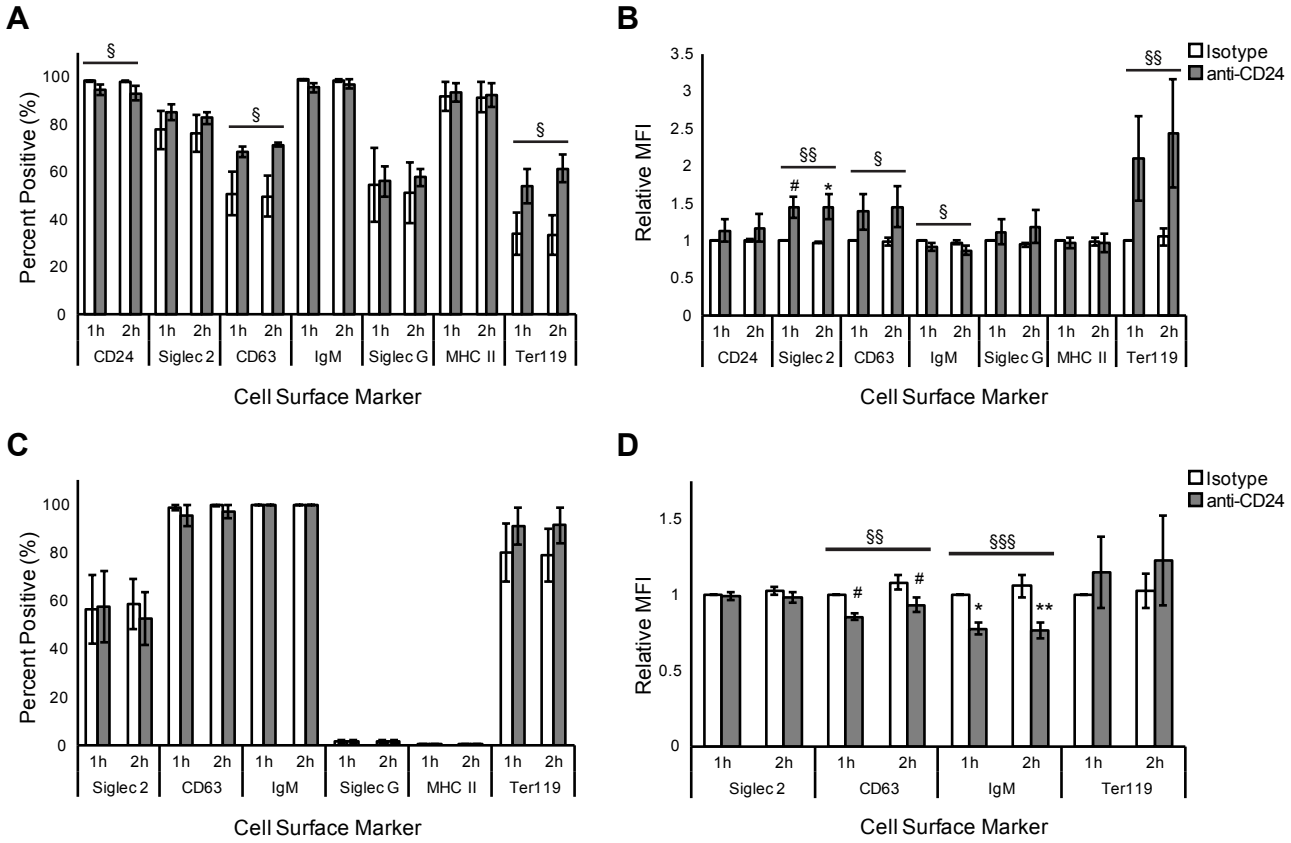

Figure 4.6: CD24 stimulation induces the formation of a unique B cell MV surface phenotype that does not reflect the cells from which they are released. Cells (A,B) and MVs (C,D) were analyzed for their expression of the indicated cell surface markers. Data are shown as mean ± SEM at 1 h or 2 h stimulation with either isotype or anti-CD24 Ab. n=3-4. Cells or CD24-bearing MVs bound to beads were assessed for the percentage of (A) cells or (C) MVs positive for the individual markers, and (B/D) their relative mean fluorescent intensities (MFI). Significant differences were assessed by two-way ANOVA followed by Tukey post-hoc test, if significant. Main effect of stimulation: § $P<0.05$, §§ $P<0.01$. Significant changes compared to time-matched control: $^{\#}P<0.1$, * $P<0.05$, ** $P<0.01$. Non-statistically significant changes have no indicators.

response to CD24 stimulation. I previously established that Ter119 is not expressed on isolated splenic B cells (data not shown) consistent with literature reports (246), but unexpectedly, I found that it is expressed on WEHI-231 cells. Furthermore, significantly more cells express Ter119 in response to anti-CD24 stimulation.

There were also statistically significant changes in the relative abundance (measured by mean fluorescent intensity; MFI) of Siglec-2, CD63, Ter119 and IgM on the cell surface in response to anti-CD24 stimulation (**Figure 4.6**B). The relative MFI of Siglec-2 and CD63 each increased by 1.4-fold at 1 h and 2 h post-stimulation. There was a 2.1-fold increase in Ter119 after 1 h, and a 2.4-fold increase after 2 h of CD24 stimulation. In contrast, there was a slight, but significant decrease in the relative MFI of IgM, as anti-CD24-stimulated cells had a relative MFI of 0.91 after 1 h and 0.87 after 2 h, compared with isotype-treated controls. Overall, the changes in MFI were due to the stimulation of CD24, but were independent of stimulation duration.

I have shown previously that EVs can transfer CD24 protein between cells (60). Therefore, I analyzed the expression of the same proteins as above on the population of immunoaffinity-isolated, CD24+ EVs to determine if the surface composition differs in this population of EVs. This strategy also improves the detection of proteins on the overall EV population, as all EVs are measured regardless if they are too small to be analyzed by FACS.

I found that there were no statistically significant differences at 1 h or 2 h in the number of beads positive for IgM, Siglec-2, CD63 or Ter119 EVs from isotype or anti-CD24-stimulated cells (**Figure 4.6**c). Essentially 100% of beads were positive for IgM (99.9 ± 0.1 %) and CD63 (97.7 ± 2.1%); however, only 56.3 ± 12.6% of the beads were

positive for Siglec-2. While 79.4% of beads with EVs from isotype-stimulated cells and 91.2% of beads with EVs from anti-CD24-stimulated cells were positive for Ter119, this difference was not statistically significant. Surprisingly, I was unable to detect EVs containing Siglec-G or MHC-II from either condition, despite cells being positive for both.

While cells showed an increase in the MFI of Siglec-2 in response to anti-CD24 stimulation, no difference was observed in EVs (**Figure 4.6**d), The MFI of CD63 on cells increased after anti-CD24 stimulation, which was opposite to the statistically significant decrease in CD63 MFI on the EVs at 1 and 2 h. Finally, I found that anti-CD24 stimulation induced significant decreases in the MFI of IgM on bead-captured EVs, which was similar in direction but not magnitude to the change seen with the cells. Overall, I found that anti-CD24 stimulation can induce significant effects on the surface composition of cells and EVs. Furthermore, I found that select surface receptors are excluded from EVs, irrespective of cell stimulation, demonstrating that the membrane components of EVs do not necessarily reflect the bulk cell surface, but can be selected for via an unknown process.

4.4 Chapter 4 Discussion

Cells produce a variety of different vesicle subtypes, defined in part through their mechanism of biogenesis, and in part based on their morphology and composition (113). As such, there is considerable overlap between population definitions, and no "gold-standard" exists to delineate vesicle sub-groups (247). I have therefore followed recommendations to examine multiple EV components, including their RNA, representative membrane, cytosolic and intracellular proteins, as well as overall morphology to define the EV subtype I have isolated in this study (247).

First, my analysis of the RNA and protein cargo carried by these B cell EV is more consistent with reports on MVs rather than exosomes. While RNA profiling is relatively new for EV, the RNA cargo carried by the EVs described here resembles that of MVs, but not exosomes or apoptotic bodies (204). Specifically, the lack of 18S and 28S rRNA in the BioAnalyzer analysis, and confirmed by sequencing analyses, and the shorter length of the RNA transcripts is more consistent with MVs than with apoptotic bodies, or exosomes (204). In the protein cargo, I identified the presence of several HSPs, including HSP90α/β, and exploited the presence of membrane-integral HSPs to isolate EVs using the Vn96 peptide (221). My MS analysis also identified other proteins associated with intracellular compartments under-represented in exosomes, such as Calreticulin from the endoplasmic reticulum and Histone cluster 1h4a, providing further support that the EV population is primarily composed of MVs and not exosomes (247).

Secondly, I detected the presence of several integral membrane cell surface receptors, including Siglec-2, the IgM, and CD63 by FACS. While CD63 was previously

considered an exosome marker, it is now appreciated that different EV species share compositional overlaps, and that this marker is not likely to be exclusive to exosomes (113, 138). I identified the presence of phosphatidylserine (PS) via Annexin V-staining, which is typically associated with MVs rather than exosomes (97). I also found that these EVs lack MHC-II, known to be present on exosomes from activated B cells (235).

Finally, through multiple techniques, including TEM, NPT and my previous FACS analysis (Section 3.3.3 and 3.3.4), I have established that the EVs described herein range in size from 70 nm to 170 nm. This is on the larger end of sizes reported for exosomes, but in line with reports on MVs (75). My previous analysis suggested the EVs released from WEHI-231 cells in response to CD24 are plasma membrane derived (as are MV) as there was no evidence of multivesicular body formation, as seen in figure 3.5 (60). Taken together, these data strongly support that most the EV population in this case is comprised of MVs, and not exosomes or apoptotic bodies, and that CD24 stimulation promotes the genesis of additional phosphatidylserine-positive MVs.

Within the cargo of these MVs, I observed considerable variability in MV RNA and protein composition. My analysis suggests B cells produce MVs with a spectrum of compositions following isotype and CD24 stimulation (**Figure 4.7**). There are several potential reasons for this variability. First, vesicle packaging is limited by available lumen area. The interior space of exosomes (or similarly sized MVs such as described here) is calculated to be 20 nm to 90 nm^3 (248). Thus, RNA and proteins compete for limited space. My measurements of MV RNA, averaging under 5 ng of total RNA per EV isolation from 2 mL of conditioned media (data not shown), agree with other assessments and indicate that these MVs package very few transcripts per vesicle (249).

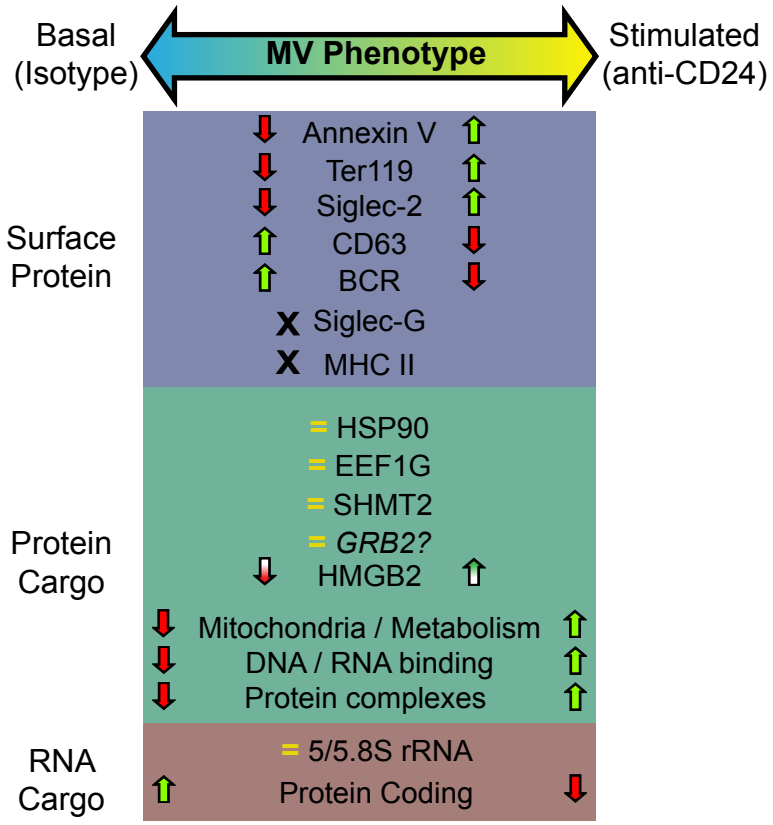

Figure 4.7: Summary diagram of the cargo and surface composition of MVs from isotype or CD24 stimulated cells. The differences in surface protein, luminal protein, and RNA transcriptome between basal and CD24 induced MVs are shown. No change indicated by =, absence indicated by X, a significant change indicated by arrows where arrows coloured with a gradient indicate a variable difference in abundance as detected by Western blot.

Thus, small differences in packaging, or skewing towards increased protein inclusion will lead to increased heterogeneity.

Secondly, cells can produce multiple vesicle populations simultaneously (138), which may increase the variability of cargo observed when isolating total EV populations, as was performed here. Studies using methods that select for a single EV sub-population (such as differential centrifugation, sucrose gradient floatation, or size-exclusion filtration) may exclude some EV populations and thus underestimate total EV cargo complexity (250). Additionally, the use of larger sample volumes (158, 251) or highly enriched cell culture supernatants (158) may also underestimate heterogeneity by reporting the dominant cargo species rather than capturing the population heterogeneity. In comparison, my analysis was on a small number of cells in a low volume of media with short duration of stimulation.

Finally, I detected the presence of HSPs, which can participate in protein degradation (252-254), and multiple proteasome sub-units in all six of the MV samples. This suggests that these MVs may contain proteolytically active components, which could result in the degradation of packaged vesicle proteins. This may explain the inability to detect some proteins by Western blot that were detected by MS, which relies on measurement of peptide fragments and not intact proteins. If degraded in this way, the protein may become smaller than is resolvable by SDS-PAGE gels. The loss of an epitope can prevent detection of proteins by western blot for various reasons, including splice variants of the protein that do not contain the antibody-specific sequence, or unappreciated post-translational modifications which may mask the availability of an epitope for antibody binding. Another potential cause of discrepancy between the MS and

Western blot detection of specific proteins owes to the sensitivity of the techniques. Whereas MS can detect single peptide fragments, Western blot requires substantially more protein to provide adequate signal, thus low abundance proteins in some samples may be detectable by MS whereas not identified via Western blotting.

The RNA cargo within the B cell MVs was primarily composed of 5.8S and 5S rRNA. Since I did not detect the presence of 18S or 28S rRNA by BioAnalyzer or by sequencing, I believe that these MVs do not carry these components. This agrees with other analyses of MVs from human HMC-1 mast cells and mouse BV-2 microglia cells which also lack 18S and 28S rRNA (204). It is unknown what the functional consequence of this apparent differential selection of rRNA species may be.

These B cell MVs carry protein-coding transcripts from both nuclear and mitochondrial genes, with the majority encoding components of the electron transport chain; however, I did not identify any differentially included transcripts in response to CD24 stimulation. I observed a reduction in the overall abundance of protein coding RNA and a trend towards increased miRNA incorporation following stimulation. As described in section 1.5, transcripts carried by MVs and EVs are functional, thus the inclusion of additional miRNA by these MVs may result in altering of protein translation in recipient cells. Only two of the miRNAs were annotated: mir6236 and mir5099. There is little information on the function of these miRNAs, however mir5099 expression is associated with B cell development (255) and binding to Argonaut, which is a key component in miRNA-induced RNA silencing, in helper T cells (256). Overall, the purpose of these transcripts and compositional changes in B cell MVs are unknown and may therefore be of interest in future studies on the biological function of these MVs.

My proteomics analysis suggested that CD24 may affect the protein cargo carried by B cell MVs. I found there were 41 unique proteins, identified by MS, carried in all six MV samples. A substantial number of these were canonical HSPs, which is expected as the Vn96 capture is known to depend, at least partially, on binding to HSPs, which are known to be enriched in EVs (113, 221). As previously discussed, a second major group of proteins identified in all six MV samples belong to the proteasome complex involved in protein degradation. While there were no unique proteins associated with MVs released following CD24 stimulation, there were 77 proteins identified as selectively enriched in at least 2 of 3 anti-CD24 stimulated MV samples.

Many proteins enriched in MVs from CD24 stimulated cells were involved in RNA shuttling, processing or stability. These include the KH-type splicing regulatory protein (Khsrp), Karyopherin (Importin) β-1 (Kpnb1), Ran binding protein 1 (Ranbp1), Heterogenous nuclear ribonucleoprotein A2/B1 (Hnrpa2b1), Poly(A) binding protein, cytoplasmic 1 (Pabpc1), and Poly(rC) binding protein 1 (PCBP1). These enriched proteins, along with the loss of protein coding mRNA and a trend towards increasing miRNA incorporation into MVs from CD24-stimulated cells, suggest a mechanism by which select miRNA transcripts could be enriched in MVs and influence recipient cell behaviour through their MV-mediated delivery and subsequent effect on the gene expression profile of the recipient cells. Future studies are planned to examine how the RNA and protein cargo of these MVs could influence recipient cell behaviour.

When I attempted to validate the CD24-mediated changes in protein cargo using four different proteins, representing different biological functions, I found that while all

the proteins were present in the cells, only EEF1G, SHMT2, and HMGB2, but not GRB2, were detectable in the EVs; however, the abundance of EEF1G and SHMT2 was not altered with CD24 stimulation. Interestingly, I found that HMGB2 had variable inclusion into MVs from CD24-stimulated cells, with it being highly enriched in MVs in response to CD24-stimulation in two biological replicates, but undetectable in MVs in additional replicates, regardless of the stimulation. I do not believe that this is a technical error, as other MV proteins (such as HSP90) were easily detected in the same replicate and there were very high levels of HMGB2 when it was detected. HMGB2 is closely related to HMGB1 and HMGB3, which are DAMPS that act in response to cellular stress (241, 242). Thus, I believe that there may be an additional stress event, which I have not yet identified, that allows HMGB2 to be released in response to CD24 stimulation. Studies are ongoing to identify additional signals that regulate HMGB2 release.

Overall, regardless of stimulation, a significant contribution to the MV RNA and protein cargo was related to mitochondrial components and functions. This included mitochondrial transcripts and proteins involved in metabolite generation and electron transport activity. I therefore propose these MVs, regardless of CD24 stimulation, are associated with proper mitochondrial maintenance. As with other cancers, B cell leukemia or lymphoma cells show increased markers of oxidative stress and reactive oxygen species (ROS) formation (257). Increased ROS production can negatively affect cell viability, leading to increased caspase activation, and ultimately cell death (258). As CD24 stimulation in B cells also results in caspase activation leading to apoptosis (62), the additional stress from CD24 stimulation may compound the challenge of dealing with ROS in these cells. Thus, the release of mitochondria components in B cell MVs, and the

enrichment of these components following CD24 stimulation, may act as a mechanism to regulate mitochondrial health. This is consistent with a recently-described process termed mitoptosis, which involves the selective sequestering, destruction and disposal of dysfunctional mitochondria to mitigate ROS stress and preserve cell viability (259). During mitoptosis, these dysfunctional mitochondria may be selectively discarded through plasma membrane blebbing (such as occurs in MV formation) in vesicles 50 nm to 200 nm in size (259). Therefore, the association reported herein between CD24 stimulation and an increase in the release of MVs enriched in mitochondrial components and cell stress markers, like HMGB2 may be related to mitoptosis, or a similar process, to regulate cell health and viability. Future studies will be necessary to test this hypothesis

Despite the variability in RNA and protein cargo, I observed clear phenotypic differences with respect to the cell surface receptor composition of cells and EVs, and that CD24 can induce specific changes to this composition. Approximately 50% of cells were positive for Siglec-G, regardless of stimulation, and all were positive for MHC-II; however, MVs carried neither protein. As both these proteins are integral membrane proteins, they must be excluded from the membrane domain from which MVs are released. In addition, following CD24 stimulation, cells increased their relative expression of Siglec-2 (CD22) but this was not reflected in the MVs. Similarly, CD24-stimulation caused an increase in the percentage of cells expressing CD63 from approximately 50% to 68.3% at 1 h and to 71.5% at 2 h, as well as increasing its relative abundance. In contrast, nearly 100% of the MV populations from both conditions expressed CD63, and CD24 stimulation caused a *decrease* in the relative abundance of CD63 carried by MVs. These observations clearly demonstrate that MVs are not merely

representative of the cells from which they originate, and that aspects of their surface composition must be regulated during formation.

The release of exosomes by B cells is associated with their activation during immune signalling (260, 261). My analysis suggests the MVs isolated here are not related to B cell activation. First, B cell activation requires BCR stimulation, which was not performed here. Also, Siglec-2 is antagonistic to BCR signalling (262), thus the observed increase in Siglec-2 expression would be expected to inhibit BCR signalling. Additionally, B cell exosomes carry antigen-presenting MHC-II (235) whereas I found no MHC-II expression on the MVs captured. Therefore, the distinct surface composition, as well as the abundance of mitochondrial contents, argues these MVs are formed and released to perform a distinct function compared with exosomes released during B cell activation. The functional consequences of these compositional differences are unknown, but will likely be an important consideration in understanding the function of exosomes compared to MVs.

The ability of CD24 to promote MV cargo composition changes likely affects the function of these MVs, and the specific changes in surface receptors on the MVs may influence their intended extracellular targets. Compositionally, the mitochondrial cargo carried by these B cell MVs, and potentially enriched by CD24, suggest they may have a role in regulating mitochondrial health or stress.

Chapter 5: General Discussion

5.1 Functional potential of CD24 in EV

While it is clear that CD24 can induce changes in microvesicle (MV) composition, a mechanistic role of CD24 itself has yet to be identified. Several studies propose that CD24 may be useful as a marker of extracellular vesicles (EVs) (158, 221); however, its function has not been elucidated. An examination of the established biological functions of CD24 suggests several potential roles. First, it may act as an adhesion molecule, potentially for the recognition and binding of EV/MV to cells. Alternatively, CD24 present on EV may act as a signalling entity for immune cells, with its established ability to affect lymphocyte survival and activation.

CD24 can mediate cell adhesion events through cell-specific ligands, such as selectins (24-26). The ability to enable cell to cell recognition and binding is easily extendable to suggest it may enable cell to EV binding. Its heavy glycosylation further promotes this hypothesis. It was recently shown that Siglec-1 (CD169) expressed on the cell surface is required for exosome capture by macrophages, and for apoptotic vesicle recognition by immune cells. This recognition occurs through binding to EV-incorporated proteins modified with α2,3 sialic acids (112, 263).

CD24 is modified by the addition of α2,3- and α2,6 sialic acids, thus it is possible that the α2,3 and/or α2,6 sialic acids on CD24 promote interaction of EVs with Siglec-expressing cells. The data presented in this work demonstrates that Siglec-G, which is structurally similar to Siglec-1 (31, 184), is retained on the B cell surface rather than incorporated into their MVs. This creates a dynamic whereby cells can create an intrinsic

receptor-ligand distribution to facilitate EV recognition. By controlling specific glycosylation moieties on their surface, cells may be able to direct EV to specific binding partners. For example, not all Siglecs demonstrate equal binding to sialic acid. Siglec-1 bind preferentially to α2,3 sialic acid, whereas Siglec 2 (CD22) bind to α2,6 sialic acid, and Siglec-G (Siglec-10) has an affinity to both (264, 265). In fact, CD24-Siglec-G interactions have been documented via both α2,3 and α2,6 mechanisms (31). By enriching the EV surface with specific combinations of glycosylation, cells may be specifically targeted by their expression of appropriate Siglec receptors. With its highly variable, cell-specific glycosylation patterns CD24 could potentially act as a universal "addressing" molecule, by acting as a protein core to which a specific "glyco-address" could be attached.

In addition, protein glycosylation may influence EV formation. Proteins heavily enriched for N-linked glycosylation (notably α2,6 sialic acids) are preferentially sorted into EV when compared to their relative abundance on the cell surface (101). The selective inhibition of α2,6 sialyation was capable of preventing protein inclusion into EVs, without altering the quantity of EVs released from a cell, demonstrating that the N-glycan modification may serve as a determinant of EV protein inclusion. As CD24 is heavily enriched for these same structures, it is not necessarily surprising that it is enriched in EVs. By extension, however, it is known that CD24 can alter the localization of other proteins, such as integrins on the cell surface (71). Furthermore, following its stimulation, CD24 induces redistribution of other proteins into lipid raft (or glycolipid-enriched membrane) domains, such as Lyn and the BCR (61). Therefore, the selective

sorting of CD24, and other N-linked glycated proteins, may have direct implications on the selection of other cell surface proteins selected for release in EVs.

5.2 Sorting of CD24 in EVs may have immune cell signalling and survival repercussions

The presence of CD24 on EV released from B cells may have direct implications on the signalling, activation, or survival of other cells in their microenvironment. CD24 is most highly expressed in B cells during their bone marrow development, with a re-activation in transitional, splenic B cells (13, 33, 54). During these periods, CD24-expressing B cells are resident in areas of high cell density, with large numbers of other B cells as well as other developing immune cells, antigen presenting cells, and stromal cells. Therefore, the release of CD24-bearing EVs into a heterogeneous, high cell-density environment may allow for these EVs to interact with a broad range of cellular targets.

CD24-bearing EV may retain the ability to induce intracellular signalling in recipient cells by co-transporting CD24 with transmembrane signalling partners. Thus, these EVs may be capable of directly influencing the induction of apoptosis or activation in recipient cells. For B cells, this means CD24-bearing EVs may be able to modulate the induction of apoptosis *de novo*. Therefore, the release of CD24-bearing EV from one cell may serve as a pro-apoptotic factor upon their incorporation into a neighbouring cell. The potential for a positive-feedback cascade whereby a single B cell releasing CD24-positive EV induces apoptosis, and EV release from recipient B cells may spread through a population. This possibility may have implications into our understanding of autoimmune

disease or leukemia where the balance between pro-apoptotic, pro-proliferative and pro-activation signalling becomes dysregulated.

CD24-bearing EV may inhibit the function of the BCR on neighbouring B cells owing to their composition which I have identified in this work. The inclusion of CD24 and CD22 in EVs is likely to be a potent inhibitor of BCR-mediated signalling and activation. It has been well-established that CD22 is a negative regulator of the BCR (266). CD22 is also known to operate through Lyn, supporting potential complementarity with CD24, which can activate these same proteins (262). The transport of CD22 via EV to neighbouring B cells thus carries the potential to depress the responsiveness of the BCR to stimulation. In congruence with this idea, CD24 is known to affect the localization of the BCR on the plasma membrane. Indeed, CD24 stimulation results in co-localization with the BCR (61). Therefore, EV transport of CD24 may serve to cluster the BCR into EV-interacting domains on the PM surface. This would bring these BCRs into proximity of CD22, potentiating its ability to inhibit BCR activation. Other components of the EVs described in chapter 4 further suggest these vesicles are not involved in activation of the B cell since B cells release MCH-II-positive EV in response to activation (86). The lack of MCH-II in EV described herein argues they serve a distinct function, which is compatible with their potential to inhibit activation.

These MVs may therefore participate in multiple roles. First, their ability to act as mitoptosis-enabling entities may act as a mechanism to attempt to protect B cells from BCR-mediated apoptosis. In recipient cells, these MVs may act directly as a BCR-activation suppressor, to protect cells from the induction of apoptosis in the first place.

The composition of these CD24-bearing MVs may act as an anti-activation mechanism for other immune cells in the local environment. The ability of CD24 to restrain T cell homeostatic proliferation, or to induce apoptosis in neutrophils suggest these MVs could potentially act as an immunomodulatory vector in areas of high immune cell density. The lack of MHC-II would similarly prevent these MVs from acting as a means of CD4+ T cell antigen presentation, and the generation of a T-cell mediated immune response. Therefore, overall the composition of the MVs released from CD24-stimulated B cells would suggest their role in recipient cells is to act as an immune down-regulating agent, potentially as a means of maintaining a homeostatic balance of immune cell activation and survival (**Figure 5.1**).

5.3 A Generalized mechanism of CD24 signalling

5.3.1 CD24 is a signalling rheostat

A broader question which remains to be answered is the mechanism through which the CD24 protein can signal to engage any intracellular effects, such as Src tyrosine kinase activation, calcium signalling or the formation of EV, since CD24 lacks a transmembrane domain. By examining the wealth of published data on CD24 interactions and effects, I propose that rather than act as a signalling receptor in its own right, CD24 functions as a rheostat to modulate responses transduced by a cell surface transmembrane receptor(s) to which it is partnered, and that the partner receptor defines the biological outcome. Mechanistically, CD24 likely modulates activation of the receptor through direct physical interaction mediated by its modifiable glycoslyations.

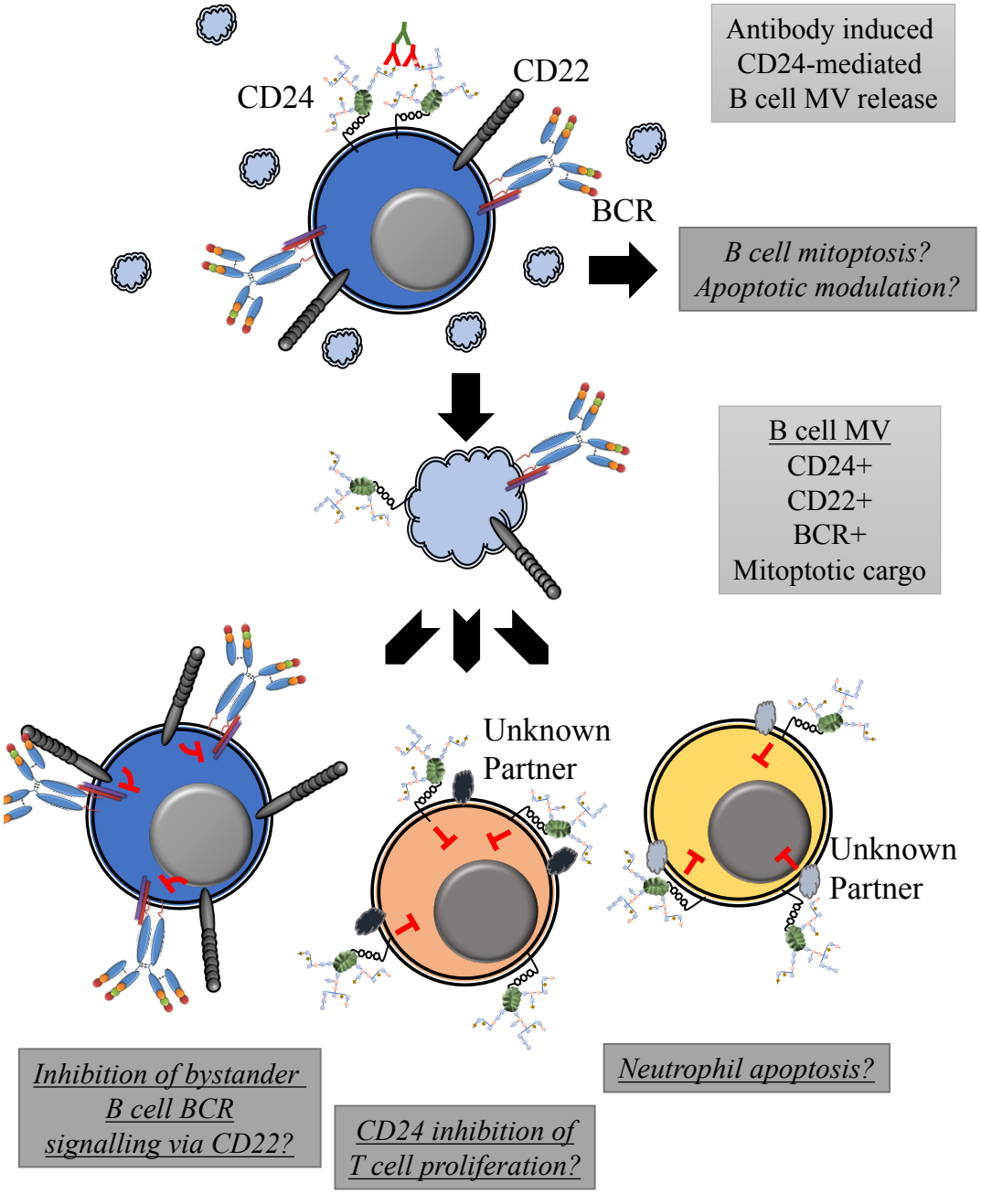

Figure 5.1 Potential signalling functions of CD24-MVs released from B cells. Following antibody-mediated stimulation of CD24, B cell MVs are released containing CD24, CD22 and the BCR (among other cargo). These MVs may act to suppress local immune responses through several means. They may act to directly inhibit neighbouring B cells via CD24/CD22-mediated repression of BCR signalling (left), CD24-mediated restriction of T cell proliferation (centre) and regulation of neutrophil cell survival (right).

The variable nature of CD24-mediated effects can be explained by its *in cis* association with unique, cell-type specific signalling partners (**Figure 5.2**). The activity of the partner receptor could be further modulated through additional *cis* or *trans* elements acting via multi-receptor complexes. Moreover, the activity of the partner receptor could have additional effects on downstream receptors. The presence of CD24 may alter the association of cell surface receptors with their canonical ligands, to promote or inhibit receptor activation. Ligand - receptor interactions may also promote association, or displacement, of CD24 from its receptor partner, which we have termed an associative or dissociative ligand, respectively.

While it is our opinion this is the most parsimonious explanation for the cell-specific effects mediated by CD24, it does not necessarily suggest a generalized mechanism of GPI-anchored protein signalling. GPI-anchored proteins have been shown to work through specific transmembrane proteins, as well as to signal via endocytosis or lipid kinases (203, 267-271), thus consideration of specific GPI anchored protein signalling should be considered on a case-by-case basis. Importantly, we believe that CD24 is unique in that it partners with different cell-specific signalling receptors in a cell-type dependent manner.

5.3.2 Physical Interactions with Cell Surface Receptors

CD24 interacts *in cis* with L1CAM on neuroblastoma cells in a predicted 5:1 ratio (19). L1CAM/CD24 associates *in cis* with NCAM1, forming a tri-molecular complex, however no direct interaction between CD24 and NCAM1 was observed. The

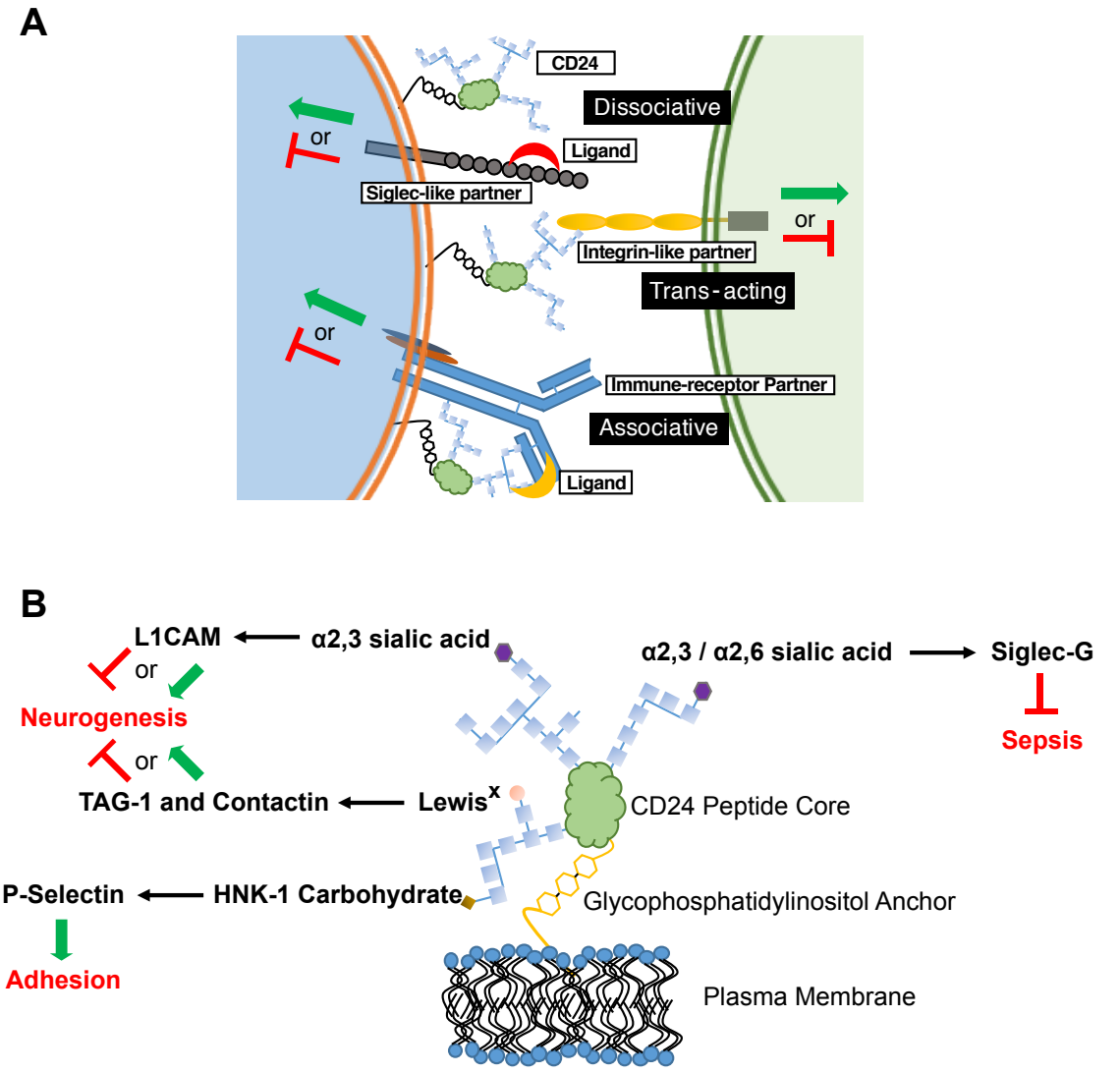

Figure 5.2. CD24 operates through a combination of *in cis* and *in trans* partners to affect cell behaviour in a cell-specific manner. A) Schematic diagram showing the possible associations of CD24 with partner receptors and ligands. These associations selectively tune cellular responses. CD24 association with a signalling partner may be enhanced or inhibited through associative and dissociative ligands, respectively. The various CD24 interactions may not be mutually exclusive on a single cell, thus leading to a mosaic of cellular interactions and activation (green arrow) or inhibitory (red line) effects. B) Interactions between specific CD24 glycosylations, ligands and known biological outcomes. Glycosylations are depicted as chains of carbohydrate monomers (blue squares) but do not represent a specific structure. The ligand-interacting, terminal carbohydrate moiety is indicated. L1CAM, Contactin and TAG-1 show both activating and inhibitory signals for neurogenesis as both effects can be mediated in discrete regions during CNS development.

use of Ab against both CD24 or L1CAM to mimic ligand induced a calcium influx, with co-stimulation having a synergistic effect (19). This strongly suggests that the physical interaction between CD24 and L1CAM is associated with shared signalling processes.

CD24 also acts *in cis* with Siglec-G to moderate DC activation (29, 31). In dendritic cells from the liver, CD24 forms a complex between Siglec-G and extracellular DAMP proteins, such as HMGB1, to alter the activity of Toll-Like Receptors (TLR) (28, 29). Here, Siglec-G was the signalling partner of CD24, via interaction with the glycosylations on CD24. In the presence of CD24, signalling downstream from Siglec-G prevents the activation of TLRs by DAMPS. However, in the absence of CD24, the inhibition of TLR is lost. Moreover, CD24 is a necessary mediator in this system as Siglec-G and HMGB1 were shown to be associative ligands with CD24, but neither HMGB1 nor TLR interact directly with Siglec-G in this system.

5.3.3 Interactions with signalling proteins and receptors

Studies in B cells have shown that CD24 alters the localization of the B Cell Receptor (BCR) and associated intracellular signalling proteins within lipid rafts (61). Furthermore, engagement of the BCR results in many of the same outcomes regulated by CD24, including apoptosis, Protein Tyrosine Kinase (PTK) and Mitogen Activated Protein Kinase (MAPK) activity (61, 62). Moreover, co-ligation of both CD24 and the BCR with sub-optimal doses of Ab can induce apoptosis, whereas ligation of either alone could not, suggesting cooperative signalling (61).

CD24 is important in regulating T cell survival. T cells must regulate their proliferation to support a long-lived cell population, but can expand their numbers during immune activation (272). In the absence of CD24, homeostatic proliferation of T cells is markedly reduced. In total-body CD24 knockout mice, homeostatic T cell proliferation is dysregulated, causing excessive and destructive T proliferation (67). In contrast, immune-driven proliferation is less affected by the absence of CD24 (66), likely because it depends on TCR co-receptors (273). However, the presence of CD24 on either T cells or dendritic cells is sufficient to control homeostatic T cell proliferation, suggesting that CD24 can act either *in cis* on the T cell to regulate TCR signalling, or *in trans,* where DC-expressed CD24 can bind and modulate its partner(s) on the T cell.

5.3.4 Regulation of plasma membrane organization and signalling

As CD24 lacks an intracellular domain, it cannot directly activate signalling pathways. CD24 is resident in highly fluid, cholesterol-rich microdomains, termed lipid rafts (274). In B cells and in breast cancer cells the presence of CD24 in lipid rafts excludes the CXCR4, the chemokine receptor for Stromal Cell Derived Factor-1 (SDF-1), from lipid rafts whereas in the absence of CD24, CXCR4 can enter lipid rafts (275). This exclusion prevents the SDF-1 activation of CXCR4-mediated signalling. In contrast, β-integrin is normally found in non-lipid raft membrane domains, but in the presence of CD24 it can translocate into lipid rafts (276) to promote cell-cell adhesion (72). These studies suggest that regulating the physical location of receptors is also a function of CD24.

The ability of CD24 to act as a membrane-organizing factor further supports a role for CD24 in interacting with receptors partners to regulate receptor oligomerization and localization. It is also possible that CD24 can rapidly or contextually alter its associations, which may be another mechanism through which it exerts context-specific effects.

5.3.5 Identifying CD24 mechanisms

If the ability for CD24 to mediate intracellular signalling is dependent on its association with cell-type specific surface receptors, then identification of these partners is essential. In some cases, transcriptomic data may be used to predict potential partners by their co-expression with CD24 (13). Alternatively, knowledge of common biological outcomes between CD24 and cell specific surface receptors could be used to predict receptor partners. Visualization of co-localized receptors through high resolution microscopy may be employed to demonstrate co-localization on intact cells. Alternatively, if there are no known or predicted CD24 interactors expressed in the cell of interest, a non-biased approach, such as mass-spectrometry based identification of CD24 interacting proteins would be necessary.

Confirming the functional interaction between CD24 and its partner could be accomplished *in vivo* with the use of knockout and transgenic animals and *in vitro* using gene knockout or over-expression vectors, to alter the expression of CD24 and its putative signalling partner. Altering the expression of CD24 should disrupt the signalling through its partner. For example, if CD24 acts to restrict signalling, then the receptor

partner may become hyper-responsive in a CD24 knockout. The inverse relationship would be seen if CD24 is a positive regulator of signalling. This relationship may explain the loss of developing B cells in both CD24 knockout and CD24-overexpressing mice, since the BCR can transduce pro-survival or pro-apoptotic signals, depending on B cell developmental status and the strength of BCR stimulation (277, 278). In CD24-knockout animals, the BCR may be over-sensitive leading to apoptosis, whereas in transgenic mice with constitutively high levels of CD24, the BCR no longer provides supportive tonic signalling, leading to apoptosis.

With whole-body knockout animals, compensatory changes to the expression of the signalling partner may occur due to the absence of CD24, to re-establish its signalling potential. These changes may be observed by comparing the expression of partner receptors in wild type vs. CD24 knockout mice. The generation of inducible CD24 knock-out models, to prevent compensatory changes in partnered receptors or signalling pathways, would negate these concerns.

Importantly, knockdown or over-expression of the signalling partner would have the same biological outcomes as the loss or gain of CD24, respectively. In this case, CD24 could still be engaged with ligand or Ab, but would not exert any effect in the absence of its partner.

Determining the mechanism for CD24-ligand specificity is key. CD24 has been shown to vary in size from approximately 30 to 80 kDa, depending on the tissue from which it is isolated due to the variable mosaic of different N- and O- linked glycosylations (14). The different terminal glycans exhibit unique binding potential to cell surface receptors. For example, Siglec-G binds to α2,6 and α2,3 sialic acid (31),

whereas P-selectin binds to human natural killer-1 (HNK-1) sulfated carbohydrates (279) on CD24. If the binding and activity of CD24 is glycan-dependent, tissue-specific glycosylation would create glyco-variants of CD24 capable of interacting with specific partners, allowing a selectivity of responsiveness, and preventing systemic effects. Therefore, it is our opinion that future studies to identify *in cis* and *in trans* partners of CD24 should seek to identify the glycan moieties on CD24 mediating those interactions.

5.4 Implications and Conclusions

This thesis describes a comprehensive analysis on the expression and function of CD24 in several cellular contexts, with a primary focus on its role in regulating apoptosis in immature, developing B cells from humans and mice. While there are still outstanding questions regarding the nature of CD24-ligand interactions, and their cell-specific functions, I have validated that co-expression analysis is a viable approach for identifying putative signalling partners as a first step in further elucidating these interactions. I have further developed a general schema for CD24-mediated activity which is the first to attempt to provide a unifying theory on the cell-specific effects attributed to CD24.

I propose that CD24 influences different *cis*-interacting partners**,** or that some CD24 “ligands” may not directly interact with CD24, but could interact with an associated partner. Thus, this would explain how CD24 is associated with numerous and diverse ligands and cellular activities but be widely expressed and evolutionarily conserved. As CD24 is also carried on EV, this ability to act *in cis* or *in trans* with a multitude of partners may be significant for its biological functions.

My investigation into the mechanism of CD24-mediated apoptosis in B cells is the first to identify it as a regulator of B cell EV release, and a director of B cell EV composition. As a director of cell signalling or stress, CD24-laden vesicles may be potent signalling modulators that can interact with numerous partners in the cellular microenvironment, or even at distal sites. Future studies may now focus on the role of B cell EV to alter the function of recipient cells in immune microenvironments. The data presented here thus provide a solid foundation for future studies that can elucidate a broader understanding of the function of CD24 in regulating B cell development. By gaining new insight into this function, we may identify new fundamental principles guiding CD24-mediated cell survival and activation as well as a more complete picture of how cell fate can be controlled.

Chapter 6: References

1. Springer T, Galfre G, Secher DS, Milstein C. Monoclonal xenogeneic antibodies to murine cell surface antigens: identification of novel leukocyte differentiation antigens. Eur J Immunol. 1978;8(8):539-51.

2. Alterman LA, Crispe IN, Kinnon C. Characterization of the murine heat-stable antigen: an hematolymphoid differentiation antigen defined by the J11d, M1/69 and B2A2 antibodies. Eur J Immunol. 1990;20(7):1597-602.

3. Pirruccello SJ, LeBien TW. The human B cell-associated antigen CD24 is a single chain sialoglycoprotein. J Immunol. 1986;136(10):3779-84.

4. Duperray C, Boiron JM, Boucheix C, Cantaloube JF, Lavabre-Bertrand T, Attal M, et al. The CD24 antigen discriminates between pre-B and B cells in human bone marrow. J Immunol. 1990;145(11):3678-83.

5. Kay R, Takei F, Humphries RK. Expression cloning of a cDNA encoding M1/69-J11d heat-stable antigens. J Immunol. 1990;145(6):1952-9.

6. Kay R, Rosten PM, Humphries RK. CD24, a signal transducer modulating B cell activation responses, is a very short peptide with a glycosyl phosphatidylinositol membrane anchor. J Immunol. 1991;147(4):1412-6.

7. Wenger RH, Ayane M, Bose R, Kohler G, Nielsen PJ. The genes for a mouse hematopoietic differentiation marker called the heat-stable antigen. Eur J Immunol. 1991;21(4):1039-46.

8. Fischer GF, Majdic O, Gadd S, Knapp W. Signal transduction in lymphocytic and myeloid cells via CD24, a new member of phosphoinositol-anchored membrane molecules. J Immunol. 1990;144(2):638-41.

9. Boccuni P, Del Vecchio L, Di Noto R, Rotoli B. Glycosyl phosphatidylinositol (GPI)-anchored molecules and the pathogenesis of paroxysmal nocturnal hemoglobinuria. Crit Rev Oncol Hematol. 2000;33(1):25-43.

10. Ayre DC, Christian SL. CD24: A Rheostat That Modulates Cell Surface Receptor Signaling of Diverse Receptors. Front Cell Dev Biol. 2016;4:146.

11. Hough MR, Rosten PM, Sexton TL, Kay R, Humphries RK. Mapping of CD24 and homologous sequences to multiple chromosomal loci. Genomics. 1994;22(1):154-61.

12. Pruitt KD, Brown GR, Hiatt SM, Thibaud-Nissen F, Astashyn A, Ermolaeva O, et al. RefSeq: an update on mammalian reference sequences. Nucleic Acids Res. 2014;42(Database issue):D756-63.

13. Ayre DC, Pallegar NK, Fairbridge NA, Canuti M, Lang AS, Christian SL. Analysis of the structure, evolution, and expression of CD24, an important regulator of cell fate. Gene. 2016.

14. Fang X, Zheng P, Tang J, Liu Y. CD24: From A to Z. Cell Mol Immunol. 2010;7:100-3.

15. Tan Y, Zhao M, Xiang B, Chang C, Lu Q. CD24: from a Hematopoietic Differentiation Antigen to a Genetic Risk Factor for Multiple Autoimmune Diseases. Clin Rev Allergy Immunol. 2015.

16. Hitsumoto Y, Nakano A, Ohnishi H, Hamada F, Saheki S, Takeuchi N. Purification of the murine heat-stable antigen from erythrocytes. Biochem Biophys Res Commun. 1992;187(2):773-7.

17. Kadmon G, Eckert M, Sammar M, Schachner M, Altevogt P. Nectadrin, the heat-stable antigen, is a cell adhesion molecule. J Cell Biol. 1992;118(5):1245-58.

18. Hahne M, Wenger RH, Vestweber D, Nielsen PJ. The heat-stable antigen can alter very late antigen 4-mediated adhesion. J Exp Med. 1994;179(4):1391-5.

19. Kadmon G, von Bohlen und Halbach F, Horstkorte R, Eckert M, Altevogt P, Schachner M. Evidence for cis interaction and cooperative signalling by the heat-stable antigen nectadrin (murine CD24) and the cell adhesion molecule L1 in neurons. Eur J Neurosci. 1995;7(5):993-1004.

20. Bailey CH, Kandel ER. Synaptic remodeling, synaptic growth and the storage of long-term memory in Aplysia. Prog Brain Res. 2008;169:179-98.

21. Kleene R, Yang H, Kutsche M, Schachner M. The neural recognition molecule L1 is a sialic acid-binding lectin for CD24, which induces promotion and inhibition of neurite outgrowth. J Biol Chem. 2001;276(24):21656-63.

22. Krames ES. The dorsal root ganglion in chronic pain and as a target for neuromodulation: a review. Neuromodulation. 2015;18(1):24-32; discussion

23. Fine EJ, Ionita CC, Lohr L. The history of the development of the cerebellar examination. Semin Neurol. 2002;22(4):375-84.

24. Aigner S, Ruppert M, Hubbe M, Sammar M, Sthoeger Z, Butcher EC, et al. Heat stable antigen (mouse CD24) supports myeloid cell binding to endothelial and platelet P-selectin. Int Immunol. 1995;7(10):1557-65.

25. Sammar M, Aigner S, Altevogt P. Heat-stable antigen (mouse CD24) in the brain: dual but distinct interaction with P-selectin and L1. Biochim Biophys Acta. 1997;1337(2):287-94.

26. Myung JH, Gajjar KA, Pearson RM, Launiere CA, Eddington DT, Hong S. Direct measurements on CD24-mediated rolling of human breast cancer MCF-7 cells on E-selectin. Anal Chem. 2011;83(3):1078-83.

27. Aigner S, Ramos CL, Hafezi-Moghadam A, Lawrence MB, Friederichs J, Altevogt P, et al. CD24 mediates rolling of breast carcinoma cells on P-selectin. Faseb j. 1998;12(12):1241-51.

28. Liu Y, Chen GY, Zheng P. CD24-Siglec G/10 discriminates danger- from pathogen-associated molecular patterns. Trends Immunol. 2009;30(12):557-61.

29. Chen GY, Tang J, Zheng P, Liu Y. CD24 and Siglec-10 selectively repress tissue damage-induced immune responses. Science. 2009;323:1722-5.

30. Tang D, Kang R, Coyne CB, Zeh HJ, Lotze MT. PAMPs and DAMPs: signal 0s that spur autophagy and immunity. Immunol Rev. 2012;249(1):158-75.

31. Chen GY, Chen X, King S, Cavassani KA, Cheng J, Zheng X, et al. Amelioration of sepsis by inhibiting sialidase-mediated disruption of the CD24-SiglecG interaction. Nat Biotechnol. 2011;29(5):428-35.

32. Hough MR, Chappel MS, Sauvageau G, Takei F, Kay R, Humphries RK. Reduction of early B lymphocyte precursors in transgenic mice overexpressing the murine heat-stable antigen. J Immunol. 1996;156(2):479-88.

33. Chappel MS, Hough MR, Mittel A, Takei F, Kay R, Humphries RK. Cross-Linking the Murine Heat-Stable Antigen Induces Apoptosis in B Cell Precursors and

Suppresses the Anti-CD40-Induced Proliferation of Mature Resting B Lymphocytes. J Exp Med. 1996;184:1639-49.

34. Keller G, Lacaud G, Robertson S. Development of the hematopoietic system in the mouse. Exp Hematol. 1999;27(5):777-87.

35. Sasaki K, Sonoda Y. Histometrical and three-dimensional analyses of liver hematopoiesis in the mouse embryo. Arch Histol Cytol. 2000;63(2):137-46.

36. Fernandez KS, de Alarcon PA. Development of the hematopoietic system and disorders of hematopoiesis that present during infancy and early childhood. Pediatr Clin North Am. 2013;60(6):1273-89.

37. Orkin SH, Zon LI. Hematopoiesis: An Evolving Paradigm for Stem Cell Biology. Cell. 2008;132(4):631-44.

38. Seita J, Weissman IL. Hematopoietic stem cell: self-renewal versus differentiation. Wiley Interdiscip Rev Syst Biol Med. 2010;2(6):640-53.

39. Elghetany MT, Patel J. Assessment of CD24 expression on bone marrow neutrophilic granulocytes: CD24 is a marker for the myelocytic stage of development. Am J Hematol. 2002;71(4):348-9.

40. Raife TJ, Lager DJ, Kemp JD, Dick FR. Expression of CD24 (BA-1) predicts monocytic lineage in acute myeloid leukemia. Am J Clin Pathol. 1994;101(3):296-9.

41. Sammar M, Aigner S, Hubbe M, Schirrmacher V, Schachner M, Vestweber D, et al. Heat-stable antigen (CD24) as ligand for mouse P-selectin. Int Immunol. 1994;6(7):1027-36.

42. Parlato M, Souza-Fonseca-Guimaraes F, Philippart F, Misset B, Adib-Conquy M, Cavaillon JM. CD24-triggered caspase-dependent apoptosis via mitochondrial membrane

depolarization and reactive oxygen species production of human neutrophils is impaired in sepsis. J Immunol. 2014;192(5):2449-59.

43. del Hoyo GM, Martin P, Vargas HH, Ruiz S, Arias CF, Ardavin C. Characterization of a common precursor population for dendritic cells. Nature. 2002;415(6875):1043-7.

44. Martinez del Hoyo G, Martin P, Arias CF, Marin AR, Ardavin C. CD8alpha+ dendritic cells originate from the CD8alpha- dendritic cell subset by a maturation process involving CD8alpha, DEC-205, and CD24 up-regulation. Blood. 2002;99(3):999-1004.

45. Chaplin DD. Overview of the immune response. J Allergy Clin Immunol. 2010;125(2 Suppl 2):S3-23.

46. Dal Porto JM, Gauld SB, Merrell KT, Mills D, Pugh-Bernard AE, Cambier J. B cell antigen receptor signaling 101. Mol Immunol. 2004;41(6-7):599-613.

47. Tonegawa S. Somatic generation of antibody diversity. Nature. 1983;302(5909):575-81.

48. Hardy RR, Hayakawa K. B cell development pathways. Annu Rev Immunol. 2001;19:595-621.

49. Monroe JG. ITAM-mediated tonic signalling through pre-BCR and BCR complexes. Nat Rev Immunol. 2006;6(4):283-94.

50. Defrance T, Casamayor-Palleja M, Krammer PH. The life and death of a B cell. Adv Cancer Res. 2002;86:195-225.

51. Hardy RR, Hayakawa K, Parks DR, Herzenberg LA, Herzenberg LA. Murine B cell differentiation lineages. J Exp Med. 1984;159(4):1169-88.

52. Stavnezer J, Guikema JE, Schrader CE. Mechanism and regulation of class switch recombination. Annu Rev Immunol. 2008;26:261-92.

53. Cerutti A, Zan H, Schaffer A, Bergsagel L, Harindranath N, Max EE, et al. CD40 ligand and appropriate cytokines induce switching to IgG, IgA, and IgE and coordinated germinal center and plasmacytoid phenotypic differentiation in a human monoclonal IgM+IgD+ B cell line. J Immunol. 1998;160(5):2145-57.

54. Hardy RR, Carmack CE, Shinton SA, Kemp JD, Hayakawa K. Resolution and characterization of pro-B and pre-pro-B cell stages in normal mouse bone marrow. J Exp Med. 1991;173(5):1213-25.

55. Shah DK, Zuniga-Pflucker JC. An overview of the intrathymic intricacies of T cell development. J Immunol. 2014;192(9):4017-23.

56. Germain RN. T-cell development and the CD4-CD8 lineage decision. Nat Rev Immunol. 2002;2(5):309-22.

57. Porritt HE, Rumfelt LL, Tabrizifard S, Schmitt TM, Zuniga-Pflucker JC, Petrie HT. Heterogeneity among DN1 prothymocytes reveals multiple progenitors with different capacities to generate T cell and non-T cell lineages. Immunity. 2004;20(6):735-45.

58. Wenger RH, Kopf M, Nitschke L, Lamers MC, Köhler G, Nielsen PJ. B-cell Maturation in Chimaeric Mice Deficient for the Heat Stable Antigen (HSA/mouse CD24). Transgenic Research. 1995;4:173-83.

59. Hough MR, Takei F, Humphries RK, Kay R. Defective development of thymocytes overexpressing the costimulatory molecule, heat-stable antigen. J Exp Med. 1994;179(1):177-84.

60. Ayre DC, Elstner M, Smith NC, Moores ES, Hogan AM, Christian SL. Dynamic regulation of CD24 expression and release of CD24-containing microvesicles in immature B cells in response to CD24 engagement. Immunology. 2015;146(2):217-33.

61. Suzuki T, Kiyokawa N, Taguchi T, Sekino T, Katagiri YU, Fujimoto J. CD24 Induces Apoptosis in Human B Cells Via The Glycolipid-Enriched Membrane Domains/Rafts-Mediated Signaling System. J Immunol. 2001;166:5567-77.

62. Taguchi T, Kiyokawa N, Mimori H, Suzuki T, Sekino T, Nakajima H, et al. Pre-B Cell Antigen Receptor-Mediated Signal Inhibits CD24-Induced Apoptosis in Human Pre-B Cells. J Immunol. 2003;170:252-60.

63. Liu Y, Jones B, Aruffo A, Sullivan KM, Linsley PS, Janeway CA, Jr. Heat-stable antigen is a costimulatory molecule for CD4 T cell growth. J Exp Med. 1992;175(2):437-45.

64. Hubbe M, Altevogt P. Heat-stable antigen/CD24 on mouse T lymphocytes: evidence for a costimulatory function. Eur J Immunol. 1994;24(3):731-7.

65. Prlic M, Blazar BR, Khoruts A, Zell T, Jameson SC. Homeostatic expansion occurs independently of costimulatory signals. J Immunol. 2001;167(10):5664-8.

66. Li O, Zheng P, Liu Y. CD24 expression on T cells is required for optimal T cell proliferation in lymphopenic host. J Exp Med. 2004;200(8):1083-9.

67. Li O, Chang X, Zhang H, Kocak E, Ding C, Zheng P, et al. Massive and destructive T cell response to homeostatic cue in CD24-deficient lymphopenic hosts. J Exp Med. 2006;203(7):1713-20.

68. Toubai T, Hou G, Mathewson N, Liu C, Wang Y, Oravecz-Wilson K, et al. Siglec-G-CD24 axis controls the severity of graft-versus-host disease in mice. Blood. 2014;123:3512-23.

69. Zarn JA, Zimmermann SM, Pass MK, Waibel R, Stahel RA. Association of CD24 with the kinase c-fgr in a small cell lung cancer cell line and with the kinase lyn in an erythroleukemia cell line. Biochem Biophys Res Commun. 1996;225(2):384-91.

70. Parsons SJ, Parsons JT. Src family kinases, key regulators of signal transduction. Oncogene. 2004;23(48):7906-9.

71. Sammar M, Gulbins E, Hilbert K, Lang F, Altevogt P. Mouse CD24 as a signaling molecule for integrin-mediated cell binding: functional and physical association with src-kinases. Biochem Biophys Res Commun. 1997;234(2):330-4.

72. Baumann P, Thiele W, Cremers N, Muppala S, Krachulec J, Diefenbacher M, et al. CD24 interacts with and promotes the activity of c-src within lipid rafts in breast cancer cells, thereby increasing integrin-dependent adhesion. Cell Mol Life Sci. 2012;69(3):435-48.

73. Wang W, Wang X, Peng L, Deng Q, Liang Y, Qing H, et al. CD24-dependent MAPK pathway activation is required for colorectal cancer cell proliferation. Cancer Sci. 2010;101(1):112-9.

74. Jung KC, Park WS, Kim HJ, Choi EY, Kook MC, Lee HW, et al. TCR-independent and caspase-independent apoptosis of murine thymocytes by CD24 cross-linking. J Immunol. 2004;172(2):795-802.

75. Akers JC, Gonda D, Kim R, Carter BS, Chen CC. Biogenesis of extracellular vesicles (EV): exosomes, microvesicles, retrovirus-like vesicles, and apoptotic bodies. J Neurooncol. 2013;113(1):1-11.

76. Piper RC, Katzmann DJ. Biogenesis and function of multivesicular bodies. Annu Rev Cell Dev Biol. 2007;23:519-47.

77. Huotari J, Helenius A. Endosome maturation. Embo j. 2011;30(17):3481-500.

78. Stoorvogel W. Resolving sorting mechanisms into exosomes. Cell Res. 2015;25(5):531-2.

79. Pols MS, Klumperman J. Trafficking and function of the tetraspanin CD63. Exp Cell Res. 2009;315(9):1584-92.

80. Baietti MF, Zhang Z, Mortier E, Melchior A, Degeest G, Geeraerts A, et al. Syndecan-syntenin-ALIX regulates the biogenesis of exosomes. Nat Cell Biol. 2012;14(7):677-85.

81. Stenmark H. Rab GTPases as coordinators of vesicle traffic. Nat Rev Mol Cell Biol. 2009;10(8):513-25.

82. Zerial M, McBride H. Rab proteins as membrane organizers. Nat Rev Mol Cell Biol. 2001;2(2):107-17.

83. Grosshans BL, Ortiz D, Novick P. Rabs and their effectors: achieving specificity in membrane traffic. Proc Natl Acad Sci U S A. 2006;103(32):11821-7.

84. Wandinger-Ness A, Zerial M. Rab proteins and the compartmentalization of the endosomal system. Cold Spring Harb Perspect Biol. 2014;6(11):a022616.

85. Harding C, Heuser J, Stahl P. Endocytosis and intracellular processing of transferrin and colloidal gold-transferrin in rat reticulocytes: demonstration of a pathway for receptor shedding. Eur J Cell Biol. 1984;35(2):256-63.

86. Raposo G, Nijman HW, Stoorvogel W, Liejendekker R, Harding CV, Melief CJ, et al. B lymphocytes secrete antigen-presenting vesicles. J Exp Med. 1996;183(3):1161-72.

87. Raposo G, Stoorvogel W. Extracellular vesicles: exosomes, microvesicles, and friends. J Cell Biol. 2013;200(4):373-83.

88. Heijnen HF, Schiel AE, Fijnheer R, Geuze HJ, Sixma JJ. Activated platelets release two types of membrane vesicles: microvesicles by surface shedding and exosomes derived from exocytosis of multivesicular bodies and alpha-granules. Blood. 1999;94(11):3791-9.

89. Del Conde I, Shrimpton CN, Thiagarajan P, Lopez JA. Tissue-factor-bearing microvesicles arise from lipid rafts and fuse with activated platelets to initiate coagulation. Blood. 2005;106(5):1604-11.

90. Hugel B, Martinez MC, Kunzelmann C, Freyssinet JM. Membrane microparticles: two sides of the coin. Physiology (Bethesda). 2005;20:22-7.

91. Mobarrez F, Abraham-Nordling M, Aguilera-Gatica K, Friberg I, Antovic A, Pisetsky DS, et al. The expression of microvesicles in the blood of patients with Graves' disease and its relationship to treatment. Clin Endocrinol (Oxf). 2016;84(5):729-35.

92. Colombo M, Raposo G, Thery C. Biogenesis, secretion, and intercellular interactions of exosomes and other extracellular vesicles. Annu Rev Cell Dev Biol. 2014;30:255-89.

93. Pasquet JM, Dachary-Prigent J, Nurden AT. Calcium influx is a determining factor of calpain activation and microparticle formation in platelets. Eur J Biochem. 1996;239(3):647-54.

94. Weber H, Huhns S, Luthen F, Jonas L. Calpain-mediated breakdown of cytoskeletal proteins contributes to cholecystokinin-induced damage of rat pancreatic acini. Int J Exp Pathol. 2009;90(4):387-99.

95. Cooper JA, Schafer DA. Control of actin assembly and disassembly at filament ends. Curr Opin Cell Biol. 2000;12(1):97-103.

96. Muralidharan-Chari V, Clancy J, Plou C, Romao M, Chavrier P, Raposo G, et al. ARF6-regulated shedding of tumor cell-derived plasma membrane microvesicles. Curr Biol. 2009;19(22):1875-85.

97. Muralidharan-Chari V, Clancy JW, Sedgwick A, D'Souza-Schorey C. Microvesicles: mediators of extracellular communication during cancer progression. J Cell Sci. 2010;123(Pt 10):1603-11.

98. Nolte-'t Hoen E, Cremer T, Gallo RC, Margolis LB. Extracellular vesicles and viruses: Are they close relatives? Proc Natl Acad Sci U S A. 2016;113(33):9155-61.

99. Pincetic A, Leis J. The Mechanism of Budding of Retroviruses From Cell Membranes. Adv Virol. 2009;2009:6239691-9.

100. Shen B, Wu N, Yang JM, Gould SJ. Protein targeting to exosomes/microvesicles by plasma membrane anchors. J Biol Chem. 2011;286(16):14383-95.

101. Liang Y, Eng WS, Colquhoun DR, Dinglasan RR, Graham DR, Mahal LK. Complex N-linked glycans serve as a determinant for exosome/microvesicle cargo recruitment. J Biol Chem. 2014;289(47):32526-37.

102. Szostak N, Royo F, Rybarczyk A, Szachniuk M, Blazewicz J, del Sol A, et al. Sorting signal targeting mRNA into hepatic extracellular vesicles. RNA Biol. 2014;11(7):836-44.

103. Bolukbasi MF, Mizrak A, Ozdener GB, Madlener S, Strobel T, Erkan EP, et al. miR-1289 and "Zipcode"-like Sequence Enrich mRNAs in Microvesicles. Mol Ther Nucleic Acids. 2012;1:e10.

104. Lee TH, D'Asti E, Magnus N, Al-Nedawi K, Meehan B, Rak J. Microvesicles as mediators of intercellular communication in cancer--the emerging science of cellular 'debris'. Semin Immunopathol. 2011;33(5):455-67.

105. Stein JM, Luzio JP. Ectocytosis caused by sublytic autologous complement attack on human neutrophils. The sorting of endogenous plasma-membrane proteins and lipids into shed vesicles. Biochem J. 1991;274 (Pt 2):381-6.

106. Hristov M, Erl W, Linder S, Weber PC. Apoptotic bodies from endothelial cells enhance the number and initiate the differentiation of human endothelial progenitor cells in vitro. Blood. 2004;104(9):2761-6.

107. Elmore S. Apoptosis: a review of programmed cell death. Toxicol Pathol. 2007;35(4):495-516.

108. Atkin-Smith GK, Tixeira R, Paone S, Mathivanan S, Collins C, Liem M, et al. A novel mechanism of generating extracellular vesicles during apoptosis via a beads-on-a-string membrane structure. Nat Commun. 2015;6:7439.

109. Kurosaka K, Takahashi M, Watanabe N, Kobayashi Y. Silent cleanup of very early apoptotic cells by macrophages. J Immunol. 2003;171(9):4672-9.

110. Suzuki J, Umeda M, Sims PJ, Nagata S. Calcium-dependent phospholipid scrambling by TMEM16F. Nature. 2010;468(7325):834-8.

111. Fadok VA, Bratton DL, Henson PM. Phagocyte receptors for apoptotic cells: recognition, uptake, and consequences. J Clin Invest. 2001;108(7):957-62.

112. Black LV, Saunderson SC, Coutinho FP, Muhsin-Sharafaldine MR, Damani TT, Dunn AC, et al. The CD169 sialoadhesin molecule mediates cytotoxic T-cell responses to tumour apoptotic vesicles. Immunol Cell Biol. 2016;94(5):430-8.

113. Yanez-Mo M, Siljander PR, Andreu Z, Zavec AB, Borras FE, Buzas EI, et al. Biological properties of extracellular vesicles and their physiological functions. J Extracell Vesicles. 2015;4:27066.

114. Steppich B, Mattisek C, Sobczyk D, Kastrati A, Schomig A, Ott I. Tissue factor pathway inhibitor on circulating microparticles in acute myocardial infarction. Thromb Haemost. 2005;93(1):35-9.

115. Walker JD, Maier CL, Pober JS. Cytomegalovirus-infected human endothelial cells can stimulate allogeneic CD4+ memory T cells by releasing antigenic exosomes. J Immunol. 2009;182(3):1548-59.

116. Hwang I, Shen X, Sprent J. Direct stimulation of naive T cells by membrane vesicles from antigen-presenting cells: distinct roles for CD54 and B7 molecules. Proc Natl Acad Sci U S A. 2003;100(11):6670-5.

117. Alvarez-Erviti L, Seow Y, Yin H, Betts C, Lakhal S, Wood MJ. Delivery of siRNA to the mouse brain by systemic injection of targeted exosomes. Nat Biotechnol. 2011;29(4):341-5.

118. Hedlund M, Nagaeva O, Kargl D, Baranov V, Mincheva-Nilsson L. Thermal- and oxidative stress causes enhanced release of NKG2D ligand-bearing immunosuppressive exosomes in leukemia/lymphoma T and B cells. PLoS One. 2011;6(2):e16899.

119. Raulet DH. Roles of the NKG2D immunoreceptor and its ligands. Nat Rev Immunol. 2003;3(10):781-90.

120. Monleon I, Martinez-Lorenzo MJ, Monteagudo L, Lasierra P, Taules M, Iturralde M, et al. Differential secretion of Fas ligand- or APO2 ligand/TNF-related apoptosis-inducing ligand-carrying microvesicles during activation-induced death of human T cells. J Immunol. 2001;167(12):6736-44.

121. Xie Y, Zhang H, Li W, Deng Y, Munegowda MA, Chibbar R, et al. Dendritic cells recruit T cell exosomes via exosomal LFA-1 leading to inhibition of CD8+ CTL responses through downregulation of peptide/MHC class I and Fas ligand-mediated cytotoxicity. J Immunol. 2010;185(9):5268-78.

122. Aalberts M, Stout TA, Stoorvogel W. Prostasomes: extracellular vesicles from the prostate. Reproduction. 2014;147(1):R1-14.

123. Moskovtsev SI, Jarvi K, Legare C, Sullivan R, Mullen JB. Epididymal P34H protein deficiency in men evaluated for infertility. Fertil Steril. 2007;88(5):1455-7.

124. Frenette G, Thabet M, Sullivan R. Polyol pathway in human epididymis and semen. J Androl. 2006;27(2):233-9.

125. Tannetta DS, Dragovic RA, Gardiner C, Redman CW, Sargent IL. Characterisation of syncytiotrophoblast vesicles in normal pregnancy and pre-eclampsia: expression of Flt-1 and endoglin. PLoS One. 2013;8(2):e56754.

126. De Toro J, Herschlik L, Waldner C, Mongini C. Emerging roles of exosomes in normal and pathological conditions: new insights for diagnosis and therapeutic applications. Front Immunol. 2015;6:203.

127. Stenqvist AC, Nagaeva O, Baranov V, Mincheva-Nilsson L. Exosomes secreted by human placenta carry functional Fas ligand and TRAIL molecules and convey apoptosis in activated immune cells, suggesting exosome-mediated immune privilege of the fetus. J Immunol. 2013;191(11):5515-23.

128. Kshirsagar SK, Alam SM, Jasti S, Hodes H, Nauser T, Gilliam M, et al. Immunomodulatory molecules are released from the first trimester and term placenta via exosomes. Placenta. 2012;33(12):982-90.

129. Friend C, Marovitz W, Henie G, Henie W, Tsuei D, Hirschhorn K, et al. Observations on cell lines derived from a patient with Hodgkin's disease. Cancer Res. 1978;38(8):2581-91.

130. Poste G, Nicolson GL. Arrest and metastasis of blood-borne tumor cells are modified by fusion of plasma membrane vesicles from highly metastatic cells. Proc Natl Acad Sci U S A. 1980;77(1):399-403.

131. Park JE, Tan HS, Datta A, Lai RC, Zhang H, Meng W, et al. Hypoxic tumor cell modulates its microenvironment to enhance angiogenic and metastatic potential by secretion of proteins and exosomes. Mol Cell Proteomics. 2010;9(6):1085-99.

132. Ghosh AK, Secreto CR, Knox TR, Ding W, Mukhopadhyay D, Kay NE. Circulating microvesicles in B-cell chronic lymphocytic leukemia can stimulate marrow stromal cells: implications for disease progression. Blood. 2010;115(9):1755-64.

133. Al-Nedawi K, Meehan B, Micallef J, Lhotak V, May L, Guha A, et al. Intercellular transfer of the oncogenic receptor EGFRvIII by microvesicles derived from tumour cells. Nat Cell Biol. 2008;10(5):619-24.

134. Kruger S, Abd Elmageed ZY, Hawke DH, Worner PM, Jansen DA, Abdel-Mageed AB, et al. Molecular characterization of exosome-like vesicles from breast cancer cells. BMC Cancer. 2014;14:44.

135. Zomer A, Maynard C, Verweij FJ, Kamermans A, Schafer R, Beerling E, et al. In Vivo imaging reveals extracellular vesicle-mediated phenocopying of metastatic behavior. Cell. 2015;161(5):1046-57.

136. Zhou W, Fong MY, Min Y, Somlo G, Liu L, Palomares MR, et al. Cancer-secreted miR-105 destroys vascular endothelial barriers to promote metastasis. Cancer Cell. 2014;25(4):501-15.

137. Tominaga N, Kosaka N, Ono M, Katsuda T, Yoshioka Y, Tamura K, et al. Brain metastatic cancer cells release microRNA-181c-containing extracellular vesicles capable of destructing blood-brain barrier. Nat Commun. 2015;6:6716.

138. Willms E, Johansson HJ, Mager I, Lee Y, Blomberg KE, Sadik M, et al. Cells release subpopulations of exosomes with distinct molecular and biological properties. Sci Rep. 2016;6:22519.

139. Lazaro-Ibanez E, Lunavat TR, Jang SC, Escobedo-Lucea C, Oliver-De La Cruz J, Siljander P, et al. Distinct prostate cancer-related mRNA cargo in extracellular vesicle subsets from prostate cell lines. BMC Cancer. 2017;17(1):92.

140. Galindo-Hernandez O, Villegas-Comonfort S, Candanedo F, Gonzalez-Vazquez MC, Chavez-Ocana S, Jimenez-Villanueva X, et al. Elevated concentration of

microvesicles isolated from peripheral blood in breast cancer patients. Arch Med Res. 2013;44(3):208-14.

141. Logozzi M, De Milito A, Lugini L, Borghi M, Calabro L, Spada M, et al. High levels of exosomes expressing CD63 and caveolin-1 in plasma of melanoma patients. PLoS One. 2009;4(4):e5219.

142. Matsumoto Y, Kano M, Akutsu Y, Hanari N, Hoshino I, Murakami K, et al. Quantification of plasma exosome is a potential prognostic marker for esophageal squamous cell carcinoma. Oncol Rep. 2016.

143. Cho YE, Im EJ, Moon PG, Mezey E, Song BJ, Baek MC. Increased liver-specific proteins in circulating extracellular vesicles as potential biomarkers for drug- and alcohol-induced liver injury. PLoS One. 2017;12(2):e0172463.

144. Momen-Heravi F, Saha B, Kodys K, Catalano D, Satishchandran A, Szabo G. Increased number of circulating exosomes and their microRNA cargos are potential novel biomarkers in alcoholic hepatitis. J Transl Med. 2015;13:261.

145. Helmke A, von Vietinghoff S. Extracellular vesicles as mediators of vascular inflammation in kidney disease. World J Nephrol. 2016;5(2):125-38.

146. Sarker S, Scholz-Romero K, Perez A, Illanes SE, Mitchell MD, Rice GE, et al. Placenta-derived exosomes continuously increase in maternal circulation over the first trimester of pregnancy. J Transl Med. 2014;12:204.

147. Taylor DD, Gercel-Taylor C. MicroRNA signatures of tumor-derived exosomes as diagnostic biomarkers of ovarian cancer. Gynecol Oncol. 2008;110(1):13-21.

148. Skog J, Wurdinger T, van Rijn S, Meijer DH, Gainche L, Sena-Esteves M, et al. Glioblastoma microvesicles transport RNA and proteins that promote tumour growth and provide diagnostic biomarkers. Nat Cell Biol. 2008;10(12):1470-6.

149. Takahashi K, Yan IK, Kogure T, Haga H, Patel T. Extracellular vesicle-mediated transfer of long non-coding RNA ROR modulates chemosensitivity in human hepatocellular cancer. FEBS Open Bio. 2014;4:458-67.

150. Ciravolo V, Huber V, Ghedini GC, Venturelli E, Bianchi F, Campiglio M, et al. Potential role of HER2-overexpressing exosomes in countering trastuzumab-based therapy. J Cell Physiol. 2012;227(2):658-67.

151. Sloand EM, Maciejewski JP, Dunn D, Moss J, Brewer B, Kirby M, et al. Correction of the PNH defect by GPI-anchored protein transfer. Blood. 1998;92:4439-45.

152. Sloand EM, Mainwaring L, Keyvanfar K, Chen J, Maciejewski J, Klein HG, et al. Transfer of glycosylphosphatidylinositol-anchored proteins to deficient cells after erythrocyte transfusion in paroxysmal nocturnal hemoglobinuria. Blood. 2004;104:3782-8.

153. Dias V, Junn E, Mouradian MM. The role of oxidative stress in Parkinson's disease. J Parkinsons Dis. 2013;3(4):461-91.

154. Haney MJ, Klyachko NL, Zhao Y, Gupta R, Plotnikova EG, He Z, et al. Exosomes as drug delivery vehicles for Parkinson's disease therapy. J Control Release. 2015;207:18-30.

155. Di X, Zhang G, Zhang Y, Takeda K, Rivera Rosado LA, Zhang B. Accumulation of autophagosomes in breast cancer cells induces TRAIL resistance through

downregulation of surface expression of death receptors 4 and 5. Oncotarget. 2013;4(9):1349-64.

156. Yuan ZQ, Kolluri KK, Gowers KHC, Janes SM. TRAIL delivery by MSC-derived extracellular vesicles is an effective anticancer therapy. J Extracell Vesicles. 2017;6(1).

157. Hall J, Prabhakar S, Balaj L, Lai CP, Cerione RA, Breakefield XO. Delivery of Therapeutic Proteins via Extracellular Vesicles: Review and Potential Treatments for Parkinson's Disease, Glioma, and Schwannoma. Cell Mol Neurobiol. 2016;36(3):417-27.

158. Keller S, Rupp C, Stoeck A, Runz S, Fogel M, Lugert S, et al. CD24 is a marker of exosomes secreted into urine and amniotic fluid. Kidney Int. 2007;72(9):1095-102.

159. Rupp AK, Rupp C, Keller S, Brase JC, Ehehalt R, Fogel M, et al. Loss of EpCAM expression in breast cancer derived serum exosomes: role of proteolytic cleavage. Gynecol Oncol. 2011;122(2):437-46.

160. Palanisamy V, Sharma S, Deshpande A, Zhou H, Gimzewski J, Wong DT. Nanostructural and transcriptomic analyses of human saliva derived exosomes. PLoS One. 2010;5(1):e8577.

161. Keller S, Konig AK, Marme F, Runz S, Wolterink S, Koensgen D, et al. Systemic presence and tumor-growth promoting effect of ovarian carcinoma released exosomes. Cancer Lett. 2009;278(1):73-81.

162. Ayre DC, Chute IC, Joy AP, Barnett DA, Hogan AM, Grull MP, et al. CD24 induces changes to the surface receptors of B cell microvesicles with variable effects on their RNA and protein cargo. Sci Rep. 2017;7(1):8642.

163. Crooks GE, Hon G, Chandonia JM, Brenner SE. WebLogo: a sequence logo generator. Genome Res. 2004;14(6):1188-90.

164. Yang J, Yan R, Roy A, Xu D, Poisson J, Zhang Y. The I-TASSER Suite: protein structure and function prediction. Nat Methods. 2015;12(1):7-8.

165. Zhang T, Faraggi E, Xue B, Dunker AK, Uversky VN, Zhou Y. SPINE-D: accurate prediction of short and long disordered regions by a single neural-network based method. J Biomol Struct Dyn. 2012;29(4):799-813.

166. RStudio T. RStudio: Integrated Development for R. Boston, MA: RStudio, Inc.; 2015.

167. R Development Core Team. R: A language and environment for statistical computing. Vienna, Austria: R Foundation for Statistical Computing; 2008.

168. Gentleman RC, Carey VJ, Bates DM, Bolstad B, Dettling M, Dudoit S, et al. Bioconductor: open software development for computational biology and bioinformatics. Genome Biol. 2004;5(10):R80.

169. Carvalho BS, Irizarry RA. A framework for oligonucleotide microarray preprocessing. Bioinformatics. 2010;26(19):2363-7.

170. Heng TS, Painter MW. The Immunological Genome Project: networks of gene expression in immune cells. Nat Immunol. 2008;9(10):1091-4.

171. Li T, Huang J, Jiang Y, Zeng Y, He F, Zhang MQ, et al. Multi-stage analysis of gene expression and transcription regulation in C57/B6 mouse liver development. Genomics. 2009;93(3):235-42.

172. Hartl D, Irmler M, Romer I, Mader MT, Mao L, Zabel C, et al. Transcriptome and proteome analysis of early embryonic mouse brain development. Proteomics. 2008;8(6):1257-65.

173. Somel M, Franz H, Yan Z, Lorenc A, Guo S, Giger T, et al. Transcriptional neoteny in the human brain. Proc Natl Acad Sci U S A. 2009;106(14):5743-8.

174. Knox K, Baker JC. Genomic evolution of the placenta using co-option and duplication and divergence. Genome Res. 2008;18(5):695-705.

175. Small CL, Shima JE, Uzumcu M, Skinner MK, Griswold MD. Profiling gene expression during the differentiation and development of the murine embryonic gonad. Biol Reprod. 2005;72(2):492-501.

176. Stephens DN, Klein RH, Salmans ML, Gordon W, Ho H, Andersen B. The Ets transcription factor EHF as a regulator of cornea epithelial cell identity. J Biol Chem. 2013;288(48):34304-24.

177. Motari E, Zheng X, Su X, Liu Y, Kvaratskhelia M, Freitas M, et al. Analysis of Recombinant CD24 Glycans by MALDI-TOF-MS Reveals Prevalence of Sialyl-T Antigen. Am J Biomed Sci. 2009;1(1):1-11.

178. Medzihradszky KF. Characterization of site-specific N-glycosylation. Methods Mol Biol. 2008;446:293-316.

179. Finn RD, Bateman A, Clements J, Coggill P, Eberhardt RY, Eddy SR, et al. Pfam: the protein families database. Nucleic Acids Res. 2014;42(Database issue):D222-30.

180. Lieberoth A, Splittstoesser F, Katagihallimath N, Jakovcevski I, Loers G, Ranscht B, et al. Lewis(x) and alpha2,3-sialyl glycans and their receptors TAG-1, Contactin, and L1 mediate CD24-dependent neurite outgrowth. J Neurosci. 2009;29(20):6677-90.

181. Smith NC, Fairbridge NA, Pallegar NK, Christian SL. Dynamic upregulation of CD24 in pre-adipocytes promotes adipogenesis. Adipocyte. 2015;4(2):89-100.

182. Jeffery E, Church CD, Holtrup B, Colman L, Rodeheffer MS. Rapid depot-specific activation of adipocyte precursor cells at the onset of obesity. Nat Cell Biol. 2015;17(4):376-85.

183. Shirasawa T, Akashi T, Sakamoto K, Takahashi H, Maruyama N, Hirokawa K. Gene expression of CD24 core peptide molecule in developing brain and developing non-neural tissues. Dev Dyn. 1993;198(1):1-13.

184. Crocker PR, Varki A. Siglecs in the immune system. Immunology. 2001;103(2):137-45.

185. Mildner A, Jung S. Development and function of dendritic cell subsets. Immunity. 2014;40(5):642-56.

186. Niederkorn JY. See no evil, hear no evil, do no evil: the lessons of immune privilege. Nat Immunol. 2006;7(4):354-9.

187. Mellor AL, Munn DH. Immunology at the maternal-fetal interface: lessons for T cell tolerance and suppression. Annu Rev Immunol. 2000;18:367-91.

188. Samstein RM, Josefowicz SZ, Arvey A, Treuting PM, Rudensky AY. Extrathymic generation of regulatory T cells in placental mammals mitigates maternal-fetal conflict. Cell. 2012;150(1):29-38.

189. Riau AK, Wong TT, Lan W, Finger SN, Chaurasia SS, Hou AH, et al. Aberrant DNA methylation of matrix remodeling and cell adhesion related genes in pterygium. PLoS One. 2011;6(2):e14687.

190. Belvindrah R, Rougon G, Chazal G. Increased neurogenesis in adult mCD24-deficient mice. J Neurosci. 2002;22(9):3594-607.

191. Qiu Q, Hernandez JC, Dean AM, Rao PH, Darlington GJ. CD24-positive cells from normal adult mouse liver are hepatocyte progenitor cells. Stem Cells Dev. 2011;20(12):2177-88.

192. Gracz AD, Ramalingam S, Magness ST. Sox9 expression marks a subset of CD24-expressing small intestine epithelial stem cells that form organoids in vitro. Am J Physiol Gastrointest Liver Physiol. 2010;298(5):G590-600.

193. Cremers N, Deugnier MA, Sleeman J. Loss of CD24 expression promotes ductal branching in the murine mammary gland. Cell Mol Life Sci. 2010;67(13):2311-22.

194. Lindblom P, Rafter I, Copley C, Andersson U, Hedberg JJ, Berg AL, et al. Isoforms of alanine aminotransferases in human tissues and serum--differential tissue expression using novel antibodies. Arch Biochem Biophys. 2007;466(1):66-77.

195. Michalopoulos GK. Liver regeneration. J Cell Physiol. 2007;213(2):286-300.

196. Dunker AK, Lawson JD, Brown CJ, Williams RM, Romero P, Oh JS, et al. Intrinsically disordered protein. J Mol Graph Model. 2001;19(1):26-59.

197. Perez RB, Tischer A, Auton M, Whitten ST. Alanine and proline content modulate global sensitivity to discrete perturbations in disordered proteins. Proteins. 2014;82(12):3373-84.

198. Jentoft N. Why are proteins O-glycosylated? Trends Biochem Sci. 1990;15(8):291-4.

199. Askew D, Harding CV. Antigen processing and CD24 expression determine antigen presentation by splenic CD4+ and CD8+ dendritic cells. Immunology. 2008;123(3):447-55.

200. Shakiba N, White CA, Lipsitz YY, Yachie-Kinoshita A, Tonge PD, Hussein SM, et al. CD24 tracks divergent pluripotent states in mouse and human cells. Nat Commun. 2015;6:7329.

201. Nieoullon V, Belvindrah R, Rougon G, Chazal G. Mouse CD24 is required for homeostatic cell renewal. Cell Tissue Res. 2007;329(3):457-67.

202. Fukushima K, Ikehara Y, Yamashita K. Functional role played by the glycosylphosphatidylinositol anchor glycan of CD48 in interleukin-18-induced interferon-gamma production. J Biol Chem. 2005;280(18):18056-62.

203. Deckert M, Ticchioni M, Bernard A. Endocytosis of GPI-anchored proteins in human lymphocytes: role of glycolipid-based domains, actin cytoskeleton, and protein kinases. J Cell Biol. 1996;133(4):791-9.

204. Crescitelli R, Lasser C, Szabo TG, Kittel A, Eldh M, Dianzani I, et al. Distinct RNA profiles in subpopulations of extracellular vesicles: apoptotic bodies, microvesicles and exosomes. J Extracell Vesicles. 2013;2.

205. Lacroix R, Robert S, Poncelet P, Dignat-George F. Overcoming limitations of microparticle measurement by flow cytometry. Semin Thromb Hemost. 2010;36(8):807-18.

206. Poncelet P, Robert S, Bouriche T, Bez J, Lacroix R, Dignat-George F. Standardized counting of circulating platelet microparticles using currently available flow cytometers and scatter-based triggering: Forward or side scatter? Cytometry A. 2015.

207. Lindstrom ML, Bates DM. Nonlinear mixed effects models for repeated measures data. Biometrics. 1990;46(3):673-87.

208. Lanzavecchia A. Receptor-mediated antigen uptake and its effect on antigen presentation to class II-restricted T lymphocytes. Annu Rev Immunol. 1990;8:773-93.

209. Ketchum C, Miller H, Song W, Upadhyaya A. Ligand mobility regulates B cell receptor clustering and signaling activation. Biophys J. 2014;106(1):26-36.

210. Denzer K, Kleijmeer MJ, Heijnen HF, Stoorvogel W, Geuze HJ. Exosome: from internal vesicle of the multivesicular body to intercellular signaling device. J Cell Sci. 2000;113 Pt 19:3365-74.

211. Lin RC, Scheller RH. Mechanisms of synaptic vesicle exocytosis. Annu Rev Cell Dev Biol. 2000;16:19-49.

212. Cocucci E, Racchetti G, Meldolesi J. Shedding microvesicles: artefacts no more. Trends Cell Biol. 2009;19(2):43-51.

213. Ratajczak J, Wysoczynski M, Hayek F, Janowska-Wieczorek A, Ratajczak MZ. Membrane-derived microvesicles: important and underappreciated mediators of cell-to-cell communication. Leukemia. 2006;20(9):1487-95.

214. Camussi G, Deregibus MC, Bruno S, Cantaluppi V, Biancone L. Exosomes/microvesicles as a mechanism of cell-to-cell communication. Kidney Int. 2010;78(9):838-48.

215. Thery C, Ostrowski M, Segura E. Membrane vesicles as conveyors of immune responses. Nat Rev Immunol. 2009;9(8):581-93.

216. McIlwain DR, Berger T, Mak TW. Caspase functions in cell death and disease. Cold Spring Harb Perspect Biol. 2013;5(4):a008656.

217. van der Pol E, Boing AN, Harrison P, Sturk A, Nieuwland R. Classification, functions, and clinical relevance of extracellular vesicles. Pharmacol Rev. 2012;64(3):676-705.

218. Camussi G, Deregibus MC, Bruno S, Grange C, Fonsato V, Tetta C. Exosome/microvesicle-mediated epigenetic reprogramming of cells. Am J Cancer Res. 2011;1(1):98-110.

219. Müller G. Release of exosomes and microvesicles harbouring specific RNAs and glycosylphosphatidylinositol-anchored proteins from rat and human adipocytes is controlled by histone methylation. American Journal of Molecular Biology. 2012;02(03):187-209.

220. Thery C, Amigorena S, Raposo G, Clayton A. Isolation and characterization of exosomes from cell culture supernatants and biological fluids. Curr Protoc Cell Biol. 2006;Chapter 3:Unit 3.22.

221. Ghosh A, Davey M, Chute IC, Griffiths SG, Lewis S, Chacko S, et al. Rapid isolation of extracellular vesicles from cell culture and biological fluids using a synthetic Peptide with specific affinity for heat shock proteins. PLoS One. 2014;9(10):e110443.

222. Anders S, Pyl PT, Huber W. HTSeq--a Python framework to work with high-throughput sequencing data. Bioinformatics. 2015;31(2):166-9.

223. Durinck S, Moreau Y, Kasprzyk A, Davis S, De Moor B, Brazma A, et al. BioMart and Bioconductor: a powerful link between biological databases and microarray data analysis. Bioinformatics. 2005;21(16):3439-40.

224. Robinson MD, McCarthy DJ, Smyth GK. edgeR: a Bioconductor package for differential expression analysis of digital gene expression data. Bioinformatics. 2010;26(1):139-40.

225. Eng JK, McCormack AL, Yates JR. An approach to correlate tandem mass spectral data of peptides with amino acid sequences in a protein database. J Am Soc Mass Spectrom. 1994;5(11):976-89.

226. Consortium U. Update on activities at the Universal Protein Resource (UniProt) in 2013. Nucleic Acids Res. 2013;41(Database issue):D43-7.

227. Craig R, Cortens JP, Beavis RC. Open source system for analyzing, validating, and storing protein identification data. J Proteome Res. 2004;3(6):1234-42.

228. Nesvizhskii AI, Keller A, Kolker E, Aebersold R. A statistical model for identifying proteins by tandem mass spectrometry. Anal Chem. 2003;75(17):4646-58.

229. Chen J, Bardes EE, Aronow BJ, Jegga AG. ToppGene Suite for gene list enrichment analysis and candidate gene prioritization. Nucleic Acids Res. 2009;37(Web Server issue):W305-11.

230. Supek F, Bosnjak M, Skunca N, Smuc T. REVIGO summarizes and visualizes long lists of gene ontology terms. PLoS One. 2011;6(7):e21800.

231. Jenjaroenpun P, Kremenska Y, Nair VM, Kremenskoy M, Joseph B, Kurochkin IV. Characterization of RNA in exosomes secreted by human breast cancer cell lines using next-generation sequencing. PeerJ. 2013;1:e201.

232. Kubota H, Hynes G, Willison K. The chaperonin containing t-complex polypeptide 1 (TCP-1). Multisubunit machinery assisting in protein folding and assembly in the eukaryotic cytosol. Eur J Biochem. 1995;230(1):3-16.

233. Gupta SK, Bhandari B, Shrestha A, Biswal BK, Palaniappan C, Malhotra SS, et al. Mammalian zona pellucida glycoproteins: structure and function during fertilization. Cell Tissue Res. 2012;349(3):665-78.

234. Gonzales PA, Pisitkun T, Hoffert JD, Tchapyjnikov D, Star RA, Kleta R, et al. Large-scale proteomics and phosphoproteomics of urinary exosomes. J Am Soc Nephrol. 2009;20(2):363-79.

235. Buschow SI, van Balkom BW, Aalberts M, Heck AJ, Wauben M, Stoorvogel W. MHC class II-associated proteins in B-cell exosomes and potential functional implications for exosome biogenesis. Immunol Cell Biol. 2010;88(8):851-6.

236. Principe S, Jones EE, Kim Y, Sinha A, Nyalwidhe JO, Brooks J, et al. In-depth proteomic analyses of exosomes isolated from expressed prostatic secretions in urine. Proteomics. 2013;13(10-11):1667-71.

237. Prunotto M, Farina A, Lane L, Pernin A, Schifferli J, Hochstrasser DF, et al. Proteomic analysis of podocyte exosome-enriched fraction from normal human urine. J Proteomics. 2013;82:193-229.

238. Mootha VK, Bunkenborg J, Olsen JV, Hjerrild M, Wisniewski JR, Stahl E, et al. Integrated analysis of protein composition, tissue diversity, and gene regulation in mouse mitochondria. Cell. 2003;115(5):629-40.

239. Corbi N, Batassa EM, Pisani C, Onori A, Di Certo MG, Strimpakos G, et al. The eEF1gamma subunit contacts RNA polymerase II and binds vimentin promoter region. PLoS One. 2010;5(12):e14481.

240. Riis B, Rattan SI, Clark BF, Merrick WC. Eukaryotic protein elongation factors. Trends Biochem Sci. 1990;15(11):420-4.

241. Yang H, Wang H, Chavan SS, Andersson U. High Mobility Group Box Protein 1 (HMGB1): The Prototypical Endogenous Danger Molecule. Mol Med. 2015;21 Suppl 1:S6-s12.

242. Yanai H, Ban T, Taniguchi T. High-mobility group box family of proteins: ligand and sensor for innate immunity. Trends Immunol. 2012;33(12):633-40.

243. Pusterla T, de Marchis F, Palumbo R, Bianchi ME. High mobility group B2 is secreted by myeloid cells and has mitogenic and chemoattractant activities similar to high mobility group B1. Autoimmunity. 2009;42(4):308-10.

244. Ackermann JA, Radtke D, Maurberger A, Winkler TH, Nitschke L. Grb2 regulates B-cell maturation, B-cell memory responses and inhibits B-cell Ca2+ signalling. Embo j. 2011;30(8):1621-33.

245. Cheng S, Hsia CY, Feng B, Liou ML, Fang X, Pandolfi PP, et al. BCR-mediated apoptosis associated with negative selection of immature B cells is selectively dependent on Pten. Cell Res. 2009;19(2):196-207.

246. Kina T, Ikuta K, Takayama E, Wada K, Majumdar AS, Weissman IL, et al. The monoclonal antibody TER-119 recognizes a molecule associated with glycophorin A and specifically marks the late stages of murine erythroid lineage. Br J Haematol. 2000;109(2):280-7.

247. Lotvall J, Hill AF, Hochberg F, Buzas EI, Di Vizio D, Gardiner C, et al. Minimal experimental requirements for definition of extracellular vesicles and their functions: a position statement from the International Society for Extracellular Vesicles. J Extracell Vesicles. 2014;3:26913.

248. Ung TH, Madsen HJ, Hellwinkel JE, Lencioni AM, Graner MW. Exosome proteomics reveals transcriptional regulator proteins with potential to mediate downstream pathways. Cancer Sci. 2014;105(11):1384-92.

249. Li M, Zeringer E, Barta T, Schageman J, Cheng A, Vlassov AV. Analysis of the RNA content of the exosomes derived from blood serum and urine and its potential as biomarkers. Philos Trans R Soc Lond B Biol Sci. 2014;369(1652).

250. Van Deun J, Mestdagh P, Sormunen R, Cocquyt V, Vermaelen K, Vandesompele J, et al. The impact of disparate isolation methods for extracellular vesicles on downstream RNA profiling. J Extracell Vesicles. 2014;3.

251. Lobb RJ, Becker M, Wen SW, Wong CS, Wiegmans AP, Leimgruber A, et al. Optimized exosome isolation protocol for cell culture supernatant and human plasma. J Extracell Vesicles. 2015;4:27031.

252. McClellan AJ, Scott MD, Frydman J. Folding and quality control of the VHL tumor suppressor proceed through distinct chaperone pathways. Cell. 2005;121(5):739-48.

253. Kundrat L, Regan L. Balance between folding and degradation for Hsp90-dependent client proteins: a key role for CHIP. Biochemistry. 2010;49(35):7428-38.

254. Theodoraki MA, Caplan AJ. Quality control and fate determination of Hsp90 client proteins. Biochim Biophys Acta. 2012;1823(3):683-8.

255. Spierings DC, McGoldrick D, Hamilton-Easton AM, Neale G, Murchison EP, Hannon GJ, et al. Ordered progression of stage-specific miRNA profiles in the mouse B2 B-cell lineage. Blood. 2011;117(20):5340-9.

256. Polikepahad S, Corry DB. Profiling of T helper cell-derived small RNAs reveals unique antisense transcripts and differential association of miRNAs with argonaute proteins 1 and 2. Nucleic Acids Res. 2013;41(2):1164-77.

257. Jitschin R, Hofmann AD, Bruns H, Giessl A, Bricks J, Berger J, et al. Mitochondrial metabolism contributes to oxidative stress and reveals therapeutic targets in chronic lymphocytic leukemia. Blood. 2014;123(17):2663-72.

258. Izeradjene K, Douglas L, Tillman DM, Delaney AB, Houghton JA. Reactive oxygen species regulate caspase activation in tumor necrosis factor-related apoptosis-inducing ligand-resistant human colon carcinoma cell lines. Cancer Res. 2005;65(16):7436-45.

259. Lyamzaev KG, Nepryakhina OK, Saprunova VB, Bakeeva LE, Pletjushkina OY, Chernyak BV, et al. Novel mechanism of elimination of malfunctioning mitochondria (mitoptosis): formation of mitoptotic bodies and extrusion of mitochondrial material from the cell. Biochim Biophys Acta. 2008;1777(7-8):817-25.

260. Knight AM. Regulated release of B cell-derived exosomes: do differences in exosome release provide insight into different APC function for B cells and DC? Eur J Immunol. 2008;38(5):1186-9.

261. McLellan AD. Exosome release by primary B cells. Crit Rev Immunol. 2009;29(3):203-17.

262. Sato S, Jansen PJ, Tedder TF. CD19 and CD22 expression reciprocally regulates tyrosine phosphorylation of Vav protein during B lymphocyte signaling. Proc Natl Acad Sci U S A. 1997;94:13158-62.

263. Saunderson SC, Dunn AC, Crocker PR, McLellan AD. CD169 mediates the capture of exosomes in spleen and lymph node. Blood. 2014;123(2):208-16.

264. O'Reilly MK, Paulson JC. Multivalent ligands for siglecs. Methods Enzymol. 2010;478:343-63.

265. Varki A, Angata T. Siglecs--the major subfamily of I-type lectins. Glycobiology. 2006;16(1):1r-27r.

266. Jellusova J, Nitschke L. Regulation of B cell functions by the sialic acid-binding receptors siglec-G and CD22. Front Immunol. 2011;2:96.

267. Horejsi V, Cebecauer M, Cerny J, Brdicka T, Angelisova P, Drbal K. Signal transduction in leucocytes via GPI-anchored proteins: an experimental artefact or an aspect of immunoreceptor function? Immunol Lett. 1998;63(2):63-73.

268. Paulick MG, Bertozzi CR. The glycosylphosphatidylinositol anchor: a complex membrane-anchoring structure for proteins. Biochemistry. 2008;47(27):6991-7000.

269. Stulnig TM, Berger M, Sigmund T, Stockinger H, Horejsi V, Waldhausl W. Signal transduction via glycosyl phosphatidylinositol-anchored proteins in T cells is inhibited by lowering cellular cholesterol. J Biol Chem. 1997;272(31):19242-7.

270. Kamen BA, Wang MT, Streckfuss AJ, Peryea X, Anderson RG. Delivery of folates to the cytoplasm of MA104 cells is mediated by a surface membrane receptor that recycles. J Biol Chem. 1988;263(27):13602-9.

271. Suzuki KG, Fujiwara TK, Edidin M, Kusumi A. Dynamic recruitment of phospholipase C gamma at transiently immobilized GPI-anchored receptor clusters induces IP3-Ca2+ signaling: single-molecule tracking study 2. J Cell Biol. 2007;177(4):731-42.

272. Boyman O, Letourneau S, Krieg C, Sprent J. Homeostatic proliferation and survival of naive and memory T cells. Eur J Immunol. 2009;39(8):2088-94.

273. Chen L, Flies DB. Molecular mechanisms of T cell co-stimulation and co-inhibition. Nat Rev Immunol. 2013;13(4):227-42.

274. Lingwood D, Simons K. Lipid rafts as a membrane-organizing principle. Science. 2010;327(5961):46-50.

275. Schabath H, Runz S, Joumaa S, Altevogt P. CD24 affects CXCR4 function in pre-B lymphocytes and breast carcinoma cells. J Cell Sci. 2006;119(Pt 2):314-25.

276. Runz S, Mierke CT, Joumaa S, Behrens J, Fabry B, Altevogt P. CD24 induces localization of beta1 integrin to lipid raft domains. Biochem Biophys Res Commun. 2008;365(1):35-41.

277. Rajewsky K. Clonal selection and learning in the antibody system. Nature. 1996;381(6585):751-8.

278. Chen W, Wang HG, Srinivasula SM, Alnemri ES, Cooper NR. B cell apoptosis triggered by antigen receptor ligation proceeds via a novel caspase-dependent pathway. J Immunol. 1999;163(5):2483-91.

279. Aigner S, Sthoeger ZM, Fogel M, Weber E, Zarn J, Ruppert M, et al. CD24, a mucin-type glycoprotein, is a ligand for P-selectin on human tumor cells. Blood. 1997;89(9):3385-95.

Appendices and Supplemental Files

Appendix A: Copyright licenses.

Chapter 2: Elsevier, for Ayre and Pallegar, et al. (2016) *Gene*

ELSEVIER LICENSE TERMS AND CONDITIONS

Aug 07, 2017

This Agreement between Mr. Craig Ayre ("You") and Elsevier ("Elsevier") consists of your license details and the terms and conditions provided by Elsevier and Copyright Clearance Center.

License Number	4155911382642
License date	Jul 25, 2017
Licensed Content Publisher	Elsevier
Licensed Content Publication	Gene
Licensed Content Title	Analysis of the structure, evolution, and expression of CD24, an important regulator of cell fate
Licensed Content Author	D. Craig Ayre,Nikitha K. Pallegar,Nicholas A. Fairbridge,Marta Canuti,Andrew S. Lang,Sherri L. Christian
Licensed Content Date	Sep 30, 2016
Licensed Content Volume	590
Licensed Content Issue	2
Licensed Content Pages	14
Start Page	324
End Page	337
Type of Use	reuse in a thesis/dissertation
Intended publisher of new work	other
Portion	full article

Format	both print and electronic
Are you the author of this Elsevier article?	Yes
Will you be translating?	No
Title of your thesis/dissertation	A Generalizable Mechanism of CD24 Signalling and Its Ability to Specifically Alter the Biogenesis of B Cell Extracellular Vesicles
Expected completion date	Oct 2017
Estimated size (number of pages)	210
Requestor Location	Mr. Craig Ayre 57 Railway Avenue Moncton, NB E1C2C9 Canada Attn: Mr. Craig Ayre
Total	0.00 USD

Terms and Conditions

INTRODUCTION

1. The publisher for this copyrighted material is Elsevier. By clicking "accept" in connection with completing this licensing transaction, you agree that the following terms and conditions apply to this transaction (along with the Billing and Payment terms and conditions established by Copyright Clearance Center, Inc. ("CCC"), at the time that you opened your Rightslink account and that are available at any time at http://myaccount.copyright.com).

GENERAL TERMS

2. Elsevier hereby grants you permission to reproduce the aforementioned material subject to the terms and conditions indicated.

3. Acknowledgement: If any part of the material to be used (for example, figures) has appeared in our publication with credit or acknowledgement to another source, permission must also be sought from that source. If such permission is not obtained then that material may not be included in your publication/copies. Suitable acknowledgement to the source must be made, either as a footnote or in a reference list at the end of your publication, as follows:

"Reprinted from Publication title, Vol /edition number, Author(s), Title of article / title of chapter, Pages No., Copyright (Year), with permission from Elsevier [OR APPLICABLE SOCIETY COPYRIGHT OWNER]." Also Lancet special credit -

"Reprinted from The Lancet, Vol. number, Author(s), Title of article, Pages No., Copyright (Year), with permission from Elsevier."
4. Reproduction of this material is confined to the purpose and/or media for which permission is hereby given.
5. Altering/Modifying Material: Not Permitted. However figures and illustrations may be altered/adapted minimally to serve your work. Any other abbreviations, additions, deletions and/or any other alterations shall be made only with prior written authorization of Elsevier Ltd. (Please contact Elsevier at permissions@elsevier.com). No modifications can be made to any Lancet figures/tables and they must be reproduced in full.
6. If the permission fee for the requested use of our material is waived in this instance, please be advised that your future requests for Elsevier materials may attract a fee.
7. Reservation of Rights: Publisher reserves all rights not specifically granted in the combination of (i) the license details provided by you and accepted in the course of this licensing transaction, (ii) these terms and conditions and (iii) CCC's Billing and Payment terms and conditions.
8. License Contingent Upon Payment: While you may exercise the rights licensed immediately upon issuance of the license at the end of the licensing process for the transaction, provided that you have disclosed complete and accurate details of your proposed use, no license is finally effective unless and until full payment is received from you (either by publisher or by CCC) as provided in CCC's Billing and Payment terms and conditions. If full payment is not received on a timely basis, then any license preliminarily granted shall be deemed automatically revoked and shall be void as if never granted. Further, in the event that you breach any of these terms and conditions or any of CCC's Billing and Payment terms and conditions, the license is automatically revoked and shall be void as if never granted. Use of materials as described in a revoked license, as well as any use of the materials beyond the scope of an unrevoked license, may constitute copyright infringement and publisher reserves the right to take any and all action to protect its copyright in the materials.
9. Warranties: Publisher makes no representations or warranties with respect to the licensed material.
10. Indemnity: You hereby indemnify and agree to hold harmless publisher and CCC, and their respective officers, directors, employees and agents, from and against any and all claims arising out of your use of the licensed material other than as specifically authorized pursuant to this license.
11. No Transfer of License: This license is personal to you and may not be sublicensed, assigned, or transferred by you to any other person without publisher's written permission.
12. No Amendment Except in Writing: This license may not be amended except in a writing signed by both parties (or, in the case of publisher, by CCC on publisher's behalf).
13. Objection to Contrary Terms: Publisher hereby objects to any terms contained in any purchase order, acknowledgment, check endorsement or other writing prepared by you, which terms are inconsistent with these terms and conditions or CCC's Billing and

Payment terms and conditions. These terms and conditions, together with CCC's Billing and Payment terms and conditions (which are incorporated herein), comprise the entire agreement between you and publisher (and CCC) concerning this licensing transaction. In the event of any conflict between your obligations established by these terms and conditions and those established by CCC's Billing and Payment terms and conditions, these terms and conditions shall control.
14. Revocation: Elsevier or Copyright Clearance Center may deny the permissions described in this License at their sole discretion, for any reason or no reason, with a full refund payable to you. Notice of such denial will be made using the contact information provided by you. Failure to receive such notice will not alter or invalidate the denial. In no event will Elsevier or Copyright Clearance Center be responsible or liable for any costs, expenses or damage incurred by you as a result of a denial of your permission request, other than a refund of the amount(s) paid by you to Elsevier and/or Copyright Clearance Center for denied permissions.
LIMITED LICENSE
The following terms and conditions apply only to specific license types:
15. **Translation**: This permission is granted for non-exclusive world **English** rights only unless your license was granted for translation rights. If you licensed translation rights you may only translate this content into the languages you requested. A professional translator must perform all translations and reproduce the content word for word preserving the integrity of the article.
16. **Posting licensed content on any Website**: The following terms and conditions apply as follows: Licensing material from an Elsevier journal: All content posted to the web site must maintain the copyright information line on the bottom of each image; A hyper-text must be included to the Homepage of the journal from which you are licensing at http://www.sciencedirect.com/science/journal/xxxxx or the Elsevier homepage for books at http://www.elsevier.com; Central Storage: This license does not include permission for a scanned version of the material to be stored in a central repository such as that provided by Heron/XanEdu.
Licensing material from an Elsevier book: A hyper-text link must be included to the Elsevier homepage at http://www.elsevier.com . All content posted to the web site must maintain the copyright information line on the bottom of each image.

Posting licensed content on Electronic reserve: In addition to the above the following clauses are applicable: The web site must be password-protected and made available only to bona fide students registered on a relevant course. This permission is granted for 1 year only. You may obtain a new license for future website posting.
17. **For journal authors:** the following clauses are applicable in addition to the above:
Preprints:
A preprint is an author's own write-up of research results and analysis, it has not been peer-reviewed, nor has it had any other value added to it by a publisher (such as formatting, copyright, technical enhancement etc.).
Authors can share their preprints anywhere at any time. Preprints should not be added to or enhanced in any way in order to appear more like, or to substitute for, the final

versions of articles however authors can update their preprints on arXiv or RePEc with their Accepted Author Manuscript (see below).
If accepted for publication, we encourage authors to link from the preprint to their formal publication via its DOI. Millions of researchers have access to the formal publications on ScienceDirect, and so links will help users to find, access, cite and use the best available version. Please note that Cell Press, The Lancet and some society-owned have different preprint policies. Information on these policies is available on the journal homepage.
Accepted Author Manuscripts: An accepted author manuscript is the manuscript of an article that has been accepted for publication and which typically includes author-incorporated changes suggested during submission, peer review and editor-author communications.
Authors can share their accepted author manuscript:

- immediately
    - via their non-commercial person homepage or blog
    - by updating a preprint in arXiv or RePEc with the accepted manuscript
    - via their research institute or institutional repository for internal institutional uses or as part of an invitation-only research collaboration work-group
    - directly by providing copies to their students or to research collaborators for their personal use
    - for private scholarly sharing as part of an invitation-only work group on commercial sites with which Elsevier has an agreement
- After the embargo period
    - via non-commercial hosting platforms such as their institutional repository
    - via commercial sites with which Elsevier has an agreement

In all cases accepted manuscripts should:

- link to the formal publication via its DOI
- bear a CC-BY-NC-ND license - this is easy to do
- if aggregated with other manuscripts, for example in a repository or other site, be shared in alignment with our hosting policy not be added to or enhanced in any way to appear more like, or to substitute for, the published journal article.

Published journal article (JPA): A published journal article (PJA) is the definitive final record of published research that appears or will appear in the journal and embodies all value-adding publishing activities including peer review co-ordination, copy-editing, formatting, (if relevant) pagination and online enrichment.
Policies for sharing publishing journal articles differ for subscription and gold open access articles:
Subscription Articles: If you are an author, please share a link to your article rather than the full-text. Millions of researchers have access to the formal publications on ScienceDirect, and so links will help your users to find, access, cite, and use the best available version.

Theses and dissertations which contain embedded PJAs as part of the formal submission can be posted publicly by the awarding institution with DOI links back to the formal publications on ScienceDirect.
If you are affiliated with a library that subscribes to ScienceDirect you have additional private sharing rights for others' research accessed under that agreement. This includes use for classroom teaching and internal training at the institution (including use in course packs and courseware programs), and inclusion of the article for grant funding purposes.
Gold Open Access Articles: May be shared according to the author-selected end-user license and should contain a CrossMark logo, the end user license, and a DOI link to the formal publication on ScienceDirect.
Please refer to Elsevier's posting policy for further information.
18. **For book authors** the following clauses are applicable in addition to the above: Authors are permitted to place a brief summary of their work online only. You are not allowed to download and post the published electronic version of your chapter, nor may you scan the printed edition to create an electronic version. **Posting to a repository:** Authors are permitted to post a summary of their chapter only in their institution's repository.
19. **Thesis/Dissertation**: If your license is for use in a thesis/dissertation your thesis may be submitted to your institution in either print or electronic form. Should your thesis be published commercially, please reapply for permission. These requirements include permission for the Library and Archives of Canada to supply single copies, on demand, of the complete thesis and include permission for Proquest/UMI to supply single copies, on demand, of the complete thesis. Should your thesis be published commercially, please reapply for permission. Theses and dissertations which contain embedded PJAs as part of the formal submission can be posted publicly by the awarding institution with DOI links back to the formal publications on ScienceDirect.

Elsevier Open Access Terms and Conditions
You can publish open access with Elsevier in hundreds of open access journals or in nearly 2000 established subscription journals that support open access publishing. Permitted third party re-use of these open access articles is defined by the author's choice of Creative Commons user license. See our open access license policy for more information.
Terms & Conditions applicable to all Open Access articles published with Elsevier:
Any reuse of the article must not represent the author as endorsing the adaptation of the article nor should the article be modified in such a way as to damage the author's honour or reputation. If any changes have been made, such changes must be clearly indicated.
The author(s) must be appropriately credited and we ask that you include the end user license and a DOI link to the formal publication on ScienceDirect.
If any part of the material to be used (for example, figures) has appeared in our publication with credit or acknowledgement to another source it is the responsibility of

Chapter 3: John Wiley and Sons, for Ayre, et al. (2015) *Immunology*

JOHN WILEY AND SONS LICENSE TERMS AND CONDITIONS

Aug 07, 2017

This Agreement between Mr. Craig Ayre ("You") and John Wiley and Sons ("John Wiley and Sons") consists of your license details and the terms and conditions provided by John Wiley and Sons and Copyright Clearance Center.

License Number	4155910410682
License date	Jul 25, 2017
Licensed Content Publisher	John Wiley and Sons
Licensed Content Publication	Immunology
Licensed Content Title	Dynamic regulation of CD24 expression and release of CD24-containing microvesicles in immature B cells in response to CD24 engagement
Licensed Content Author	D. Craig Ayre,Marcus Elstner,Nicole C. Smith,Emily S. Moores,Andrew M. Hogan,Sherri L. Christian
Licensed Content Date	Jul 15, 2015
Licensed Content Pages	17
Type of use	Dissertation/Thesis
Requestor type	Author of this Wiley article
Format	Print and electronic
Portion	Full article
Will you be translating?	No
Title of your thesis / dissertation	A Generalizable Mechanism of CD24 Signalling and Its Ability to Specifically Alter the Biogenesis of B Cell Extracellular Vesicles
Expected completion date	Oct 2017
Expected size (number of pages)	210
Requestor Location	Mr. Craig Ayre 57 Railway Avenue

	Moncton, NB E1C2C9 Canada Attn: Mr. Craig Ayre
Publisher Tax ID	EU826007151
Billing Type	Invoice
Billing Address	Mr. Craig Ayre 57 Railway Avenue Moncton, NB E1C2C9 Canada Attn: Mr. Craig Ayre
Total	0.00 USD

Terms and Conditions

TERMS AND CONDITIONS

This copyrighted material is owned by or exclusively licensed to John Wiley & Sons, Inc. or one of its group companies (each a"Wiley Company") or handled on behalf of a society with which a Wiley Company has exclusive publishing rights in relation to a particular work (collectively "WILEY"). By clicking "accept" in connection with completing this licensing transaction, you agree that the following terms and conditions apply to this transaction (along with the billing and payment terms and conditions established by the Copyright Clearance Center Inc., ("CCC's Billing and Payment terms and conditions"), at the time that you opened your RightsLink account (these are available at any time at http://myaccount.copyright.com).

Terms and Conditions

- The materials you have requested permission to reproduce or reuse (the "Wiley Materials") are protected by copyright.
- You are hereby granted a personal, non-exclusive, non-sub licensable (on a stand-alone basis), non-transferable, worldwide, limited license to reproduce the Wiley Materials for the purpose specified in the licensing process. This license, **and any CONTENT (PDF or image file) purchased as part of your order,** is for a one-time use only and limited to any maximum distribution number specified in the license. The first instance of republication or reuse granted by this license must be completed within two years of the date of the grant of this license (although copies prepared before the end date may be distributed thereafter). The Wiley Materials shall not be used in any other manner or for any other purpose, beyond what is granted in the license. Permission is granted subject to an appropriate acknowledgement given to the author, title of the material/book/journal and the publisher. You shall also duplicate the copyright notice that appears in the Wiley publication in your

use of the Wiley Material. Permission is also granted on the understanding that nowhere in the text is a previously published source acknowledged for all or part of this Wiley Material. Any third party content is expressly excluded from this permission.

- With respect to the Wiley Materials, all rights are reserved. Except as expressly granted by the terms of the license, no part of the Wiley Materials may be copied, modified, adapted (except for minor reformatting required by the new Publication), translated, reproduced, transferred or distributed, in any form or by any means, and no derivative works may be made based on the Wiley Materials without the prior permission of the respective copyright owner.**For STM Signatory Publishers clearing permission under the terms of the STM Permissions Guidelines only, the terms of the license are extended to include subsequent editions and for editions in other languages, provided such editions are for the work as a whole in situ and does not involve the separate exploitation of the permitted figures or extracts,**You may not alter, remove or suppress in any manner any copyright, trademark or other notices displayed by the Wiley Materials. You may not license, rent, sell, loan, lease, pledge, offer as security, transfer or assign the Wiley Materials on a stand-alone basis, or any of the rights granted to you hereunder to any other person.
- The Wiley Materials and all of the intellectual property rights therein shall at all times remain the exclusive property of John Wiley & Sons Inc, the Wiley Companies, or their respective licensors, and your interest therein is only that of having possession of and the right to reproduce the Wiley Materials pursuant to Section 2 herein during the continuance of this Agreement. You agree that you own no right, title or interest in or to the Wiley Materials or any of the intellectual property rights therein. You shall have no rights hereunder other than the license as provided for above in Section 2. No right, license or interest to any trademark, trade name, service mark or other branding ("Marks") of WILEY or its licensors is granted hereunder, and you agree that you shall not assert any such right, license or interest with respect thereto
- NEITHER WILEY NOR ITS LICENSORS MAKES ANY WARRANTY OR REPRESENTATION OF ANY KIND TO YOU OR ANY THIRD PARTY, EXPRESS, IMPLIED OR STATUTORY, WITH RESPECT TO THE MATERIALS OR THE ACCURACY OF ANY INFORMATION CONTAINED IN THE MATERIALS, INCLUDING, WITHOUT LIMITATION, ANY IMPLIED WARRANTY OF MERCHANTABILITY, ACCURACY, SATISFACTORY QUALITY, FITNESS FOR A PARTICULAR PURPOSE, USABILITY, INTEGRATION OR NON-INFRINGEMENT AND ALL SUCH WARRANTIES ARE HEREBY EXCLUDED BY WILEY AND ITS LICENSORS AND WAIVED BY YOU.
- WILEY shall have the right to terminate this Agreement immediately upon breach of this Agreement by you.

- You shall indemnify, defend and hold harmless WILEY, its Licensors and their respective directors, officers, agents and employees, from and against any actual or threatened claims, demands, causes of action or proceedings arising from any breach of this Agreement by you.
- IN NO EVENT SHALL WILEY OR ITS LICENSORS BE LIABLE TO YOU OR ANY OTHER PARTY OR ANY OTHER PERSON OR ENTITY FOR ANY SPECIAL, CONSEQUENTIAL, INCIDENTAL, INDIRECT, EXEMPLARY OR PUNITIVE DAMAGES, HOWEVER CAUSED, ARISING OUT OF OR IN CONNECTION WITH THE DOWNLOADING, PROVISIONING, VIEWING OR USE OF THE MATERIALS REGARDLESS OF THE FORM OF ACTION, WHETHER FOR BREACH OF CONTRACT, BREACH OF WARRANTY, TORT, NEGLIGENCE, INFRINGEMENT OR OTHERWISE (INCLUDING, WITHOUT LIMITATION, DAMAGES BASED ON LOSS OF PROFITS, DATA, FILES, USE, BUSINESS OPPORTUNITY OR CLAIMS OF THIRD PARTIES), AND WHETHER OR NOT THE PARTY HAS BEEN ADVISED OF THE POSSIBILITY OF SUCH DAMAGES. THIS LIMITATION SHALL APPLY NOTWITHSTANDING ANY FAILURE OF ESSENTIAL PURPOSE OF ANY LIMITED REMEDY PROVIDED HEREIN.
- Should any provision of this Agreement be held by a court of competent jurisdiction to be illegal, invalid, or unenforceable, that provision shall be deemed amended to achieve as nearly as possible the same economic effect as the original provision, and the legality, validity and enforceability of the remaining provisions of this Agreement shall not be affected or impaired thereby.
- The failure of either party to enforce any term or condition of this Agreement shall not constitute a waiver of either party's right to enforce each and every term and condition of this Agreement. No breach under this agreement shall be deemed waived or excused by either party unless such waiver or consent is in writing signed by the party granting such waiver or consent. The waiver by or consent of a party to a breach of any provision of this Agreement shall not operate or be construed as a waiver of or consent to any other or subsequent breach by such other party.
- This Agreement may not be assigned (including by operation of law or otherwise) by you without WILEY's prior written consent.
- Any fee required for this permission shall be non-refundable after thirty (30) days from receipt by the CCC.
- These terms and conditions together with CCC's Billing and Payment terms and conditions (which are incorporated herein) form the entire agreement between you and WILEY concerning this licensing transaction and (in the absence of fraud) supersedes all prior agreements and representations of the parties, oral or written. This Agreement may not be amended except in writing signed by both parties. This Agreement shall be binding upon and inure to the

benefit of the parties' successors, legal representatives, and authorized assigns.

- In the event of any conflict between your obligations established by these terms and conditions and those established by CCC's Billing and Payment terms and conditions, these terms and conditions shall prevail.
- WILEY expressly reserves all rights not specifically granted in the combination of (i) the license details provided by you and accepted in the course of this licensing transaction, (ii) these terms and conditions and (iii) CCC's Billing and Payment terms and conditions.
- This Agreement will be void if the Type of Use, Format, Circulation, or Requestor Type was misrepresented during the licensing process.
- This Agreement shall be governed by and construed in accordance with the laws of the State of New York, USA, without regards to such state's conflict of law rules. Any legal action, suit or proceeding arising out of or relating to these Terms and Conditions or the breach thereof shall be instituted in a court of competent jurisdiction in New York County in the State of New York in the United States of America and each party hereby consents and submits to the personal jurisdiction of such court, waives any objection to venue in such court and consents to service of process by registered or certified mail, return receipt requested, at the last known address of such party.

WILEY OPEN ACCESS TERMS AND CONDITIONS

Wiley Publishes Open Access Articles in fully Open Access Journals and in Subscription journals offering Online Open. Although most of the fully Open Access journals publish open access articles under the terms of the Creative Commons Attribution (CC BY) License only, the subscription journals and a few of the Open Access Journals offer a choice of Creative Commons Licenses. The license type is clearly identified on the article.

The Creative Commons Attribution License

The Creative Commons Attribution License (CC-BY) allows users to copy, distribute and transmit an article, adapt the article and make commercial use of the article. The CC-BY license permits commercial and non-

Creative Commons Attribution Non-Commercial License

The Creative Commons Attribution Non-Commercial (CC-BY-NC)License permits use, distribution and reproduction in any medium, provided the original work is properly cited and is not used for commercial purposes.(see below)

Creative Commons Attribution-Non-Commercial-NoDerivs License

The Creative Commons Attribution Non-Commercial-NoDerivs License (CC-BY-NC-ND) permits use, distribution and reproduction in any medium, provided the original work is properly cited, is not used for commercial purposes and no modifications or adaptations are made. (see below)

Use by commercial "for-profit" organizations

Use of Wiley Open Access articles for commercial, promotional, or marketing purposes requires further explicit permission from Wiley and will be subject to a fee.

Further details can be found on Wiley Online Library http://olabout.wiley.com/WileyCDA/Section/id-410895.html

Other Terms and Conditions:

v1.10 Last updated September 2015

Questions? customercare@copyright.com or +1-855-239-3415 (toll free in the US) or +1-978-646-2777.

Chapter 4: Scientific Reports, for Ayre, et al. (2017) *Scientific Reports*.

Attribution statement:
1. Scientific Reports does not require authors to assign copyright of their published original research papers to the journal. Articles are published under a CC BY license (Creative Commons Attribution 4.0 International License). The CC BY license allows for maximum dissemination and re-use of open access materials and is preferred by many research funding bodies. Under this license users are free to share (copy, distribute and transmit) and remix (adapt) the contribution including for commercial purposes, providing they attribute the contribution in the manner specified by the author or licensor

Chapter 5: Frontiers, for Ayre and Christian (2016) *Frontiers in Cell and Developmental Biology.*

Attribution statement:
1. Under the Frontiers Terms and Conditions, authors retain the copyright to their work. All Frontiers articles are Open Access and currently distributed under the terms of the Creative Commons Attribution License, which permits the use, distribution and reproduction of material from published articles, provided the original authors and source are credited, and subject to any copyright notices concerning any third-party content.

Creative Commons Attribution 4.0 International

Creative Commons Corporation ("Creative Commons") is not a law firm and does not provide legal services or legal advice. Distribution of Creative Commons public licenses does not create a lawyer-client or other relationship. Creative Commons makes its licenses and related information available on an "as-is" basis. Creative Commons gives no warranties regarding its licenses, any material licensed under their terms and conditions, or any related information. Creative Commons disclaims all liability for damages resulting from their use to the fullest extent possible.

Using Creative Commons Public Licenses
Creative Commons public licenses provide a standard set of terms and conditions that creators and other rights holders may use to share original works of authorship and other material subject to copyright and certain other rights specified in the public license below. The following considerations are for informational purposes only, are not exhaustive, and do not form part of our licenses.

Considerations for licensors: Our public licenses are intended for use by those authorized to give the public permission to use material in ways otherwise restricted by copyright and certain other rights. Our licenses are irrevocable. Licensors should read and understand the terms and conditions of the license they choose before applying it. Licensors should also secure all rights necessary before applying our licenses so that the public can reuse the material as expected. Licensors should clearly mark any material not subject to the license. This includes other CC-licensed material, or material used under an exception or limitation to copyright. More considerations for licensors.

Considerations for the public: By using one of our public licenses, a licensor grants the public permission to use the licensed material under specified terms and conditions. If the licensor's permission is not necessary for any reason–for example, because of any applicable exception or limitation to copyright–then that use is not regulated by the license. Our licenses grant only permissions under copyright and certain other rights that a licensor has authority to grant. Use of the licensed material may still be restricted for other reasons, including because others have copyright or other rights in the material. A licensor may make special requests, such as asking that all changes be marked or described. Although not required by our licenses, you are encouraged to respect those requests where reasonable. More considerations for the public.

Creative Commons Attribution 4.0 International Public License
By exercising the Licensed Rights (defined below), You accept and agree to be bound by the terms and conditions of this Creative Commons Attribution 4.0 International Public License ("Public License"). To the extent this Public License may be interpreted as a contract, You are granted the Licensed Rights in consideration of Your acceptance of these terms and conditions, and the Licensor grants You such rights in consideration of benefits the Licensor receives from making the Licensed Material available under these terms and conditions.

Section 1 – Definitions.
a. Adapted Material means material subject to Copyright and Similar Rights that is derived from or based upon the Licensed Material and in which the Licensed Material is translated, altered, arranged, transformed, or otherwise modified in a manner requiring permission under the Copyright and Similar Rights held by the Licensor. For purposes of this Public License, where the Licensed Material is a musical work, performance, or sound recording, Adapted Material is always produced where the Licensed Material is synched in timed relation with a moving image.

b. Adapter's License means the license You apply to Your Copyright and Similar Rights in Your contributions to Adapted Material in accordance with the terms and conditions of this Public License.
c. Copyright and Similar Rights means copyright and/or similar rights closely related to copyright including, without limitation, performance, broadcast, sound recording, and Sui Generis Database Rights, without regard to how the rights are labeled or categorized. For purposes of this Public License, the rights specified in Section 2(b)(1)-(2) are not Copyright and Similar Rights.
d. Effective Technological Measures means those measures that, in the absence of proper authority, may not be circumvented under laws fulfilling obligations under Article 11 of the WIPO Copyright Treaty adopted on December 20, 1996, and/or similar international agreements.
e. Exceptions and Limitations means fair use, fair dealing, and/or any other exception or limitation to Copyright and Similar Rights that applies to Your use of the Licensed Material.
f. Licensed Material means the artistic or literary work, database, or other material to which the Licensor applied this Public License.
g. Licensed Rights means the rights granted to You subject to the terms and conditions of this Public License, which are limited to all Copyright and Similar Rights that apply to Your use of the Licensed Material and that the Licensor has authority to license.
h. Licensor means the individual(s) or entity(ies) granting rights under this Public License.
i. Share means to provide material to the public by any means or process that requires permission under the Licensed Rights, such as reproduction, public display, public performance, distribution, dissemination, communication, or importation, and to make material available to the public including in ways that members of the public may access the material from a place and at a time individually chosen by them.
j. Sui Generis Database Rights means rights other than copyright resulting from Directive 96/9/EC of the European Parliament and of the Council of 11 March 1996 on the legal protection of databases, as amended and/or succeeded, as well as other essentially equivalent rights anywhere in the world.
k. You means the individual or entity exercising the Licensed Rights under this Public License. Your has a corresponding meaning.

Section 2 – Scope.
a. License grant.
1. Subject to the terms and conditions of this Public License, the Licensor hereby grants You a worldwide, royalty-free, non-sublicensable, non-exclusive, irrevocable license to exercise the Licensed Rights in the Licensed Material to:
A. reproduce and Share the Licensed Material, in whole or in part; and
B. produce, reproduce, and Share Adapted Material.
2. Exceptions and Limitations. For the avoidance of doubt, where Exceptions and Limitations apply to Your use, this Public License does not apply, and You do not need to comply with its terms and conditions.

3. Term. The term of this Public License is specified in Section 6(a).
4. Media and formats; technical modifications allowed. The Licensor authorizes You to exercise the Licensed Rights in all media and formats whether now known or hereafter created, and to make technical modifications necessary to do so. The Licensor waives and/or agrees not to assert any right or authority to forbid You from making technical modifications necessary to exercise the Licensed Rights, including technical modifications necessary to circumvent Effective Technological Measures. For purposes of this Public License, simply making modifications authorized by this Section 2(a)(4) never produces Adapted Material.
5. Downstream recipients.
A. Offer from the Licensor – Licensed Material. Every recipient of the Licensed Material automatically receives an offer from the Licensor to exercise the Licensed Rights under the terms and conditions of this Public License.
B. No downstream restrictions. You may not offer or impose any additional or different terms or conditions on, or apply any Effective Technological Measures to, the Licensed Material if doing so restricts exercise of the Licensed Rights by any recipient of the Licensed Material.
6. No endorsement. Nothing in this Public License constitutes or may be construed as permission to assert or imply that You are, or that Your use of the Licensed Material is, connected with, or sponsored, endorsed, or granted official status by, the Licensor or others designated to receive attribution as provided in Section 3(a)(1)(A)(i).
b. Other rights.
1. Moral rights, such as the right of integrity, are not licensed under this Public License, nor are publicity, privacy, and/or other similar personality rights; however, to the extent possible, the Licensor waives and/or agrees not to assert any such rights held by the Licensor to the limited extent necessary to allow You to exercise the Licensed Rights, but not otherwise.
2. Patent and trademark rights are not licensed under this Public License.
3. To the extent possible, the Licensor waives any right to collect royalties from You for the exercise of the Licensed Rights, whether directly or through a collecting society under any voluntary or waivable statutory or compulsory licensing scheme. In all other cases the Licensor expressly reserves any right to collect such royalties.

Section 3 – License Conditions.
Your exercise of the Licensed Rights is expressly made subject to the following conditions.
a. Attribution.
1. If You Share the Licensed Material (including in modified form), You must:
A. retain the following if it is supplied by the Licensor with the Licensed Material:
i. identification of the creator(s) of the Licensed Material and any others designated to receive attribution, in any reasonable manner requested by the Licensor (including by pseudonym if designated);
ii. a copyright notice;
iii. a notice that refers to this Public License;
iv. a notice that refers to the disclaimer of warranties;

v. a URI or hyperlink to the Licensed Material to the extent reasonably practicable;
B. indicate if You modified the Licensed Material and retain an indication of any previous modifications; and
C. indicate the Licensed Material is licensed under this Public License, and include the text of, or the URI or hyperlink to, this Public License.
2. You may satisfy the conditions in Section 3(a)(1) in any reasonable manner based on the medium, means, and context in which You Share the Licensed Material. For example, it may be reasonable to satisfy the conditions by providing a URI or hyperlink to a resource that includes the required information.
3. If requested by the Licensor, You must remove any of the information required by Section 3(a)(1)(A) to the extent reasonably practicable.
4. If You Share Adapted Material You produce, the Adapter's License You apply must not prevent recipients of the Adapted Material from complying with this Public License.

Section 4 – Sui Generis Database Rights.
Where the Licensed Rights include Sui Generis Database Rights that apply to Your use of the Licensed Material:
a. for the avoidance of doubt, Section 2(a)(1) grants You the right to extract, reuse, reproduce, and Share all or a substantial portion of the contents of the database;
b. if You include all or a substantial portion of the database contents in a database in which You have Sui Generis Database Rights, then the database in which You have Sui Generis Database Rights (but not its individual contents) is Adapted Material; and

c. You must comply with the conditions in Section 3(a) if You Share all or a substantial portion of the contents of the database.
For the avoidance of doubt, this Section 4 supplements and does not replace Your obligations under this Public License where the Licensed Rights include other Copyright and Similar Rights.

Section 5 – Disclaimer of Warranties and Limitation of Liability.
a. Unless otherwise separately undertaken by the Licensor, to the extent possible, the Licensor offers the Licensed Material as-is and as-available, and makes no representations or warranties of any kind concerning the Licensed Material, whether express, implied, statutory, or other. This includes, without limitation, warranties of title, merchantability, fitness for a particular purpose, non-infringement, absence of latent or other defects, accuracy, or the presence or absence of errors, whether or not known or discoverable. Where disclaimers of warranties are not allowed in full or in part, this disclaimer may not apply to You.
b. To the extent possible, in no event will the Licensor be liable to You on any legal theory (including, without limitation, negligence) or otherwise for any direct, special, indirect, incidental, consequential, punitive, exemplary, or other losses, costs, expenses, or damages arising out of this Public License or use of the Licensed Material, even if the Licensor has been advised of the possibility of such losses, costs, expenses, or damages.

Where a limitation of liability is not allowed in full or in part, this limitation may not apply to You.

c. The disclaimer of warranties and limitation of liability provided above shall be interpreted in a manner that, to the extent possible, most closely approximates an absolute disclaimer and waiver of all liability.

Section 6 – Term and Termination.

a. This Public License applies for the term of the Copyright and Similar Rights licensed here. However, if You fail to comply with this Public License, then Your rights under this Public License terminate automatically.

b. Where Your right to use the Licensed Material has terminated under Section 6(a), it reinstates:

1. automatically as of the date the violation is cured, provided it is cured within 30 days of Your discovery of the violation; or

2. upon express reinstatement by the Licensor.

For the avoidance of doubt, this Section 6(b) does not affect any right the Licensor may have to seek remedies for Your violations of this Public License.

c. For the avoidance of doubt, the Licensor may also offer the Licensed Material under separate terms or conditions or stop distributing the Licensed Material at any time; however, doing so will not terminate this Public License.

d. Sections 1, 5, 6, 7, and 8 survive termination of this Public License.

Section 7 – Other Terms and Conditions.

a. The Licensor shall not be bound by any additional or different terms or conditions communicated by You unless expressly agreed.

b. Any arrangements, understandings, or agreements regarding the Licensed Material not stated herein are separate from and independent of the terms and conditions of this Public License.

Section 8 – Interpretation.

a. For the avoidance of doubt, this Public License does not, and shall not be interpreted to, reduce, limit, restrict, or impose conditions on any use of the Licensed Material that could lawfully be made without permission under this Public License.

b. To the extent possible, if any provision of this Public License is deemed unenforceable, it shall be automatically reformed to the minimum extent necessary to make it enforceable. If the provision cannot be reformed, it shall be severed from this Public License without affecting the enforceability of the remaining terms and conditions.

c. No term or condition of this Public License will be waived and no failure to comply consented to unless expressly agreed to by the Licensor.

d. Nothing in this Public License constitutes or may be interpreted as a limitation upon, or waiver of, any privileges and immunities that apply to the Licensor or You, including from the legal processes of any jurisdiction or authority.

Creative Commons is not a party to its public licenses. Notwithstanding, Creative Commons may elect to apply one of its public licenses to material it publishes and in those instances will be considered the “Licensor.” The text of the Creative Commons

Appendix B: R Scripts

1. **CD24 expression, endocytosis and exocytosis inhibition, epitope saturation**

```
#SURFACE EXPRESSION, WEHI231
wehi<- read.csv("wehi_rel_cd24.csv", header=T)
wehi
colnames(wehi)
wehi$TIME=as.factor(wehi$TIME)
summary(wehi)
wehiMEANAOV<-aov(wehi$MEAN~wehi$TIME)
summary(wehiMEANAOV)
TukeyHSD(wehiMEANAOV)

wehiMODEAOV<-aov(wehi$MODE~wehi$TIME)
summary(wehiMODEAOV)
TukeyHSD(wehiMODEAOV)

wehi0<-subset(wehi, TIME=="0")
wehi1<-subset(wehi, TIME=="1")
wehi.t<-rbind(wehi1,wehi0)
wehi.t
t.test(MEAN~TIME, alternative=c("greater"), var.equal=FALSE,
data=wehi.t)
t.test(MODE~TIME, alternative=c("greater"), var.equal=FALSE,
data=wehi.t)

#LINEAR MODEL TIME 1 to 60, WEHI231
wehi2<-read.csv("wehi_rel_cd24_glm.csv", header=T)
wehi2
colnames(wehi2)
#wehi2$TIME=as.factor(wehi2$TIME)
wehi2MEANglm<-glm(wehi2$MEAN~wehi2$TIME)
anova(wehi2MEANglm)
summary(wehi2MEANglm)
plot(wehi2MEANglm)
coef(wehi2MEANglm)

wehi2MODEglm<-glm(wehi2$MODE~wehi2$TIME)
anova(wehi2MODEglm)
summary(wehi2MODEglm)
plot(wehi2MODEglm)
coef(wehi2MODEglm)

#LINEAR MODEL TIME 1 to 60, WEHI231
```

```
wehiendo2<-read.csv("wehiendo2.csv", header=T)
wehiendo2
colnames(wehiendo2)
wehiendo2$TIME=as.factor(wehiendo2$TIME)
wehiendo2glm<-
glm(wehiendo2$CD24~wehiendo2$TIME*wehiendo2$INHIBIT)
anova(wehiendo2glm)
summary(wehiendo2glm)
plot(wehiendo2glm)

#LINEAR MODEL TIME 1 to 60, WEHI231
wehiexo2<-read.csv("wehiexo2.csv", header=T)
wehiexo2
colnames(wehiexo2)
wehiexo2$TIME=as.factor(wehiexo2$TIME)
wehiexo2glm<-
glm(wehiexo2$CD24~wehiexo2$TIME*wehiexo2$INHIBIT)
anova(wehiexo2glm)
summary(wehiexo2glm)
plot(wehiexo2glm)

#ENDOCYTOSIS INHIBITION, WEHI231
wehiendo<- read.csv("wehiendo.csv", header=T)
wehiendo
colnames(wehiendo)
wehiendo$TIME=as.factor(wehiendo$TIME)
summary(wehiendo)
wehiendoAOV<-
aov(wehiendo$CD24~wehiendo$TIME*wehiendo$INHIBIT)
summary(wehiendoAOV)

#One-way anova, Time zero
wehiendo0<-subset(wehiendo, TIME=="0")
wehiendo0
wehiendo0AOV<-aov(wehiendo0$CD24~wehiendo0$INHIBIT)
summary(wehiendo0AOV)
TukeyHSD(wehiendo0AOV)

#One-way anova, Time 1
wehiendo1<-subset(wehiendo, TIME=="1")
wehiendo1
wehiendo1AOV<-aov(wehiendo1$CD24~wehiendo1$INHIBIT)
summary(wehiendo1AOV)
TukeyHSD(wehiendo1AOV)

#One-way anova, Time 5
```

```
wehiendo5<-subset(wehiendo, TIME=="5")
wehiendo5
wehiendo5AOV<-aov(wehiendo5$CD24~wehiendo5$INHIBIT)
summary(wehiendo5AOV)
TukeyHSD(wehiendo5AOV)

#One-way anova, Time 15
wehiendo15<-subset(wehiendo, TIME=="15")
wehiendo15
wehiendo15AOV<-aov(wehiendo15$CD24~wehiendo15$INHIBIT)
summary(wehiendo15AOV)
TukeyHSD(wehiendo15AOV)

#One-way anova, Time 40
wehiendo40<-subset(wehiendo, TIME=="40")
wehiendo40
wehiendo40AOV<-aov(wehiendo40$CD24~wehiendo40$INHIBIT)
summary(wehiendo40AOV)
TukeyHSD(wehiendo40AOV)

#One-way anova, Time 60
wehiendo60<-subset(wehiendo, TIME=="60")
wehiendo60
wehiendo60AOV<-aov(wehiendo60$CD24~wehiendo60$INHIBIT)
summary(wehiendo60AOV)
TukeyHSD(wehiendo60AOV)


#EXOCYTOSIS INHIBITION, WEHI231
wehiexo<- read.csv("wehiexo.csv", header=T)
wehiexo
colnames(wehiexo)
wehiexo$TIME=as.factor(wehiexo$TIME)
summary(wehiexo)
wehiexoAOV<-aov(wehiexo$CD24~wehiexo$TIME*wehiexo$INHIBIT)
summary(wehiexoAOV)

#One-way anova, Time zero
wehiexo0<-subset(wehiexo, TIME=="0")
wehiexo0
wehiexo0AOV<-aov(wehiexo0$CD24~wehiexo0$INHIBIT)
summary(wehiexo0AOV)
TukeyHSD(wehiexo0AOV)

#One-way anova, Time 1
wehiexo1<-subset(wehiexo, TIME=="1")
```

```
wehiexo1
wehiexo1AOV<-aov(wehiexo1$CD24~wehiexo1$INHIBIT)
summary(wehiexo1AOV)
TukeyHSD(wehiexo1AOV)

#One-way anova, Time 5
wehiexo5<-subset(wehiexo, TIME=="5")
wehiexo5
wehiexo5AOV<-aov(wehiexo5$CD24~wehiexo5$INHIBIT)
summary(wehiexo5AOV)
TukeyHSD(wehiexo5AOV)

#One-way anova, Time 15
wehiexo15<-subset(wehiexo, TIME=="15")
wehiexo15
wehiexo15AOV<-aov(wehiexo15$CD24~wehiexo15$INHIBIT)
summary(wehiexo15AOV)
TukeyHSD(wehiexo15AOV)

#One-way anova, Time 40
wehiexo40<-subset(wehiexo, TIME=="40")
wehiexo40
wehiexo40AOV<-aov(wehiexo40$CD24~wehiexo40$INHIBIT)
summary(wehiexo40AOV)
TukeyHSD(wehiexo40AOV)

#One-way anova, Time 60
wehiexo60<-subset(wehiexo, TIME=="60")
wehiexo60
wehiexo60AOV<-aov(wehiexo60$CD24~wehiexo60$INHIBIT)
summary(wehiexo60AOV)
TukeyHSD(wehiexo60AOV)
```

CD24 exchange between cells

```
setwd("~/Desktop")
getwd()
exchange<-read.csv("exchange.csv", header=T)
exchange
colnames(exchange)
summary(exchange)
exchangeAOV<-aov(exchange$DBLPOS~exchange$TIME)
summary(exchangeAOV)

exchangeglm<-glm(exchange$DBLPOS~exchange$TIME)
anova(exchangeglm)
summary(exchangeglm)
```

```
plot(exchangeglm)

# Saturation and Epitopes
sat<-read.csv("saturation.csv", header=T)
sat
colnames(sat)
sat$COND=as.factor(sat$COND)
summary(sat)
satMEANAOV<-aov(sat$FITC~sat$COND)
summary(satMEANAOV)
TukeyHSD(satMEANAOV)

satMODEAOV<-aov(sat$APC~sat$COND)
summary(satMODEAOV)
TukeyHSD(satMODEAOV)

#LINEAR MODEL TIME 1 to 60, WEHI231
sat2<-read.csv("saturation_glm.csv", header=T)
sat2
colnames(sat2)
#wehi2$TIME=as.factor(wehi2$TIME)
sat2APCglm<-glm(sat2$APC~sat2$COND)
anova(sat2APCglm)
summary(sat2APCglm)
plot(sat2APCglm)
coef(sat2APCglm)

sat2FITCglm<-glm(sat2$FITC~sat2$COND)
anova(sat2FITCglm)
summary(sat2FITCglm)
plot(sat2FITCglm)
coef(sat2FITCglm)
```

2. Gene expression analysis

```
#Normalizing and Background Correcting
library(oligo)
celfiles=list.celfiles()
celfiles
data=read.celfiles(celfiles)
data
hist(data)
boxplot(data)
genes=rma(data, target="core")
genes
hist(genes)
boxplot(genes)
```

```
list<-c("10362896", "10351197", "10351206", "10351182",
"10605113", "10562132", "10552369", "10552380", "10435704",
"10439312", "10557862", "10412760", "10547894", "10567863",
"10545765", "10524718", "10571653", "10547894", "10538979",
"10538993", "10535381")
genesint<-genes[list]
genesint
write.exprs(genesint, file="Dendritic interest.txt")
write.exprs(genes, file="Dendritic_all.txt")
```

3. **RNA-Seq Analysis**

```
setwd("~/Documents/Graduate Degree/Research/Paper 3 - Ayre
et al - Vesicles/RNA-Seq")
getwd()
source("http://bioconductor.org/biocLite.R")
biocLite("biomaRt")
biocLite("edgeR")

#getting the RNA subtypes
library("biomaRt")
library("edgeR")
listMarts()
ensembl=useMart("ensembl")
listDatasets(ensembl)
ensembl =
useMart("ensembl",dataset="mmusculus_gene_ensembl")
genes=read.csv("ensmbl.csv",header=TRUE)
colnames(genes)
biomart_gene=getBM(attributes=c("ensembl_gene_id",
"transcript_biotype"),mart=ensembl)
genes$type=biomart_gene$transcript_biotype[match(genes$Ensem
ble, biomart_gene$ensembl_gene_id)]
write.csv(genes, file="BiomaRt_Transcript_Annotation.csv")

#Counting RNA species
features=table(genes$type)
features

#Reading counts
setwd("~/Documents/Graduate Degree/Research/Paper 3 - Ayre
et al - Vesicles/RNA-Seq")
getwd()
source("http://bioconductor.org/biocLite.R")
#biocLite("biomaRt")
#biocLite("edgeR")
```

```
#biocLite("locfit")
#biocLite("statmod")

#getting the RNA subtypes
library("biomaRt")
library("edgeR")
library("locfit")
library("statmod")
rawdata=read.delim("Counts_all.txt", header=TRUE,
row.names="Ensmbl")
summary(rawdata)
head(rawdata)
colnames(rawdata)
seq=DGEList(counts=rawdata[,3:8], genes=rawdata[,1])
group=c(rep("Isotype",3),rep("M1/69",3))
y=DGEList(counts=seq, group=group)
y
nonint=rownames(y) %in%
c("no_feature","ambiguous","too_low_aQual","alignment_not_un
ique","not_aligned")
cpms=cpm(y)
keep = rowSums(cpms>0.1)>=2 &!nonint
counts=y[keep, ,keep.lib.sizes=FALSE]
table(keep)
d=DGEList(counts=counts, group=group)
plotMDS(d)
d=calcNormFactors(d)
d$samples
plotMDS(d)
d=estimateCommonDisp(d, verbose=T)
d=estimateTagwiseDisp(d)
plotBCV(d)
de=exactTest(d, pair=c("Isotype","M1/69"))
tt=topTags(de, n=nrow(d))
head(tt$table)
nc=cpm(d, normalized.lib.sizes = TRUE)
rn=rownames(tt$table)
deg=rn[tt$table$PValue<0.001]
plotSmear(d, de.tags = deg)
write.csv(tt$table, file="toptags_edgeR.csv")
```

Supplemental File 1: The mean and standard deviations from the microarray data analyzed, for all genes shown in Chapter 2

Supplemental File 2: Gene ontology enrichment analysis of the top 50 protein coding transcripts identified in EV from B cells released under isotype or anti-CD24 stimulation.

Supplemental File 3: Gene ontology, pathway, process and disease enrichments identified from the proteins enriched in EV released from B cells following anti-CD24 stimulation.